



**This electronic thesis or dissertation has been
downloaded from Explore Bristol Research,
<http://research-information.bristol.ac.uk>**

Author:

O'Sullivan, Dominic

Title:

The effect of implant geometry upon the primary stability of dental implants.

General rights

Access to the thesis is subject to the Creative Commons Attribution - NonCommercial-No Derivatives 4.0 International Public License. A copy of this may be found at <https://creativecommons.org/licenses/by-nc-nd/4.0/legalcode>. This license sets out your rights and the restrictions that apply to your access to the thesis so it is important you read this before proceeding.

Take down policy

Some pages of this thesis may have been removed for copyright restrictions prior to having it been deposited in Explore Bristol Research. However, if you have discovered material within the thesis that you consider to be unlawful e.g. breaches of copyright (either yours or that of a third party) or any other law, including but not limited to those relating to patent, trademark, confidentiality, data protection, obscenity, defamation, libel, then please contact collections-metadata@bristol.ac.uk and include the following information in your message:

- Your contact details
- Bibliographic details for the item, including a URL
- An outline nature of the complaint

Your claim will be investigated and, where appropriate, the item in question will be removed from public view as soon as possible.

The effect of implant geometry upon the primary stability of dental implants

Dominic O'Sullivan BDS., FDSRCS.

**A thesis submitted to the University of Bristol in accordance with the
requirements of the degree of Doctor of Philosophy in the
Faculty of Medicine**

**Department of Restorative Dentistry
Bristol Dental School
Lower Maudlin Street
Bristol, BS1 2LY**

May 2001

38 989

ABSTRACT

The effect of variation in implant geometry upon oral implant primary stability has been investigated. Comparison has been made of the primary stability characteristics of three implant designs, two commercially available (standard Brånemark and Mark II) and one tapered experimental design (Mark IV). The experimental design has been produced with the aim of enhancing implant primary stability in implant sites of poor bone quality. A review of the relevant literature with particular reference to the relationship between surgery, the oral implant and the bone site as well as factors associated with implant primary and secondary stability is presented. A comparison of the clinical primary stability characteristics of standard Brånemark implants (placed with a modified surgical technique) and the experimental Mark IV implant was made. The results indicate that the modified surgical technique and the Mark IV can enhance implant primary stability. A comparative study of the primary stability characteristics of five designs of oral implant is presented using a human cadaver model and a polyurethane foam model used to simulate Type IV bone. Electrical resistance strain gauges were used to examine the effect of implant taper on bovine cortical bone strain in vitro. Strain gauges were used to study the post insertion changes in strain and implant stability relating to the initial postoperative phase for the differing implant designs. Results indicate that changes in strain and stability continue for several hours following implant insertion. The taper of the Mark IV implant appears to give rise to increased primary stability when compared to the other implant types. Although a similar level of primary stability can be achieved using other implant types by the use of an altered surgical technique the Mark IV achieves this level of primary stability with a reduced level of energy imparted to the peri-implant bone.

ACKNOWLEDGEMENTS

I owe a debt of gratitude to a number of people for their help and support.

Firstly I am greatly indebted to my supervisors, Professor Neil Meredith and Professor Alan Harrison for their advice and encouragement throughout the period of this work. Particular thanks must go to Professor Neil Meredith who inspired this work and whose enthusiasm has carried me through some times when my own enthusiasm was flagging. A note of thanks must also go on a more personal level to both Professor Neil Meredith and his wife Susan who generously gave me a roof over my head in the first few months when my experimental work transferred to Leeds University and who always made me feel welcome – thank you.

My thanks must go to Frederik Engman and Tomas Bäck of Nobel Biocare, Sweden for their help on numerous occasions and for the supply of implant related materials throughout this study. Without their help this work could not have taken place.

I would like to thank Dr. Lars Sennerby of the Institute of Handicap Research, Gothenburg, Sweden for his help and guidance and in particular his generous help with Chapter 5.

Louise Merrett deserves a special mention for her constant support during the three years of this study. Her help with the experimental work involved in Chapter 2 and Chapter 4 was invaluable. I must especially thank her for the seemingly endless hours standing in a cold mortuary helping with the data acquisition for Chapter 4, a job that I know she did not relish.

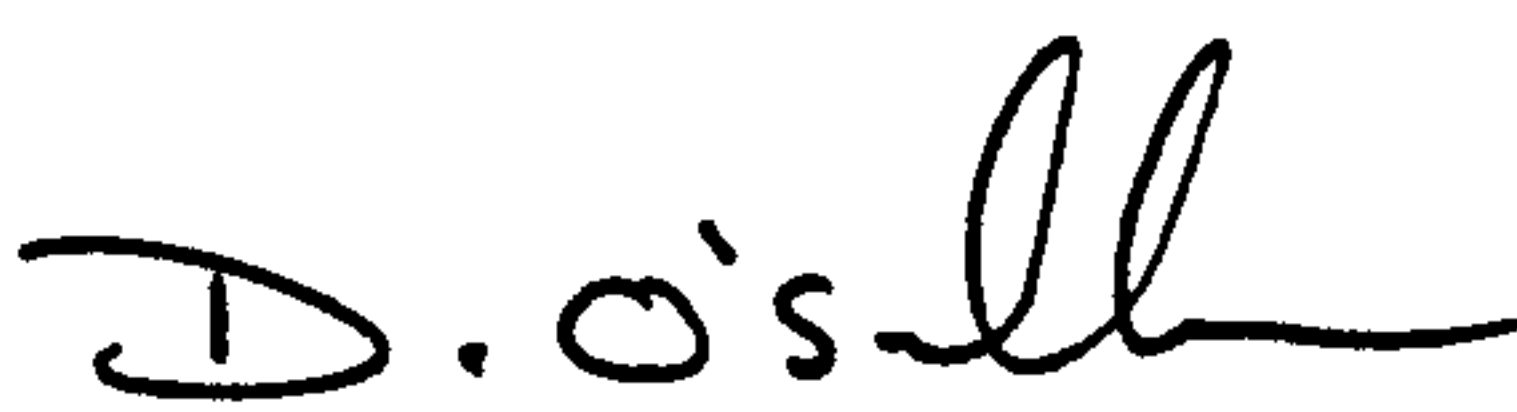
Special thanks must go to my parents and family who have understood my apparent absence from their lives for three years.

AUTHOR'S DECLARATION

The accompanying thesis entitled *The effect of implant geometry upon the primary stability of dental implants* is submitted for the degree of Doctor of Philosophy in the Faculty of Medicine at the University of Bristol. Any views expressed in the dissertation are those of the author and in no way represent those of the University of Bristol.

I certify that this thesis has been based on my own independent work, except where acknowledged in the text or by reference.

The work in this thesis has not been submitted previously for a degree or diploma at this or any other University or examining body.

Signature: 

Date: 9.9.01

DOMINIC J O'SULLIVAN

TABLE OF CONTENTS

TITLE PAGE	i
ABSTRACT	ii
ACKNOWLEDGEMENTS	iii
AUTHORS DECLARATION	iv
LIST OF CONTENTS	v
LIST OF FIGURES	xiii
LIST OF TABLES	xix
NOTATION	xx

CHAPTER 1 –

LITERATURE REVIEW AND AIMS OF THE PRESENT STUDY

1.1	Introduction	2
1.1.1	History of implant design	2
1.2	Implant success	5
1.2.1	Defining implant success and failure	5
1.2.2	Factors related to implant success and failure	6
1.3	Primary stability and implant success	7
1.3.1	The importance of primary oral implant stability	7
1.3.2	Relationship of primary to secondary implant stability	8
1.3.3	The factors affecting primary stability	11
1.4	The objectives of the present work	12
1.5	The assessment of primary implant stability	13

1.5.1	Primary stability assessment techniques	13
1.5.1.1	Percussion and manual testing	13
1.5.1.2	Radiographic examination	13
1.5.1.3	Periotest	16
1.5.1.4	Reverse Torque Testing	18
1.5.1.5	Removal Torque	20
1.5.1.6	Immediate Removal Torque	22
1.5.1.7	Resonance Frequency Analysis (RFA)	23
1.6	Bone Quality	26
1.6.1	Definitions of jaw bone quality	26
1.6.2	Assessment of bone quality	28
1.6.2.1	Radiographic examination	28
1.6.2.2	Quantitative Computed Tomography (QCT)	28
1.6.2.3	Bone mineral density (BMD)	30
1.6.2.4	Ultrasound attenuation velocity	31
1.6.2.5	Magnetic Resonance Imaging (MRI)	31
1.6.2.6	Bone biopsies	31
1.6.2.7	Insertion Torque (true cutting resistance)	32
1.7	Bone Quantity	33
1.7.1	Assessment techniques for jaw bone quantity	33
1.8	Surgical technique	33
1.8.1	Surgical technique and implant success	33
1.9	Bone healing	36
1.9.1	Bone response to surgery	36
1.9.2	Bone response to thermal injury	36

1.9.3	Bone response to mechanical stress and strain	37
1.9.4	Measurement of bone strain	39
1.10	Implant design	41
1.10.1	Bone stress in relation to implant design	41
1.10.2	Biomechanics of implant design	43
1.10.3	Rationale for implant design changes	45

CHAPTER 2 –

IN VIVO DATA RELATING TO THE PRIMARY AND SECONDARY STABILITY OF DENTAL IMPLANTS

2.1	Aims and objectives	48
2.2	Method	49
2.2.1	Patient selection and implant placement	49
2.2.2	Data collection	52
2.2.3	Calibration of the Osseocare unit	54
2.2.4	Bone Quality Assessment	58
2.2.5	Resonance Frequency Analysis	62
2.2.6	Evaluating Insertion Torque Peaks	62
2.2.7	Calculation of Energy required during implant insertion	64
2.2.8	Statistics	64
2.3	Results	64
2.3.1	Insertion Torque	66
2.3.2	Resonance Frequency Analysis (RFA)	69
2.4	Discussion	73

2.4.1	Discussion of the method	73
2.4.2	Discussion of the results	76

CHAPTER 3 –

THE DEVELOPMENT OF AN IN-VITRO MODEL TO COMPARE THE PRIMARY STABILITIES OF DENTAL IMPLANTS

3.1	Aims and objectives	86
3.2	Method	86
3.2.1	Baseline clinical data	86
3.2.2	Specimen preparation	87
3.2.3	Implant characteristics	91
3.2.4	Surgical techniques and implant placement	91
3.2.5	Data collection	91
3.2.6	Statistics	93
3.3	Results	93
3.4	Discussion	97
3.4.1	Discussion of the method	97
3.4.2	Discussion of the results	99

CHAPTER 4 –

THE COMPARISON OF THE PRIMARY STABILITY OF DIFFERING IMPLANT DESIGNS IN A CADAVER MODEL

4.1	Aims and objectives	103
-----	---------------------	-----

4.2	Method	103
4.2.1	Subjects	103
4.2.2	Implant characteristics	104
4.2.3	Surgical technique and implant placement	104
4.2.4	Assessment of bone quality	105
4.2.5	Data collection	105
4.2.6	Statistics	106
4.3	Results	106
4.3.1	Insertion Torque	106
4.3.2	Resonance Frequency Analysis (RFA)	110
4.4	Discussion	114
4.4.1	Discussion of the method	113
4.4.2	Discussion of the results	114

CHAPTER 5 –

THE COMPARISON OF THE PRIMARY STABILITY OF IMPLANTS WITH DIFFERING GEOMETRY IN AN IN-VIVO RABBIT MODEL

5.1	Aims and objectives	120
5.2	Method	120
5.2.1	Animals and anaesthesia	120
5.2.2	Implant materials	121
5.2.3	Resonance Frequency Analysis (RFA)	123
5.2.4	Insertion Torque	123
5.2.5	Removal Torque	125

5.2.6	Statistics	125
5.3	Results	125
5.4	Discussion	128
5.4.1	Discussion of the method	128
5.4.2	Discussion of the results	129

CHAPTER 6 –

MEASUREMENT OF THE SURFACE BONE STRAINS AND PRIMARY STABILITY OF IMPLANTS WITH DIFFERING GEOMETRY DURING IMPLANT PLACEMENT

6.1	Aims and objectives	134
6.2	Method	134
6.2.1	Specimen Preparation	134
6.2.2	Strain gauge attachment	135
6.2.3	Strain gauge calibration	140
6.2.4	Testing procedures	143
6.2.5	Data acquisition	148
6.2.6	Statistics	149
6.3	Results	149
6.3.1	Implant site preparation	155
6.3.2	Implant insertion	155
6.4	Discussion	162
6.4.1	Discussion of the method	162
6.4.2	Discussion of the results	168

6.4.2.1	Implant site preparation	168
6.4.2.2	Implant insertion	169

CHAPTER 7 –

THE MEASUREMENT OF PRIMARY STABILITY AND STRESS RELAXATION OF IMPLANTS WITH DIFFERING GEOMETRY IMMEDIATELY FOLLOWING IMPLANT PLACEMENT

7.1	Aims and objectives	174
7.2	Method	175
7.2.1	Specimen Preparation	175
7.2.2	Strain gauge attachment	175
7.2.3	Data acquisition	177
7.2.4	Testing procedures	178
7.2.5	Statistics	182
7.3	Results	182
7.4	Discussion	187
7.4.1	Discussion of the method	187
7.4.2	Discussion of the results	191

CHAPTER 8 –

CLINICAL IMPLICATIONS, PROPOSED FURTHER WORK AND CONCLUSIONS

8.1	Clinical implications	198
-----	-----------------------	-----

8.2	Proposed further work	201
8.3	Conclusions	202
Appendix I	– Labview 5.1 virtual instruments used in this work	204
Appendix II	– Materials	211
Appendix III	- Work from this thesis previously published	212
References		213

LIST OF FIGURES

Figure	Description	Page
1.1	Factors influencing implant secondary stability	10
1.2	Periapical radiograph of two failing implants	15
1.3	Schematic of Figure 1.2 demonstrating perifixtural and angular bone loss shaded grey	15
1.4	Periotest unit	17
1.5	Diagram of Periotest handpiece in use	17
1.6	Tohnichi torque gauge	19
1.7	Photograph and schematic of Removal Torque rig	21
1.8	Photograph of Resonance Frequency Analysis system in use	24
1.9	Schematic of Resonance Frequency system	24
1.10	Bone quality scoring system (after Lekholm & Zarb 1985)	27
1.11	Bone quantity scoring system (after Lekholm and Zarb 1985)	27
1.12	CT scan	29
1.13	OPT radiographic view used for bone quantity assessment	34
1.14	Schematic of bone mapping	34
2.1	Standard surgical protocol for Standard Nobelbiocare implants	51
2.2	Osseocare unit	53
2.3	Close view of Osseocare unit control panel	52
2.4	Tohnichi torque gauge	55
2.5	Tohnichi torque gauge with surgical tap in place	55
2.6	Osseocare torque calibration results. Mean values with 95% confidence Intervals are shown where appropriate	57
2.7	Hewlett Packard HEDS-550S optical rotary encoder	59

2.8	Osseocare rotation calibration results. Mean values and 95% confidence Intervals are shown.	60
2.9	Implant insertion torque plot with annotation	63
2.10	Derivation of implant insertion energy	65
2.11	Mean maximum insertion torque at implant insertion. Mean values with 95% confidence intervals are shown.	67
2.12	Slope of the tangent to the maximum insertion torque peak at implant insertion. Mean values with 95% confidence intervals are shown.	67
2.13	Mean maximum insertion torque at implant insertion per implant type. Mean values with 95% confidence intervals are shown.	68
2.14	Slope of the tangent to the maximum Insertion torque peak per implant type. Mean values with 95% confidence intervals are shown.	68
2.15	Energy required during implant insertion. Mean values with 95% confidence intervals are shown.	70
2.16	Energy required during implant insertion per implant type. Mean values with 95% confidence intervals are shown.	70
2.17	RFA values at implant placement. Mean values with 95% confidence intervals are shown.	71
2.18	RFA values at second stage surgery. Mean values with 95% confidence intervals are shown.	71
2.19	RFA values at implant placement per implant type. Mean values with 95% confidence intervals are shown.	72
2.20	RFA values per implant type at second stage surgery. Mean values with 95% confidence intervals are shown.	72
2.21	Maximum insertion torque against RFA at implant placement.	74
2.22	Maximum insertion torque against RFA at second stage surgery.	74
2.23	Comparison of insertion torque traces in this study with a standard Brånemark implant placed into a pre-tapped hole.	79
2.24	Insertion torque profile plots for 3.75mm diameter standard Nobelbiocare implant inserted into bovine spine using varying drill diameters.	80

3.1	Baseline insertion torque data from cadaver specimens	88
3.2	Aluminium polyurethane foam moulds	89
3.3	Comparison of baseline insertion torque data from cadaver specimens and polyurethane foam models	90
3.4	Implant types	92
3.5	Mean peak insertion torque values for the five implant types placed into the polyurethane foam model. Mean values with 95% confidence intervals are shown.	95
3.6	Mean RFA values for the five implant types placed into the polyurethane foam model. Mean values with 95% confidence intervals are shown.	96
4.1	Insertion torque/displacement profile for a Mark II implant	107
4.2	Insertion torque/displacement profile for a Mark IV implant	107
4.3	Insertion torque/displacement profile for an Osseotite implant	107
4.4	Peak insertion torque values for each implant type in Type 2 bone. Mean values and 95% confidence intervals are shown	108
4.5	Peak insertion torque values for each implant type in Type 3 bone. Mean values and 95% confidence intervals are shown	108
4.6	Peak insertion torque values for each implant type in Type 4 bone. Mean values and 95% confidence intervals are shown	108
4.7	Peak immediate removal torque values for each implant type in Type 2 bone. Mean values and 95% confidence intervals are shown	109
4.8	Peak immediate removal torque values for each implant type in Type 3 bone. Mean values and 95% confidence intervals are shown	109
4.9	Peak immediate removal torque values for each implant type in Type 4 bone. Mean values and 95% confidence intervals are shown	109
4.10	Insertion torque profiles for standard Branemark, Mark II and Mark IV implants.	111
4.11	Mean RFA values for each implant type in Type 2 bone. Mean values with 95% confidence intervals are shown	112
4.12	Mean RFA values for each implant type in Type 3 bone. Mean	112

	values with 95% confidence intervals are shown	
4.13	Mean RFA values for each implant type in Type 4 bone. Mean values with 95% confidence intervals are shown	112
5.1	Surgical technique used in the placement of implants in the rabbit study	122
5.2	Implant distribution in the rabbit	124
5.3	Removal torque rig	127
6.1	Strain gauge details	136
6.2	Experimental set-up for strain gauge experiment	138
6.3	Implant site preparation and insertion through strain gauge	139
6.4	Temperature fluctuation of dummy strain gauge	141
6.5	Instron mechanical testing machine and handpiece rig	145
6.6	Labview display and schematic	150
6.7	Strain gauge response to implant site preparation plotted against time	151
6.8	Strain gauge response to implant site preparation plotted against depth	152
6.9	Strain gauge response to Standard implant insertion plotted against time	153
6.10	Strain gauge response to Mark II implant insertion plotted against time	153
6.11	Strain gauge response to Mark IV implant insertion plotted against time	153
6.12	Strain gauge response to standard implant insertion plotted against depth	154
6.13	Strain gauge response to Mark II implant insertion plotted against depth	154
6.14	Strain gauge response to Mark IV implant insertion plotted against depth	154
6.15	Maximum principal strains during the stages of implant site preparation. Mean values with 95% confidence intervals are	156

	shown	
6.16	Minimum principal strains during the stages of implant site preparation. Mean values with 95% confidence intervals are shown	156
6.17	Angle of principal strains during the stages of implant site preparation. Mean values with 95% confidence intervals are shown	157
6.18	Mean maximum principal strains during the stages of implant Site preparation. Mean values with 95% confidence intervals are shown	158
6.19	Mean minimum principal strains during the stages of implant site preparation. Mean values with 95% confidence intervals are shown	158
6.20	Maximum principal strains during implant insertion. Mean Values. With 95% confidence intervals are shown	159
6.21	Minimum principal strains during implant insertion. Mean values With 95% confidence intervals are shown	159
6.22	Angle of principal strains during implant insertion. Mean values With 95% confidence intervals are shown	160
6.23	Mean max principal strains during implant insertion. Mean values With 95% confidence intervals are shown	161
6.24	Mean min principal strains during implant insertion. Mean values With 95% confidence intervals are shown	161
6.25	Mean maximum principal stresses during implant site preparation calculated with a range of values for Poisson's ratio and Young's modulus	165
6.26	Mean minimum principal stresses during implant site preparation calculated with a range of values for Poisson's ratio and Young's modulus	165
6.27	Mean maximum principal stresses during implant insertion calculated with a range of values for Poisson's ratio and Young's modulus	166
6.28	Mean minimum principal stresses during implant insertion calculated with a range of values for Poisson's ratio and Young's modulus	166

6.29	Illustration of maximum and minimum principal strain direction in relation to anatomical form	170
7.1	Stress relaxation setup	179
7.2	Implant insertion stopping position. Demonstrating space between implant flange and cortical bone surface	181
7.3	Representative stress/RFA changes for a Mark II implant in bovine bone following insertion	183
7.4	Mean starting RFA values. Mean values with 95% confidence intervals are shown	184
7.5	Mean changes in RFA for each implant. Mean values with 95% confidence intervals are shown	184
7.6	Mean changes in maximum principal strain during the test period. Mean values with 95% confidence intervals are shown	185
7.7	Mean changes in minimum principal strain during the test period. Mean values with 95% confidence intervals are shown	185
7.8	Load-deformation curve for bovine bone specimen	189

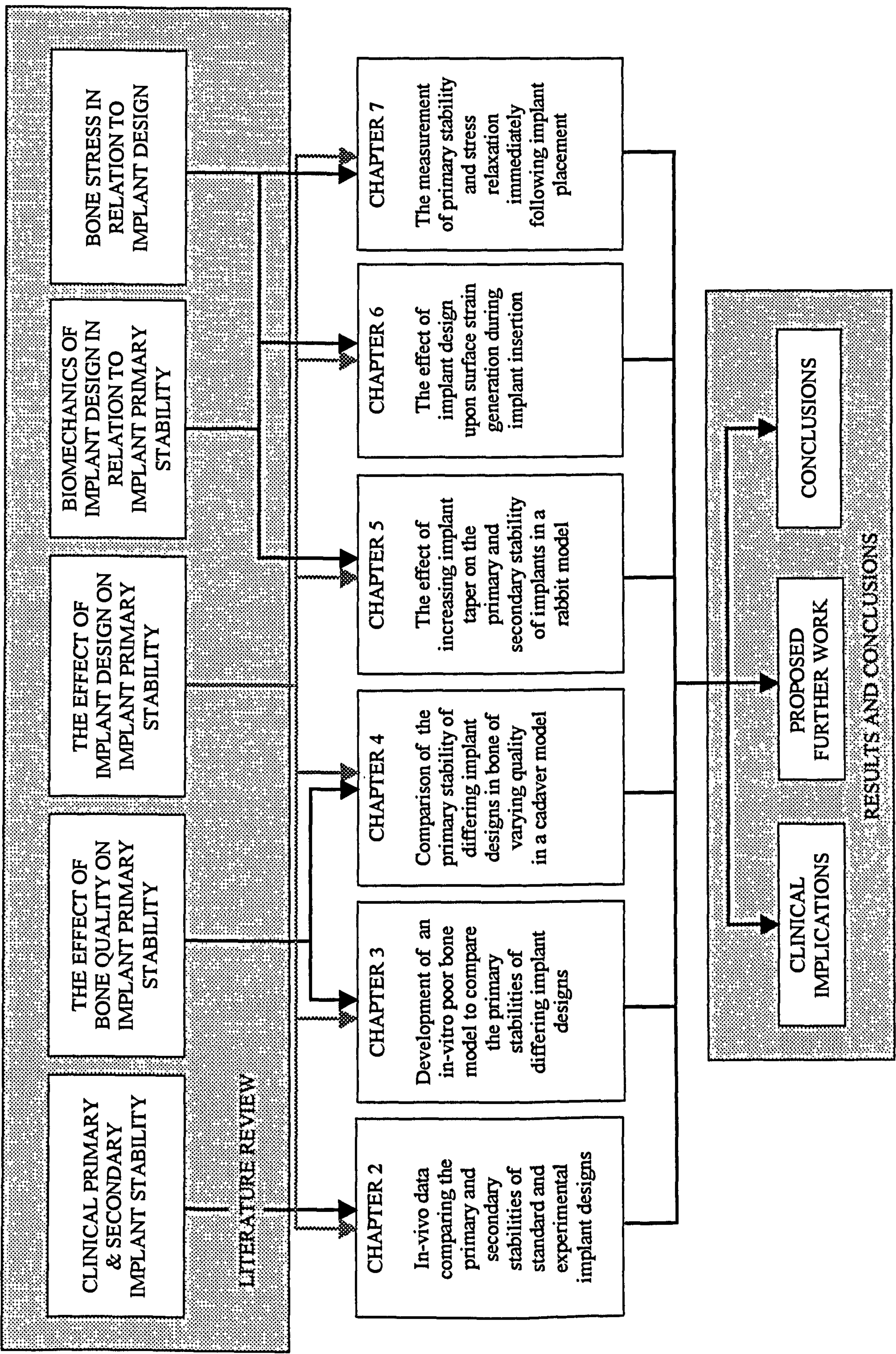
LIST OF TABLES

Table	Description	Page
1.1	Design criteria for dental implants (After Grenoble 1974)	44
2.1	Implant distribution table	50
2.2	Torque calibration results	56
2.3	Rotation calibration results	61
3.1	Summary of Insertion Torque and RFA data	94
5.1	Rabbit summary data	127
6.1	Summary of implant site preparation stages	146
6.2	Summary of implant insertion details	147
6.3	Implant site preparation – summary of data	163
6.4	Implant types - summary of data	164
7.1	Summary of RFA data	186

NOTATION

A	angular displacement
b wt	by weight
cm ³	cubic centimetre
c.p.	commercially pure
°C	degrees centigrade
CT	contact time
D ₁₀₀₀	strain reading during 1000µε calibration test
D ₀	strain reading at zero strain
D.C.	direct current
D _χ	strain reading at measured strain
E	Young's modulus
E _χ	energy in joules
g	gram
Hz	hertz
ID	insertion depth in mm
Kg	kilogram
KHz	kilohertz
ml	millilitres
mm	millimetres
ms	milliseconds
Nm	Newton metres
Ncm	Newton centimetres
PTV	Periotest value
RFA	Resonance Frequency Analysis

TP	thread pitch
T_{θ}	Torque in Ncm
ν	Poisson's ratio
ϵ_{χ}	absolute strain in microstrain units
ϵ	principal strain in microstrain units
ρ	principal stress
θ	angular displacement in degrees
s	seconds
$\mu\epsilon$	microstrain



CHAPTER 1

LITERATURE REVIEW AND AIMS OF THE PRESENT STUDY

LITERATURE REVIEW AND AIMS OF THE PRESENT STUDY

1.1 Introduction

The loss of teeth through trauma or pathology of the teeth or their supporting structures can have a wide variety of detrimental functional and psychological effects for the patient concerned. If the tooth loss is limited and the teeth adjacent to the site are suitable, a fixed prosthesis may be provided. For cases where the adjacent teeth are not suitable for the provision of a fixed prosthesis or for areas of more extensive tooth loss traditionally a removable prostheses may be provided. Many patients cope well with these forms of treatment, which offer a relatively low cost and durable solution to tooth loss. They are not, however, appropriate for all patients. For those patients with a combination of anatomical, physiological or psychological factors endosseous implants offer an alternative treatment modality. Since the 1960's with the discovery of biocompatible implant materials and the development of surgical protocols, improving success rates for this form of treatment have meant that a wide variety of oral implants are now available. There have been a number of studies over the past thirty years on a variety of implant systems. The results of the studies are often compared to studies involving the Brånemark implant system, a system with the longest and best documented clinical history of any implant type.

1.1.1 History of implant design

Implanted pieces of stone or mollusc shell have been reported in the jaws of the ancient Mayan people in Guatemala and the Ulloa Valley of Honduras (Bobbio 1972) as replacements for lost teeth. These skulls, over 1000 years old, are amongst the earliest recorded forms of dental implant. These 'implants' were placed more for

cosmetic reasons than to truly restore the function of a lost tooth. Although they appear to have remained in situ for some time (judged by the formation of calculus deposits on the 'implant' surface) they would not have integrated into the hard or soft tissues in the manner we expect from modern implants.

Bobbio (1972) reported on a book written by Maggiolo at the beginning of the nineteenth century describing the "making of artificial roots suitable for carrying a pivot tooth". This implant consisted of a hollow gold tube and the author described how to make the implant and perform the surgery to implant it after extracting the tooth. A number of references exist in the literature indicating that experiments into dental implantology continued throughout the end of the nineteenth and the beginning of the twentieth century (Edmunds, 1889; Znamensky, 1891; Bonwill, 1895; Goldberg and Gershkoff, 1949).

Greenfield (1913) reported the use of iridio-platinum implants. The implant itself consisted of iridio-platinum wires soldered together with 24-carat gold to form a latticework cylinder. The author stated that the first trials were not successful. Undeterred, he attributed the lack of success to poor instrumentation and poor preparation of the surgical bed. In an attempt to improve this, Greenfield designed cutting burs to match the size and shape of the implant and stated that the implants placed in this way were firm after placement with no evidence of radiolucency. With Greenfield we have the first indication of a methodical approach to implant and instrumentation design, which may have led to a limited improvement in success. Goldberg and Gershkoff introduced the subperiosteal implant in 1949. Initially the technique involved trimming a cast to resemble the exposed bone at the implant site;

a metal framework was then waxed up and constructed. The framework was placed onto the bone and the mucosa sutured over the frame with pillars protruding through to support a prosthesis. Later, the taking of a direct impression of the bone surface improved the initial fit of the framework. Some designs incorporated screws to enhance the stability by fixing the implant to the bone. The success rates of these early implants were low and the techniques unpredictable. In 1972 the Council on Dental Materials and Devices of the American Dental Association declared that “the Council has been following with both interest and concern, the insufficient information that exists regarding the causes of failures as well as the reasons for success of implants” (Natiella et. al. 1972).

The transosteal implant was inserted through an extraoral submandibular approach. The implant was made up of a number of posts, which penetrated the mandible, with some of the posts exiting the bone intraorally to support a prosthesis. The posts were then joined together by a horseshoe shaped plate on the inferior border of the mandible. Small (1975) reported that the survival rate for transosteal implants over 5 years was in the region of 86%, Cranin et al, (1986) reported the results of 17 years of follow up to be a survival rate of 81%. Albrektsson and Sennerby (1991) stated that the results reported for the transosteal implant were acceptable and well documented.

The major breakthrough in modern dental implantology occurred with the research by Brånemark et al (1977), using commercially pure titanium screw shaped implants. The authors stated that a relationship existed between clinical mobility and implant failure. Using a careful surgical technique under strictly sterile conditions they were

able to achieve greater reproducibility and a higher success rate than previous authors had reported. A successful implant was one that was deemed to be clinically stable with no mobility. Histologically bone was demonstrated to grow in direct contact with the titanium surface providing support to the implant and ultimately the prosthesis attached to it. The authors called this osseointegration. They further defined it as “the direct apposition of ordered living bone at the surface of a load carrying implant as revealed under the light microscope”. Development of their research produced a commercially available implant system with a proven clinical success rate. Other systems have been developed with nearly 200 different implant systems currently commercially available based upon the use of titanium cylindrical implants.

1.2 Implant success

1.2.1 Defining implant success and failure

The Brånemark system has been examined by a number of authors (Cox and Zarb, 1987; van Steenberghe et al, 1987; Albrektsson, 1988; Adell et al, 1990a; Bahat, 1993; Jemt and Pettersson, 1993; Nevins and Langer, 1993; Wyatt and Zarb, 1998) with implant survival of the order of magnitude of 82-99% after up to 10 years of loading. Despite such high survival rates implant failures are higher in certain clinical situations (Lekholm and Zarb, 1985; Worthington et al, 1987; Engquist et al, 1988; Zarb and Schmitt, 1990; Jaffin and Berman, 1991; Jemt, 1991; Sennerby, 1991; van Steenberghe, 1991; Jemt and Lekholm, 1995; Bryant, 1998). Esposito et al (1998a and b) used a meta analytical approach to examine implant failure using a sample of 2,812 Brånemark implants. The biologically related implant failure rate over a 5-year period was 7.7%, with the early failure rate (those for which successful

healing did not take place) accounting for 3.6%. Implants in partially edentulous patients failed less often than in fully edentulous patients. In fully edentulous patients implant failure rates were approximately 3 times higher in the maxilla than in the mandible.

1.2.2 Factors related to implant success and failure

Many workers have suggested criteria for the evaluation of implant success.

Albrektsson et al (1986) defined the following widely accepted criteria:

- an individual implant which is immobile when clinically assessed;
- an absence of peri-implant radiolucency;
- vertical bone loss around the implant, 0.2mm annually after the first year;
- absence of pain, infection, paraesthesia, neuropathies or obvious nerve damage.

He suggested that, using the above criteria a minimum success rate of 85% after five years and 80% after ten years should be achievable for a given implant system.

Osseointegrated implants have been widely used throughout the world and the Brånemark system is without doubt the best documented followed by the Astra and ITI systems. Survival rates for the Brånemark system are documented to be in the region of 99% after 10 years of loading intraorally. Patients and implant sites are selected carefully by surgeons although even with such careful selection, success rates vary when implants are placed in different regions of mouth and in bone of varying quality and quantity.

Failures of implants have been divided into early and late failures (Friberg et al 1991). Early failure can be defined as those implants for which osseointegration never occurs due to failure in the initial healing process. Esposito (1998a and b) suggested that early failures are related to excessively traumatic surgery, together with anatomical conditions. Late implant failures can be defined as those failures taking place following the loading of the implant in function. The same author related such failures to overloading combined with insufficient bone quality and quantity.

1.3 Primary stability and implant success

1.3.1 The importance of primary oral implant stability

When an implant is placed into bone the aim is to drill a hole in the bone into which the implant will be placed so that the implant surface and bone surfaces are closely apposed. In practice this is not possible with the current drilling and implant placement techniques. Hobkirk and Rusiniak (1977) when investigating factors associated with drilling bone found that the design of drill and interoperator variability had a significant effect upon the forces applied to bone during drilling. Interoperator variability was found to be the most significant factor. Due to changes in hand position of the surgeon and chatter and movement of the drill in the handpiece the hole drilled will often deviate from the ideal. In a study in sheep tibia, Haider et al (1993) found that up to 30% of preparations showed such deviations. This mismatch between the implant site and the implant creates gaps between the implant surface and the bone and if a load is applied to the implant before bone has been able to grow into this space micromotion may occur. In a severe case motion may be detectable clinically. Salonen et. al. (1993) and Tricio et. al. (1995) have

suggested that implants may more commonly show signs of subclinical mobility which may have an effect upon implant integration. Cameron et. al. (1973); Schatzker et. al. (1975); Pilliar et. al. (1986); Brunski (1988) and Goodman et. al. (1993) have all shown that micromotion between the implant and the bone promotes the formation of a soft tissue capsule around the implant. A degree of motion appears to be tolerated before soft tissue formation occurs. Pilliar et. al. (1986) found that motion of 150 μ m amplitude will cause a fibrous tissue interface whilst 28 μ m would not. The absolute value of tolerated differential movement of the implant and bone surfaces has yet to be fully defined for intraoral implants and certainly such a precise level of motion is impossible to control in vivo. In practice, surgeons aim for the maximum stability achievable. The stability of an implant immediately after surgical placement is defined as the primary implant stability.

1.3.2 Relationship of primary to secondary implant stability

Following the placement of implants a number of complex biological events can occur. Schenk and Willenegger (1977), Frost (1989b) and Schenk (1994) identified ample blood supply and mechanical stability as the two basic requirements for healing of bony deficiencies. The surgical preparation of the implant bed inevitably leads to a layer of damaged tissue at the cut bone surfaces of the implant site. The tissue damage results from mechanical damage to cells, thermal damage due to insufficient cooling of the drills and surgical taps and the damage to the microcirculation within the bone resulting in inadequate local blood supply to living osteocytes. When the implant is placed in the bone the initial interface zone is made up of a mixture of bone fragments and blood constituents. After a few days, mesenchymal cells and macrophages invade the interface zone and an osteoblast

seam will form at the endosteal surface of the cortex (Sennerby et al, 1993; Masuda et al, 1997). After 7 days, immature woven bone will develop from the osteoblasts, forming ribbons of hard tissue, which approach the implant surface. This bone later matures into lamellar bone, Roberts et al (1993) extrapolating from a rabbit model estimated that this maturation process takes 4-12 months in the human.

The healing process around the implant alters the initial primary implant stability. It may be expected that an implant with an initially high stability may exhibit a loss of stability due the activity of resorptive cells whilst stability will be enhanced by the formation of new bone in close contact with the implant surface. The interaction between these factors is complex and as yet unquantified. It is summarised in Figure 1.1.

Sennerby et al (1992) reported a correlation between the removal torque of titanium implants and the amount of compact bone surrounding them when placed into the tibia and cancellous bone adjacent to the knee joints of rabbits. The cortical bone appeared to provide improved implant support in the immediate post operative period. With time the stability of the implants placed into the cancellous bone reached the same levels but the implants were relatively vulnerable in the immediate post operative period. Ivanoff et al (1996) used a rabbit model to compare implants placed with mono- and bicortical anchorage. The bicortical implants showed two to three times higher removal torque after 6 and 12 weeks, respectively, compared to the monocortical ones. The bicortical implants showed higher bone/implant contact area than the monocortical.

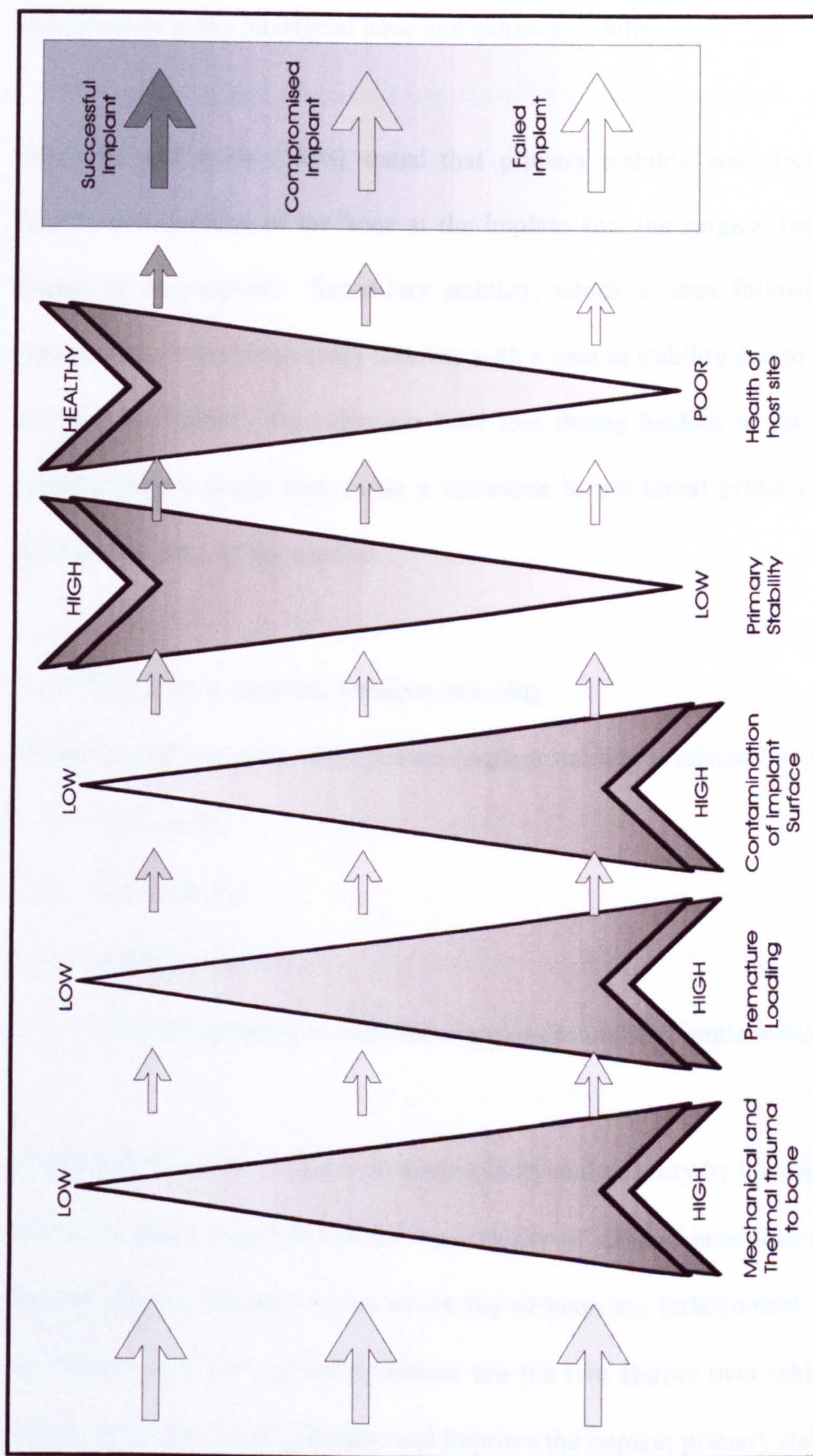


Figure 1.1: Factors influencing implant secondary stability.

Sennerby (1991) suggested omitting the pre-tapping of a threaded bone channel at placement in cases where minimal cortical bone is present in order to induce compression in the interfacial bone and enhance stability.

Sennerby and Roos (1998) stated that primary stability was determined by the density and quantity of the bone at the implant site, the surgical technique and the design of the implant. Secondary stability, which is seen following the healing period, was viewed as primary stability with a gain in stability due to bone formation around the implant. By extension bone loss during healing or the formation of a fibrous tissue capsule may cause a reduction in the initial primary stability value indicating failure of the implant.

1.3.3 The factors affecting primary stability

Meredith (1997) reported that primary implant stability is affected by several factors:

- bone quality
- bone quantity
- implant geometry
- relationship between pilot hole/tapped channel and implant diameter.

Efforts may be made to affect the bone quality and quantity by the use of bone grafts or augmentation materials but for the majority of implant insertions the bone at the implant site is a parameter over which the surgeon has little control. The design of the implant and the surgical technique are the two factors over which the surgeon may be able to exert an influence and improve the implant primary stability.

1.4 The objectives of the present work

Recent work, particularly in the field of resonance frequency, has helped to expand our understanding of primary implant stability and its relationship with secondary implant stability and clinical outcome Meredith (1997; 1998a and b) and Meredith et al (1996a and b; 1997a and b; 1998). Following the successful implant work by Brånemark et al (1969; 1977), the standard Brånemark screw form c.p. titanium implant has become the most widely studied implant design. During the initial development period from 1965 to 1971 Brånemark and co-workers made several refinements to their initial implant design and surgical technique (Adell et al, 1981), but the basic screw form implant was retained. In 1980, 4.0mm diameter implants were introduced as well as the 3.75mm diameter traditional implants. Langer et al (1993), reported the use of 5.0mm and 5.5mm diameter wide platform implants to be used in poor bone qualities, in posterior regions with reduced bone height and as a 'rescue' implant in regions where an implant has failed to integrate or where the implant site has been damaged. An increase in the diameter of the implant has the advantage of engaging the denser buccal and linguopalatal cortical bone as well as having a larger surface area available for bone apposition. In 1983/1984 a self-tapping implant design was introduced initially with the aim of increasing implant primary stability in maxillary bone. In 1997, Friberg et al reported on a new variation of the self-tapping implant with improved cutting characteristics suitable for use in the denser bone of the mandible. In 1998 a further design change was introduced with the introduction of a tapered implant for improved primary stability in poor bone quality. However, there are no studies reported in the dental literature to compare the primary stability of these variations and to look at the effect changes

in implant design have upon implant primary stability and the mechanism by which design changes may alter primary stability.

1.5 The assessment of primary implant stability

1.5.1 Primary stability assessment techniques

1.5.1.1 Percussion and manual testing

Adell et al (1985) recommended that striking the implant abutment lightly could assess the degree of osseointegration of an implant. If the implant is osseointegrated the pitch will be high when the implant is struck, if the implant is surrounded by fibrous tissue the pitch produced will be lower.

The test is obviously easy to carry out but is flawed for several reasons. The angle, direction, magnitude of the strike and point of contact is impossible to reproduce and it is also difficult for the human ear to interrogate the subtle changes in resonance frequency, damping and amplitude (Meredith, 1997).

Coupled with the percussion test all clinicians assess the degree of rotational and lateral mobility of an implant by gentle application of a gentle rotational force to the implant and abutment complex by the use of an appropriate screwdriver (Friberg et al 1999). In a successful implant case no mobility or pain should be noted.

1.5.1.2 Radiographic examination

Radiographic examination is the most commonly used technique in clinical practice as an extension of its traditional use in monitoring the natural dentition. The implant is commonly monitored with radiographs taken at abutment connection, six and 12

months post abutment connection and then every 12 months. The aim of radiographic monitoring is to identify marginal bone loss and perifixtural radiolucencies (Gröndahl et al, 1996; 1997).

Strid (1985) found that a degree of marginal bone remodelling occurs around an implant following insertion. The reduction in marginal bone height from implant insertion to the end of the first year following loading is approximately 1.2mm for the Brånemark system with an average marginal bone loss of 0.1mm per year. If loading of the implant is favourable it appears that an equilibrium state can occur following the initial remodelling phase with negligible further bone loss. Strid (1985) also reported that for implants where there have been mechanical failures of implant components, or where there has been evidence of excessive loading, the marginal bone loss can be up to 3mm per year. Implant design appears to play a part in the degree of marginal bone loss, Roos et al (1997) found that IMZ implants have a mean annual bone loss of up to 0.5mm per year which did not appear to reach an equilibrium.

Radiographs have a poor diagnostic ability for the detection of perifixtural radiolucency (Figures 1.2 and 1.3) due to their limited discriminatory acuity (Caton et al, 1976). Variations in tube angulation, exposure, film placement and processing techniques can alter the radiographic appearance of the perifixtural region. The use of radiographic stents, aluminium step wedges and standardized processing techniques can produce effective serial radiographs but these are not commonly employed and are time consuming and expensive. Perhaps the most important

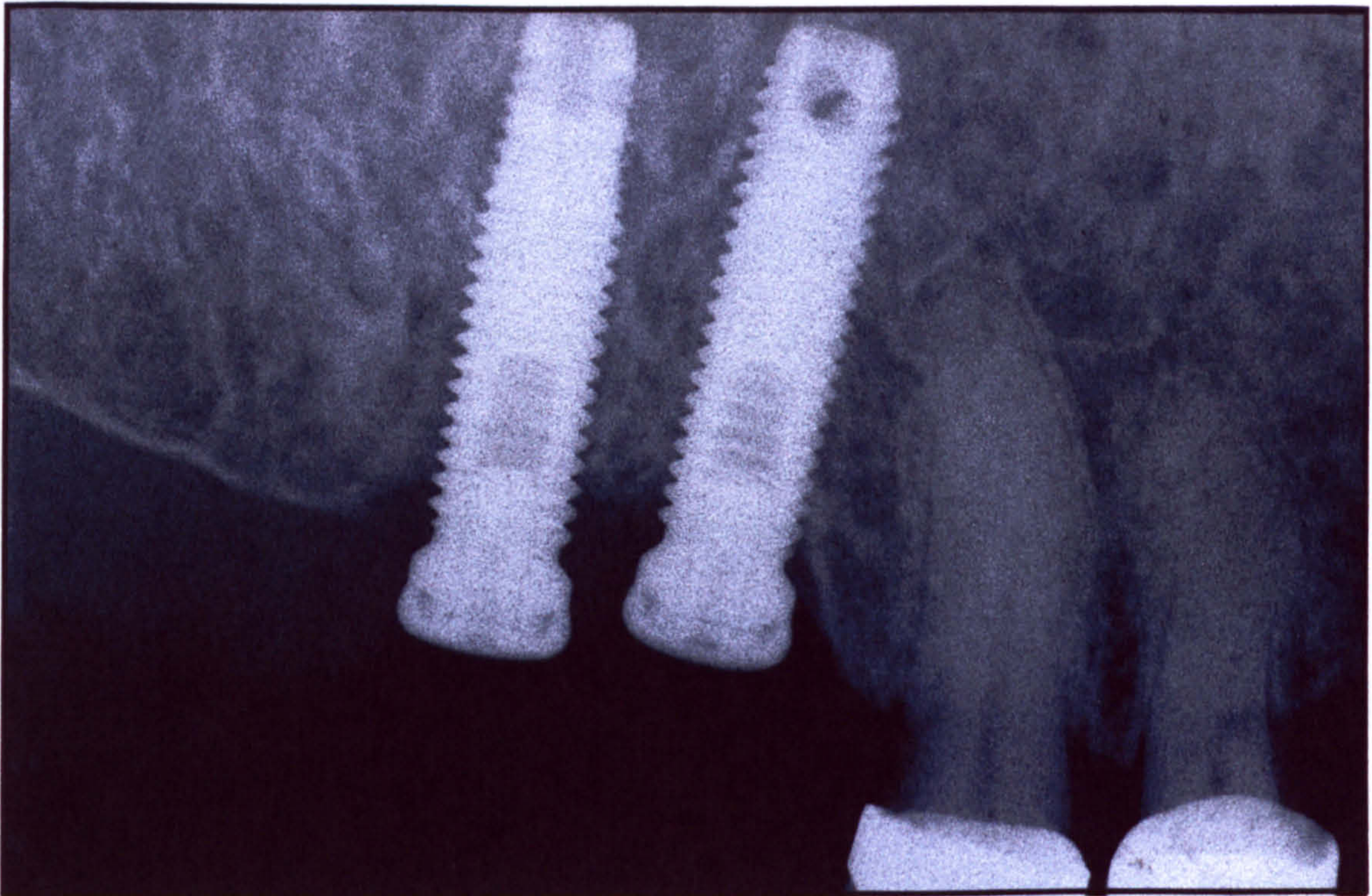


Figure 1.2: Periapical radiograph of two failing implants.

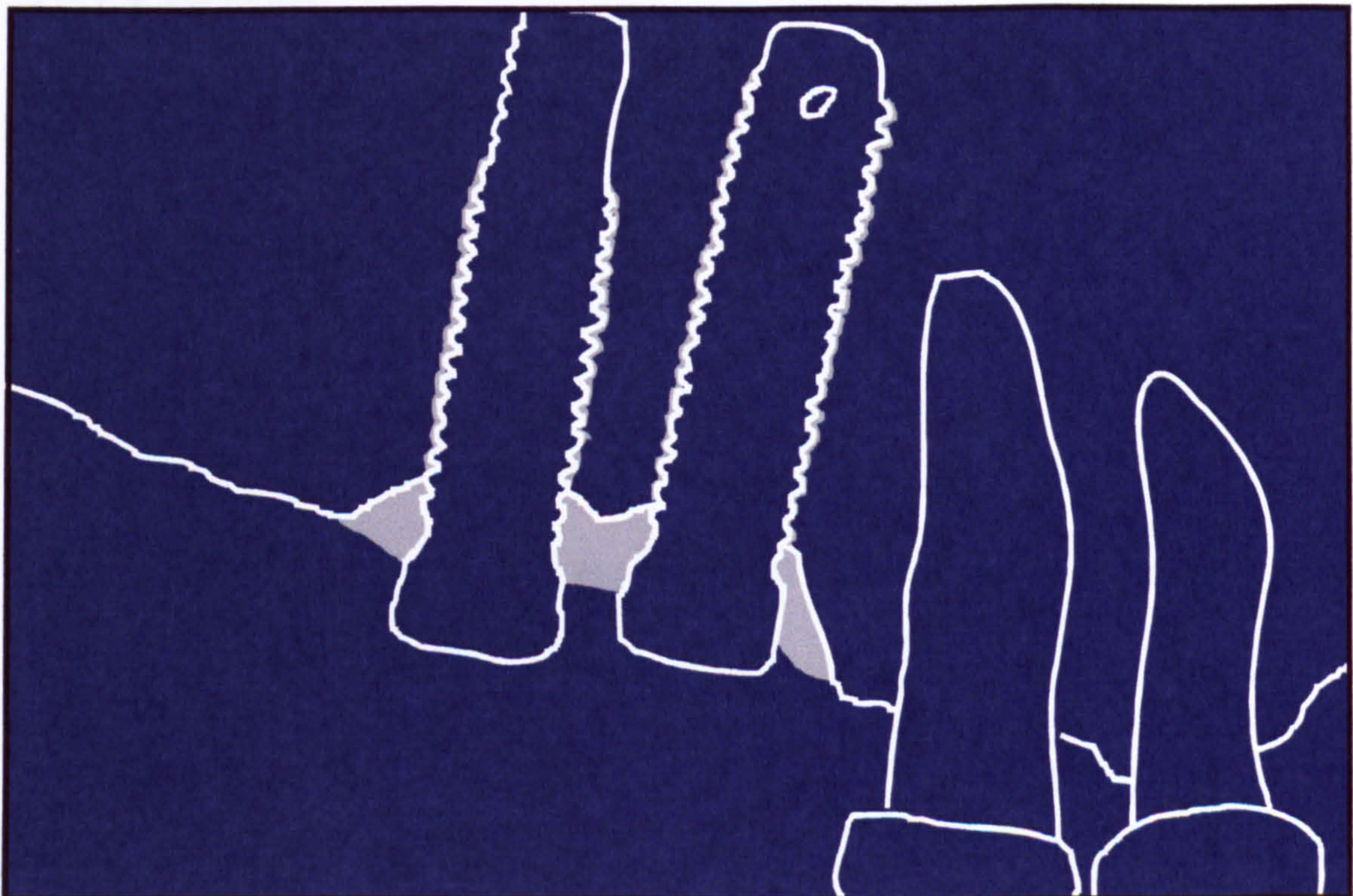


Figure 1.3: Schematic of above radiograph. Perifxtural radiolucency and angular bone loss shaded grey.

drawback of radiographic assessment is that the radiograph is a two dimensional image whilst the implant/bone interface is a cylindrical three-dimensional region. A satisfactory radiograph may be obtained in one plane while a considerable region of the interface may not be satisfactorily integrated in another plane. Sunden et al (1995) studied the agreement within and between observers during repeat examination of a number of radiographs when attempting to assess clinical instability. Eight radiologists were asked to determine the presence or absence of perifixtural radiolucencies around 62 unstable and 158 stable implants. They concluded that the probability of detecting clinical implant instability from radiographic examination was low in populations with a low prevalence of implants showing instability.

1.5.1.3 Periotest

The Periotest®, (Siemens AG, Bensheim, Germany) (Figures 1.4 and 1.5), is, in principle, a sophisticated version of the percussion method. It was developed to quantify the damping characteristics of the periodontal tissues supporting a tooth and therefore assess its mobility (Schulte, 1983). The periotest comprises a handheld probe containing a small electromagnetically driven metal pellet, which percusses the tooth or implant surface. The process is repeated 16 times and mobility is assessed by measurement of the contact time between the metal hammer and the surface under test. The result is displayed as a Periotest value (PTV) on a scale between -8 (low mobility) and +50 (high mobility). Tricio et al (1995) have described that for PTV's from -8 to +13 the following linear formula is used.

$$PTV = \frac{CT}{0.02ms} - 213$$



Figure 1.4: Periotest unit.

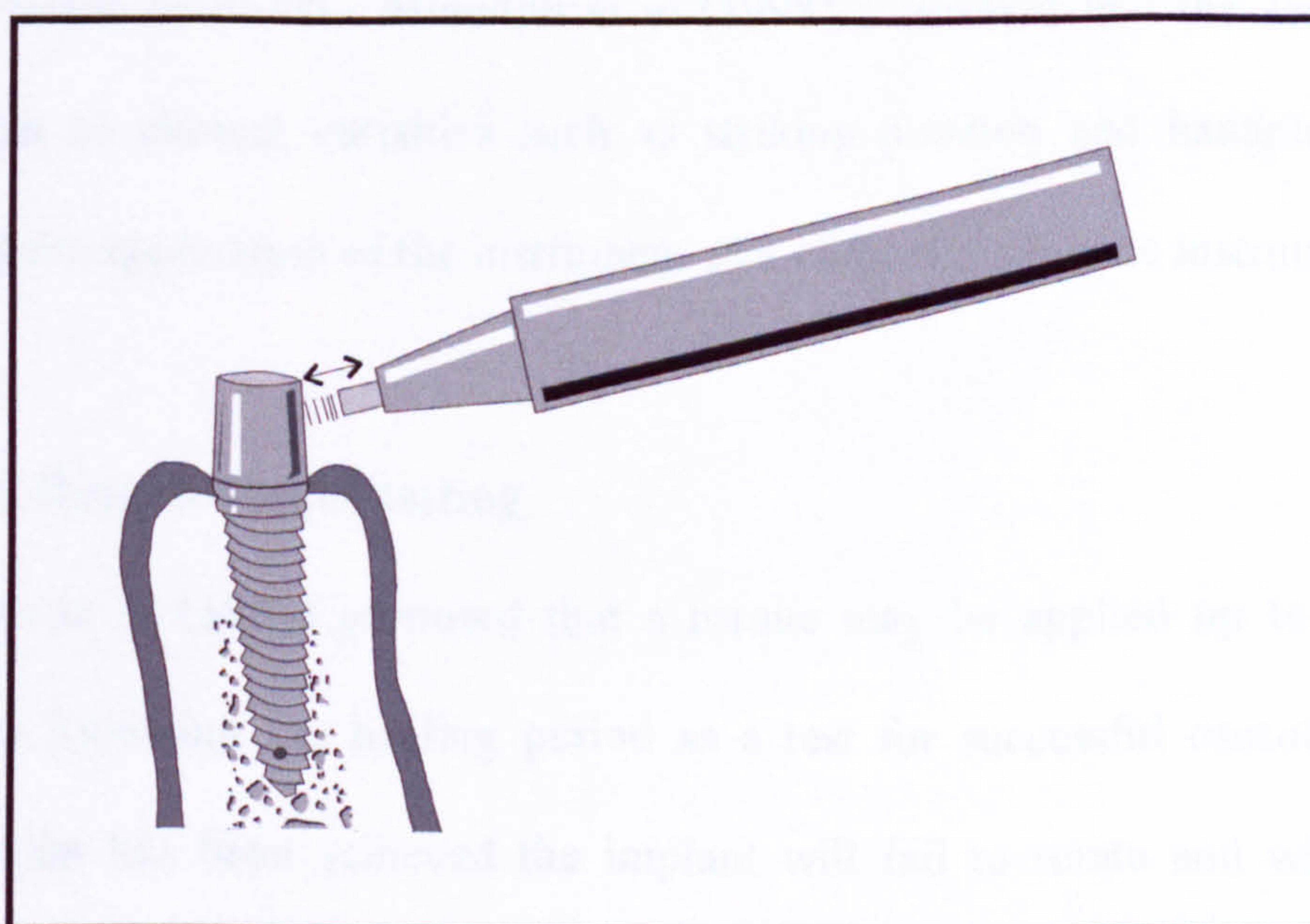


Figure 1.5: Diagram of Periotest handpiece in use.

For PTV's from +13 to +50 the following equation is used.

$$PTV = \sqrt{\left(\frac{CT}{0.06ms} - 8.493\right)} - 4.17$$

The instrument was designed to measure tooth mobility but Olivé and Aparicio (1990) described its use for measuring implant stability and found that the PTV range for implants was from -5 to +5, a small discriminatory scale when compared to the overall range of the unit. Derhami et al (1995) reported that the accuracy of the device is affected by variations in the angulation at which the probe is held, the point of contact with the abutment and the distance that the handpiece is held from the implant under test; this limits the accuracy and effectiveness of this technique as a measure of primary implant stability. The test itself is quite uncomfortable for the patient as first reported by Oka et al (1990) as the metal slug hits the tooth/implant with considerable force. Chavez et al (1993) reported that the metal slug in the handpiece results in a peak load of 4.7N as measured by firing the slug at a piezoelectric load cell. Meredith et al (1998) concluded that the sensitivity of the Periotest to clinical variables such as striking position and handpiece angulation limited the application of the instrument as a clinical diagnostic instrument.

1.5.1.4 Reverse torque testing

Sullivan et al (1996) proposed that a torque may be applied up to 20Ncm to an implant following the healing period as a test for successful osseointegration. If integration has been achieved the implant will fail to rotate and will maintain its

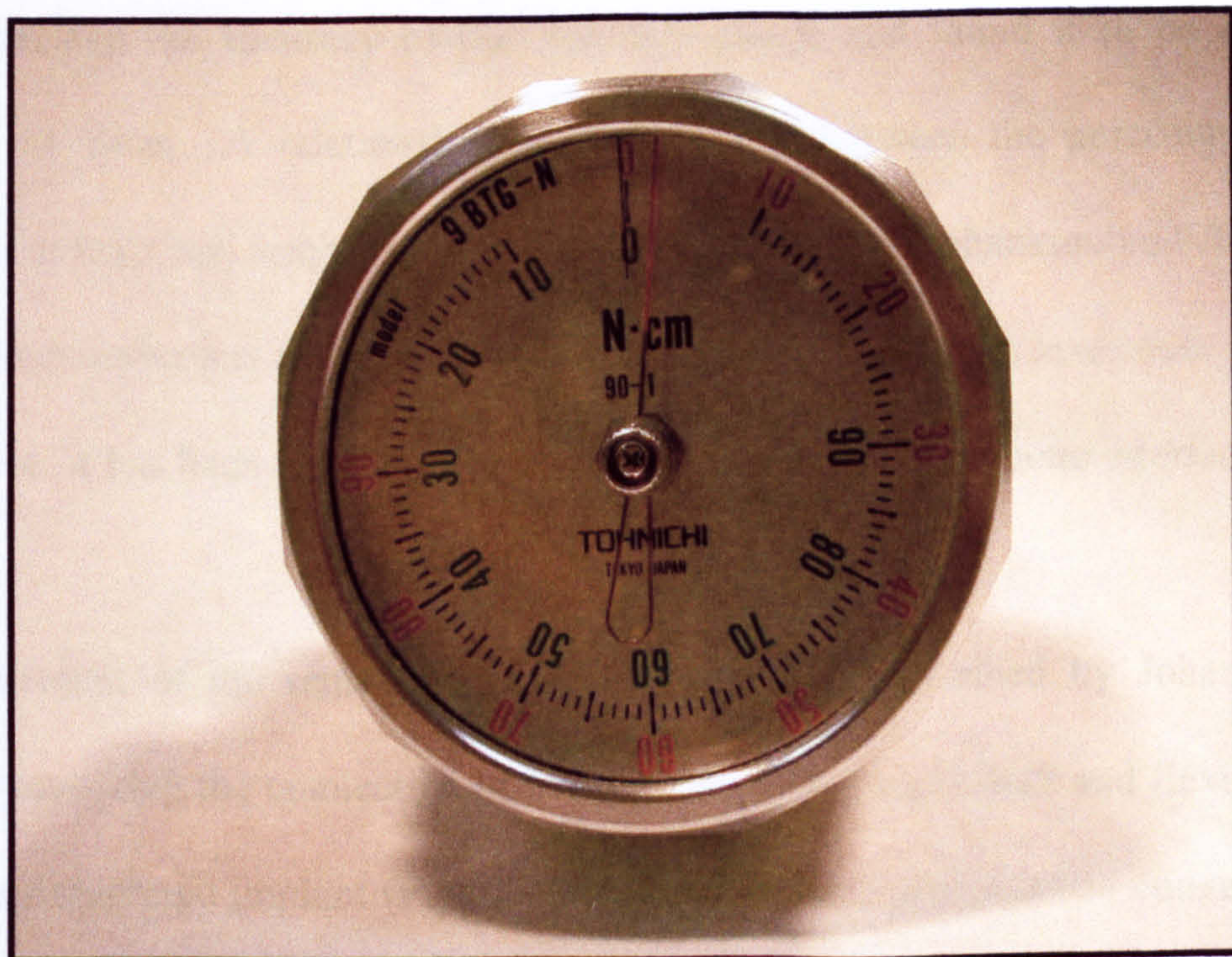
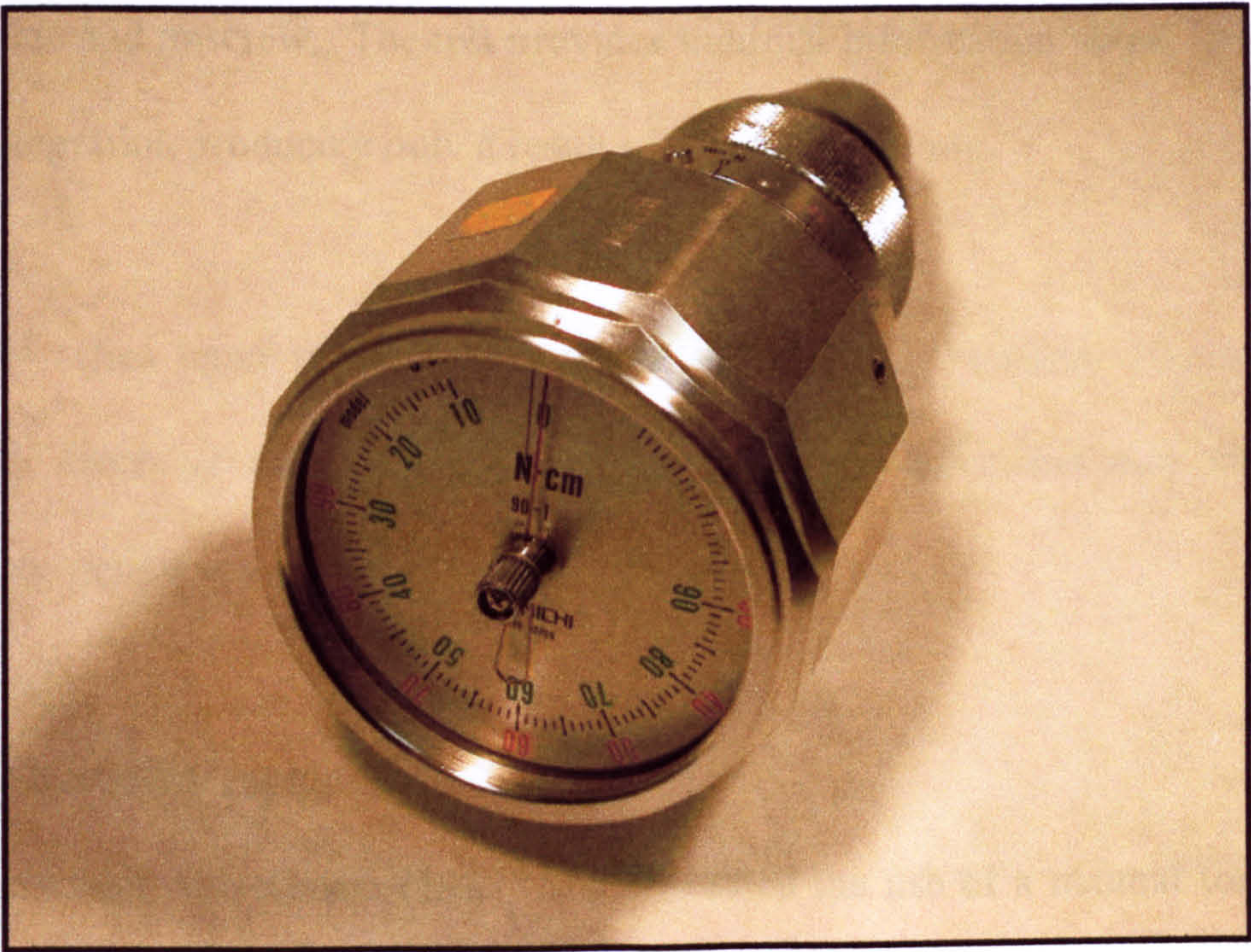


Figure 1.6: Tohnichi torque gauge.

union with the bone, if fibrous capsule formation has taken place then the implant will rotate and unscrew. The test provides minimal information about any degree of osseointegration producing only a result of success or failure.

The test relies upon placing a rotational force on the implant, which results in shearing forces at the implant bone interface. In theory this may damage this important region and can be considered undesirable.

1.5.1.5 Removal Torque

Johansson and Albrektsson (1987) first described the use of a manual torque gauge (Figures 1.6) to measure the peak removal torque of an implant. Tests were carried out in the rabbit at 3 weeks, 3 months, and 12 months which showed increasing removal torque was needed the longer the implant healing period. Carlsson et al (1988) tested the accuracy of the Tohnichi gauge and found it to be accurate to within ± 1 Ncm. A relationship has been found between the percentage bone to implant contact and removal torque (Carlsson et al 1988; Johansson and Albrektsson, 1991; Wennerberg et al 1995). As bone to implant contact increases over the healing period so, it has been argued, does the strength of the implant/bone interface.

A refinement of the removal torque technique was described by Johansson et al (1991) involving the connection of a D.C. motor via a rigid shaft and flexible joint to an osseointegrated implant (Figures 1.7). The motor is stalled when connected to the implant and increasing the current supplied to the motor by the use of an electronic ramp generator will produce a torque. If the current taken by the stalled motor is

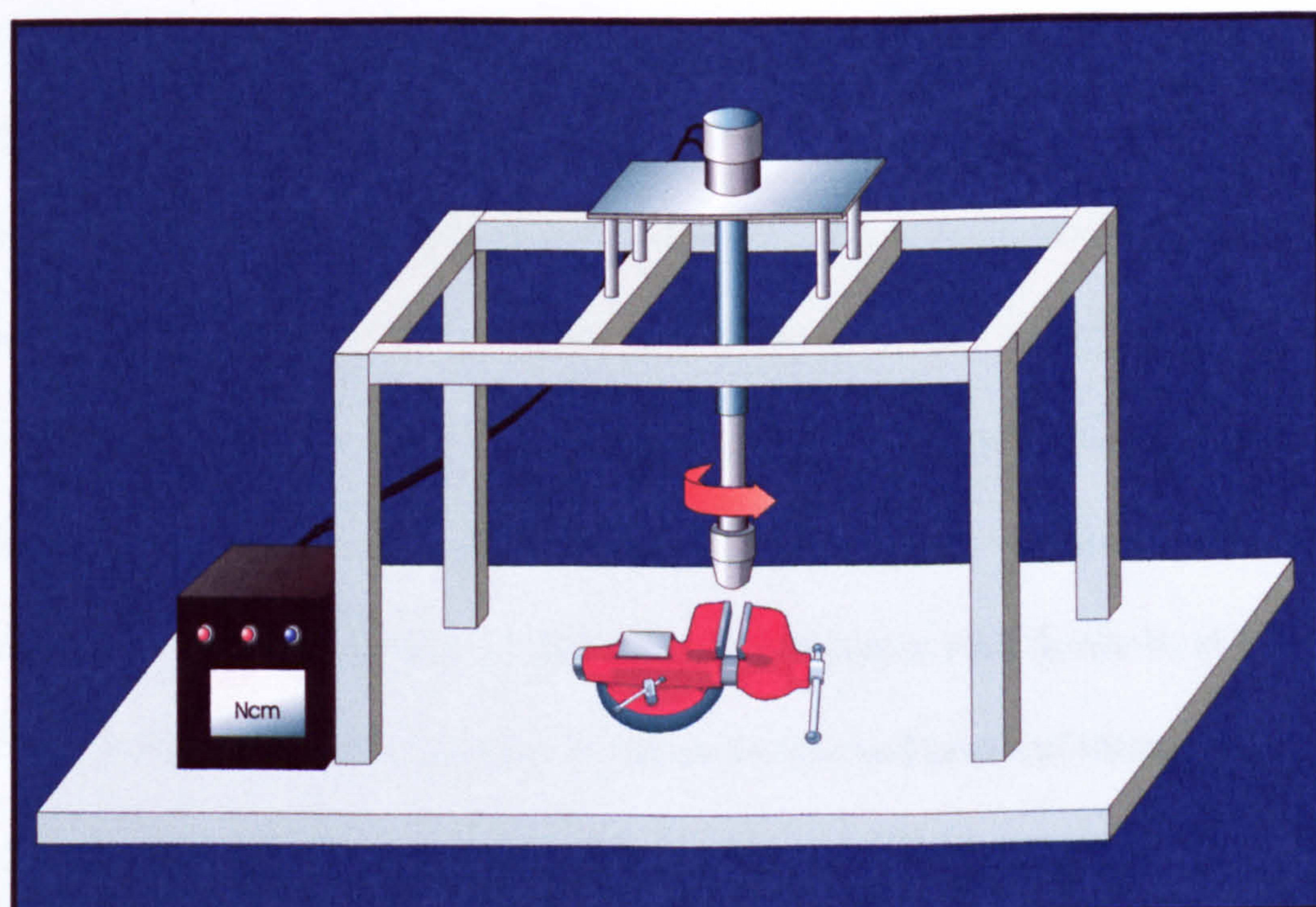
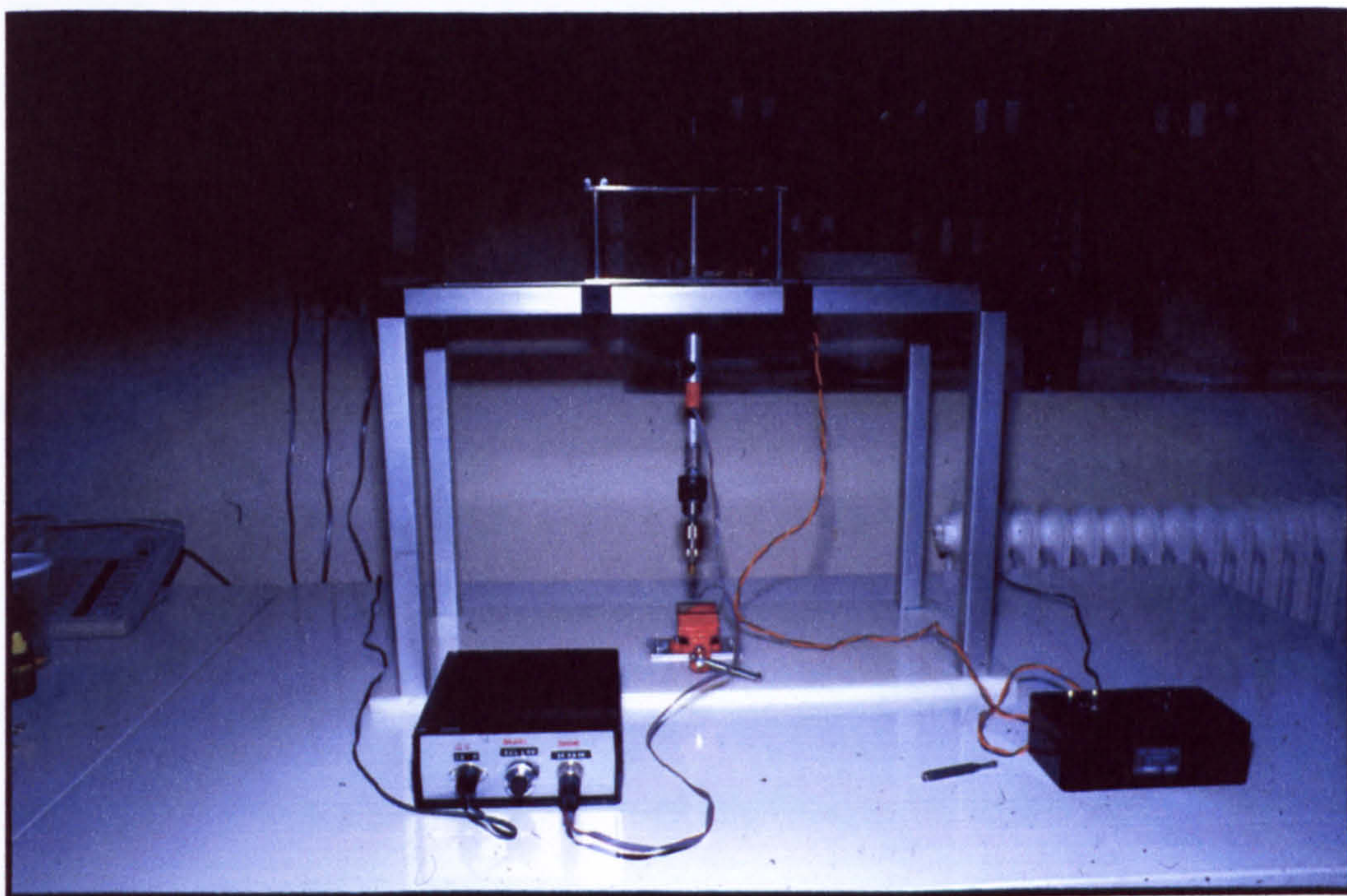


Figure 1.7: Photograph and schematic of Removal Torque rig.

recorded a torque profile of the failing implant interface can be produced. An alternative is to measure the torsion of the connecting beam using strain gauges connected in a standard Wheatstone bridge configuration with the output of the bridge connected to a computer data logger. The system can be calibrated by hanging a series of known weights from the beam and measuring the recorded strain.

The removal torque test is a destructive test. It can give an indication of interface strength, but the technique has not been standardized, with variations in the manner in which specimens are held, the rate of application of torque and the measurement of the generated torque.

1.5.1.6 Immediate Removal Torque

Removal torque of an implant immediately after placement has been used to assess the initial stability of endosseous implants. Niimi et al (1997) used this technique to assess the bone quality and cortical bone thickness of fibula, iliac crest and scapula. They found a significant correlation between cortical bone thickness and removal torque, but not between bone quality and removal torque. They also compared the results from a cadaver model with data collected clinically and found no significant differences between them indicating that the cadaver is a suitable model for the assessment of initial stability. This was in agreement with Ueda et al (1991) who looked at the relationship between insertion torque and removal torque of endosseous fixtures when placed in cadaveric temporal bone. They noted that a high removal torque was always related to a higher initial insertion torque but with the peak removal torque always of a lower magnitude than the peak insertion torque. This would be expected as the frictional component of the removal torque curve would be

the same as for the insertion torque but without the compressive/cutting force component generated during insertion.

There are obvious problems when drawing conclusions from removal torque data gathered immediately after insertion. A high immediate removal torque may not indicate that a high removal torque would be gained once osseointegration has taken place. Immediate removal torque does however provide a measure of the resistance of an implant to rotational displacement in the vulnerable post insertion healing period.

1.5.1.7 Resonance Frequency Analysis (RFA)

Meredith et al (1996a) described the use of resonance frequency analysis to quantitatively examine the implant-tissue interface. A transducer, comprising an L-shaped beam with piezoelectric crystals attached to either side of the beam upright, is attached to the implant via a screw attachment (Figures 1.8 and 1.9). One crystal is excited with a swept frequency from approximately 2kHz to 20kHz by a custom designed Frequency Response Analyser (FRA). The response is measured by the opposite piezoelectric crystal and amplified within the FRA before logging the response data on a computer. A number of studies have been conducted which show that the RFA value of the implant/transducer complex is related to the height of the implant above the bone crest and the stability of the implant/tissue interface as determined by the absence of clinical mobility (Meredith et al, 1996b; 1997a and b).

In vitro work (Meredith et al, 1996a) confirmed a relationship between Resonance Frequency value and the stiffness of the implant interface and the effective length of the transducer. Repeated RFA measurements made on healing implants in rabbit

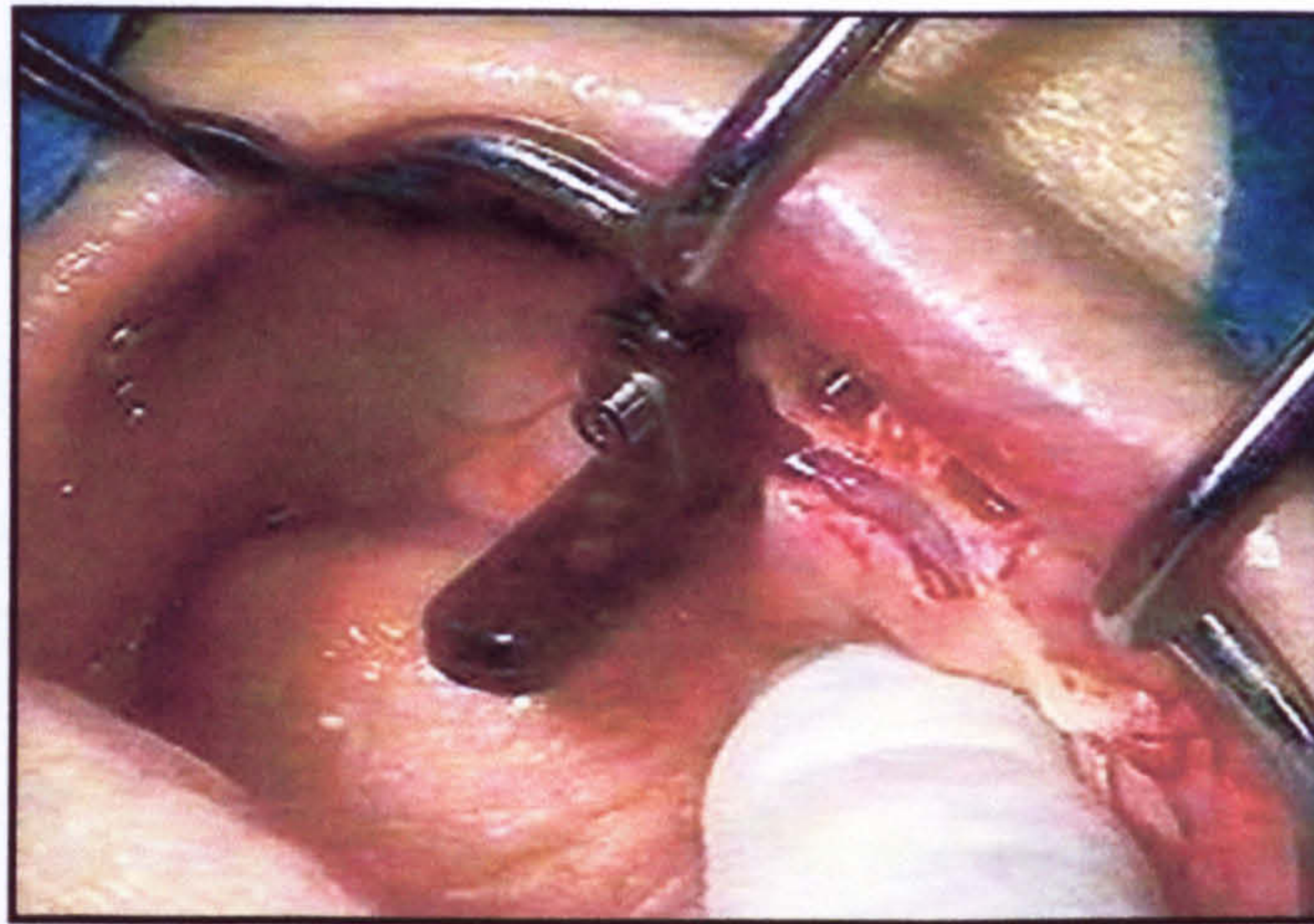


Figure 1.8: Photograph of a resonance frequency analysis transducer attached to a mandibular implant.

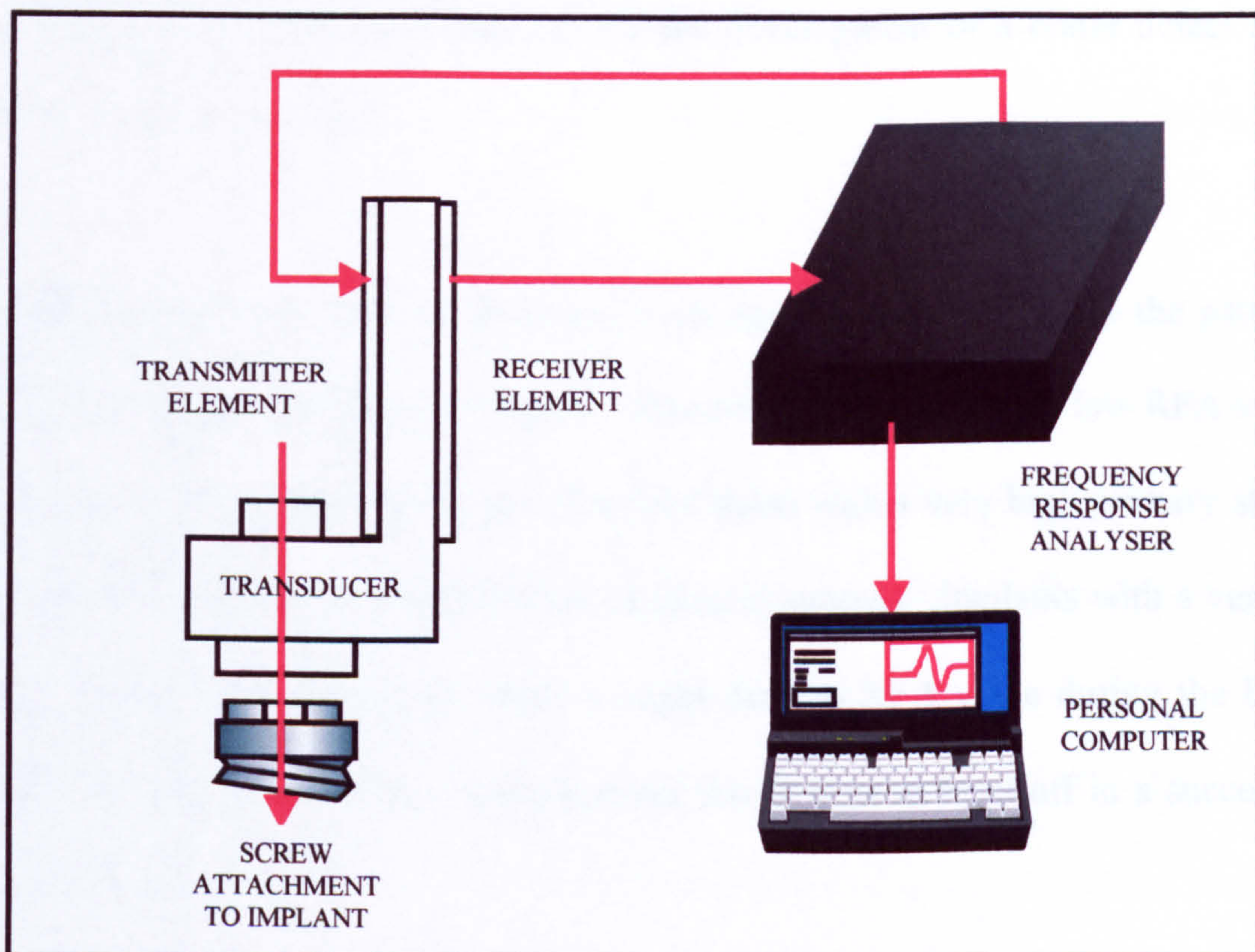


Figure 1.9: Schematic of the resonance frequency analysis system.

tibia (Meredith et al, 1997b) showed an initial rise in value, which levelled off after 43 days. Histomorphometric analysis was used to study bone formation around the implant during healing and a correlation was found between bone formation adjacent to the implant and a rise in RFA value relating to increased implant stability. A number of clinical studies and animal studies (Friberg et al, 1999; Meredith et al, 1996a and 1997b; Rasmusson et al, 1997 and 1998) have now been conducted confirming the relationship between RFA value and effective transducer length with a drop in RFA of ~200Hz for every 1mm increase in effective beam length.

Significant increases in RFA value are seen for those implants that are successfully integrating, with a drop in RFA value indicating a failure in perfixtural bone formation during healing or more rarely the development of a crater defect around the neck of the implant.

Recent unpublished work (O'Sullivan et al) appears to indicate that the pattern of change in implant stability is complex. Those implants with a very low RFA value at placement have a high chance of failure and those with a very high primary stability (high RFA value) have a high chance of clinical success. Implants with a very high RFA value at placement may show a slight drop in RFA value during the healing period as bone remodelling takes place but this is seen to level off in a successfully healing implant.

For those implants with mid range values at implant placement the clinical course of the healing period is very important. An implant with an initially low RFA value if left undisturbed with an increased healing period can show a slow increase in

stability with RFA giving a useful guide to the clinical stability of the implant. RFA may provide a clinically useful guide to the stability of an implant, helping to identify when an implant is of sufficiently high stability to be clinically loaded. Additional studies are currently being undertaken to examine whether RFA can be used to identify, which implants are of a sufficiently high primary stability to be able to be immediately loaded without compromising the long-term prognosis of the implants.

1.6 Bone Quality

1.6.1 Definitions for jaw bone quality

The term bone quality has been used for many years by clinicians but there is still no clear definition of what is meant by bone quality. Horner and Devlin (1998a and b) claimed that bone quality was related to various interrelating factors including bone mineral density, cortical thickness, trabecular density and trabecular thickness. Stulberg et al (1989) have taken a different approach by saying that bone quality relates to the ability of the bone to adapt to specific loads and the capability to remodel. The majority of reports relating to bone quality relate to the mechanical properties of the bone (Martin, 1991), the elastic modulus, stiffness, strength and strain characteristics. It has not been proved that these properties, although traditionally measured for standard engineering materials, relate to the differences in bone quality that clinicians see. Clinically bone quality is judged by the clinician by a combination of pre-operative radiographic assessments and the degree of resistance to drilling and tapping and this led to the widely used scoring system outlined by Lekholm and Zarb (1985). They proposed a scoring system from 1 to 4; in quality 1

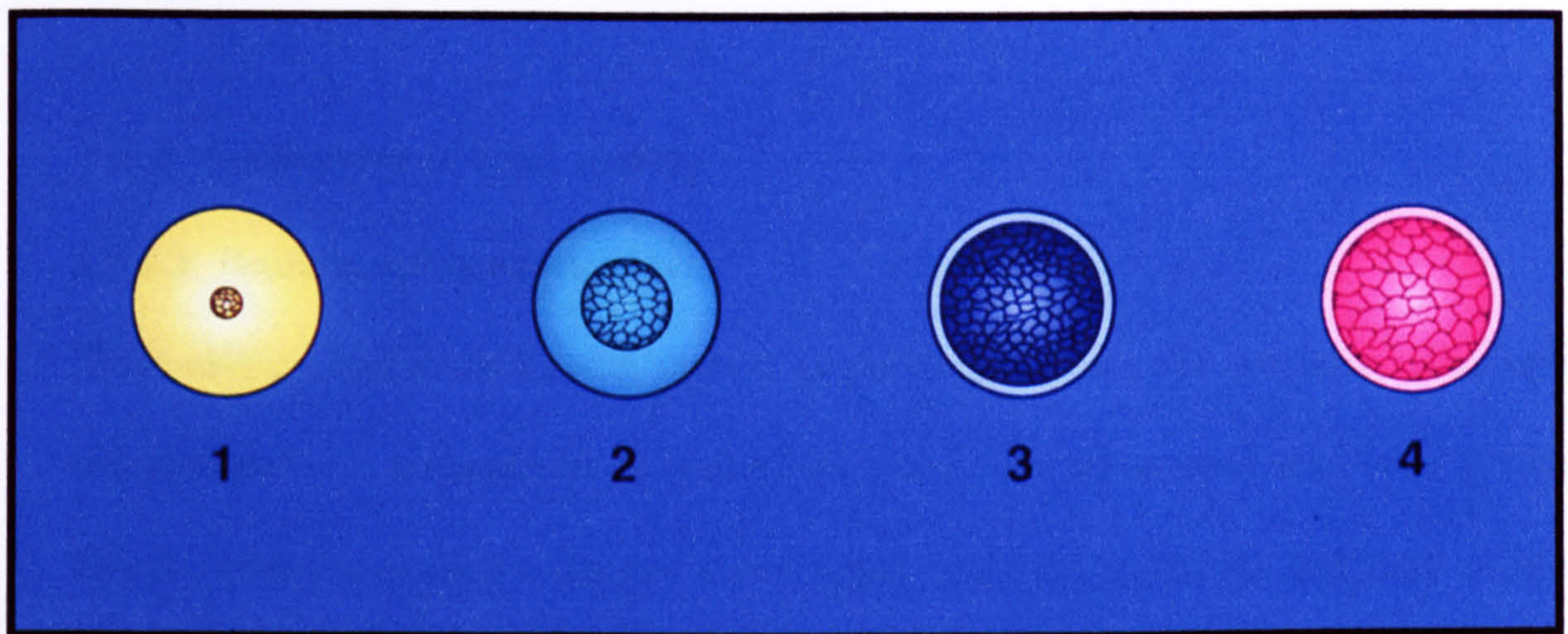


Figure 1.10: Bone quality scoring system (after Lekholm & Zarb 1985).

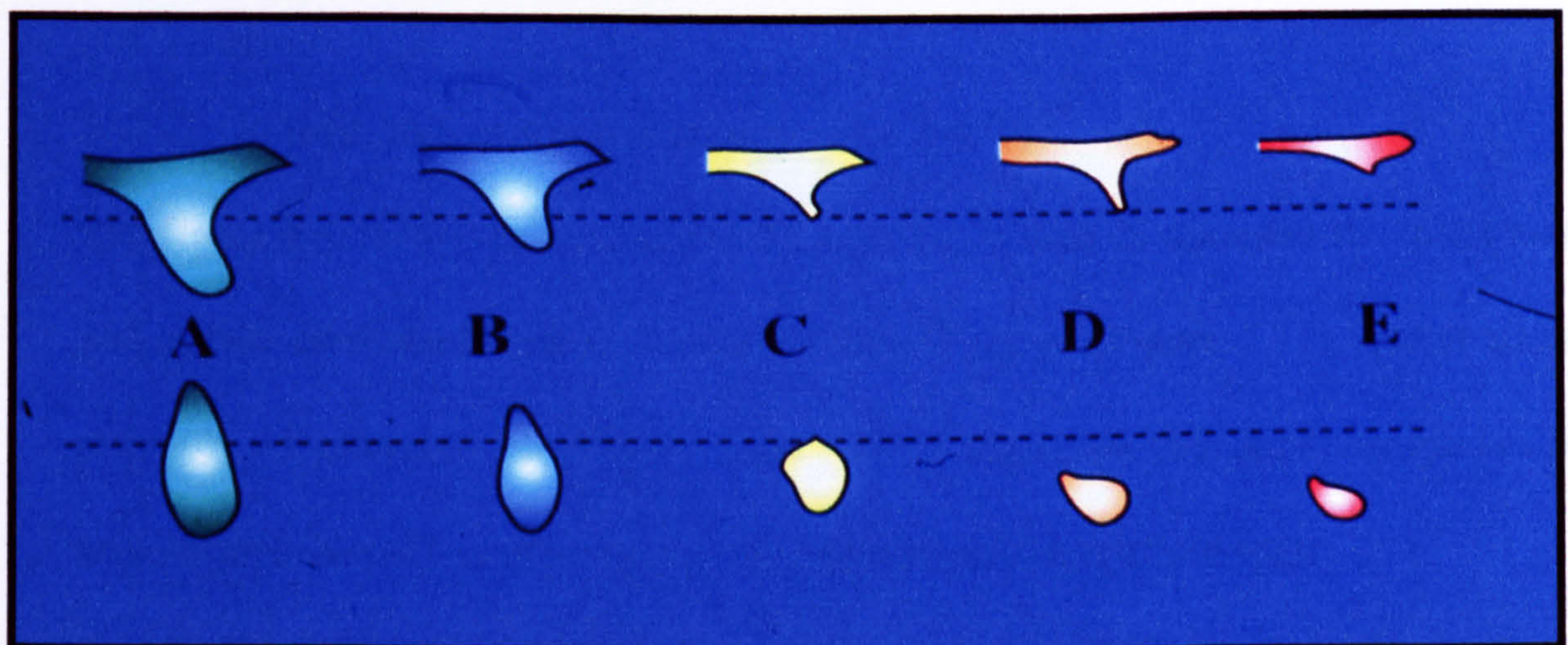


Figure 1.11: Bone quantity scoring system (after Lekholm & Zarb 1985)

compact bone predominates while in quality 4 cancellous bone predominates. The scoring system is summarised in Figures 1.10 and 1.11.

1.6.2 Assessment of bone quality

1.6.2.1 Radiographic examination

The Lekholm and Zarb scoring system as previously described partially relies upon the pre-operative radiographs as well as the perception of resistance to bone cutting. Misch (1990) proposed a density index based upon the Lekholm and Zarb scoring system giving density measurements from D1 to D4. Jensen (1989) suggested a classification of bone sites based upon radiographic examination including proximity to local structures, pathology, general disease etc. Lindh et al (1996a and b) has suggested a classification system of 3 classes based upon the trabecular appearance in periapical radiographs. None of these systems has been widely adopted with the exception of the Lekholm and Zarb system.

1.6.2.2 Quantitative computed tomography (QCT)

The Computed tomography number (CT number) is used to represent the mean x-ray attenuation associated with each pixel of the CT image (Figure 1.12). Numbers are normally expressed as Hounsfield units (HU). Measured values of attenuation are transformed into CT numbers using the international Hounsfield scale:

$$CTnumber = 1000 \frac{\mu_{material} - \mu_{water}}{\mu_{water}}$$

Where μ is the effective linear attenuation coefficient for the x-ray beam. The scale is defined so that water has a value of 0HU, air has a value of -1000 and bone

+1000. A major advantage of QCT is the ability to describe an internationally accepted value to each pixel of the image, allowing the examination of fine trabecular detail (Taguchi et al, 1991; Klemetti et al, 1993a and b; Dougherty, 1996; Lindh et al 1996a).

Duckmanton et al (1994) considered that cancellous bone with a value of +100 HU could be considered poor quality and would be expected to provide poor stability for an implant placed in the site. The use of this technique in conjunction with implant planning is still in its early stages. The radiation dose and the cost and availability of CT scanners have restricted the widespread adoption of this technique despite its obvious advantages over conventional plain radiographs.

1.6.2.3 Bone mineral density (BMD)

Von Wewern et al (1988) examined the relationship between the bone mineral content of mandibles, forearms and lumbar spine using dual energy photon absorptiometry. No relationship was found between the mandible and other sites although a correlation was seen between the bone mineral content of the forearms and lumbar spine. Klemetti et al (1993a) found that the mandibular cortical BMD was correlated with the lumbar spine and femoral neck whilst the cancellous bone was not related. It has been reported that the BMD around implants in function increases (Strid, 1985; Von Wewern et al 1990). Horner and Devlin (1998a) found a significant correlation between the Lekholm and Zarb bone quality index and the BMD of mandibular bone.

1.6.2.4 Ultrasound attenuation and velocity

A number of orthopaedic studies have looked at the use of ultrasound to examine bone quality specifically in the heel and forearm. Hans et. al (1997) found a significant correlation between ultrasound parameters and BMD. No effective work has been conducted to evaluate the usefulness of the technique in mandibular and maxillary bone.

1.6.2.5 Magnetic resonance imaging (MRI)

Hirschmann (1998) advocated the use of MRI in the pre-operative assessment of implant sites. It allows the three-dimensional analysis of the bone but without the risks associated with ionizing radiation. Although the images are certainly useful qualitatively to assist the surgeon in assessment of bone volume and morphology the assessment of mineral density and quality is not possible.

1.6.2.6 Bone biopsies

Klinge et al (1995) suggested the use of bone biopsies taken from an implant site prior to implant placement. The biopsies are then subjected to histomorphometric analysis the bone quality is assessed in terms of bone area and this information can be used to suggest an individualized healing period for each implant. They found that the bone quality score varied between implant sites necessitating a bone biopsy at each implant site. This technique has a lot to commend it as it allows the direct observation of the bone from the implant site. The need for a biopsy at each implant site, however, makes it expensive and impractical in clinical practice.

1.6.2.7 Insertion Torque – true cutting resistance

For screw form implants a common part of the procedure is the cutting of a thread in the bone either by the use of a tap or by the use of a self-tapping implant. It has been proposed by a number of authors that by measuring the torque necessary to cut a thread in the bone information may be derived regarding the bone quality and primary implant stability.

Johansson and Strid (1994) described a mathematical model from which the energy used to cut a threaded bone channel can be derived. Torque was determined by the current drawn by an electric motor whilst cutting. The authors claimed that the total insertion torque comprised a frictional component, a cutting component and a component related to shiver packing. A formula was derived that removed elements in the total torque data to leave the true cutting resistance. Bone quality was expressed as the energy to cut and remove a volume of bone and for tests conducted on bovine cortical bone a value of 0.3 J/mm^3 was reported. The authors reported a correlation between the cutting resistance and radiographic measurements of aluminium referred bone density.

Friberg in 1994 and Friberg et al in 1995 used the Johansson and Strid model to measure the cutting resistance of 31 jaw bone specimens. They found measurements to be higher for the mandible than the maxilla with the greater values tending to be found towards the incisor region. Further work by Friberg et al (1995) found that cutting resistance values were not significantly influenced by the pressure applied by the operator and the angulation of the handpiece.

1.7 Bone Quantity

1.7.1 Assessment techniques for jaw bone quantity

Bone quantity or more precisely the anatomical morphology of the bone at a potential implant site, has been difficult to assess. Plain radiographic films and bone mapping (Figures 1.13 and 1.14) have been used until the last 5-10 years to assess the quantity and distribution of bone at implant sites. The problem with plain radiographs is that they represent a two dimensional image of a complex three-dimensional structure. Bone-mapping helps to identify the contour of the oral bone surface but gives the surgeon no indication about the depth of bone at the implant site and the morphology of the bone surfaces away from the oral cavity (e.g. nasal floor, inferior margins of the maxillary sinus etc.). With the advent of CT scanning technology as previously outlined in section 1.6.2.2, the surgeon is now able to visualize the bone quantity available at the implant site with much greater accuracy and in three-dimensions.

1.8 Surgical technique

1.8.1 Surgical technique and implant success

The surgical technique involves a number of variables that may affect the successful integration of an implant. The cleanliness of the surgical field, the experience of the surgeon, the incision design used and the drilling technique have all been implicated in affecting implant prognosis.

Implant surgery is traditionally carried out under sterile conditions (Adell et al, 1985; Friberg, 1996). Kraut (1996) suggested that sterile conditions might not be necessary after observing low failure rates when clean operating room conditions were used.

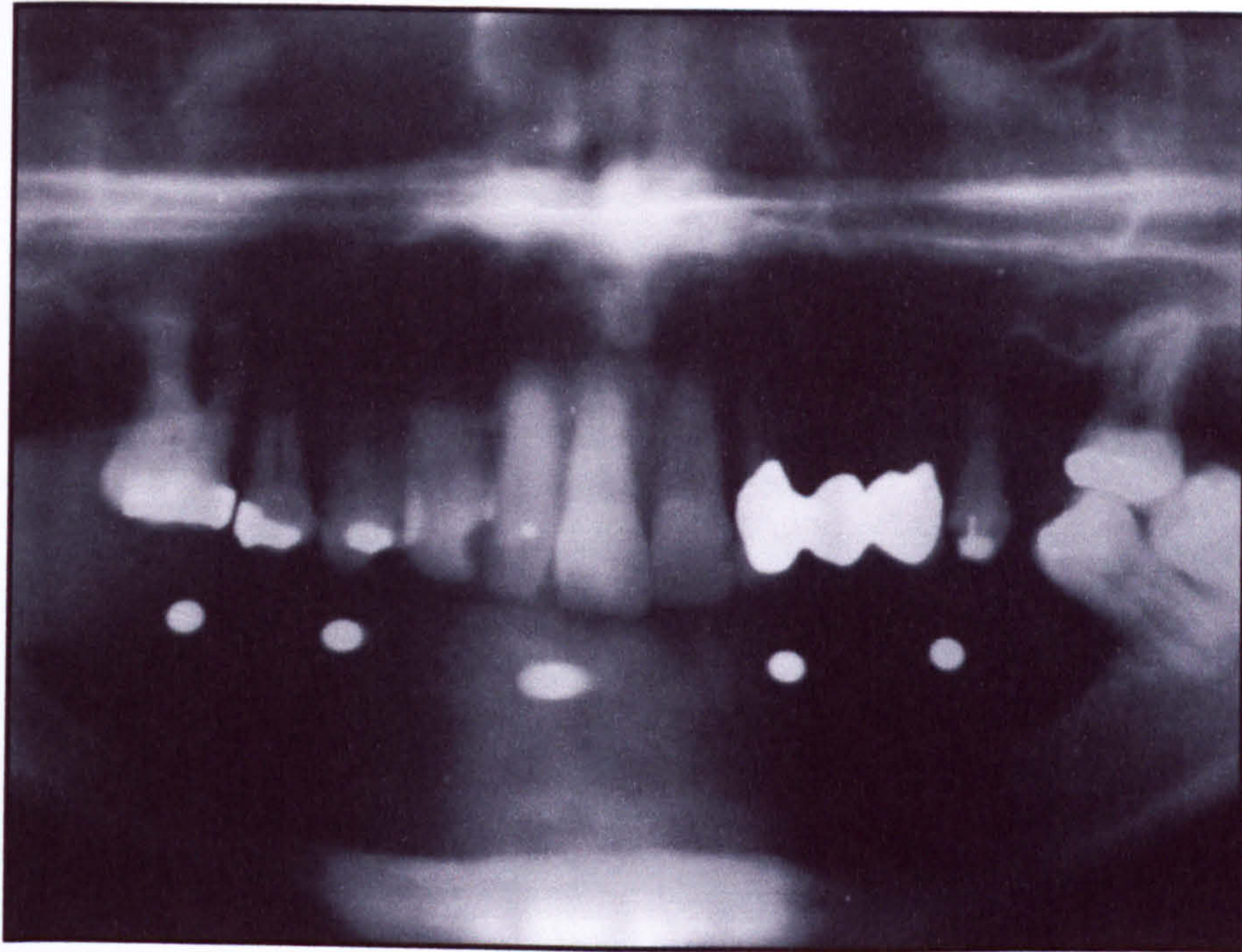


Figure 1.13: DPT radiographic view used for bone quantity assessment.

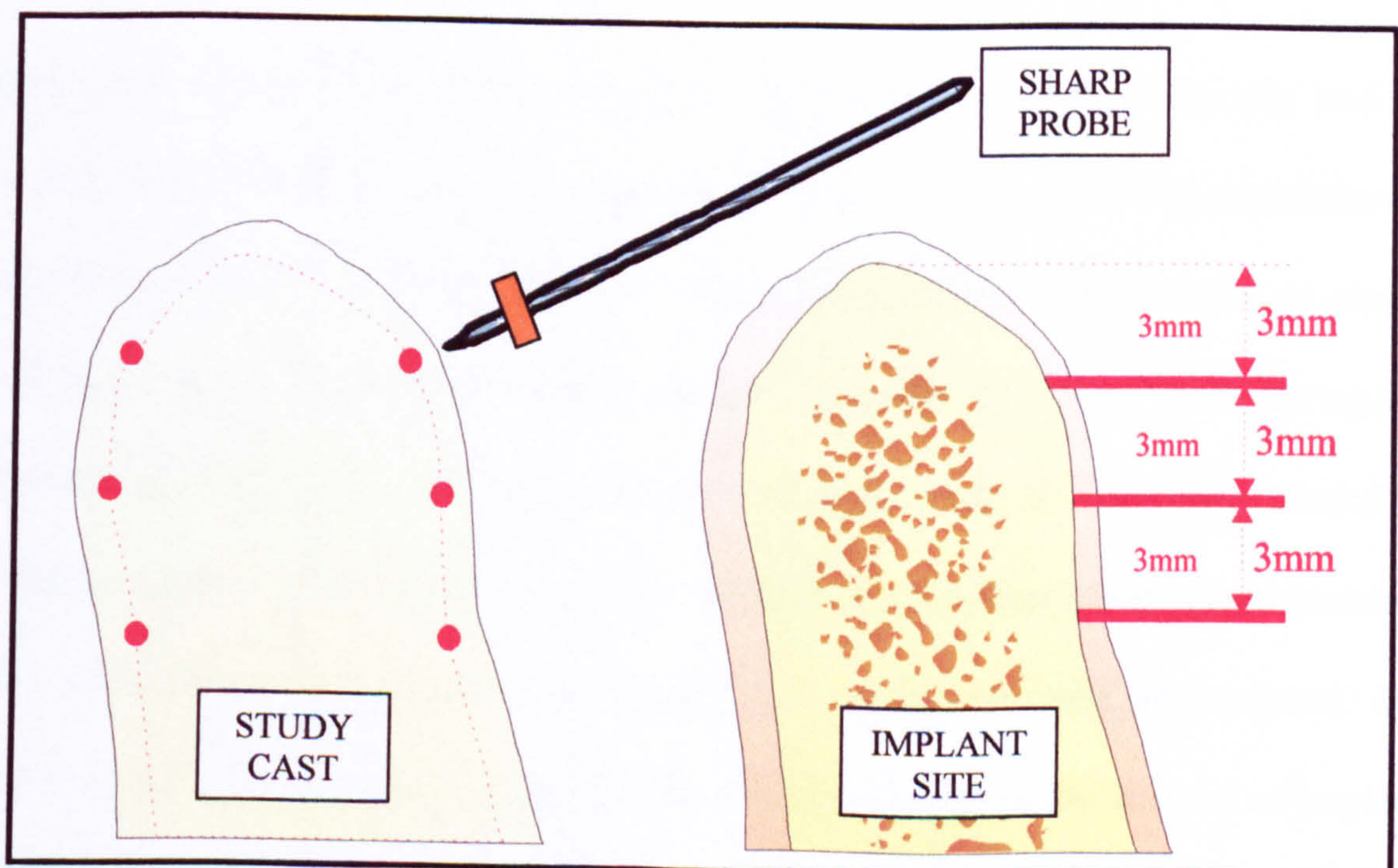


Figure 1.14: Schematic of bone mapping.

Friberg (1996), however, advocated a sterile procedure because of the lack of long term studies into the use of a clean procedure.

The experience of the surgeon appears to be of importance. Lambert et al (1997) reported that implants placed by inexperienced surgeons (<50 implants), failed twice as often as implants placed by experienced surgeons (>50 implants). Incision techniques commonly divide into crestal and buccally approaching flap designs. The original Brånemark technique advocated a mucobuccal incision in order that the incision line is kept away from the implant site. However, this has been investigated by Scharf and Tarnow (1993) and Casino et al (1997), and no difference in implant success rates could be identified.

Inadequate cooling of the drills during preparation of the implant site can lead to overheating of the bone and excessive tissue damage. Lundskog (1972) and Eriksson (1984) have investigated the threshold temperatures for osteocyte necrosis to occur, and found it to be 50°C for 30 seconds and 47°C respectively. The friction during the insertion of the implant itself will generate heat and cannot be adequately cooled as irrigants cannot reach the implant bone surfaces due to their close approximation. The importance of preparing an implant site congruent with the implant has previously been discussed, and may be an important factor in the success of implant treatment.

1.9 Bone healing

1.9.1 Bone response to surgery

Bone surgery causes damage to the bone. Initially a haematoma forms (Frost, 1989a and b) and this forms a zone around the implant composed of bone fragments and blood cells. Within a few days of surgery mesenchymal cells and macrophages from the bone marrow invade the haematoma and a layer of osteoblasts will form at the endosteal surface of the cortex (Sennerby et al, 1993; Masuda et al, 1997). After approximately 7 days, woven bone will develop from the osteoblast layer approaching the implant surface forming strands of bone tissue. Four to six weeks later the woven bone is replaced by lamellar bone (Roberts et al, 1984; Sennerby et al 1993; Masuda et al, 1997). The maturation of the bone into a lamellar form probably takes 4 to 12 months extrapolating from the 6 to 18 weeks seen in the rabbit (Roberts et al, 1984).

1.9.2 Bone response to thermal injury

A poor-drilling technique can lead to heating of the cut bone surface. Lundskog (1972) found that osteocytes were irreversibly damaged at 50°C when exposed for 30 seconds while Eriksson (1984) found 47°C to be the threshold for a similar time interval. In general a low speed (2000 rpm) and profuse saline irrigation have been suggested by Eriksson (1984) and Adell et al (1985), as means of reducing thermal damage to the bone. Some debate still exists regarding the relationship of drill speed, force application and heat generation. Abouzgia et. al. (1996) and Iyer et al (1997) found an inverse relationship between drill speed and heat generation. In general, every effort must be made clinically to minimise heat generation and energy dissipation to bone during implant insertion.

1.9.3 Bone response to mechanical stress and strain

Bone is a vital, living tissue that responds to loading by apposition and resorption. Bone modelling in response to mechanical stress is a complex process that is not fully understood. Bassett and Becker (1962) investigated the theory that bone modelling is mediated by the development of electric potentials at areas of tension and compression. They stated that the amplitude of the electric potentials generated in stressed bone is dependent upon the rate and magnitude of the bony deformation, with areas under compression developing negative potentials and those areas under tension developing positive potentials in relation to adjacent areas. The authors stated that the hydroxyapatite component in bone behaves in a piezoelectric manner similar to quartz, but that in bone the potentials decayed more slowly than in quartz.

High compressive stresses have been associated with bone resorption. An example can be seen at the compressive surface of a tooth during orthodontic tooth movement. This concept led to the analysis of implants along similar lines (Hassler et al, 1977; Farah et al, 1979; Clift et al, 1992; Sandy et al, 1993). Rieger et al (1990) stated that the optimal bone maintenance takes place with stress magnitudes around 250 psi (1.7243 N/mm²), whereas at magnitudes greater than 700 psi (4.8279 N/mm²) pathological bone resorption takes place. Continuous levels less than 200 psi (1.279 N/mm²) lead to physiological atrophy, seen clinically as the atrophy following tooth loss.

In 1992, Brunski stated that interfacial stresses and strains from loading of an implant could endanger the implant surrounding tissues, resulting in increased bone

resorption and/or implant loss. Since load divided by supporting area was considered to be an estimate of the interfacial stress magnitude, the amount of bone present as well as its mechanical properties were said to influence the success/failure of individual implants. Quirynen et al (1992) found that excessive marginal bone loss (>1mm) around implants was due to parafunctional activity, lack of anterior contacts and implant supported prostheses in both jaws, all of which suggest the presence of overload occurring for the affected implants. Hoshaw et al (1994) conducted a controlled loading study in dogs and concluded that bone resorption was overload related and a consequence of bone modelling and remodelling secondary to microfracture and damage in the interfacial bone.

Frost 1987 proposed the Mechanostat hypothesis to attempt to describe the process of mechanically induced bone adaptation. The general Mechanostat hypothesis is primarily based upon the idea that mechanically induced bone strains have an important role in governing threshold-related activation and control of bone modelling and remodelling processes. Other investigators (Carter, 1982; Rubin and Lanyon, 1987; Turner, 1991, 1998) have also suggested rules of bone adaptation that generally consider that bone homeostasis is maintained over some range of routine daily stress/strain stimuli, whilst departures above or below certain stimulus thresholds initiate formation or resorption of bone.

1.9.4 Measurement of Bone Strain

The measurement of bone strain is difficult. In general the literature relates to distinct areas of research (Little and Finlay, 1992):

- product development;
- evaluation of material properties (e.g. modulus, Poisson's ratio);
- the determination of forces and couples in vivo;
- the determination of skeletal behaviour in vivo.

A number of techniques have been used. Transmission and reflection photoelasticity, brittle coatings, thermographic stress analysis, strain gauges and finite element analysis have all been used to estimate bone strain and stress.

Transmission photoelasticity has been used widely in the field of biomechanics (Heywood, 1969; Kuske et al, 1977). Very little three dimensional work has been published and this probably relates to the difficulty in matching the moduli of the in vitro material and the bone (Hossdorf 1974). Coatings may be applied to the surface of the bone to allow reflection photoelasticity to be used for qualitative evaluation of bone strain (Blum, 1977). Quantitative work is difficult as the application of the coating can itself alter the properties of bone in thin sections and no corrective method is available for situations of anisotropy and complex geometry.

Brittle coatings have been used for many years in engineering. A brittle lacquer when sprayed onto a test material and dried will display a series of cracks when subjected to a tensile load. The technique cannot readily be applied to bone as the lacquer is affected by changes in humidity and must be applied to a dry, clean surface.

If a homogeneous, isotropic material is cyclically loaded, the thermoelastic effect produces changes in temperature. These changes in temperature are directly proportional to the sum of the principal stresses in the material under test. The technique is called Stress Pattern Analysis by Thermal Emission (SPATE). The technique requires a reference calibration to be conducted using a strain gauge or photoelastic coating on the material under test to determine the thermoelastic constant (K_m). The calibration is often difficult to do as it requires the test material to be cyclically tested to provide repeatable results (Little and Finlay, 1992). The system has been used to determine the variations in the stress distribution of different types of hip prosthesis mounted in bone (Duncan et al, 1985; 1989). They concluded that fresh bone gave a stress related thermal emission that was detectable by SPATE and had a stress distribution comparable to that obtained by conventional methods.

Of all the techniques described, electrical resistance strain gauges are the most commonly used. They have been used to identify strain changes in implant abutments and superstructures (Wang and Hobkirk, 1996; Brosh et al, 1998; Seong et al, 2000) and to measure the distortion of the mandible during function (Tashkandi et al, 1996; Hobkirk et al, 1998; Abdel-Latif et al, 2000). They have been used widely in orthopaedic studies to measure bone strains both in vitro and in vivo (Carter et al, 1980; Lanyon, 1976; Hongo et al, 1999). Although their application is difficult, methods have been described to allow their use on bone surfaces (Pople, 1979) and suggestions for the reduction in instabilities in the data recording are well documented.

Finite element analysis (FEA) has been used to develop models of bone in function and to model the interaction of bone and endosseous implants (Murphy et al, 1995; Holmgren et al, 1998; Teixeira et al, 1998; Volmer et al, 2000). It is possible to develop both two and three dimensional models and to change material properties and loading conditions to identify regions of high stress. Although the nature of FEA makes it easy to produce numerical values for the stress and strain in the bone adjacent to an implant these must be treated with caution as absolute values for the mechanical properties of a biomechanical system as complex as the bone/implant interface are still to be defined.

1.10 Implant design

1.10.1 Bone stress in relation to implant design

Photoelastic stress analysis and finite element stress analysis have been used by a number of workers to compare the potential of different implant design features to generate stresses in the peri-implant bone. Although these techniques have limitations due to their relatively low cost they have become popular in attempting to tackle the difficult issue of implant design. Privitzer et al (1975) using finite element analysis, compared a blade implant, a conically shaped implant and a cylindrical implant. They found that the most irregular stresses were recorded for the blade implant. Atmaran et al (1979) modelled implants with three differing geometries: conical, cylindrical and one resembling the root shape of a first molar tooth. The implants were modelled with the physical properties of five materials (dentine, vitallium, titanium, vitreous carbon and polymethyl methacrylate), the supporting bone was homogenous. Finite element analysis was used to study longitudinal, lateral principle and shear stresses in two-dimensional models. High stress regions

were found to lie at the implant-bone interface for all implant designs. Longitudinal compressive stresses both in the implants and in the bone were lowest for the cylindrical implants. Rigid implants with conical geometry produced high stresses around the apex of the implant with similarly large stresses being generated at the bone surface with a cylindrical design. The authors favoured a cylindrical implant with a rigid fixation to bone. Atmaran and Mohammed (1981) also reported in a similar study that a cylindrical basic geometry gave a more favourable stress distribution in the peri-implant bone.

Haraldson (1980) found in a photoelastic stress analysis study that threaded implants displayed a more favourable stress distribution in the bone when compared to unthreaded. Hobkirk (1983) demonstrated that implants with sharp corners elicited a fibrous tissue reaction and produced evidence that the implant shape in the cervical region could influence the pattern of bone behaviour. Morris and Ochi (1992) proposed a controlled multicentre clinical study to examine the influence of implant design on clinical performance and crestal bone response. The study would test the success of the differing designs of implant over a 5-year period and could be used to monitor any adverse consequences of differing implant design.

1.10.2 Biomechanics of implant design

Ivanoff (1999) suggested that the design of an implant should fulfill the following criteria:

- easy to handle;
- provide primary stability;
- give adequate distribution of load to the bone;
- easy to retrieve.

Grenoble (1974) outlined some criteria for dental implant materials which are summarized in Table 1.1. He noted that a number of dental implant design criteria relate to biological and dental considerations. Constraints such as the size and shape of endosteal implants are dictated by the anatomy of the jaws, the need to attach a restoration to the implant and the requirement that normal oral function is not impaired or impeded by the presence of the implant. Implants need to be able to tolerate the occlusal loads in the oral cavity without fracture or distortion of the component parts. Screw or cylinder implants approximating the length and diameter of tooth roots are the most common implant design in current use. Brånemark et al (1969), Lundskog (1972), and Carlsson et. al. (1986) reported that screw form implants to be superior to cylinders in terms of their primary stability. In relation to secondary stability, long-term studies have shown high survival rates and minimal marginal bone resorption for screw form implants (Adell et al, 1981 and 1990; Lekholm et al, 1994; Henry et al, 1996). Albrektsson (1993) suggested that cylinder form implants have shown signs of progressive marginal bone loss.

Biological criteria		Biomaterial criteria		Biomechanical criteria	
Medical contraindications		Corrosion resistance in oral and physiological fluids		Transmission of minimal stress to tissues	
Infection, hygiene		Carcinogenic potential		Implant retention	
Rate of alveolar ridge resorption adjacent to implant		Changes in physical properties over time		Effects of implant shape and material properties on local bone stress within bone	
Formation of gingival cuff around abutment		Tissue biocompatibility		Duration of effective function	
Surgical technique		Physical properties		Implant immobility	
Restoration design		Systemic toxicity		Bioelectric interactions	
Anatomical constraints		Formability, cost			

Table 1.1: Design criteria for dental implants (After Grenoble, 1974).

1.10.3 Rationale for implant design changes

Grenoble (1974) indicated that the evolution of dental implants was based on intuition, stating that: “Historically, dental implants have been designed and evaluated on a trial and error basis with clinical and scientific research being concentrated on development of improved biomaterials, attachments of tissues to synthetic materials, prevention of infection, surgical and restorative technique and patient selection criteria. Although countless numbers of implant designs have been conceived and many have been clinically tested, few have proven to be effective. Little documentation is available relating these clinical experiences to the design features of the various implants studied.” Most implant designs are based upon rationalization and theoretical projection rather than upon testing and evaluation based upon experimental evidence. Brunski (1988) stressed the importance of validation the design rationale with suitable design evaluation and research techniques.

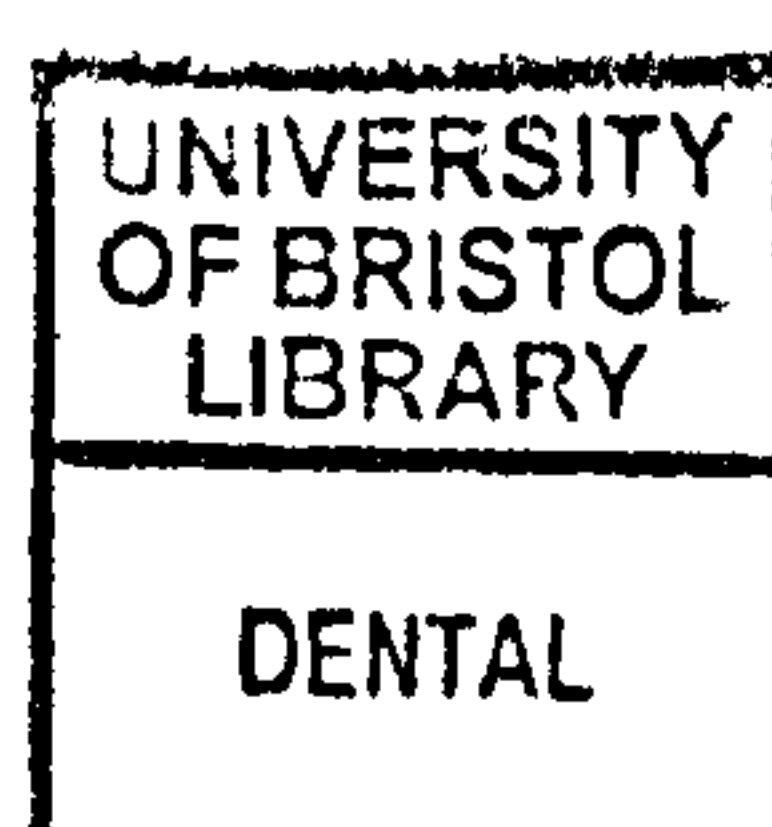
In the case of Nobelbiocare implants (Nobelbiocare AB, Gothenburg, Sweden), implant design changes away from the standard Brånemark design have been made for several reasons including:

- improved clinical handling;
- simplification of surgical technique;
- improved primary implant stability;
- enhanced osseointegration;
- improved load distribution to the bone;
- improved aesthetics of the final restorations.

Little evidence is available in the literature to identify whether these changes have significantly affected the primary stability characteristics of the implants involved.

CHAPTER 2

IN VIVO DATA RELATING TO THE PRIMARY AND SECONDARY STABILITY OF DENTAL IMPLANTS



IN VIVO DATA RELATING TO THE PRIMARY AND SECONDARY STABILITY OF DENTAL IMPLANTS

2.1 Aims and objectives

The aim of this investigation was to quantify the parameters associated with implant insertion and primary stability between two differing designs of implant in a range of bone qualities. To identify any relationship between these parameters and the change in stability of each implant during the initial six-month healing period following implant insertion. Comparison was made between standard Brånemark implants and Mark IV implants.

Standard Brånemark implants are not designed to be self-tapping and have no effective cutting facets. In order to enhance the stability of these implants at initial surgery many surgeons place these implants without the prior use of a surgical tap to prepare a threaded channel in the bone. The implant is, therefore, placed in slight compression within the bone. In theory, this compression enhances implant primary stability by developing circumferential or hoop stresses within the bone at the bone/implant interface zone. This method of enhancing the primary implant stability is purely based on intuitive reasoning and the exact effect of this technique has not been quantified.

The Mark IV implant was designed to create differential stresses within the bone at the implant site. The aim of the design was to induce circumferential stresses of greater magnitude in the cortical bone when compared to the trabecular bone in an attempt to enhance the implant primary stability in a similar manner to the technique

described above for standard implants. The implant design was developed with the aim of inducing the greatest stresses within the denser cortical bone layer, this was achieved by giving the Mark IV implant a slightly tapered profile. The Mark IV was also given a double start thread which reduces insertion time. The manufacturers claim that the taper induces compression within the cortical bone, whilst the double thread reduces the thermal energy generated at the bone implant interface due to the reduced insertion time. The reduced thermal energy transmitted to the bone has the aim of minimising osteogenic bone cell damage due to heat generation.

The aim of this study was to investigate these claims and to identify which of the two techniques was the most suitable method of enhancing clinical implant primary stability.

2.2 Method

2.2.1 Patient selection and implant placement

Data from 13 patients were used in this investigation, relating to 42 implants placed. The distribution of implant placement is shown in Table 2.1. The same operator placed all of the implants according to clinical need. Standard surgical techniques were used to prepare the surgical sites as illustrated in Figure 2.1. Full thickness mucoperiosteal flaps were raised under local anaesthesia (Xylocaine with 1:80 000 Adrenaline, AstraZeneca Pharmaceuticals, Kings Langley, Hertfordshire, UK). A 2mm round headed guide drill was first used to locate the implant position on cortical bone surface. A 2mm diameter twist drill was used, under profuse isotonic saline irrigation, to prepare the initial full depth channel at the

Implant N°:	Patient N°:	Tooth Position	Implant diameter	Implant Length	Implant Type
1	1	UL5	3.75	13	Mark IV
2	1	UL6	3.75	13	Mark IV
3	1	UL7	3.75	13	Mark IV
4	1	UR1	3.75	15	Standard
5	1	UR3	3.75	15	Standard
6	1	UR6	3.75	15	Standard
7	1	UR7	3.75	15	Standard
8	2	UL1	3.75	15	Mark IV
9	2	UL4	3.75	13	Mark IV
10	2	UL5	3.75	13	Mark IV
11	2	UL6	3.75	7	Standard
12	2	UL7	3.75	7	Standard
13	2	UR1	3.75	13	Standard
14	2	UR4	3.75	13	Standard
15	3	UL1	3.75	10	Standard
16	3	UR1	3.75	10	Standard
17	4	UL1	3.75	15	Standard
18	4	UL4	3.75	13	Standard
19	4	UR1	3.75	13	Standard
20	4	UR4	3.75	13	Standard
21	5	UL4	3.75	13	Mark IV
22	5	UL5	3.75	13	Standard
23	6	UL5	3.75	13	Mark IV
24	6	UL7	3.75	13	Mark IV
25	6	UR7	3.75	13	Standard
26	7	LL1	3.75	13	Standard
27	7	LL3	3.75	13	Standard
28	8	LL3	3.75	15	Mark IV
29	8	LR3	3.75	15	Standard
30	9	UR3	3.75	13	Standard
31	9	UL3	3.75	15	Standard
32	9	UL5	3.75	13	Standard
33	9	UR5	3.75	13	Standard
34	10	UL1	3.75	13	Standard
35	10	UL2	3.75	13	Mark IV
36	11	UL1	3.75	13	Standard
37	11	UL3	3.75	13	Standard
38	11	UR1	3.75	13	Standard
39	11	UR3	3.75	13	Standard
40	12	UR1	3.75	13	Standard
41	12	UR2	3.75	13	Standard
42	13	UL1	3.75	13	Mark IV

Table 2.1: Implant Distribution Table

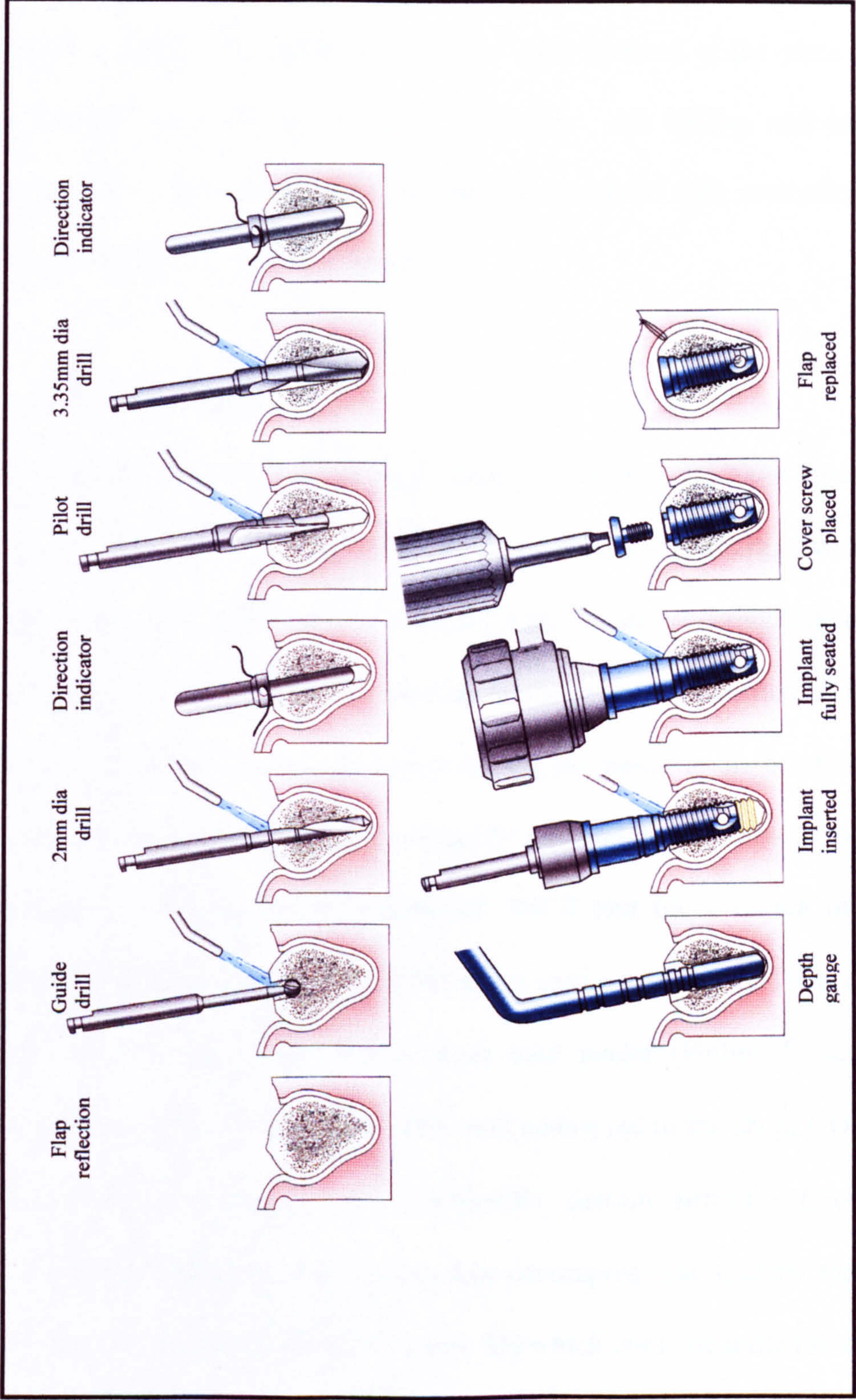


Figure 2.1: Surgical protocol for Nobel Biocare implants
(adapted from the Surgical Instruction manual – © Nobelbiocare AB, Gothenburg, Sweden).

implant site. A pilot drill was then used to enlarge the diameter of the most coronal portion of the channel; finally the channel was enlarged to 3.15mm in diameter using a twist drill. Profuse irrigation with sterile isotonic saline was used at each drilling stage. Standard and Mark IV implants were inserted at the same slow rotational speed under profuse sterile saline irrigation. All drilling and implant insertion procedures were carried out using the Osseocare™ drill controller (Nobelbiocare AB, Gothenburg, Sweden) Figure 2.2.

2.2.2 Data collection

At implant placement data were recorded onto a D32000 smart card by the Osseocare™ drill controller (NobelBiocare AB, Gothenburg, Sweden). Insertion torque was derived from the current taken by the motor during implant insertion and recorded in Ncm at every 90° rotation of the implant. Rotation of the implant was derived from the commutator pulses driving the motor in the handpiece. Processing is performed internally in the Osseocare™ unit and the insertion torque and degree of rotation are recorded as a compressed ASCII text file for each implant. Once a reading had been taken, the D32000 smart card was removed from the Osseocare™ unit and inserted into a PE122 smart card reader (Philips Electronics UK Ltd, Croydon, Surrey, UK), which in turn was connected to the serial COM port of a PC. Two pieces of Windows 95 compatible custom software (Nobelbiocare AB, Gothenburg, Sweden) were used to first decompress and transfer the data to the PC and then to convert the data into a text file which could be pulled into a conventional spreadsheet programme (Microsoft Excel, Microsoft Corporation, Redmond, WA, USA). The data recorded by the Osseocare™ unit contained the serial number of the unit which created the data, the date the files were

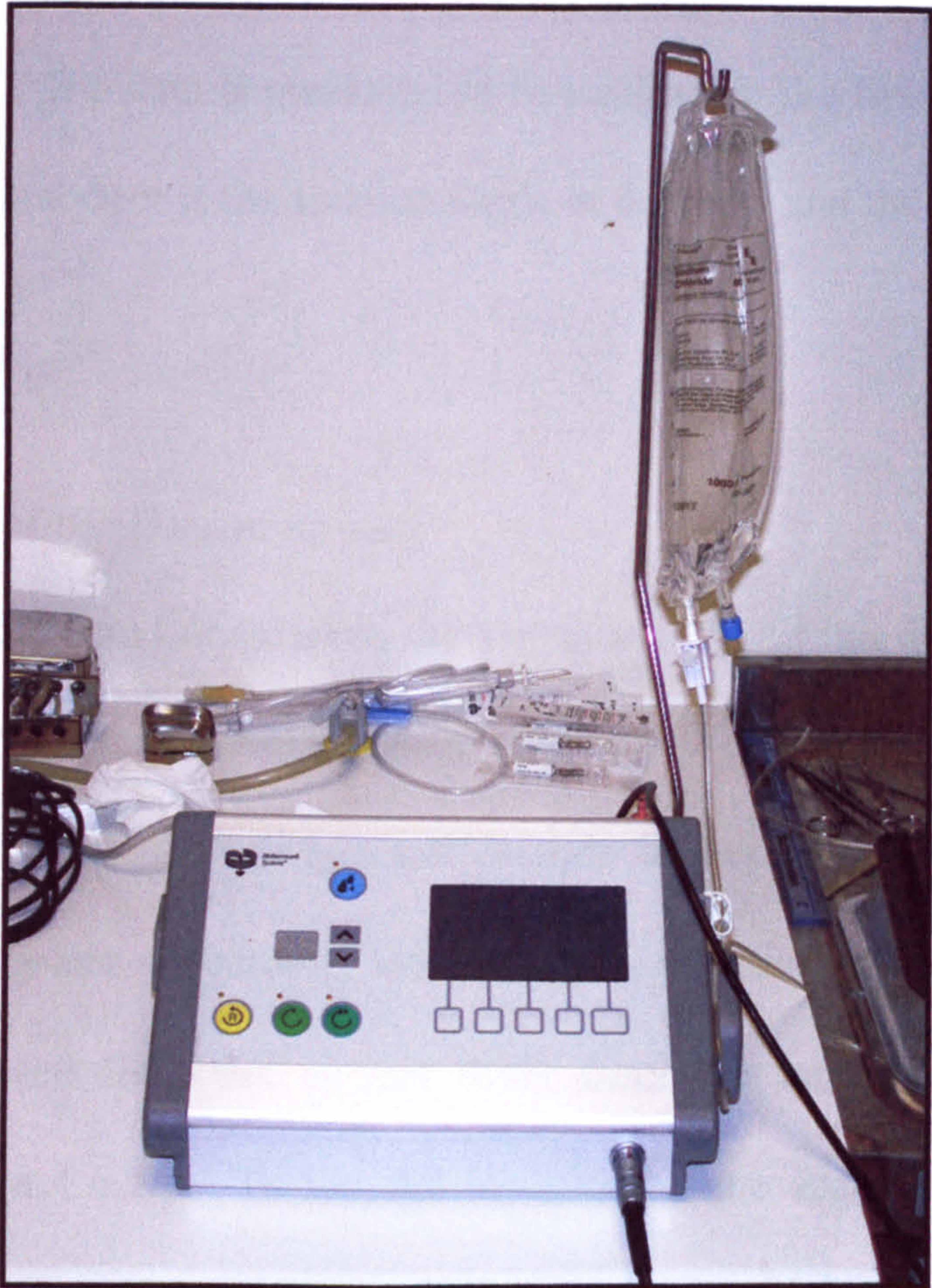


Figure 2.2: Osseocare unit.

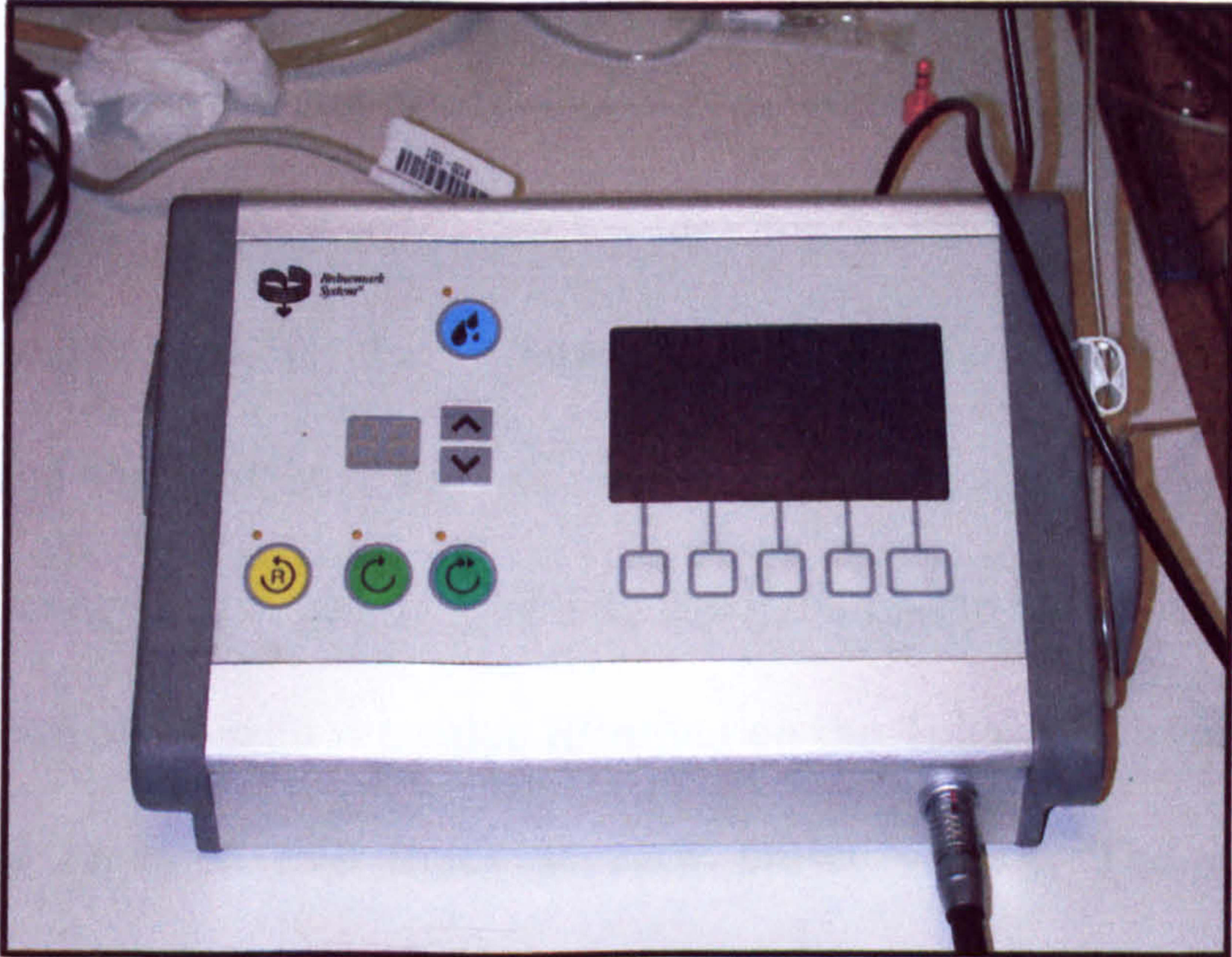


Figure 2.3: Close view of Osseocare unit control panel.

transferred to the PC, the mode of measurement (surgery or prosthetic) and the measurement data. The data is presented in two columns; the first is the number of turns (in prosthetic mode it is the rotation angle in degrees) and the second column is the torque in Ncm.

2.2.3 Calibration of the Osseocare unit

At the time this study was undertaken the Osseocare™ unit had been on the world market for only 4 months and although the manufacturers claimed that the unit was factory calibrated to calculate torque and rotation it was felt necessary to test the Osseocare™ unit against a laboratory standard. The insertion torque information for the unit is calculated from the current drain from the motor, this technique is discussed in section 1.6.2.7. To test the insertion torque accuracy of the unit the handpiece was connected to a surgical tap placed into the grips of a NAMAS certified new Tohnichi Torque gauge (Tohnichi MFG, Tokyo, Japan) (Figures 2.4 and 2.5). The Osseocare™ unit allows the operator to select preset maximum insertion torque values. When the footpedal is activated the handpiece shaft rotates at the selected speed (high or low) until the maximum insertion torque is reached, at which point the unit cuts out. For calibration, each maximum insertion torque value was selected and the footpedal activated until the preset value was reached and the cut out mechanism was triggered. The data collected on the Osseocare™ smart card and was then compared with the value recorded on the Tohnichi torque gauge. This procedure was repeated five times at each preset value. The results of the Osseocare™ torque calibration are summarized in Table 2.2 and Figure 2.6.



Figure 2.4: Tohnichi torque gauge.

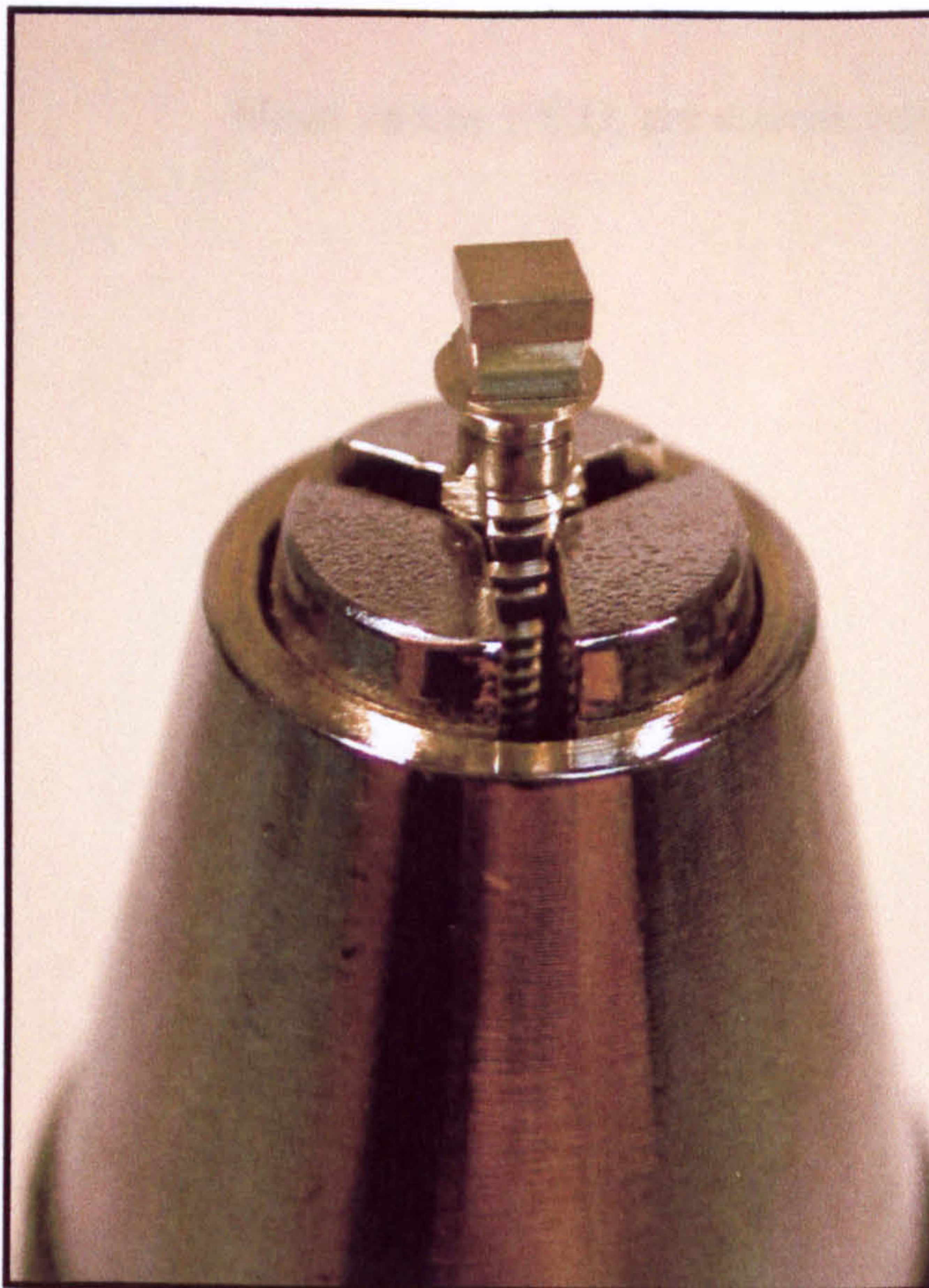


Figure 2.5: Tohnichi gauge with surgical tap in place.

Osseocare Torque setting (Ncm)	Measured mean value from Torque gauge (Ncm)
10	13.4 ± 0.6
20	17.1 ± 0.7
32	24.7 ± 0.6
45	30.5 ± 1.6

Table 2.2: Torque calibration results.

Mean values ± S.D. are shown. (n=20)

The manufacturers of the Osseocare™ joint claim that their training on the rotation of the wrist and of the handplate is derived from veterinary literature and that the device. The latest national audit was completed December 2012. The aim of this study was to determine the accuracy in calibration of the Osseocare™

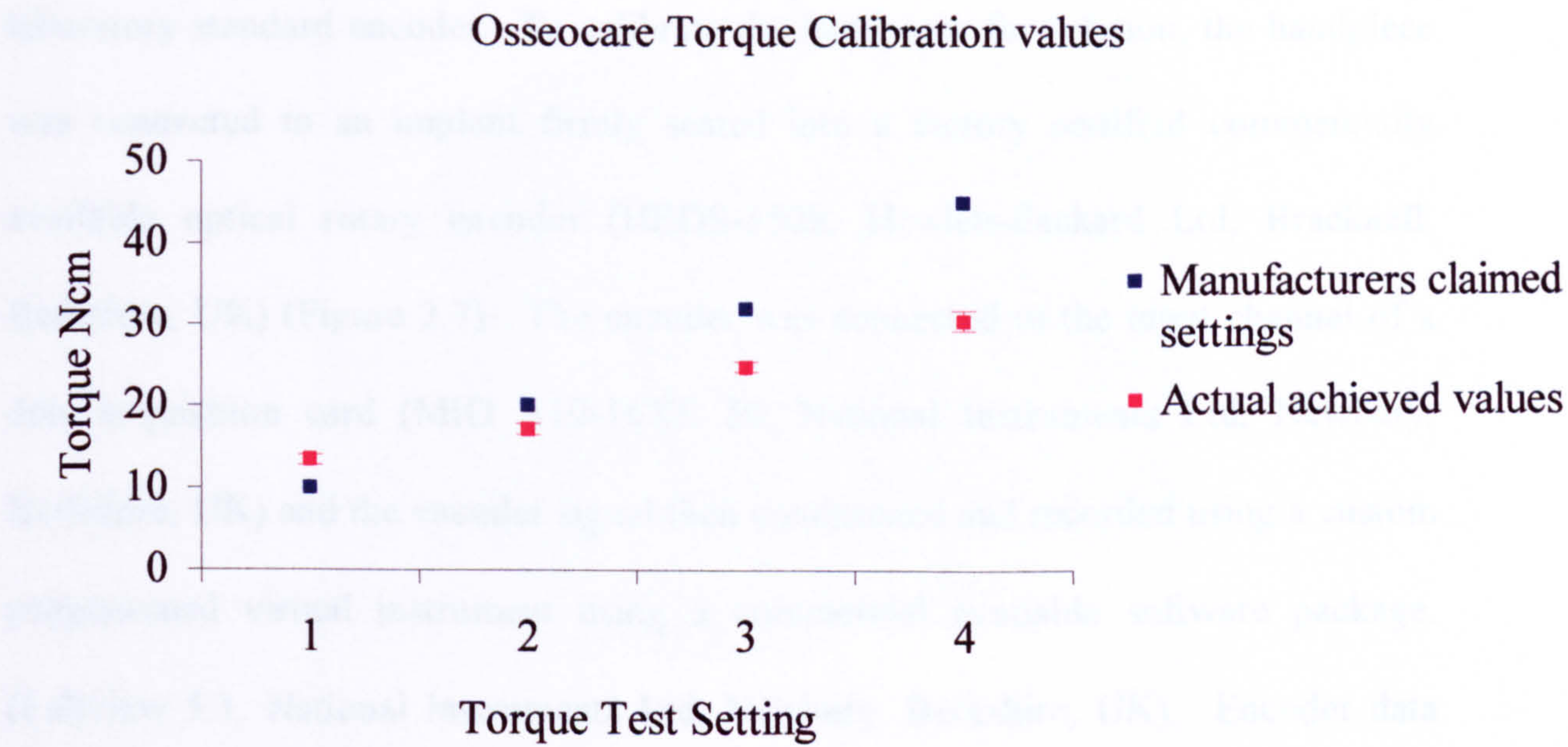


Figure 2.6: Osseocare torque calibration results.
Mean values with 95% Confidence Intervals are shown where appropriate
(n=20).

Osseocare™ and the control PC. The results of the torque calibration is shown in Table 2.1 and Figure 2.6.

2.2.2 Bone Quality Assessment

2.2.2.1 Implant site bone quality assessment
The implant site bone quality was assessed using the bone quality according to the implant system defined by Linderholm and Jansen (1993) (Figures 2.10 and 2.11). The assessment was based upon the appearance of the site on preoperative radiographs and the revision rate for revision and lifting after preparing the implant site and lifting the implant. The assessment was divided into four categories: type 1, type 2, type 3 and type 4. Type 1 was defined as the best quality and type 4 as the worst quality.

The manufacturers of the Osseocare™ unit claim that data relating to the rotation of the working end of the handpiece is derived from recording the commutator pulses from the motor. The exact method used was considered commercially sensitive at the time of this study and it was therefore felt necessary to calibrate this against a laboratory standard encoder. To calibrate the handpiece for rotation, the handpiece was connected to an implant firmly seated into a factory certified commercially available optical rotary encoder (HEDS-550S, Hewlett-Packard Ltd, Bracknell, Berkshire, UK) (Figure 2.7). The encoder was connected to the input channel of a data acquisition card (MIO A10-16XE 50, National Instruments Ltd, Newbury, Berkshire, UK) and the encoder signal then conditioned and recorded using a custom programmed virtual instrument using a commercial available software package, (Labview 5.1, National Instruments Ltd, Newbury, Berkshire, UK). Encoder data was converted into degrees of rotation and saved as an ASCII text file to a hard drive of a PC. The footpedal was activated to rotate the implant in the encoder approximately a full revolution, the data was logged simultaneously using the Osseocare™, and the encoder/PC. The results of the rotation calibration is shown in Table 2.3.and Figure 2.8.

2.2.4 Bone Quality Assessment

At each implant site the operator made an assessment of the bone quality according to the scoring system devised by Lekholm and Zarb (1985) (Figures 1.10 and 1.11). This assessment was based upon the appearance of the site on preoperative radiographs and the resistance felt to cutting and tapping when preparing the implant site and placing the implant. The operator was blinded to any of the insertion torque data,

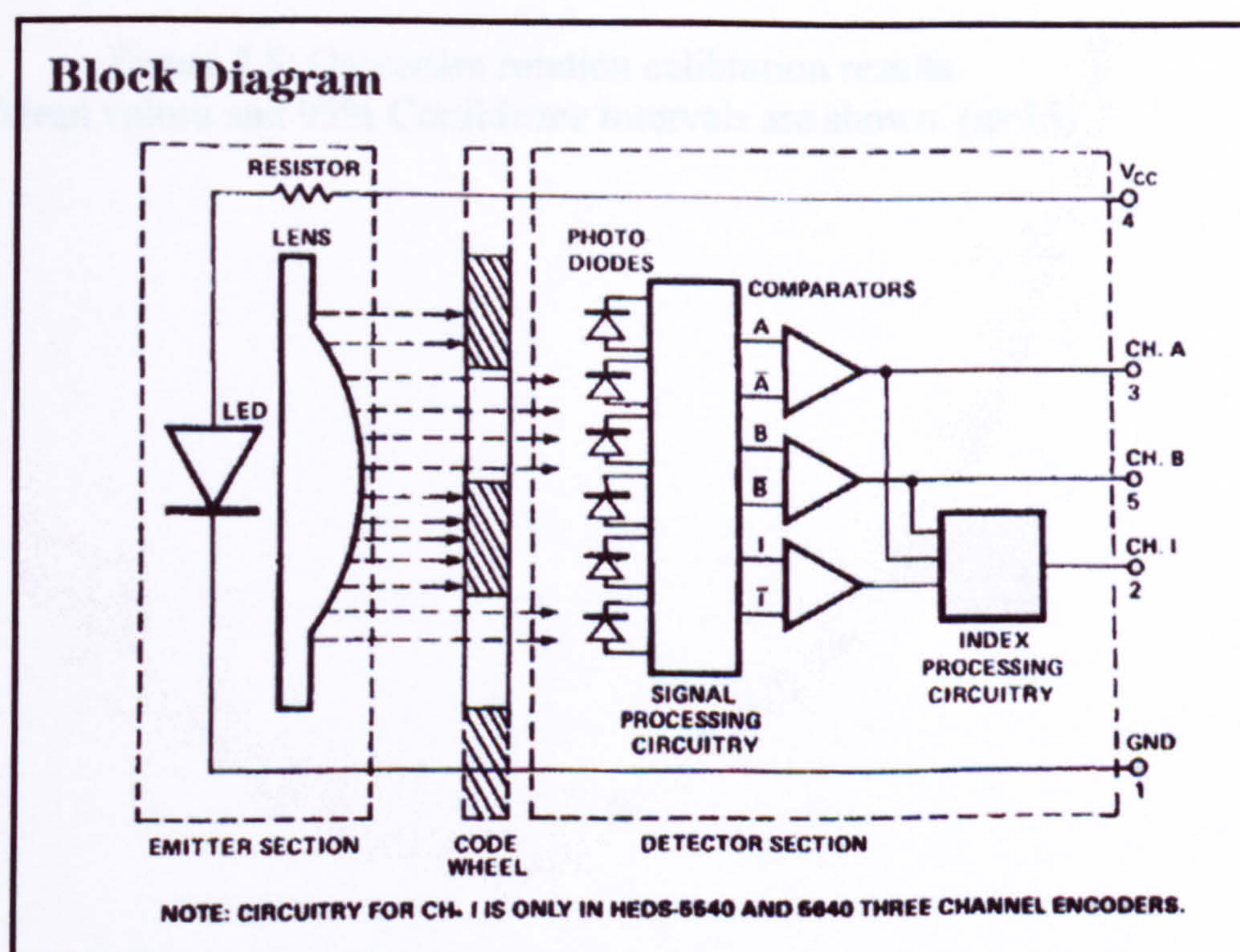
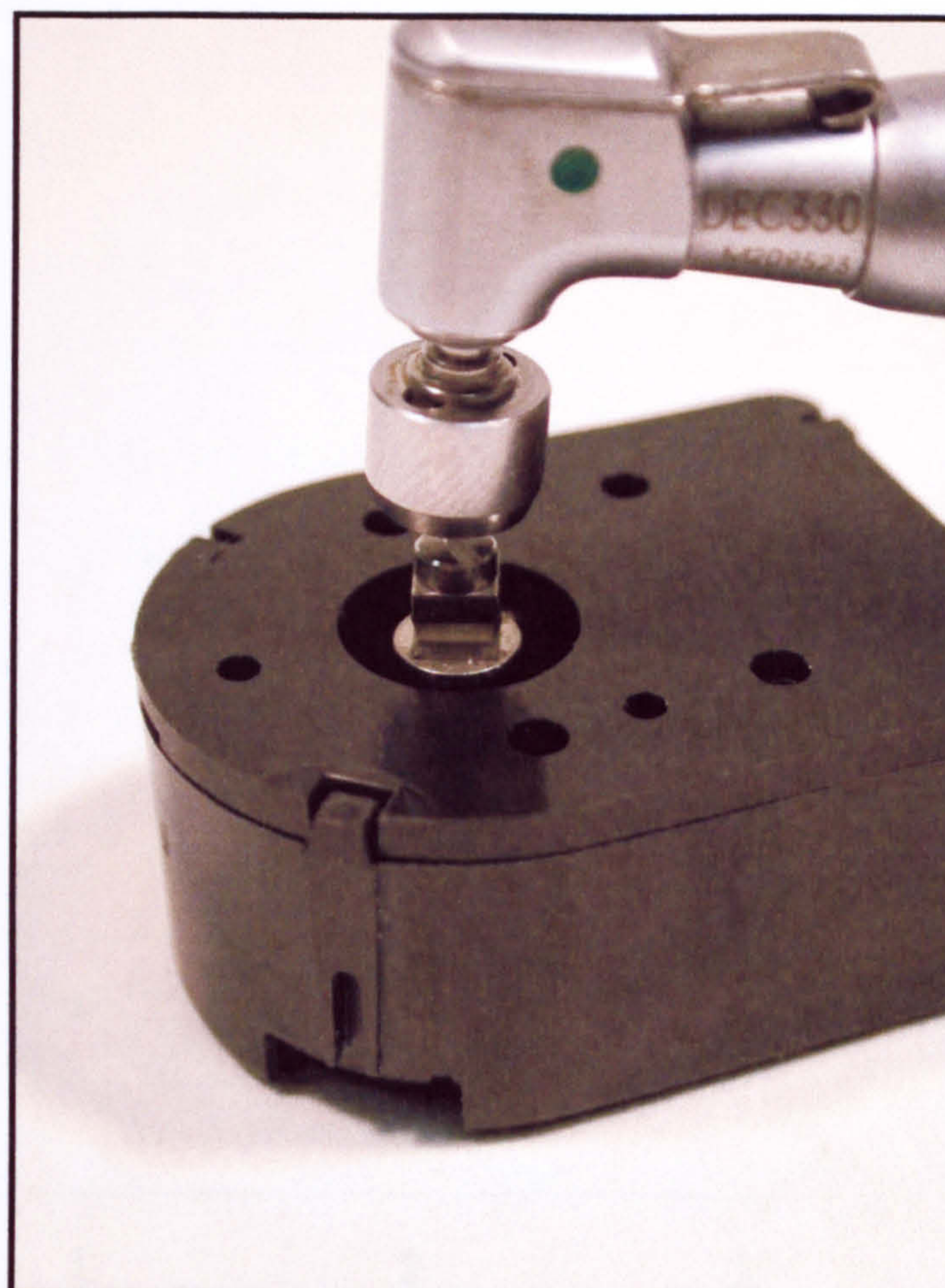


Figure 2.7: Hewlett Packard optical rotary encoder.

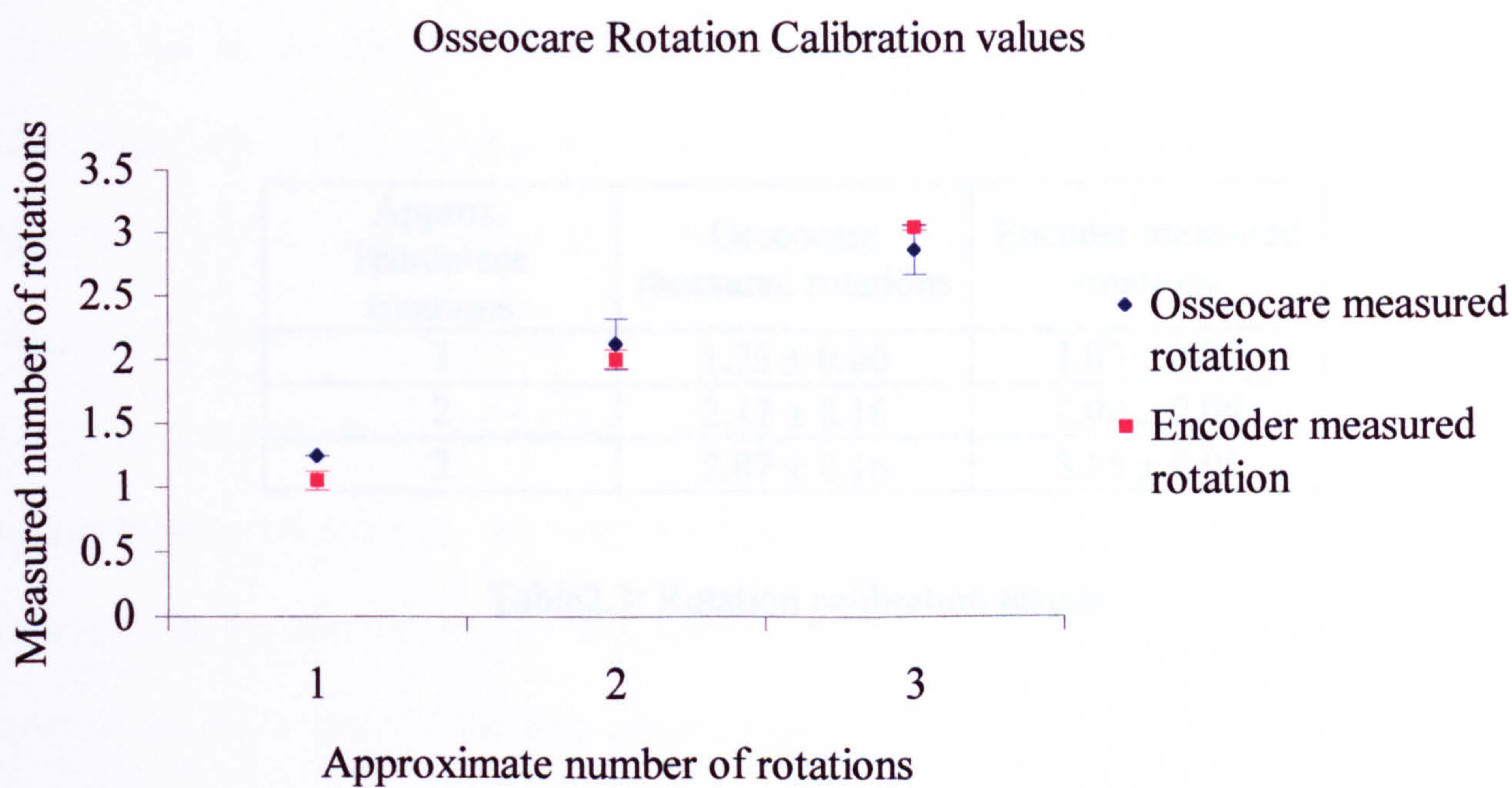


Figure 2.8: Osseocare rotation calibration results.
Mean values and 95% Confidence Intervals are shown. (n=15)

Approx. Handpiece rotations	Osseocare measured rotations	Encoder measured rotations
1	1.25 ± 0.00	1.05 ± 0.06
2	2.12 ± 0.16	2.00 ± 0.06
3	2.87 ± 0.16	3.05 ± 0.01

Table2.3: Rotation calibration results

Mean values ± S.D. are shown (n=15)

which may have influenced his response and the bone quality assessment was made prior to the Resonance Frequency test.

2.2.5 Resonance Frequency Analysis

Resonance Frequency analysis readings for each implant were taken at implant placement and six months post insertion after healing had taken place. Following implant placement resonance frequency measurements were made according to the method described by Meredith et al. (1997). The resonance frequency analysis equipment consists of a transducer which attaches to the implant; this in turn connects to a custom designed frequency response analyser and a portable laptop computer (Figure 1.8 and 1.9). The transducer is an L-shaped cantilever beam which connects to the implant via a screw attachment. The implant/transducer complex is stimulated across a swept frequency range of approximately 2 to 20 kHz, via a piezoelectric crystal attached to the upright portion of the transducer beam and the frequency range is generated by the frequency response analyser. A piezoelectric crystal on the opposite side of the beam is used as the receiving element to detect the resonance frequency peak. The data is analysed, collected and stored on a portable computer.

2.2.6 Evaluating Insertion Torque Peaks

Figure 2.9 shows a typical insertion torque plot for an implant taken from the Osseocare™ data, with a description of the relevant sections of the torque plot. The maximum insertion torque peak was taken as the maximum insertion torque value achieved during the implants insertion. The slope of the final peak relating to the

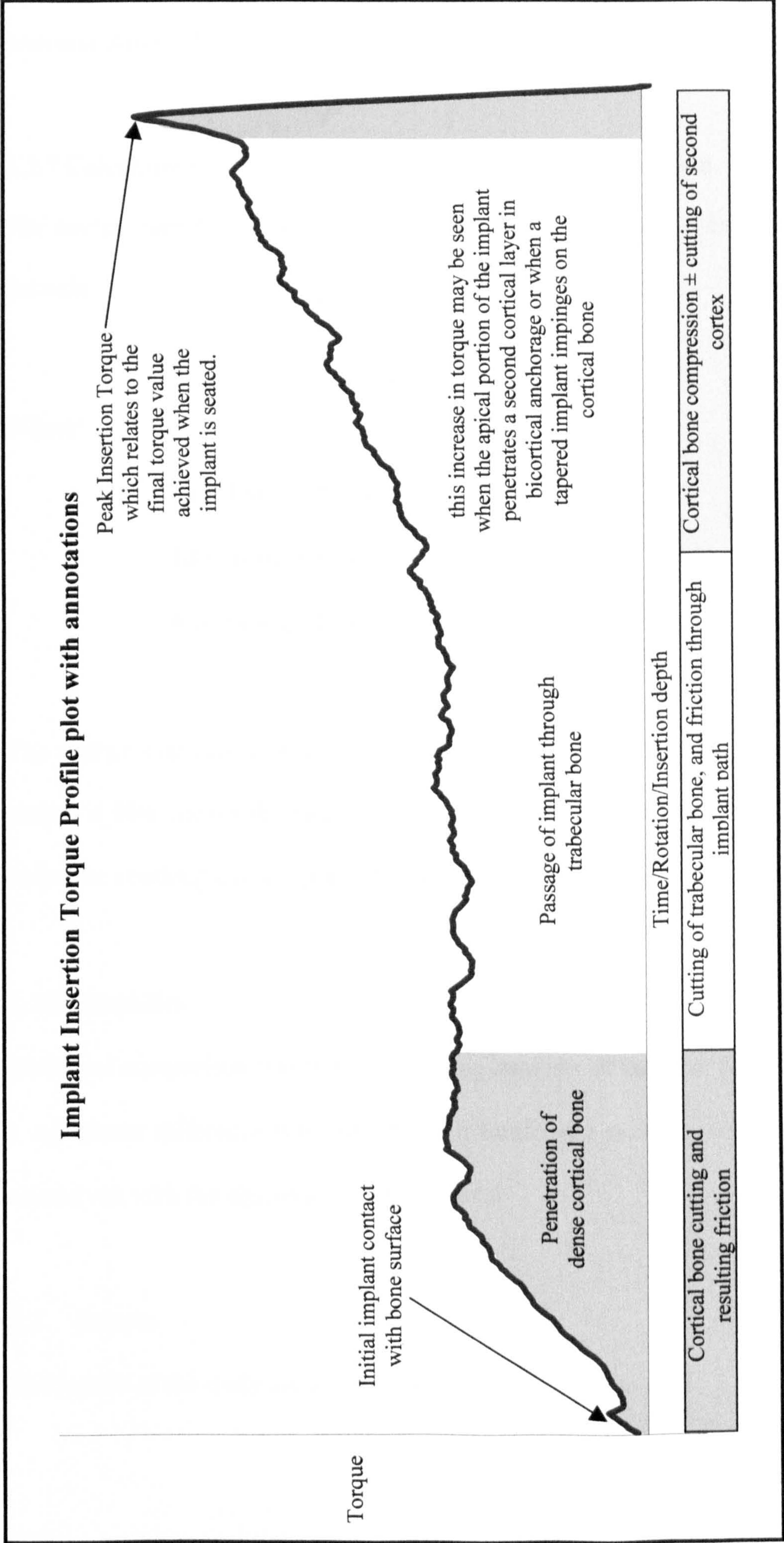


Figure 2.9: Implant Insertion Torque plot with annotation.

maximum insertion torque value was examined by taking a tangent from the insertion torque plot at this point and calculating the slope of the tangent.

2.2.7 Calculation of Energy required during implant Insertion

The energy used during implant insertion by the handpiece was calculated using the formula:

$$E_{\chi} = T\theta \times A$$

Where:

E_{χ} = Energy in joules

$T\theta$ = Torque in Nm

A = Angular displacement in radians

The energy required to insert an implant can be obtained by plotting the insertion torque in Nm against the angular displacement of the implant in radians. The area under the resulting curve represents the energy used in Joules (Figure 2.10).

2.2.8 Statistics

Statistical comparison was performed using analysis of variance (ANOVA). Where a significant difference was indicated the Bonferroni multiple comparison test was carried out with the significance set at $p=0.05$.

2.3 Results

The results of the study are summarized in Figures 2.11 to 2.22.

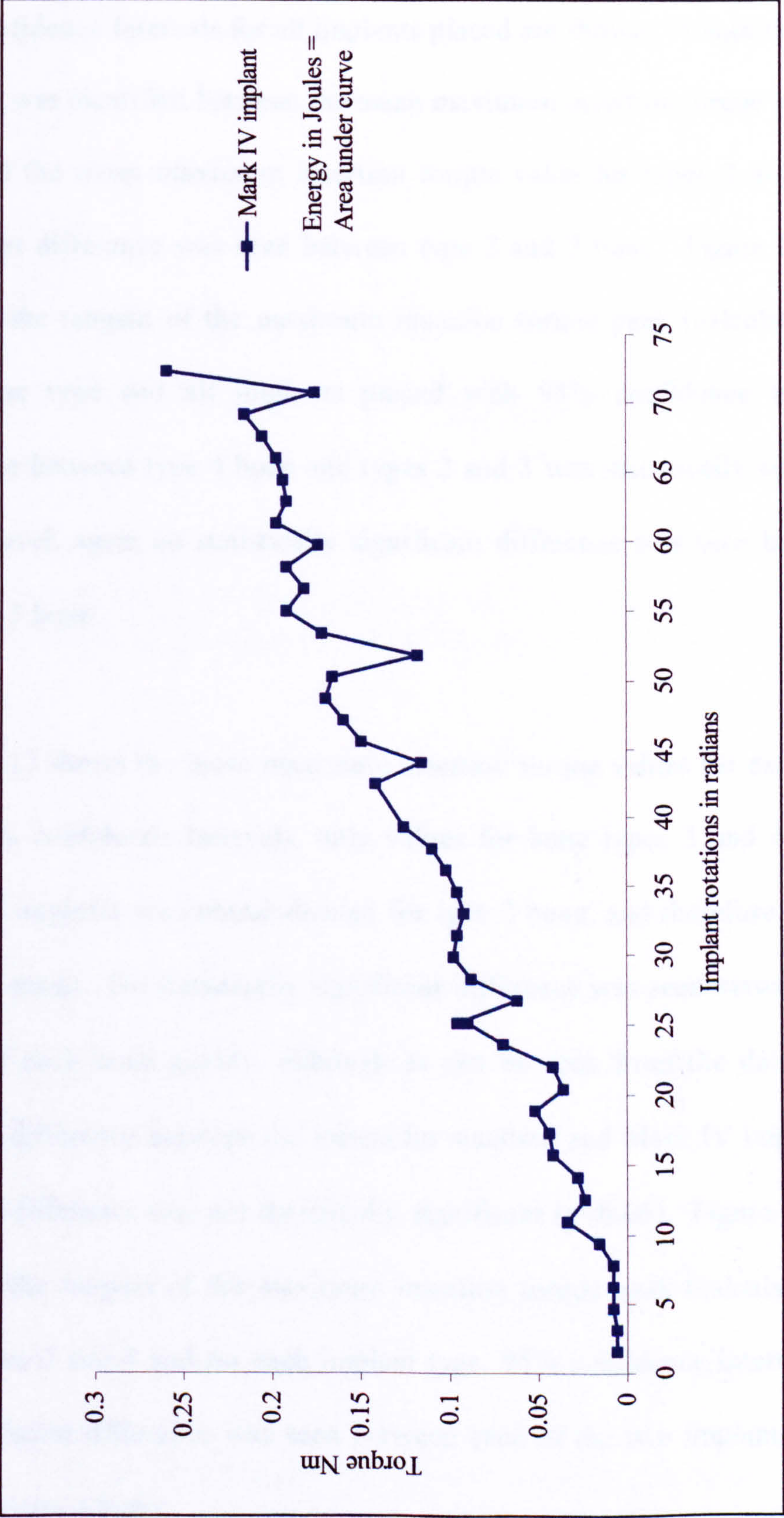


Figure 2.10: Derivation of implant insertion energy.

2.3.1 Insertion Torque

Figure 2.11 shows the mean maximum insertion torque values generated during implant insertion for each of the three bone qualities 2, 3 and 4. Mean values with 95% Confidence Intervals for all implants placed are shown. A significant difference ($p=0.05$) was identified between the mean maximum insertion torque value for type 4 bone and the mean maximum insertion torque value for types 2 and 3 bone. No significant difference was seen between type 2 and 3 bone. Figure 2.12 shows the slope of the tangent of the maximum insertion torque peak (calculated as y/x) for each bone type and all implants placed with 95% confidence intervals. The difference between type 4 bone and types 2 and 3 was statistically significant at the $p=0.05$ level, again no statistically significant difference was seen between types 2 and type 3 bone.

Figure 2.13 shows the mean maximum insertion torque values for each implant type with 95% confidence Intervals, only values for bone types 3 and 4 are shown as Mark IV implants are contraindicated for type 2 bone, and therefore no comparison could be made. No statistically significant difference was seen between the implant types for each bone quality, although as can be seen from the data there was an apparent difference between the means for standard and Mark IV implants in type 4 bone the difference was not statistically significant ($p=0.06$). Figure 2.14 shows the slope of the tangent of the maximum insertion torque peak (calculated as y/x) for bone types 3 and 4 and for each implant type, 95% confidence intervals are shown. No significant difference was seen between each of the two implant types in either type 3 or type 4 bone.

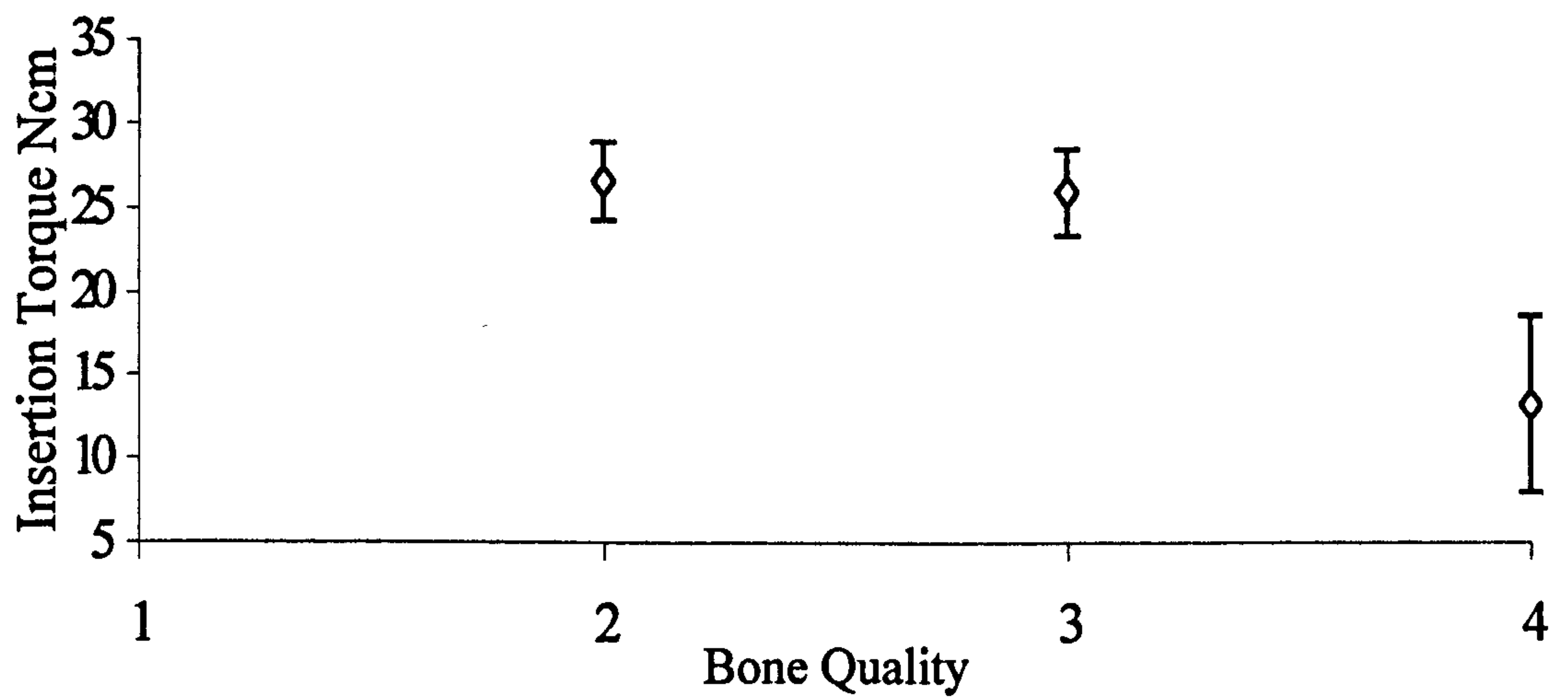


Figure 2.11: Mean maximum insertion torque at implant insertion. Mean values are shown with 95% confidence intervals (n=42)

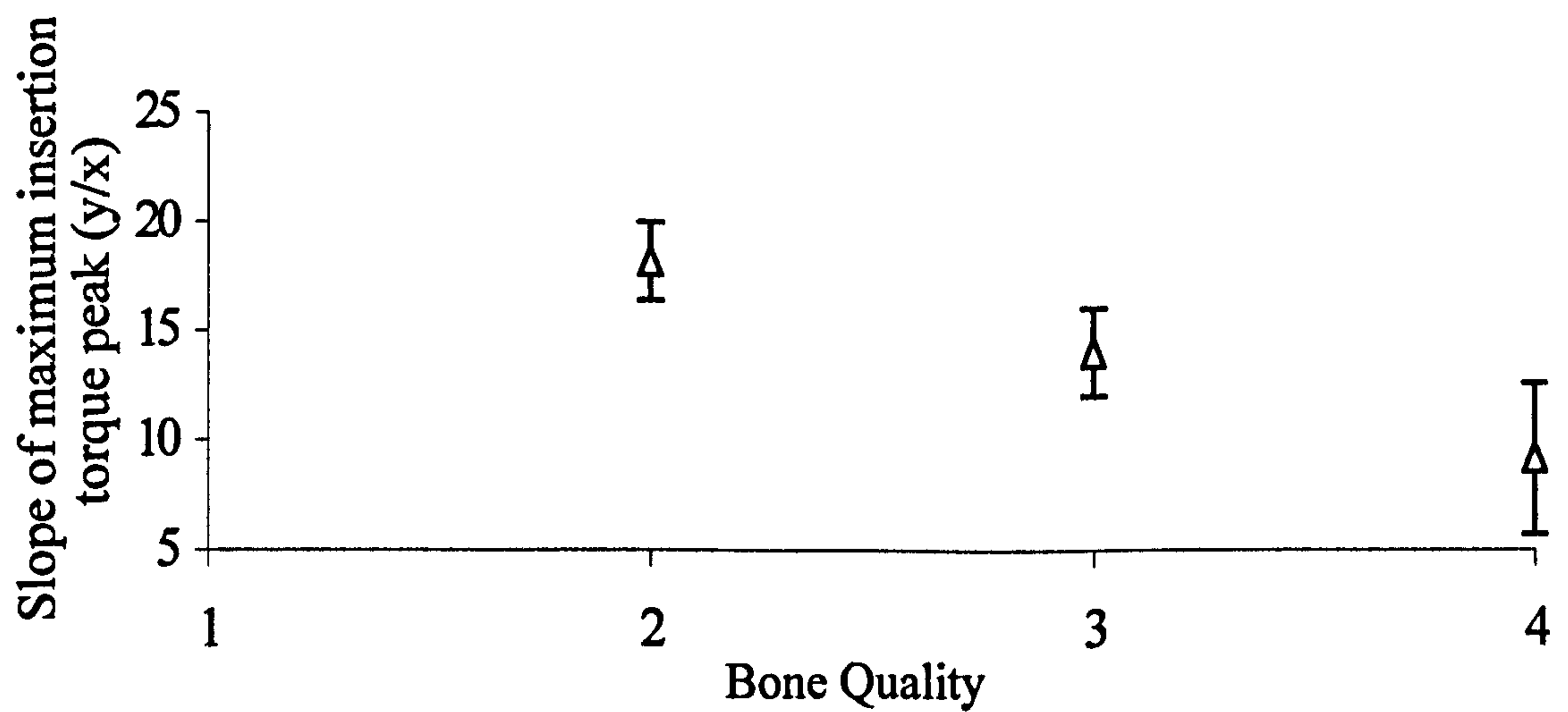


Figure 2.12: Slope of the tangent to the maximum insertion torque peak at implant insertion. Mean values are shown with 95% confidence intervals (n=42)

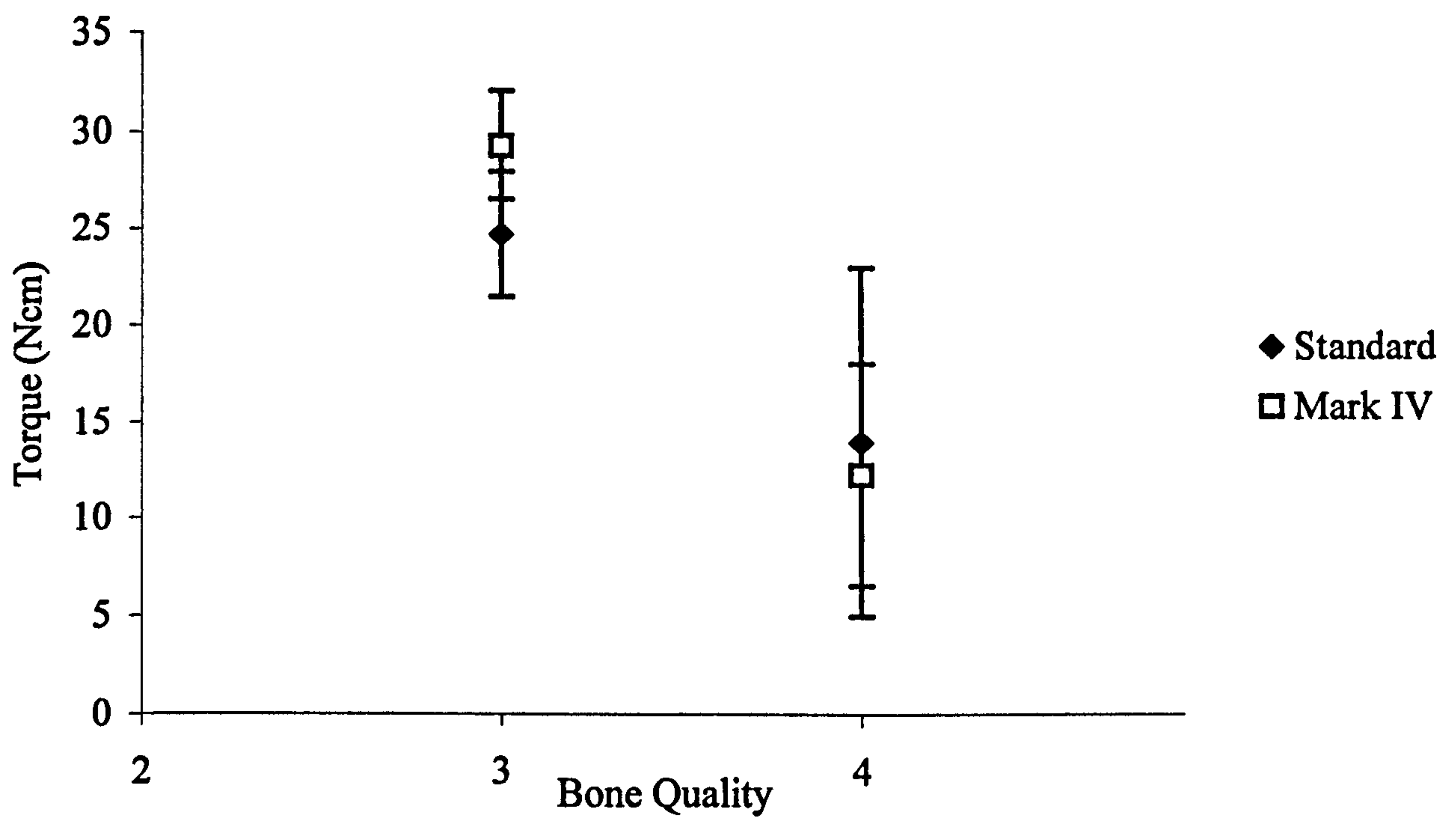


Figure 2.13: Mean maximum insertion torque at implant insertion for each implant type. Mean values are shown with 95% confidence intervals (n=23).

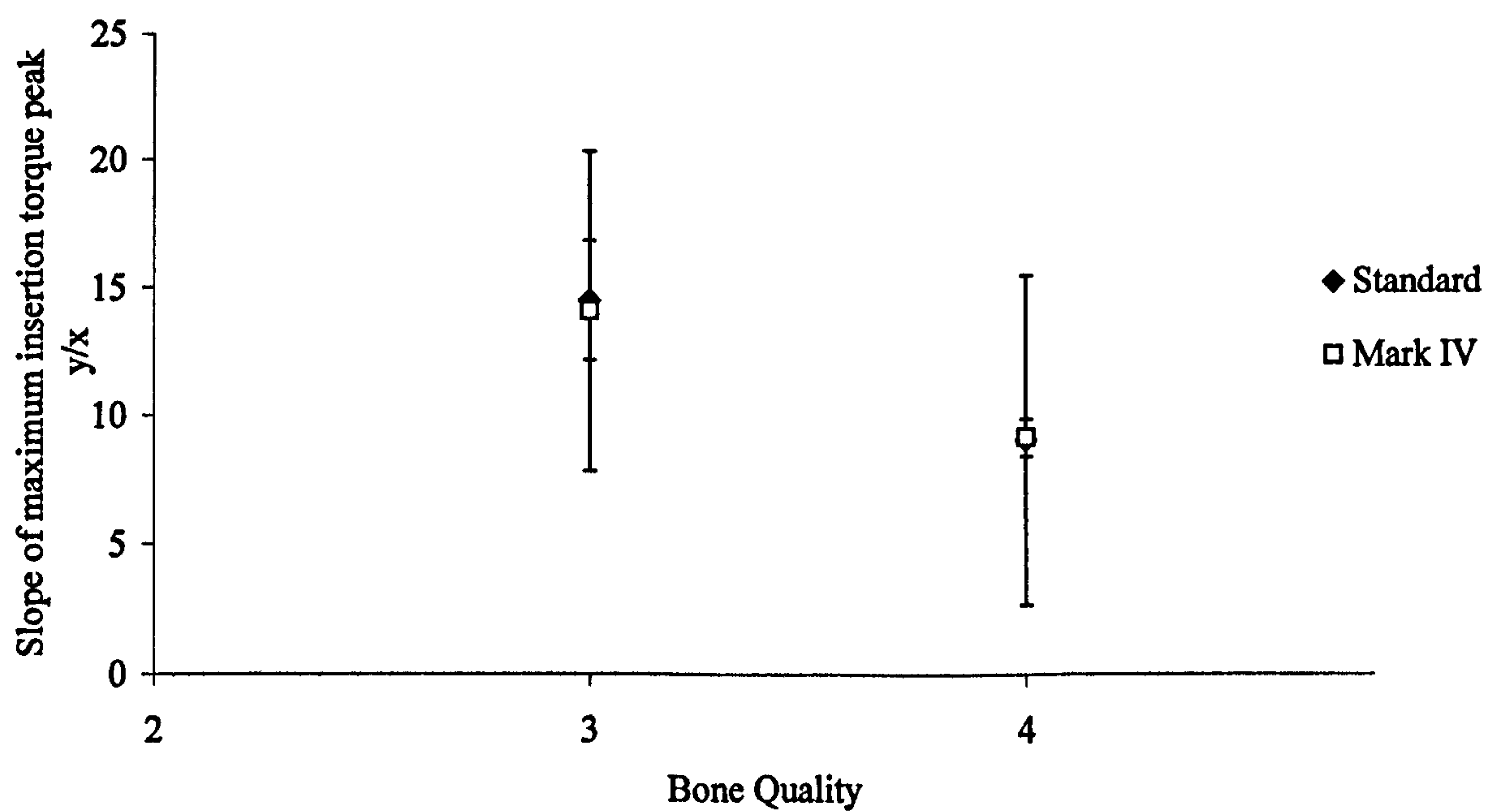


Figure 2.14: Slope of the tangent to the maximum insertion torque peak at implant insertion per implant type. Mean values are shown with 95% confidence intervals (n=23).

Energy required during implant insertion is shown in Figure 2.15 mean values with 95% Confidence Intervals shown for each bone quality. A statistically significant difference was seen between those implants placed into type 4 bone and those placed into types 2 and 3 bone. Figure 2.16 illustrates the data in Figure 2.15 divided into implant types. A significant difference ($p=0.05$) was seen between the Mark IV implants placed into type 4 bone and the other implant types/bone combinations

2.3.2 Resonance Frequency Analysis

Figure 2.17 shows the Resonance Frequency Analysis (RFA) data for all of the implants at implant placement for each bone type. Mean values with 95% confidence intervals are shown. A statistically significant difference was seen between those implants placed into type 3 and type 4 bone ($p=0.05$). No significant difference was seen between those implants in type 2 bone and types 3 or 4 bone.

The RFA data for the same implants at six-month follow-up after the initial healing has taken place and mean values with 95% confidence intervals are shown in Figure 2.18. No statistically significant difference was seen at six-month follow-up for any of the bone types.

Figure 2.19 shows the mean RFA values at implant placement for bone qualities 3 and 4 and for each implant type, 95% confidence intervals are shown. No statistically significant difference was seen between implant designs. Figure 2.20 shows the mean RFA values at second stage surgery after six months of healing had taken place for each implant type placed into bone qualities 3 and 4. 95%

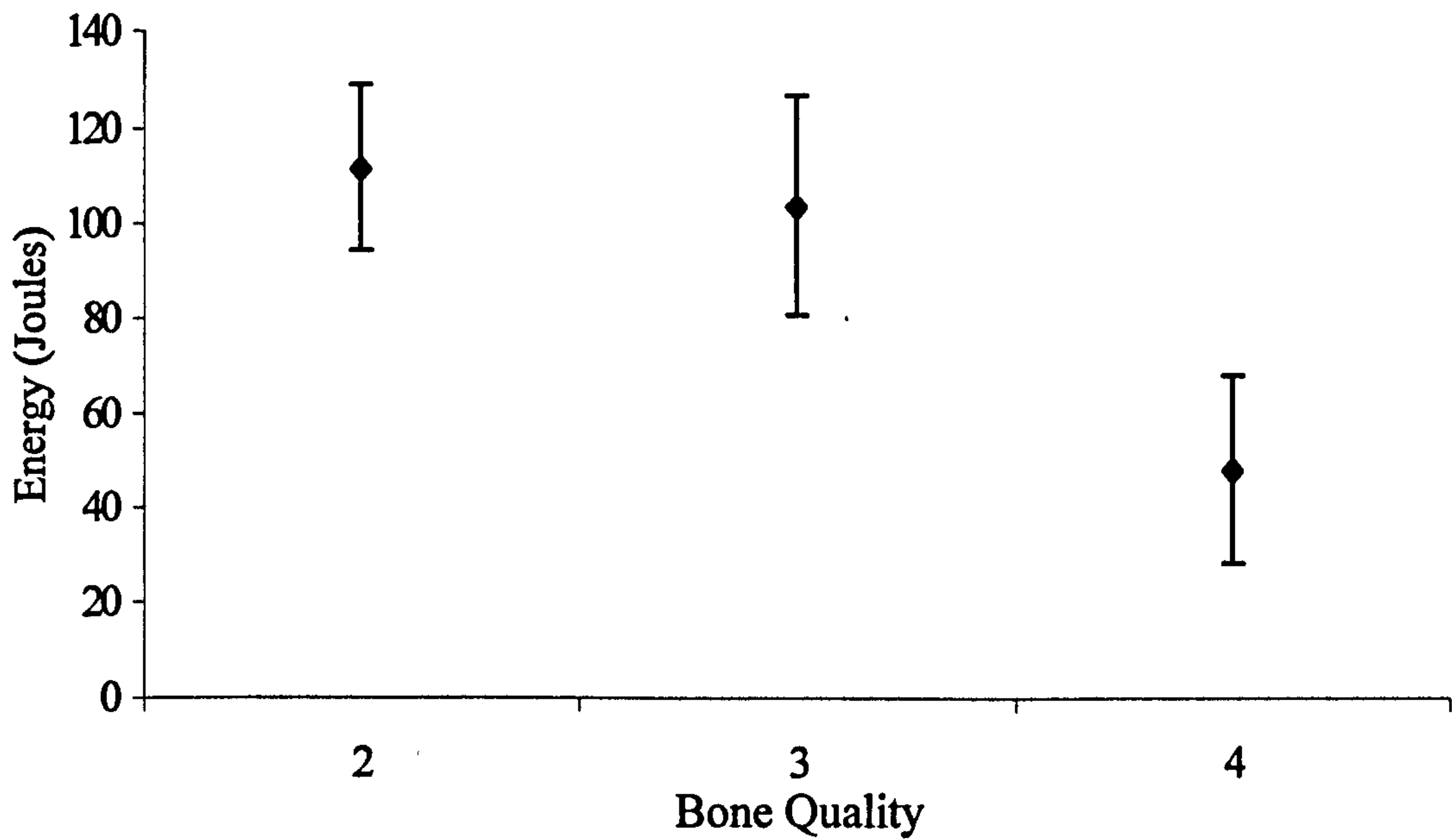


Figure 2.15: Energy required during implant insertion. Mean values with 95% confidence intervals are shown (n=42).

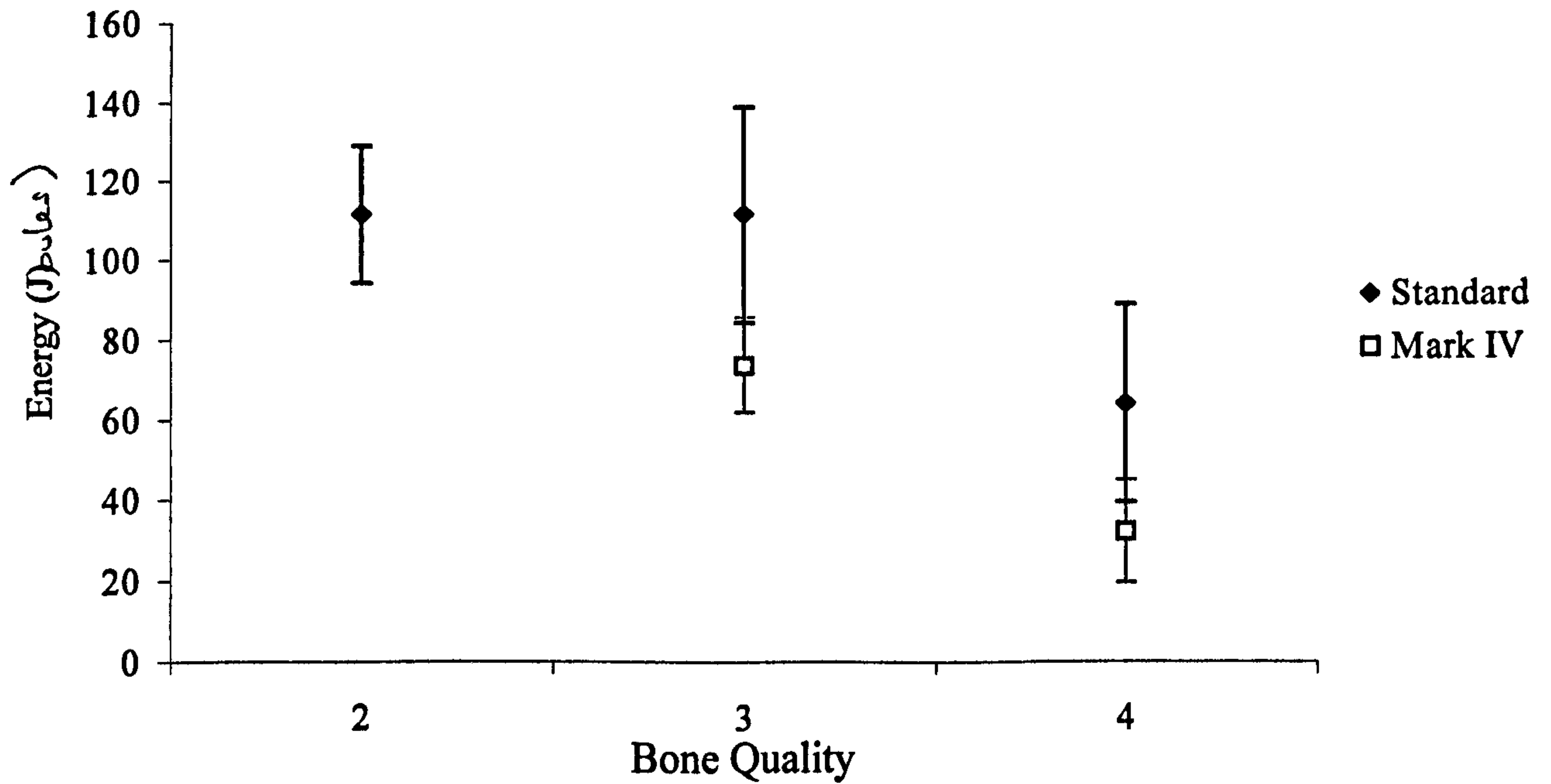


Figure 2.16: Energy required during implant insertion per implant type. Mean values with 95% confidence intervals are shown (n=42).

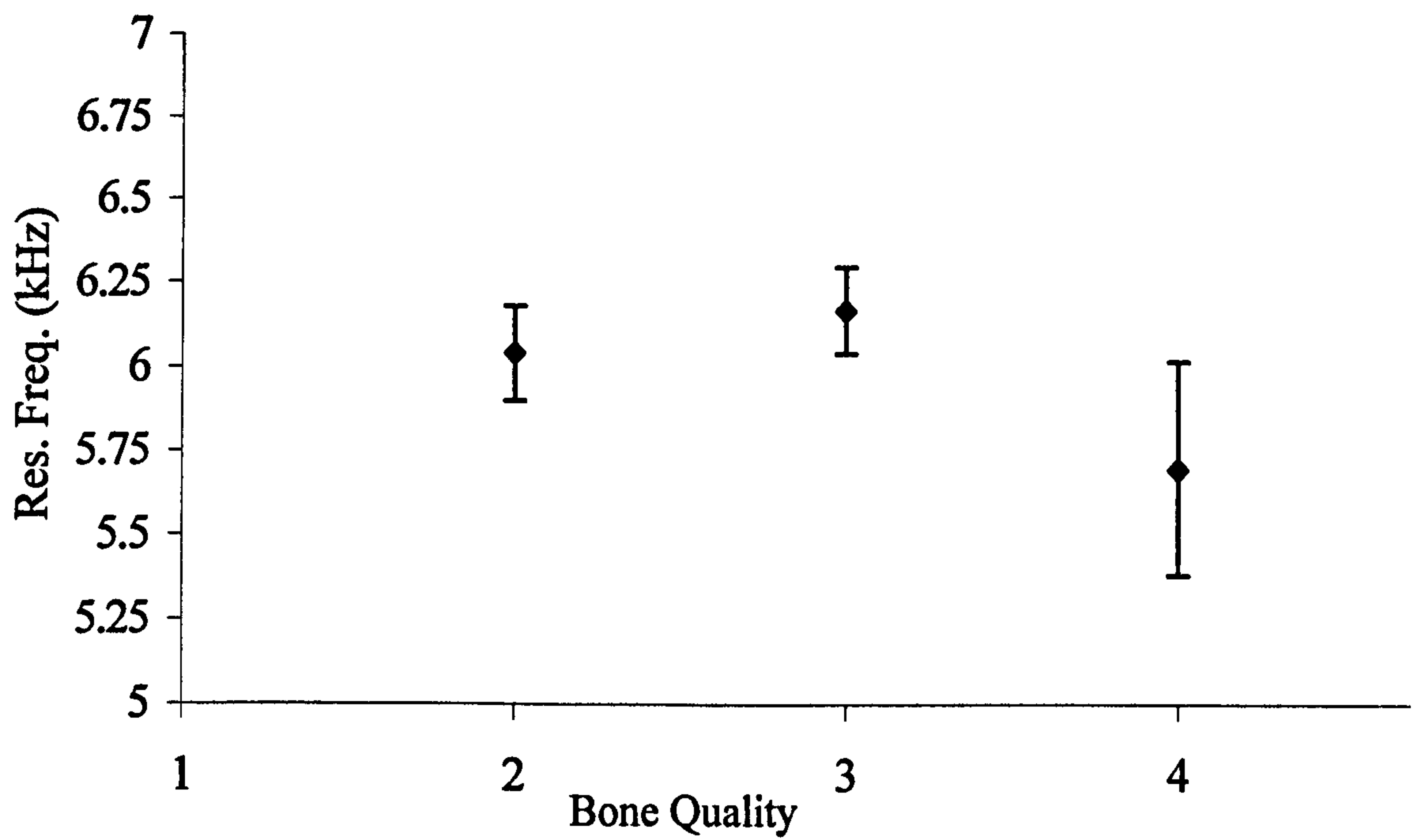


Figure 2.17: RFA values at implant placement. Mean values with 95% confidence intervals are shown (n=42).

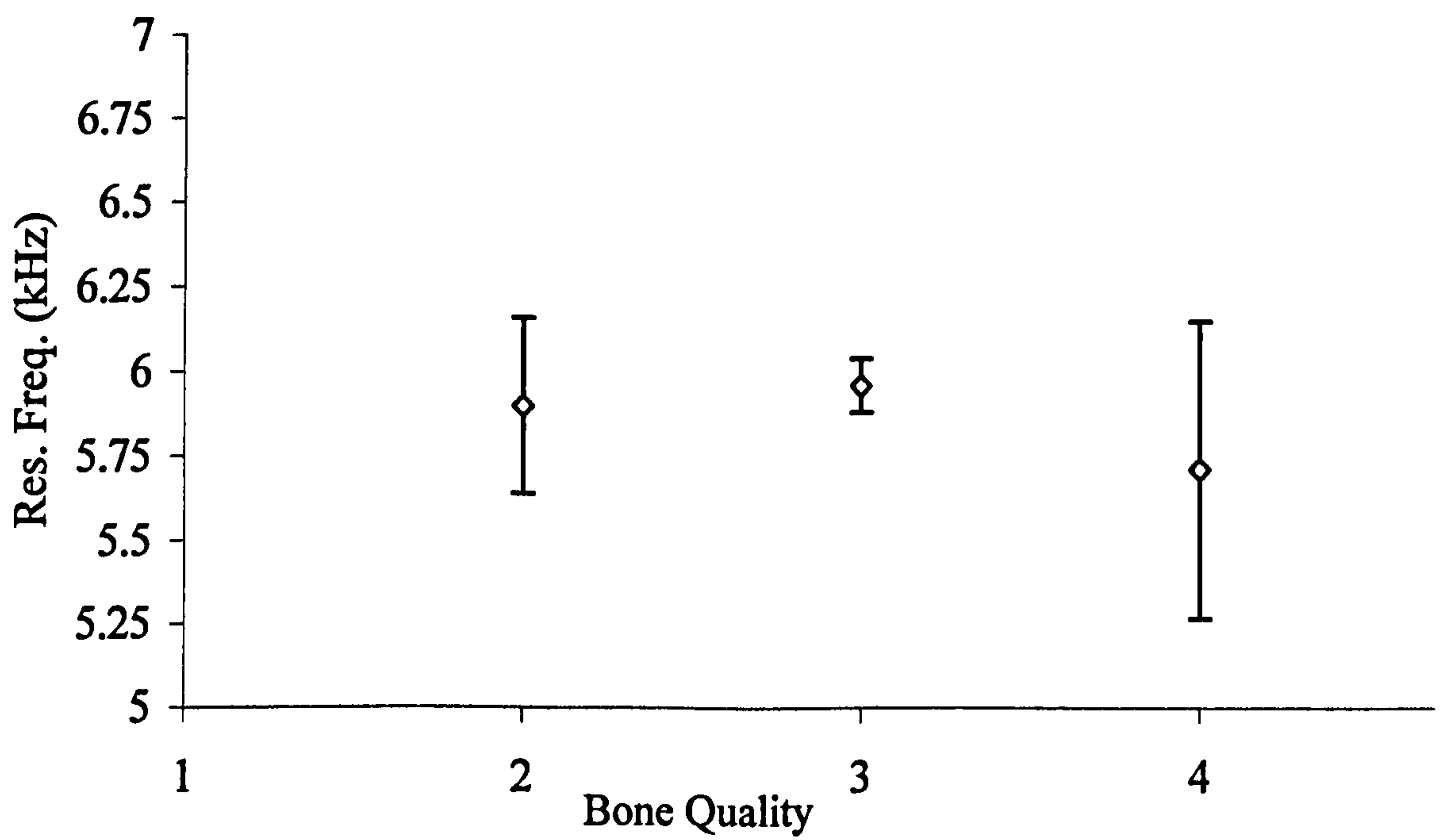


Figure 2.18: RFA values at second stage surgery. Mean values with 95% confidence intervals are shown (n=42).

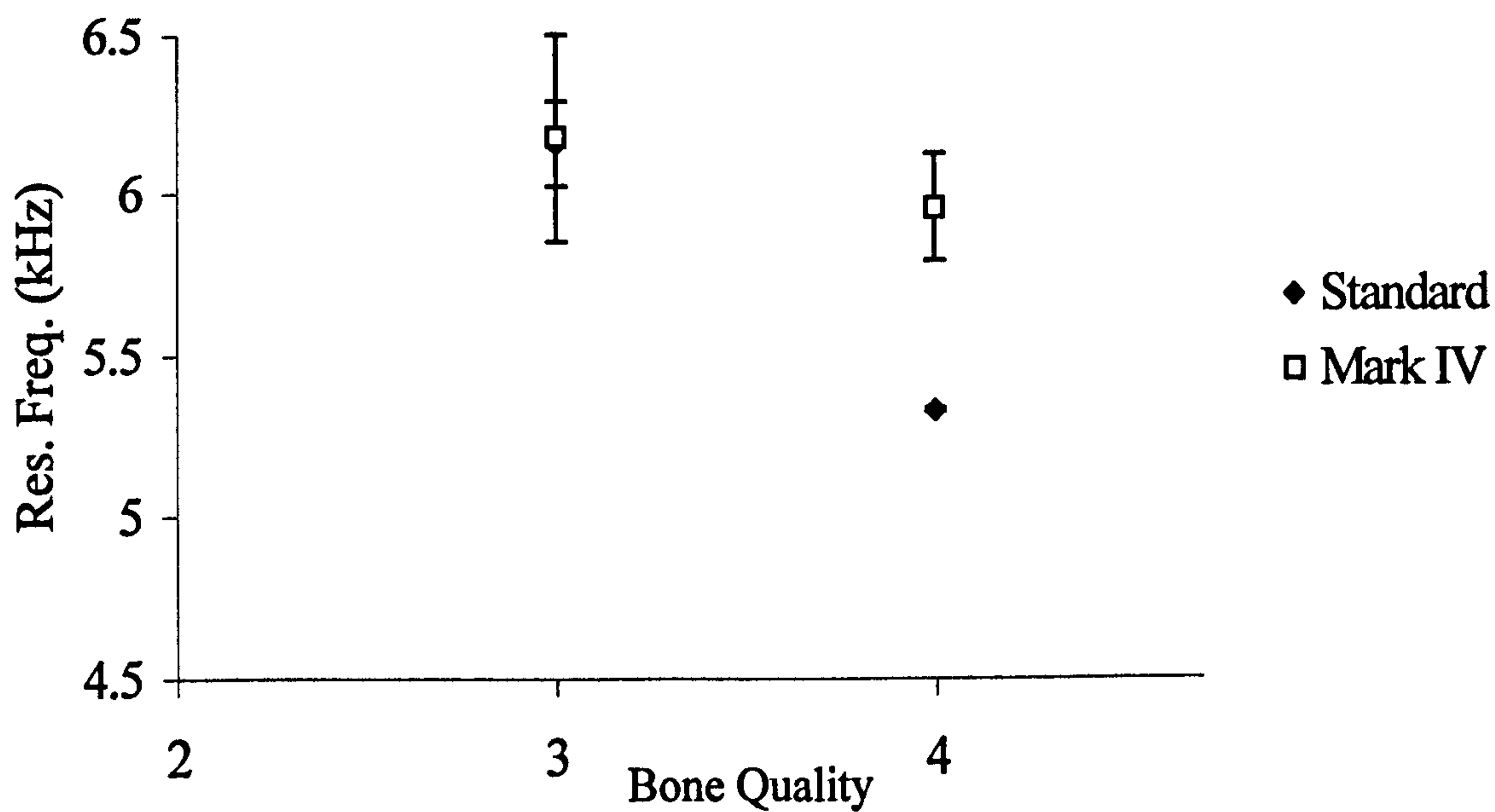


Figure 2.19: RFA values at implant placement per implant type. Mean values with 95% confidence intervals are shown (n=23).

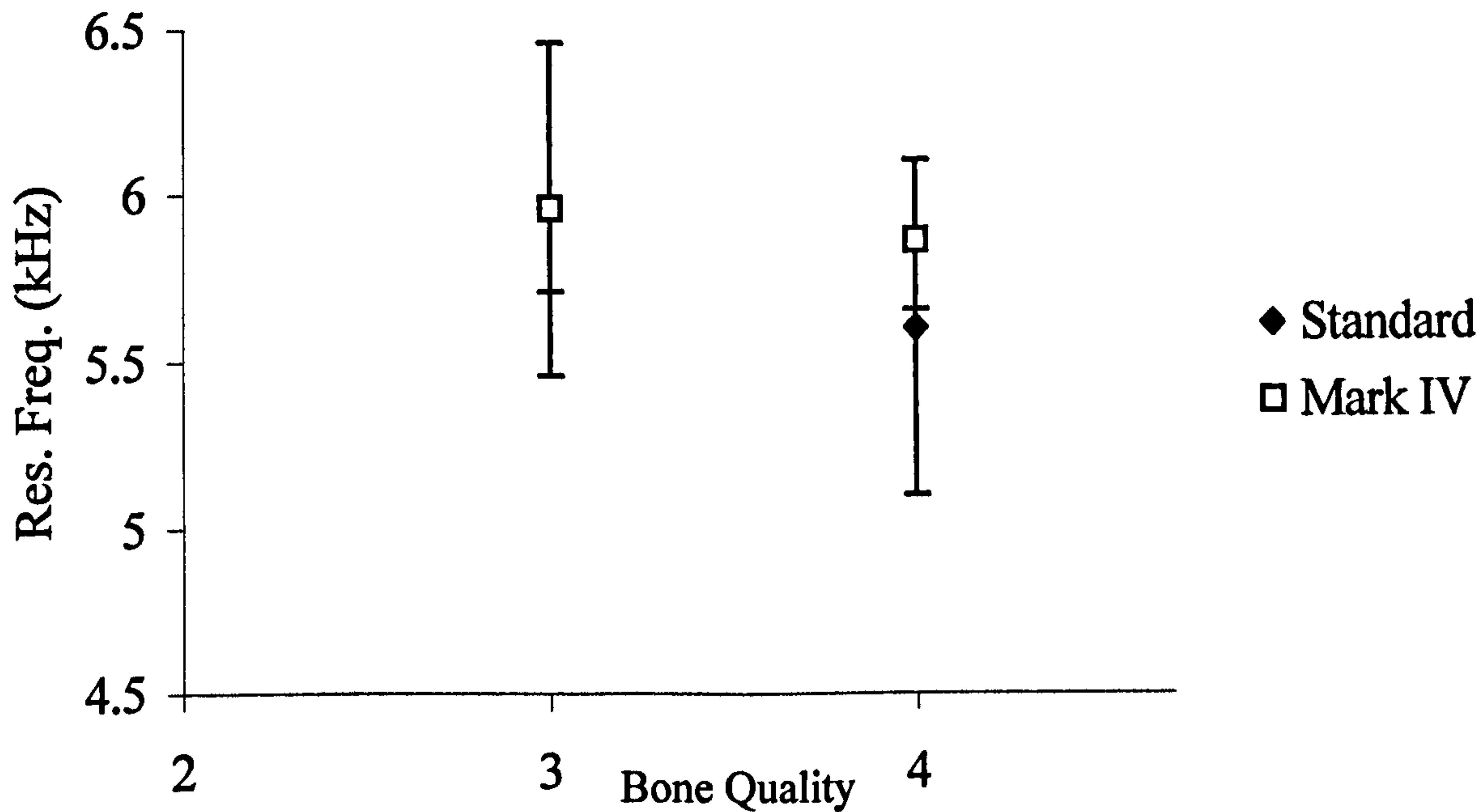


Figure 2.20: RFA values at second stage surgery per implant type. Mean values with 95% confidence intervals are shown (n=23).

confidence intervals are shown. As at implant follow-up, no statistically significant difference was seen.

Figures 2.21 and 2.22 illustrate the maximum insertion torque values for each implant plotted against RFA value at each surgical stage and for all bone types. Maximum insertion torque values are plotted against RFA values in Figure 2.21 and 2.22. Values at implant placement are shown in Figure 2.21 whilst insertion torque values at implant placement against RFA values at second stage surgery are shown in Figure 2.22. A Pearson correlation coefficient was calculated for each data set giving a value of $r = 0.285$ for the data at implant placement and $r = 0.007$ for the six month review data.

2.4 Discussion

2.4.1 Discussion of the method

The purpose of this study was to acquire information related to insertion torque and resonance frequency data in a clinical setting when attempting to maximize implant primary stability. All of the implants were placed according to clinical need as judged by the operator. Implant primary stability is currently thought to be of great importance when placing oral implants in bone and it was the view of the clinician that efforts should always be made to maximize primary stability. This led to all of the implants studied being placed in a manner that would attempt to enhance their primary stability. What was unfortunately beyond the scope of this study was the evaluation of how effective these methods are in enhancing primary stability when compared to the traditional use of a surgical tap prior to implant insertion. To be able to study this feature implants would have to have been placed in a manner

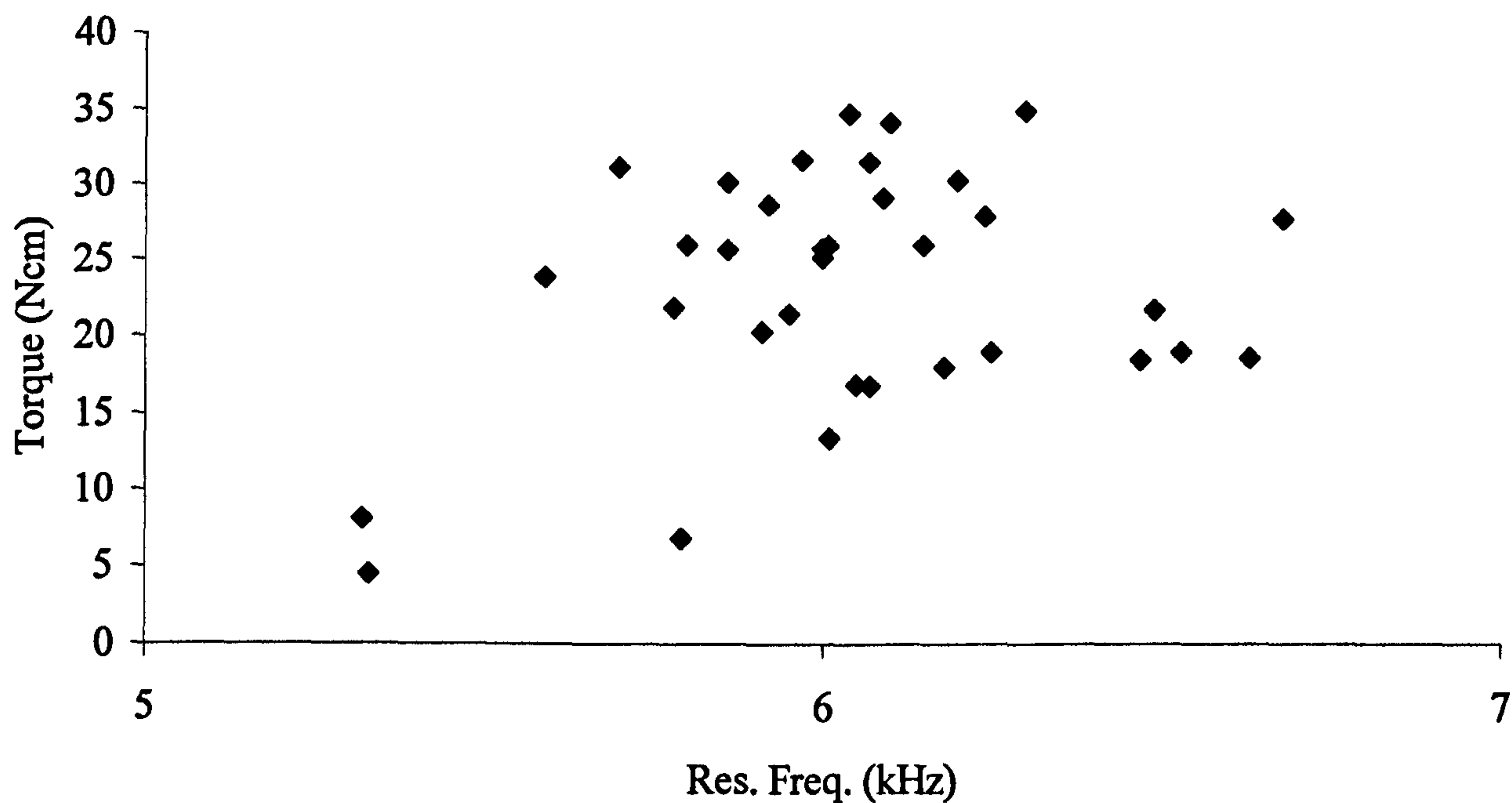


Figure 2.21: Maximum Insertion Torque against RFA value at implant placement (n=42).

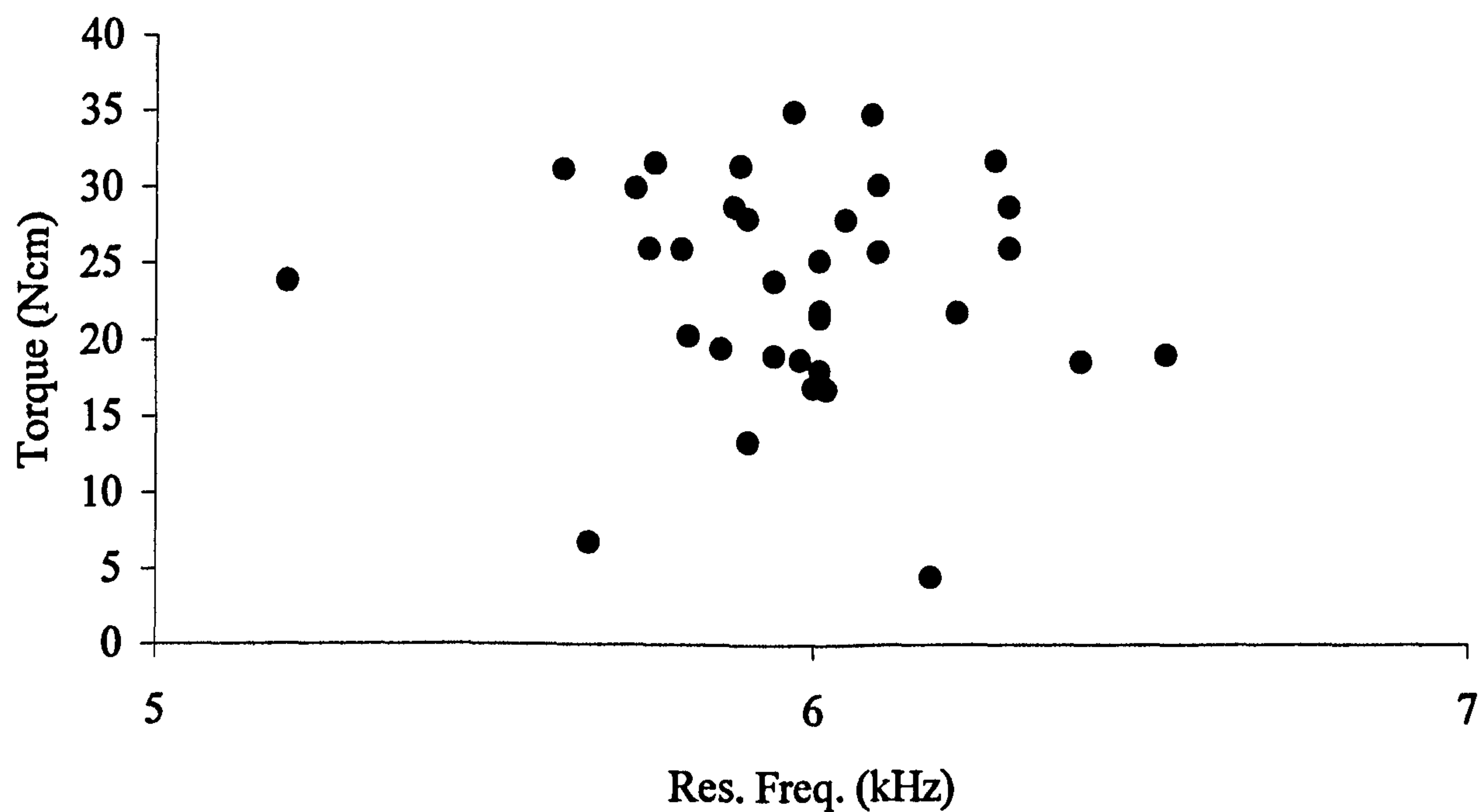


Figure 2.22: Maximum IT against RFA value at second stage surgery (n=42).

which, in the view of the clinical operator, may have led to a less successful clinical outcome for the patient. This was considered unacceptable. It is recognized that quantitative data relating to the enhanced stability gained from not using a surgical tap prior to placing a non-tapping implant is lacking, even though it has become an accepted part of current implant surgery.

The calculation of the energy used during implant insertion is a very complex area of study. Johansson and Strid (1994) described a technique using insertion torque data to calculate the energy used in cutting a prescribed unit of bone. To do this, they made a number of assumptions regarding the energy used in the development of friction between the implant and the bone and in the 'shiver packing' of bone chips into the cutting flutes and surface irregularities of the implant surface. Their assumptions were made largely without reference to experimental evidence. They also did not take into account the effect of differing implant design and variation in implant/pilot hole ratio which, as will be discussed later, has been shown to have a significant effect upon the measured insertion torque. In order to avoid these uncertainties, in this study it was decided to look at the overall energy used during the placement of the implant as a guide to the relative differences in energy imparted to the bone at the implant site during implant insertion. Looking at the overall energy used during insertion is obviously an overestimate of the energy imparted to the bone. Energy is also lost in the generation of heat within the handpiece, the generation of noise and also to friction between the components of the handpiece and motor. For the purposes of this study it was assumed that these parameters are relatively consistent and are not affected by the type of implant placed, although it is accepted that they will increase the variability between the readings.

2.4.2 Discussion of the results

When ignoring implant type as a criterion and taking all of the implants placed into account, maximum insertion torque appears to be a useful indicator of bone quality type 4. Although there is no statistical difference between type 2 and 3 bone a difference was noted in this study between types 2 and 4 and between type 3 and type 4 bone quality. The relationship between bone quality and insertion torque has been investigated by Friberg (1999). He found a significant correlation between cutting resistance (calculated using the Johansson and Strid model) and bone density measurements, as well as between cutting resistance and bone area calculations of post mortem jaws. He also found a correlation between the maximum cutting torque and assessed bone density scores in vivo. Although he discussed the Lekholm and Zarb scoring system he did not look at the comparison of Lekholm and Zarb score with cutting torque. When looking at insertion torque traces in his study, Friberg (1999) divided the insertion torque profile into equal thirds (E1, E2 and E3). He related the thirds to anatomical structure, with E1 relating to the implant passing through the upper cortical bone surface, E2 to the middle trabecular bone region and E3 to the lower apical third of the implant, which in an implant site where bicortical anchorage was achieved related to the penetration of the second cortex. Mean values were calculated and compared for each region. The peak insertion torque value was not examined as a parameter. The problem with this method of analysis is that E1:E2:E3 are not comparable between implants of differing lengths. If the torque profile is simply divided into thirds the bone depths at which E1:E2:E3 are found for a 7mm long implant will obviously differ if a 15mm long implant was to be compared. E1:E2:E3 cannot be reliably related to anatomical structure at the implant site.

Peak insertion torque can relate to a number of situations clinically. The maximum torque value generated may be due to:

- the flange of the implant impinging on the crestal cortical bone;
- the implant 'bottoming out' at the base of the prepared bone channel;
- the apical portion of the implant engaging a lower cortical bone layer;
- the generation of friction as the full length of the implant inserts into bone;
- the resistance of interfacial bone to local compression in a tapered implant.

This may explain why there does not appear to be a clear relationship between maximum insertion torque value and the Lekholm and Zarb score. The subjective nature of the Lekholm and Zarb score and the small sample size involved in this study may have lead to experimental error masking an underlying relationship and may warrant further investigation. It is then perhaps surprising, given the potential sources of error already described, that the slope of the tangent to the maximum insertion torque peak appears to demonstrate a correlation to bone quality. Implants placed into type 2 bone generated a steeper slope than those placed into type 4 bone. This difference is statistically significant ($p=0.05$) and appears either to relate to a straight line defined by the equation $y = -4.5x + 27$ or that this equation describes a straight-line section of a curve between types 2 and 4 bone. This has not been previously reported in the dental literature and appeared to be relatively unaffected by the design of implant, which is surprising. From a clinical viewpoint, the Lekholm and Zarb classification has always been seen as highly subjective and there has been little investigation into the extent to which inter and intra-operator variability affects the bone quality assessment. It is surprising then that insertion torque appears to be able to differentiate between these three bone quality groups.

Both implant types in this study are compressing the interfacial bone significantly during insertion. The resistance of the bone to this compression generates a rapid rise in insertion torque. This contrasts with the insertion torque profile which is seen when a standard Brånemark implant is placed with the prior use of the surgical tap (Figure 2.23). The slope of the graph represents the rate of application of energy to the system. From in-vitro work previously carried out this appears to be related both to the bone quality, the ratio of the pilot hole (final drill diameter) to implant diameter and the implant design. The effect of the ratio of the pilot hole (final drill diameter) to implant diameter is illustrated in Figure 2.24. A fresh bovine rib was selected and six implant sites were prepared with a variety of final drill diameters using the surgical site preparation described in Figure 2.1 and section 2.2.1. A 3.75mm diameter standard Brånemark implant was inserted into the prepared bone sites and the insertion torque was recorded using the method described in section 3.2.5. Keeping the bone quality constant but placing the implant into sequentially smaller diameter pilot holes increases the slope of the insertion torque graph. This effectively alters the ratio of pilot hole to implant diameter and thus the degree of compression induced in the interfacial bone (Figure 2.24).

Mean RFA value, like maximum insertion torque value, demonstrated no significant difference between the bone qualities 2 and 3, although a significant difference was observed between type 3 and type 4 bone. The similarity between the RFA values for implants placed into types 2 and 3 bone indicates that primary stability for these implants is close to the maximum achievable under the clinical conditions of this study. The significant drop in RFA value between types 2 and 3 bone and type 4

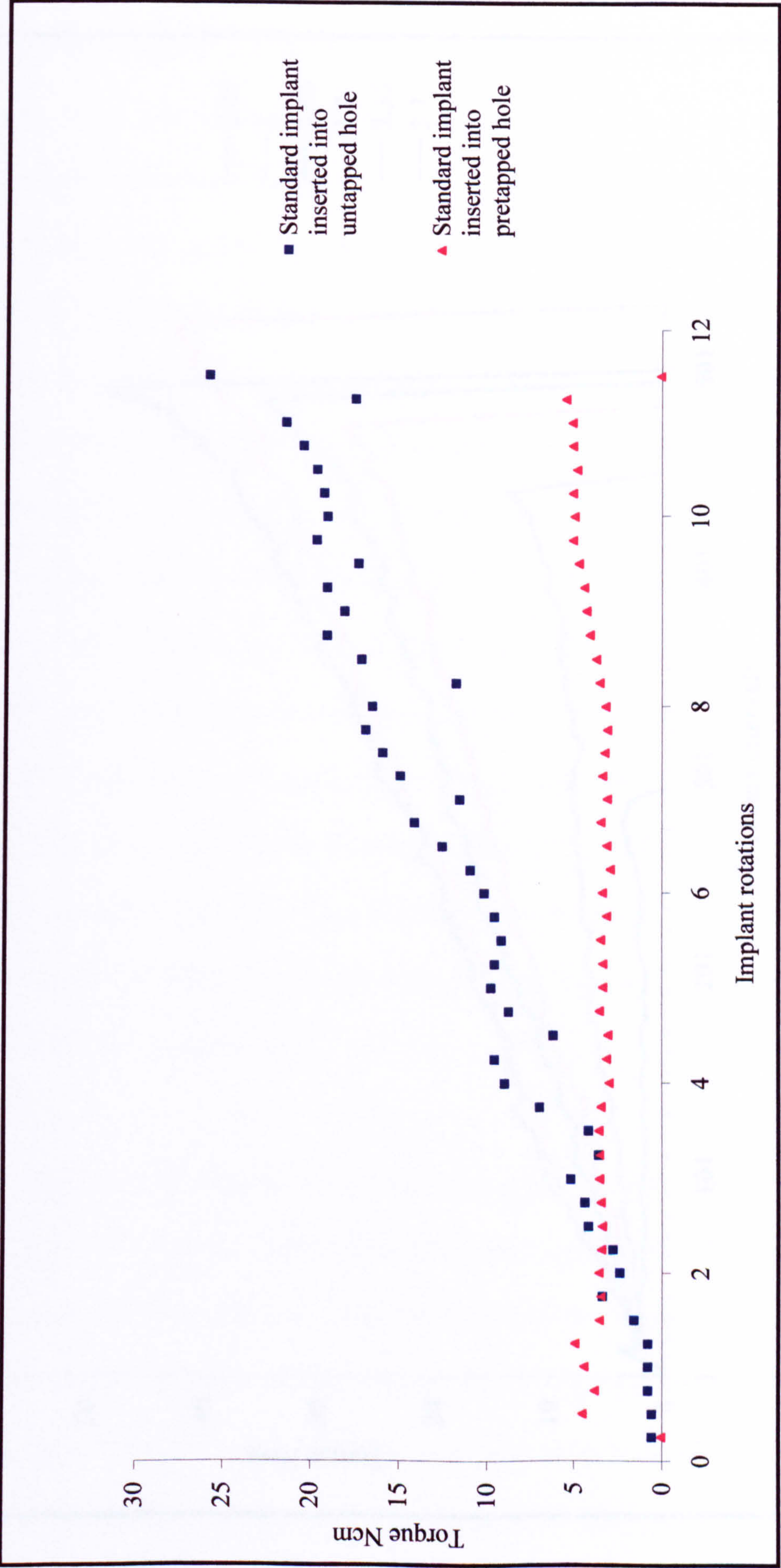


Figure 2.23: Comparison of Insertion Torque traces in this study with a standard Brånemark implant placed into a pre-tapped hole.

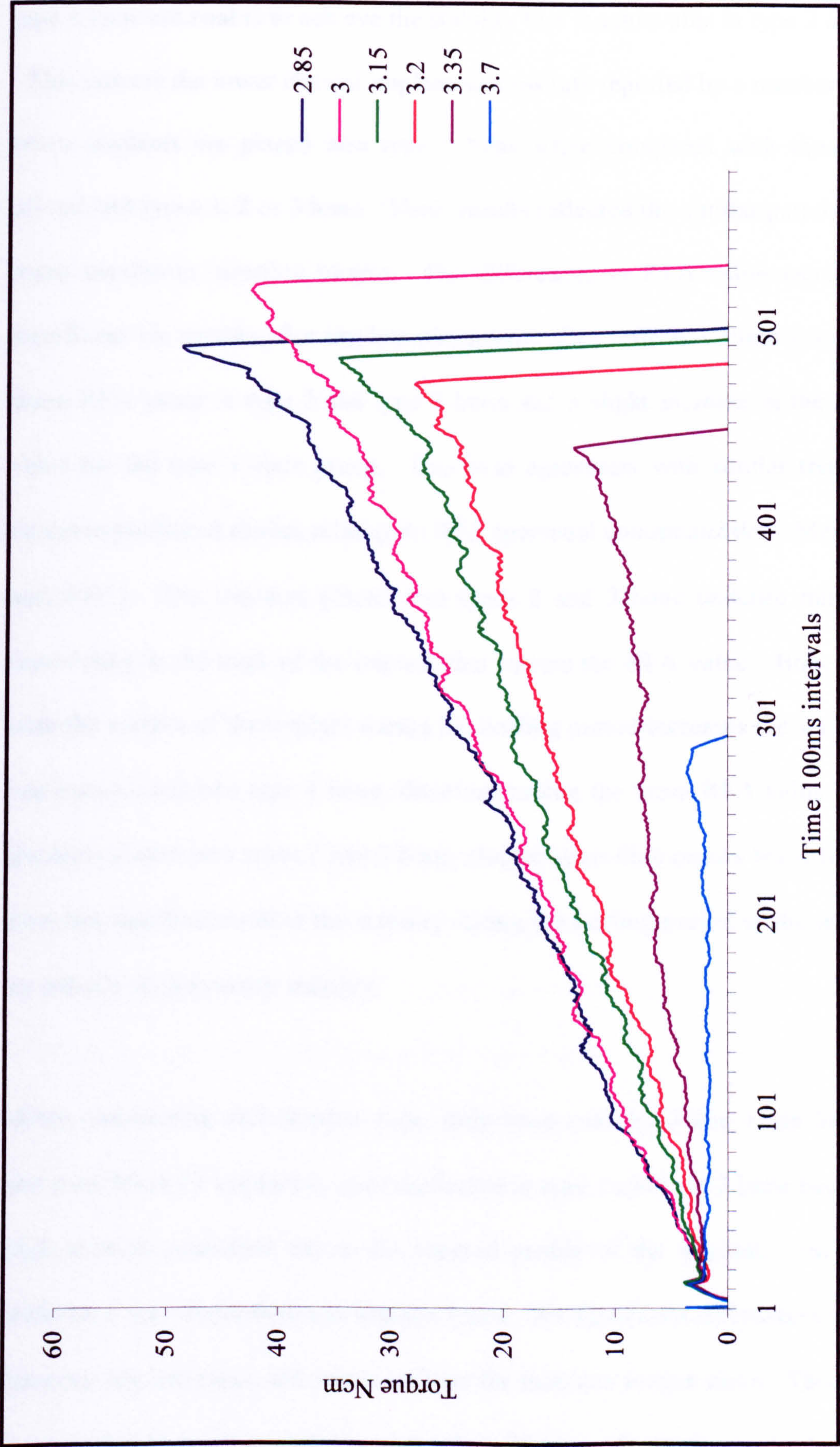


Figure 2.24: Insertion Torque profiles for 3.75mm diameter standard Nobelbiocare implant inserted into bovine spine using varying drill diameters.

bone indicates that the techniques used to maximise the primary implant stability in type 4 bone are unable to achieve the stability that is achievable in type 2 and 3 bone.

This mirrors the lower clinical implant success rate reported by a number of authors when implants are placed into type 4 bone when compared with those implants placed into types 1, 2 or 3 bone. These results reflected the similar pattern seen with mean maximum insertion torque. The differences in RFA value were no longer significant six months after implant placement. This reflects a slight decrease in the mean RFA value in type 2 and type 3 bone and a slight increase in the mean RFA value for the type 4 bone group. This is in agreement with similar trends seen in recent unpublished studies relating to RFA (personal communication, Meredith 2000 and 2001). The implants placed into types 2 and 3 bone undergo minimal bone remodeling at the neck of the implant that lowers the RFA value. Bone apposition onto the surface of the implant during the healing period increases the stability of the implants placed into type 4 bone, therefore raising the mean RFA value. For those implants placed into types 2 and 3 bone, similar apposition occurs but this apposition does not significantly alter the stability during the healing period as the implants had an initially high primary stability.

When considering each implant type, only bone qualities 3 and 4 can be compared since the Mark IV implant is contraindicated in type 1 and type 2 bone because of the high stresses generated due to the tapered profile of the implant. No significant difference was found between implant types. No significant differences were found between implant types and bone qualities for insertion torque slope. This appears to support the suggestion that the rate of application of energy to the bone in both

systems is similar and that neither implant system generates an insertion torque profile significantly different to the other.

For each implant type at implant placement mean RFA values are similar for type 3 bone quality, no significant difference was seen between standard and Mark IV implants. No significant difference was evident between Mark IV implants placed in type 3 and type 4 bone, appearing to indicate that the primary mechanical stability of Mark IV implants is less affected by bone quality. A significantly lower mean RFA value was obtained from the standard implants placed into type 4 bone quality when compared to type 3 bone quality. This appears to indicate that the method of placing standard implants without prior tapping is not as effective at maintaining a high implant primary stability. The stability of the standard implants is more affected by the quality of bone at the implant site.

For the purposes of this experiment the implants were uncovered at six months post insertion and a stability measurement was taken, this will be referred to as the secondary stability RFA value. Again, at second stage surgery, as at implant insertion no significant difference was seen between the mean RFA values for standard and Mark IV implants. For type 4 bone no significant difference is seen between standard and Mark IV. This is due to an increase in the mean RFA value for the standard implants during the healing period. This is in accordance with other studies evaluating the changes in RFA value between implant insertion and second stage surgery. The increase in mean RFA value for the standard implants during the healing period has been attributed to the deposition of bone at the bone/implant interface. This bone deposition increases the local support for the implant and

increases its stability. The Mark IV implant appears to maintain the high mean RFA value during the healing period that is seen at implant placement.

If maximum insertion torque is plotted against RFA value at implant insertion there appears to be a correlation between insertion torque and RFA value. This is in agreement with Friberg (1999) who also found a correlation. The correlation in this study is less pronounced and may be due to the use of two differing designs of implant. The poor correlation seen is of questionable value clinically and it is not surprising as RFA and insertion torque measure, and are affected by, different factors. Insertion torque is a measure of the energy required to insert an implant whilst RFA value is an indicator of interfacial stiffness and the stiffness of implant-adjacent bone in bending. At second stage surgery the spread of the data points is reduced which is a consequence of the increased stability of the standard implants placed into type 3 bone. Again this is in agreement with recent unpublished studies into RFA and the changes in RFA value following implant insertion (personal communication, Meredith 2000 and 2001).

When looking at the energy expended during implant insertion no significant difference was identified between the energy used to insert a standard implant into type 2 or type 3 bone. A difference was seen between the energy required to insert a standard implant into type 4 bone when compared to the other two bone qualities. A difference was seen between Mark IV implants placed into type 3 and type 4 bone, with less energy required to insert implants into type 4 than type 3 bone. Perhaps the most interesting finding is that less energy is used to insert a Mark IV when compared to a standard implant for each bone type. This appears to support the

manufacturers claim that the double thread reduces the insertion time and the energy dissipated to the bone at the bone/implant interface. The error in this method of measurement is unquantified but is assumed to be consistent across the implant types. Absolute values must be regarded with caution and cannot be taken to directly deduce the energy imparted to the bone, but they do reflect a definite trend. If less energy is used then less energy must be imparted to the bone.

CHAPTER 3

THE DEVELOPMENT OF AN IN-VITRO MODEL TO COMPARE THE PRIMARY STABILITIES OF DENTAL IMPLANTS

THE DEVELOPMENT OF AN IN-VITRO MODEL TO COMPARE THE PRIMARY STABILITIES OF DENTAL IMPLANTS

3.1 Aims and objectives

The comparative study of primary implant stability is affected by the natural variation in the mechanical properties of bone both between individuals and between implant sites within the same individual. Subtle differences in primary implant stability may be masked by the variations in bone properties. Particular difficulty is encountered when attempting to investigate primary implant stability in bone of poor quality. No satisfactory animal model exists for Type 4 bone (Lekholm and Zarb, 1985). Few implants are placed clinically into sites of poor bone quality. This can be attributed to the well documented high implant failure rate in bone of poor quality and the ethical consequences of putting a patient through surgery and possible implant failure. The purpose of this study was to develop a homogeneous, predictable model to simulate Type 4 quality bone. The aim was to compare the primary stability characteristics of differing designs of implant in a poor bone model material. A model was used in an attempt to overcome the inherent variability in human bone of Type 4 quality, which may introduce variability into the results and mask any differences between the implant designs.

3.2 Method

3.2.1 Baseline clinical data

Baseline insertion torque data was gathered using a modified electronic torque controller (Nobel Biocare AB, Gothenburg, Sweden) connected to an analogue to digital data acquisition card (DAQCard AI-16XE-50, National Instruments, UK Ltd,

UK) and laptop computer. Data were recorded at the rate of 10 samples per second. Eight recordings of insertion torque of a Mark II self-tapping fixture (Nobel Biocare AB, Gothenburg, Sweden) were taken from the posterior maxillary bone of four unembalmed human cadavers, which were considered clinically to be from sites of Type 4 quality bone. The same implant was used for each recording because a variation of $\pm 20\%$ cutting efficiency exists between implants (personal communication, Nobelbiocare, Sweden). A composite mean recording from these tracings of insertion torque was then produced and taken as a reference from which a synthetic bone model could be formulated (Figure 3.1).

3.2.2 Specimen preparation

Three different formulations of rigid foam polyurethane were used for the specimen manufacture: RM520W (Baxenden Chemicals Ltd., Lancashire, UK), DF0309 (Polymed, Cardiff, U.K.), and DF0314 (Polymed Ltd, Cardiff, U.K.). Foam specimens of varying density were made using an aluminium mould (Figure 3.2). The temperature of the mould was controlled at $30 \pm 5^\circ\text{C}$ by pumping water from a thermostatically controlled water bath through channels in the outer plates of the mould. Specimen density was varied by altering the shot size of polyurethane introduced into the mould. The insertion torque characteristics were tested by inserting a Mark II self-tapping fixture into each sample. The insertion torque plots for each sample were then compared to the mean Type IV bone tracing in order to identify the foam that most closely reproduced the insertion torque characteristics from the cadaver bone. It was found that DF0314 at a foam density of 0.4g/cm^3 , closely approximated the mechanical properties of Type IV bone (Figure 3.3).

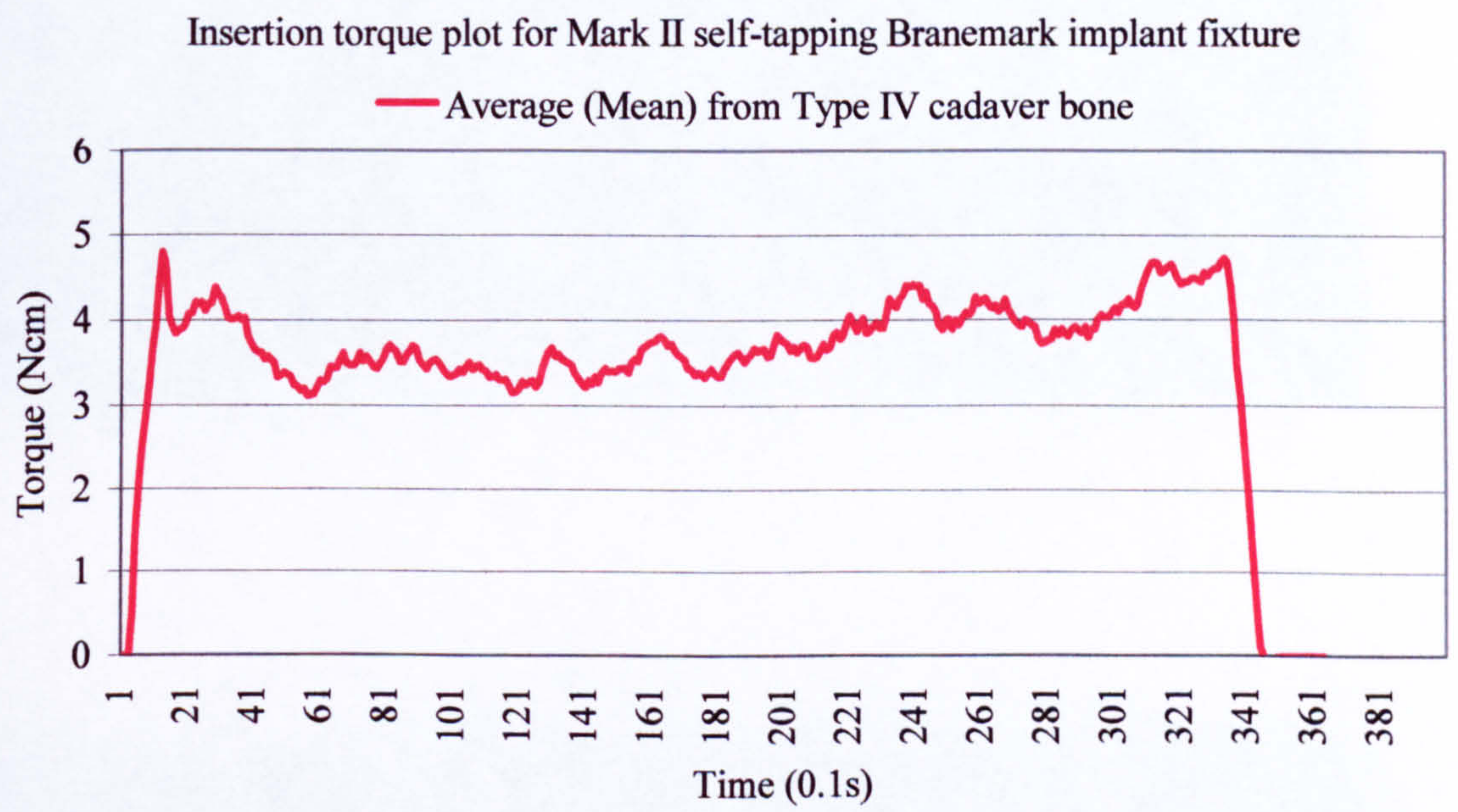


Figure 3.1: Baseline insertion torque data from cadaver specimens.

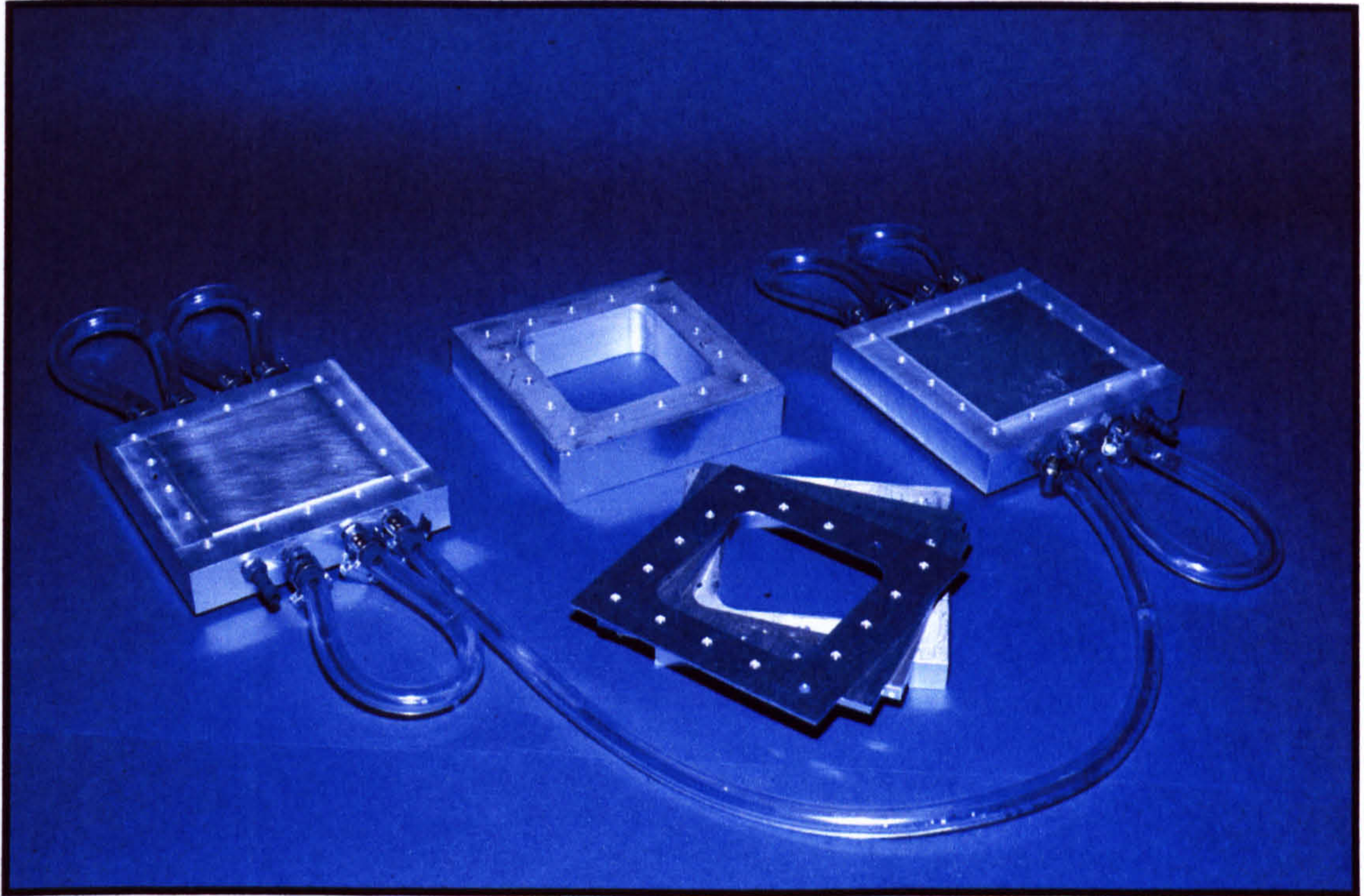


Figure 3.2: Casting moulds for polyurethane foam.

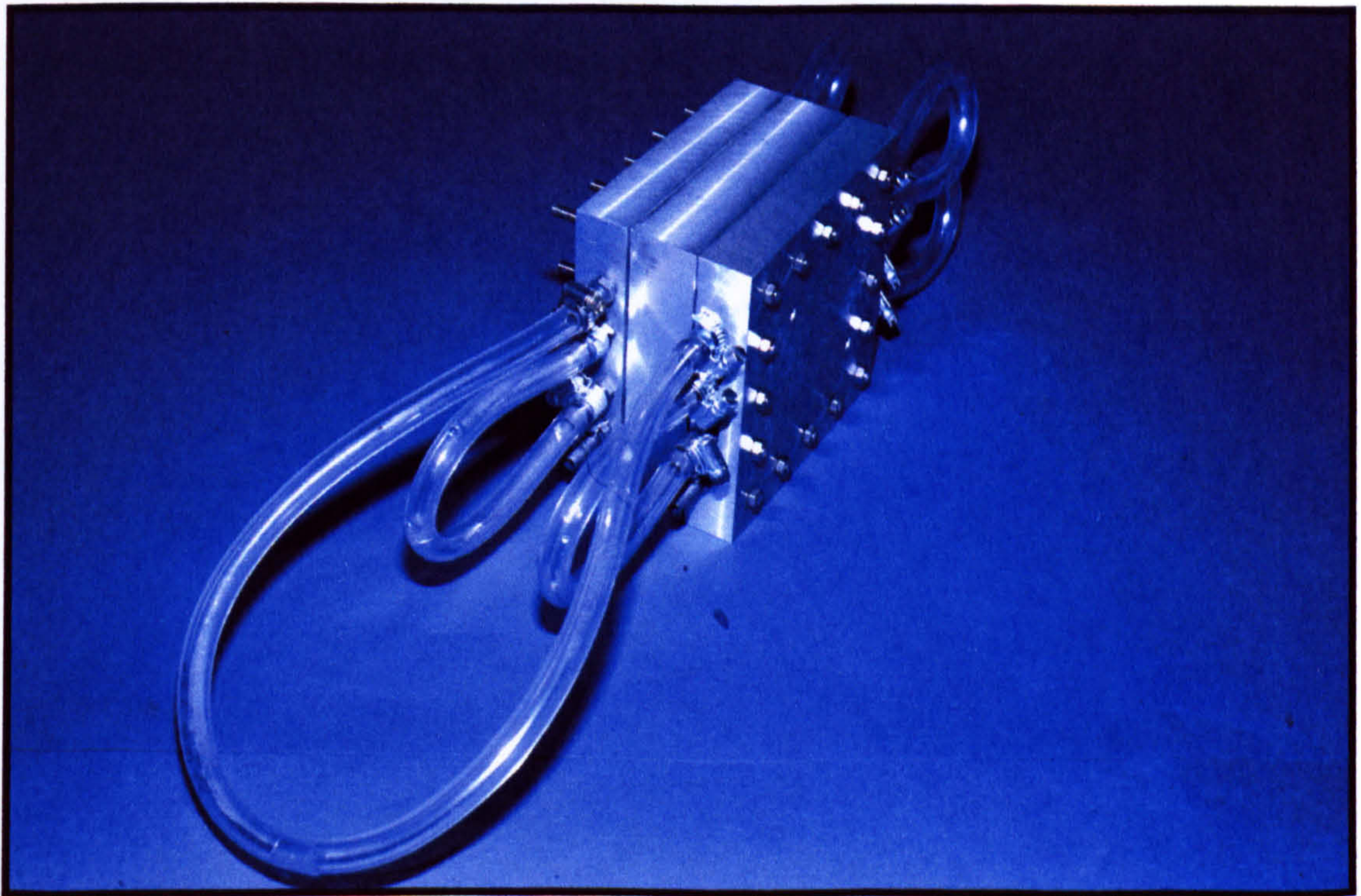


Figure 3.2: Aluminium moulds for polyurethane foam.

3.2.3 Implant insertion data

First donor implant types

Branemark fixture of Type IV

Tapping force direction

Mark IV self-tapping

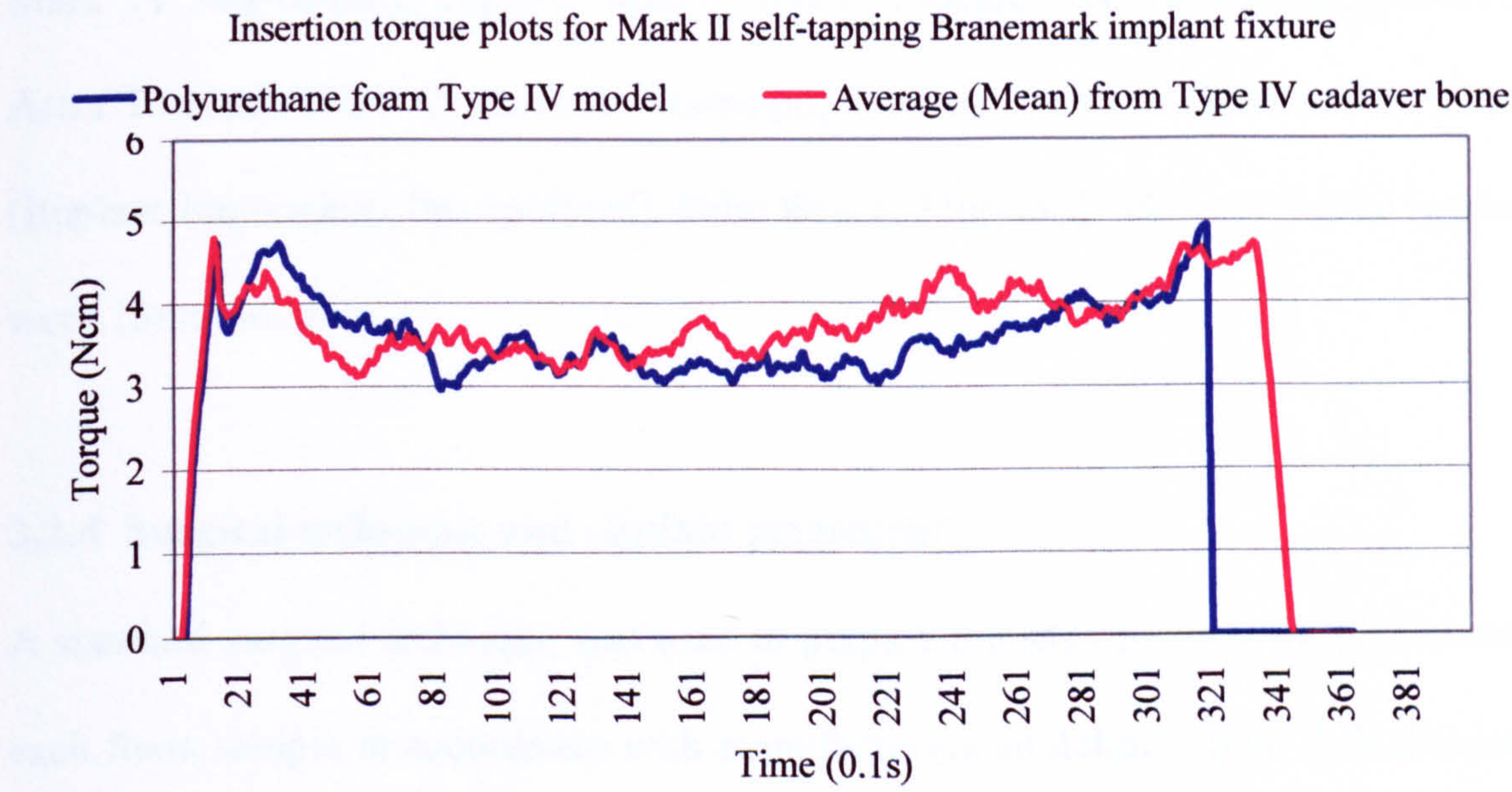


Figure 3.3: Comparison of baseline insertion torque data from cadaver specimens and polyurethane foam model.

3.2.5 Data Collection

Following the preparation, torque during implant insertion was

collected and recorded using a digital torque wrench (Model 100000, 100000

3.2.3 Implant characteristics

Five dental implant types were used (Figure 3.4). The standard 4mm diameter Brånemark implant, STA (Nobel Biocare AB, Gothenburg, Sweden), Mark II self-tapping 4mm diameter implant, MKII (Nobel Biocare AB, Gothenburg, Sweden), Mark IV self-tapping implant, MKIV (Nobel Biocare AB, Gothenburg, Sweden), Astra Tioblast, TIOB (AstraTech, Mölndahl, Sweden), and the 3i Osseotite, OTI (3i Implant Innovations Incorporated), Palm Beach, Florida, USA). All of the implants were 13mm long.

3.2.4 Surgical technique and implant placement

A standard surgical technique was used to prepare the sites for implant placement in each foam sample in accordance with manufacturers guidelines; final drill diameters of 3mm were used for the STA, MKII, OTI, and MKIV. For the TIOBL implants a final drill size of 3.7mm diameter was used in accordance with manufacturers guidelines for poor bone. The STA implant was placed using two differing techniques. In the usual clinical situation a surgical tap is used to prepare a tapped threaded channel in the bone prior to inserting the implant. Ten samples were prepared in this way and 10 samples were prepared without the use of the surgical tap in an attempt to determine the effect of tapping upon the primary stability of this implant in Type IV bone. None of the implant sites were countersunk and irrigation was not used. 60 implants were placed in total.

3.2.5 Data Collection

Following site preparation, torque during implant insertion was recorded using a modified electronic torque controller (Nobel Biocare AB, Gothenburg, Sweden)

connected to an analogue to digital data converter card (AD-16-02-03, National Instruments UK Ltd, Newbury, Berkshire, UK) and laptop computer. Data were recorded at the rate of 10 samples per second. Following implant placement, resonance frequency measurements were made according to the method described by

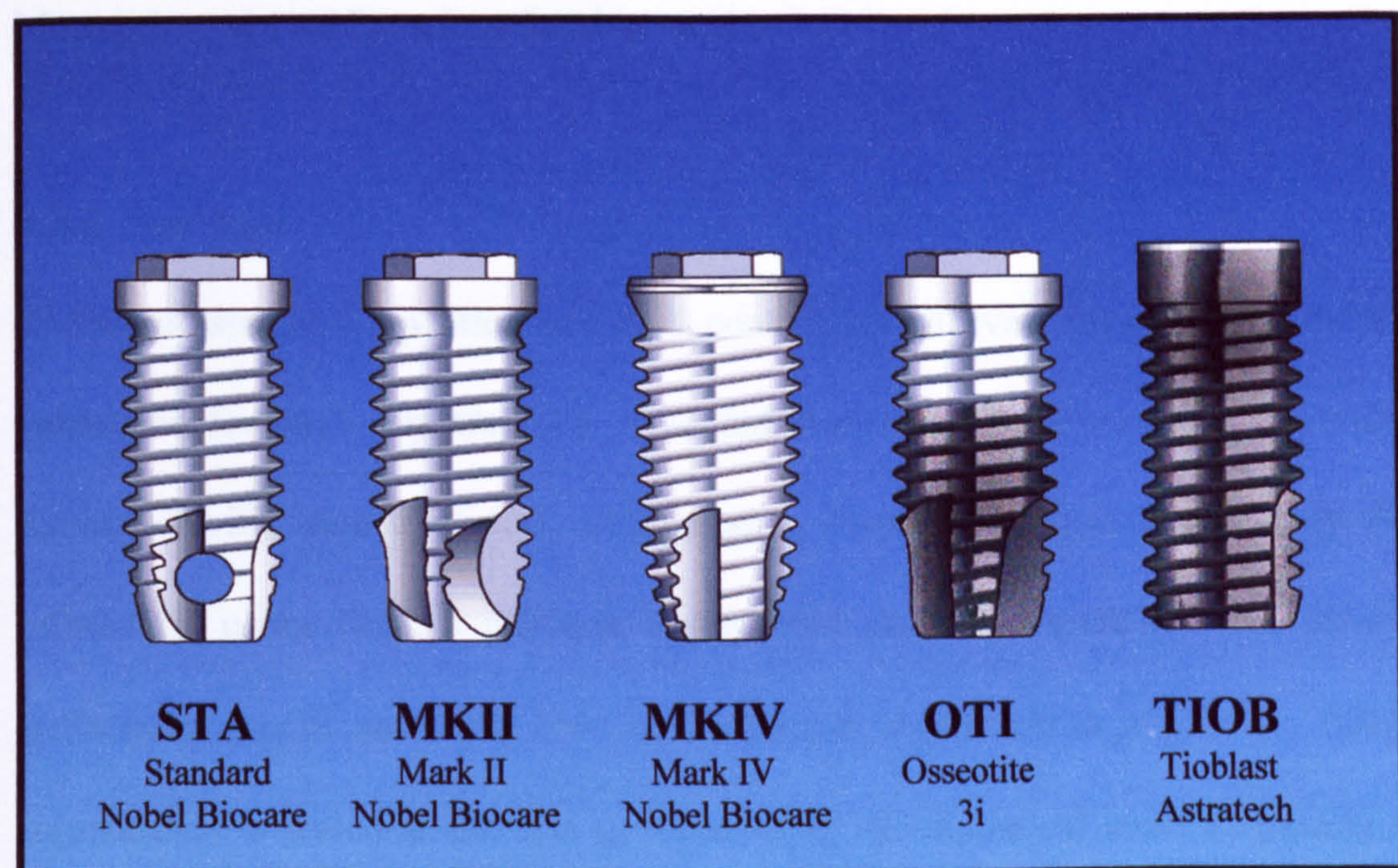


Figure 3.4: Implant types.

3.3 Results

Figure 3.5 shows the mean peak insertion torque and 95% confidence intervals for each implant type. Figure 3.6 shows the mean resonance frequency data with 95% confidence intervals against the different implant types. The resonance frequency values and mean peak torque data are summarised in Table 3.1.

connected to an analogue to digital data acquisition card (DAQCard AI-16XE-50, National Instruments UK Ltd, Newbury, Berks, UK) and laptop computer. Data were recorded at the rate of 10 samples per second. Following implant placement resonance frequency measurements were made according to the method described by Meredith et al (1997) and outlined in section 2.2.5.

3.2.6 Statistics

The mean, standard deviation and 95% confidence intervals for each parameter were calculated for each implant type. The individual values were compared using the Kruskal-Wallis statistical test, comparisons between implant types were further refined by using Dunn's multiple comparison test. Differences were considered statistically significant at $p \leq 0.05$ and extremely significant at $p \leq 0.001$. Statistical significance is stated in the text as reported by the statistical analysis package used (WinSTAT® version 2000.1 R.Fitch Software, USA). It is recognised by the author that the degree of statistical significance may be of questionable value and it is more meaningful to determine whether a significant difference is evident rather than its degree of significance.

3.3 Results

Figure 3.5 shows the mean peak insertion torque and 95% confidence intervals for each implant type. Figure 3.6 shows the mean resonance frequency data with 95% confidence intervals against the different implant types. The resonance frequency values and mean peak torque data are summarised in Table 3.1.

	STA untapped	STA	MKII	MKIV	TIOBL	OTI
Mean Peak Insertion Torque (Ncm)	5.15	3.6	5.27	8.79	4.7	5.63
S.D.	0.59	0.2	0.62	2.02	0.17	0.78
Confidence 95%	0.47	0.17	0.54	1.62	0.14	0.68
	STA untapped	STA	MKII	MKIV	TIOBL	OTI
Mean Peak Res. Freq. (kHz)	5.82	5.29	5.61	5.88	5.74	5.79
S.D.	0.14	0.61	0.14	0.21	0.25	0.28
Confidence 95%	0.11	0.53	0.12	0.17	0.2	0.27

Table 3.1: Summary of Insertion Torque and RFA data (n=60).

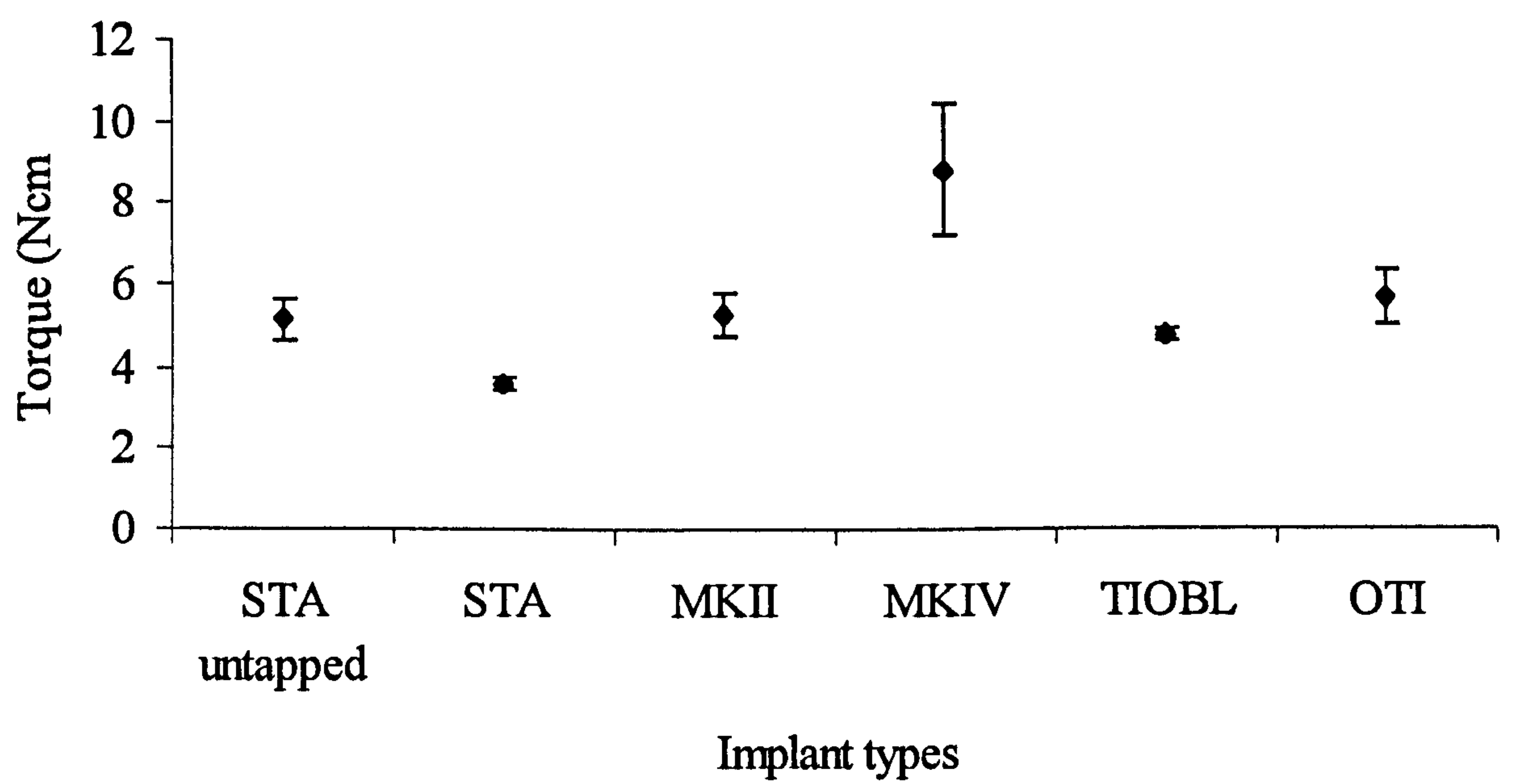


Figure 3.5: Mean peak insertion torque values for the five implant types placed into the polyurethane foam model. Mean values with 95% confidence intervals are shown (n=60).

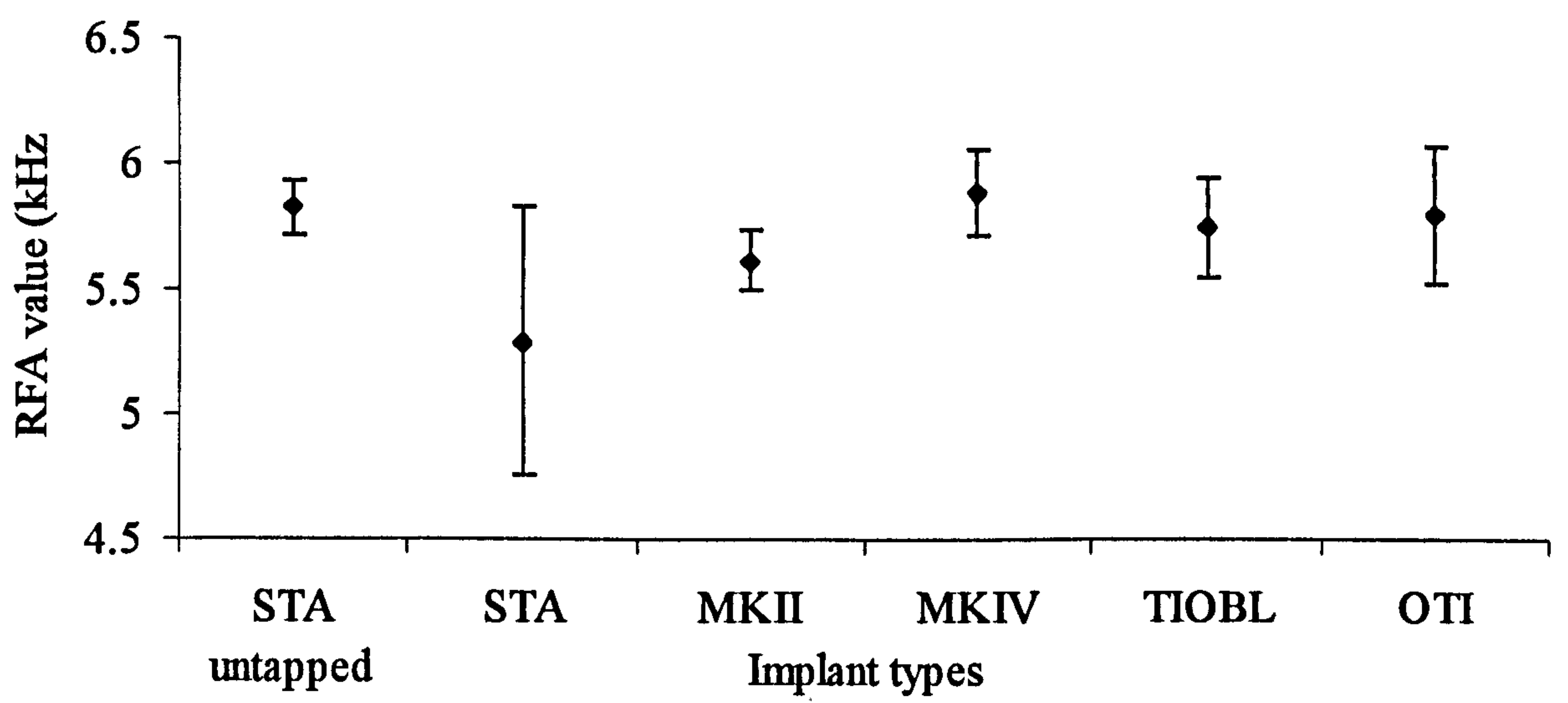


Figure 3.6: Mean resonance frequency values for the values for the five implant types placed into the polyurethane foam model. Mean values with 95% confidence intervals are shown (n=60).

No statistically significant difference in resonance frequency value was seen between different implant types ($p > 0.05$). A statistically significant difference ($p < 0.05$) was noted between the mean peak insertion torque values for the MKIV and the TIOB implants. The difference between the mean peak insertion torque values for the MKIV and the STA was identified as highly significant ($p < 0.001$).

3.4 Discussion

3.4.1 Discussion of the method

Initial primary stability of an implant is a function of bone quality and quantity, implant geometry and the placement technique. The aim of this study was to compare the primary stability characteristics of five differing designs of fixture when placed into a substrate approximating bone of poor quality. In order to predict the outcome and success rate of implant placement attempts have been made to pre-operatively assess bone quality using both conventional radiography and CT scanning. These methods can give a very good indication of bone quantity and CT scanning is of particular value in providing the surgeon with a three dimensional view of bone distribution. They can however provide only minimal data relating to bone quality. Lekholm and Zarb (1985) proposed a system based on both interpretation of radiographs and the clinical impression of cutting resistance gained by the surgeon when drilling and tapping the implant site. Bone Type 4 relates to the clinical situation where a thin layer of cortical bone surrounds a core of low density trabecular bone and this is the least favourable situation for implant placement. This classification system is a useful indicator of bone quality and quantity but it is highly subjective and can only be usefully used to provide a broad indicator of the mechanical properties and quantity of bone. In order to provide a more quantitative

method of predicting bone quality Johansson and Strid (1994) looked at the recordings of insertion torque gathered during implant placement using a modified electronic torque controller connected to a computer. They proposed a method of calculating the cutting resistance from the energy used when tapping an implant site. The aim of this would be to be able to relate the cutting resistance measurement to the bone quality at the implant site. It would be reasonable to assume that greater resistance is encountered when bone of good quality is tapped when compared to bone of poorer quality. This does indeed appear to be the case and Friberg et al (1995) have been able to demonstrate a correlation between cutting resistance measurements and bone density.

Primary stability of implants has traditionally been very difficult to assess and is often reduced to a simple assessment of mobility, this is very subjective even when attempts have been made to use electronic devices. A non-invasive technique for assessing the stability of a fixture immediately after placement has been described by Meredith et al (1996a and b) and reported upon in a number of studies both in vitro and in vivo. The technique measures the resonance frequency of a small piezoelectric transducer, which may be attached via a screw fixing to an implant or to a transmucosal abutment. The aim of the technique is to assess the interfacial stiffness between the fixture and the bone, and local bone stiffness in bending. The technique allows an initial assessment of stability to be made immediately after placement and to be able to monitor the increase in this stiffness with osseointegration over time.

A polyurethane foam model was chosen for this study because of the known variability in the mechanical properties of bone itself. This variability can present problems in the interpretation of results. De Coster et al (1990) showed that polyurethane foam has similar mechanical properties to bone. The resonance frequency technique used in this study has been shown, in preliminary work, to be sensitive to the size and shape of material samples. In certain cases the size and shape of the material sample can create a resonance mode, or multiple modes, which may interfere with the resonance mode of the fixture. A number of different sample sizes and shapes were tested and it was found that a cylindrical specimen 30mm in length and 20mm diameter reduces the formation of multiple modes and allows clear interpretation of the resonance mode relating to the fixture being tested. The model used in this study failed to show the clear differences in RFA value and insertion torque seen with bone, this may be due to the lack of a layer to represent the cortical bone layer. In bone, the cortical layer has been demonstrated previously as being of great significance in implant primary stability and its absence may have significantly affected the results in this study.

3.4.2 Discussion of the results

All of the implants when placed into the polyurethane foam gave mean resonance frequencies between 5.29 and 5.88 kHz. These values would be comparable to implants placed into bone of poor quality clinically. The STA placed into a pre-tapped hole gave the lowest mean resonance frequency values of those implants tested. The use of a surgical tap prior to implant insertion suggests that the implant meets very little resistance during insertion into the threaded channel. This leads to a very low peak insertion torque and low primary stability when placed into trabecular

bone of a loose structure such as the bone simulated by the polyurethane model. The untapped standard implant demonstrated the second highest RFA reading; which could be attributed to the insertion technique. The STA implant is a c.p. titanium screw with bone clearance chambers in the lower portion of the implant but no effective cutting surfaces and typically it is inserted into a pre-tapped hole. Experienced surgeons will, on occasion, place the implant into an untapped hole if they feel that the bone quality at the insertion site is poor and they wish to enhance stability. As the implant lacks any cutting surfaces the thread profile is formed within the bone by locally compressing the interfacial bone during insertion and this local compression is used to enhance the primary stability. Industrial thread-forming rather than thread cutting screws and fastenings are frequently used in conjunction with soft woods and plastics but the usefulness of this technique is often overlooked clinically when discussing poor bone quality. The data in this study appears to confirm the enhancement in primary implant stability. The MKII implant is a self-tapping cylindrical threaded implant, which was not specifically designed for high primary stability in poor bone. It has three large cutting surfaces at its tip and large bone clearance chambers to allow it to tap effectively into the bone. Whilst beneficial for cutting and tapping, these appear to reduce the primary stability of this implant in the poor bone model. The peak insertion torque generated by the MKII is comparable with the standard implant placed into an untapped hole, but the mean RFA value is 200Hz lower suggesting a lower primary stability. The OTI implant is a self-tapping implant by a different manufacturer but the thread form and cutting facets are broadly similar to the MKII. The lower threads of the implant have an HCl/H₂SO₄ acid etched surface which the manufacturers claim enhances osseointegration. In this study the roughened surface of the implant did not appear to

affect the insertion torque or primary stability characteristics of the implant when compared to the machined titanium surface of the MKII implant. The OTI demonstrated a peak insertion torque and RFA value similar to the MKII. The TIOB implant gave a mean peak insertion torque slightly lower than the MKII and OTI implants; this is possibly due to the implant being inserted into a wider diameter hole compared to the other two implant types. The mean RFA value for the TIOB implant was the second highest of all of those tested at 5.79 kHz indicating that a lower insertion torque does not necessarily lead to a low primary stability, with the thread profile and the implant geometry also playing a role in the stability after placement. The MKIV implant showed the highest RFA value of those implants tested. This implant has been designed with a tapered profile and combines the properties of a thread cutting and a thread-forming implant. The lower portion of the implant has thread-cutting facets that engage the bone surface and begin insertion. The upper portion of the implant is tapered to gradually compress the local bone during insertion to gain enhanced primary stability. This tapered design leads to a consistently much higher peak insertion torque than that generated during the insertion of the other implant designs tested. In this study it appears that the MKIV implant has design features that lead to an increased primary stability when compared with other implants currently available. Clinical studies are currently in progress to evaluate the performance of this MKIV fixture and it is hoped that comparison may be made between the primary stability data collected clinically with the data presented in this study. The synthetic bone model has been shown to be a useful addition to currently available testing techniques for the assessment of the insertion characteristics and primary stability of dental implants.

CHAPTER 4

THE COMPARISON OF THE PRIMARY STABILITY OF DIFFERING IMPLANT DESIGNS IN A CADAVER MODEL

THE COMPARISON OF THE PRIMARY STABILITY OF DIFFERING IMPLANT DESIGNS IN A CADAVER MODEL

4.1 Aims and objectives

The aim of this study was to assess the primary stability characteristics of five differing designs of dental implants when placed into bone of varying qualities. To do this a human cadaver model was used in an attempt to closely approximate the clinical situation. A number of different dental implant designs are currently in clinical use. A successful outcome to implant placement is thought, at least in part, to be due to the primary stability of an implant after placement. Little data is available to be able to compare the primary stability characteristics of different implant designs. This investigation compared the primary stability of five types of endosseous dental implant of varying geometry and surface topography (section 4.2.2).

4.2 Method

4.2.1 Subjects

Nine human cadavers were used in the investigation, of which 5 were female and 4 male. Their ages ranged from 65 to 79, with a mean of 71 years. All cadavers were less than 48 hours post mortem with most being tested within 30 hours; the bodies were stored at 4°C. All of the included subjects were verified free from bone pathology by a consultant pathologist and fully edentulous. All implants were placed in maxillary bone, as it was frequently impossible to gain access to the mandible due to the rigor of the facial tissues.

4.2.2 Implant characteristics

Five dental implant types were used (Figure 3.4). The standard Brånemark implant, STA (Nobel Biocare AB, Gothenburg, Sweden), Mark II self-tapping implant, MKII (Nobel Biocare AB, Gothenburg, Sweden), the Mark IV self-tapping tapered implant, MKIV (Nobel Biocare AB, Gothenburg, Sweden), the Astra Tioblast, TIOB (AstraTech, Mölndal, Sweden), and the 3i Osseotite, OTI (3i Implant Innovations Incorporated), Palm Beach, Florida, USA). All of the implants used were 13mm long.

4.2.3 Surgical technique and implant placement

A standard surgical technique was used to prepare the sites for implant placement in the maxillary bone of each cadaver. Manufacturers guidelines were followed for each of the implant systems tested. A 2 mm pilot drill was used for all implant sites. Final drill diameters of 3mm were used in bone of Type 3 and 4 quality when placing MKIV, however difficulty was experienced in fully seating the MKIV implants in Type 2 bone and a final diameter of 3.35mm was used in these sites. The same final drill diameters were used when placing STA and MKII to allow comparison with the MKIV implants. 3.35mm diameter drills were used to place the OTI, and a 3.75mm final drill was used for the TIOB in accordance with the manufacturer's guidelines for implant insertion into maxillary bone. None of the implant sites were countersunk. Due to the mean temperature of the cadavers being only 4°C irrigation was not used and all of the implants were inserted at the same low rotational speed. To enable direct comparison of different implants in bone of comparable quality and quantity, implants were placed symmetrically in opposing sides of the maxilla, with

comparison implants (STA, NBC, TIOB and OTI) in the left side of the maxilla and the MKIV in the right side. Fifty-two implants were placed in total.

4.2.4 Assessment of bone quality

The bone quality at each placement was assessed by the operator according to the system described by Lekholm and Zarb (1985). The assessment of the bone quality was achieved by the combined tactile impression of the bone quality at placement and the appearance of the bone at the implant site following implant removal. Due to the subjective nature of this test, care was taken to obscure computer measurement of insertion torque from the operator making the bone quality assessment.

4.2.5 Data Collection

Following site preparation, torque during implant insertion was recorded using a modified electronic torque controller (Nobel Biocare AB, Gothenburg, Sweden) connected to an analogue to digital data acquisition card (DAQCard AI-16XE-50, National Instruments, UK Ltd, UK) and laptop computer. Data were recorded at the rate of 10 samples per second. Angular displacement of each implant was measured using a Hall effect rotary encoder mounted on the handpiece motor. Following implant placement resonance frequency measurements were made according to the method originally described by Meredith et al (1996). The resonance frequency analysis equipment consists of a transducer, which is attached to the implant, this in turn connects to a custom designed frequency response analyser and a portable laptop computer. The transducer is an L-shaped cantilever beam, which is connected to the implant via a screw attachment. A piezoelectric crystal on the vertical of the L-shaped beam is used to stimulate the implant/transducer complex across a swept

frequency range of approximately 2 to 20 kHz, this range is generated by the frequency response analyser. A second piezoelectric crystal on the opposite side of the beam is used as the receiving element to detect the resonance frequency peak. The data was collected, stored and analysed on the computer.

4.2.6 Statistical analysis

The small number of samples (n) for each implant/bone quality subset precluded meaningful statistical analysis between these subsets. Overall comparison between implant types across all bone qualities was possible using analysis of variance (ANOVA) and where a significant difference was determined the Bonferroni multiple comparison test was performed with the significance set at $p = 0.05$.

4.3 Results

4.3.1 Insertion Torque

The insertion depth (ID) was calculated as a function of the angular displacement (θ) and the thread pitch (TP) of each implant.

$$\frac{\theta}{TP} = ID$$

Figures 4.1 to 4.3 illustrate three plots showing typical insertion torque\displacement plots for the MKII, MKIV and OTI implant types when placed into Type 2 bone. Mean values for peak insertion torque with 95% confidence intervals for bone Types 2 to 4 are illustrated in Figures 4.4 to 4.6. Peak insertion torque was calculated as the highest torque value obtained from the insertion torque plot for each implant. Figures 4.7 to 4.9 show mean values with 95% confidence intervals for peak removal

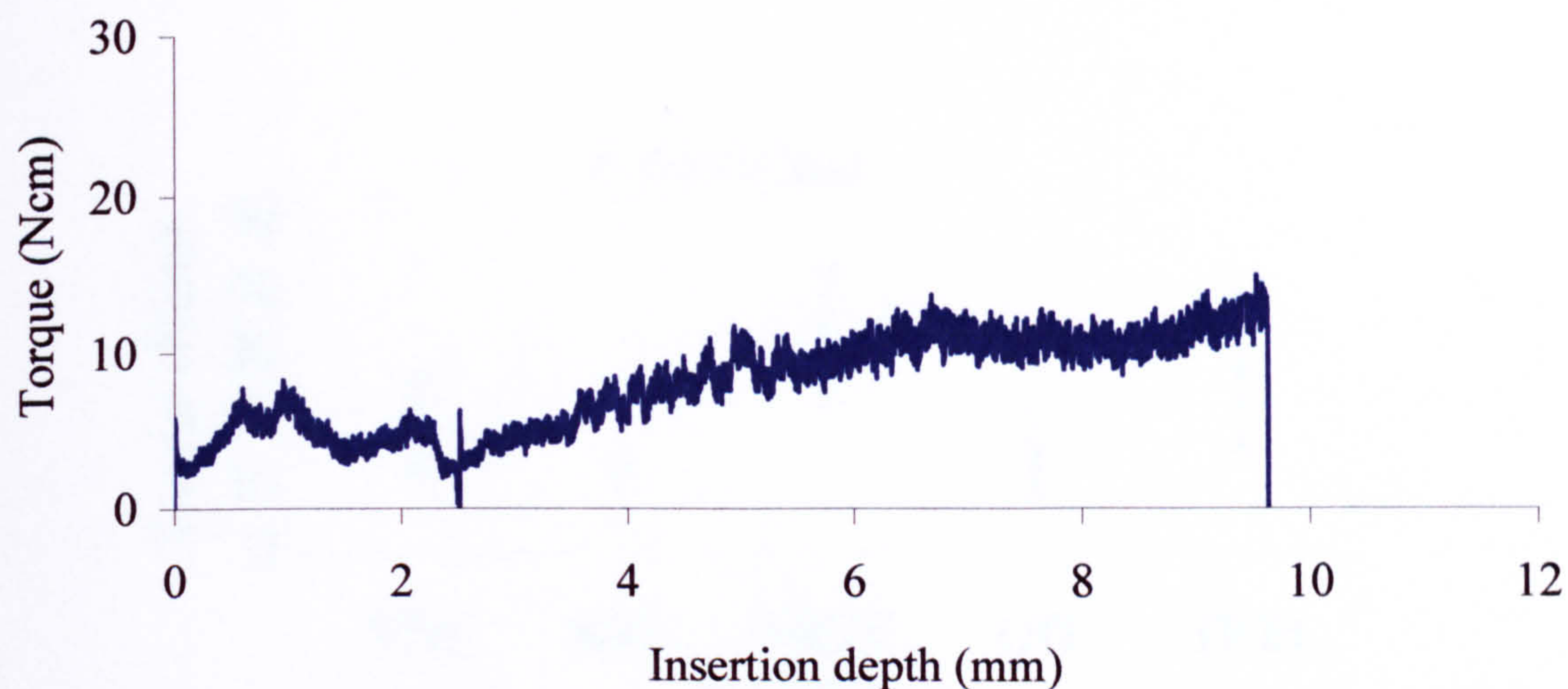


Figure 4.1: Insertion torque/displacement profile for a Mark II implant

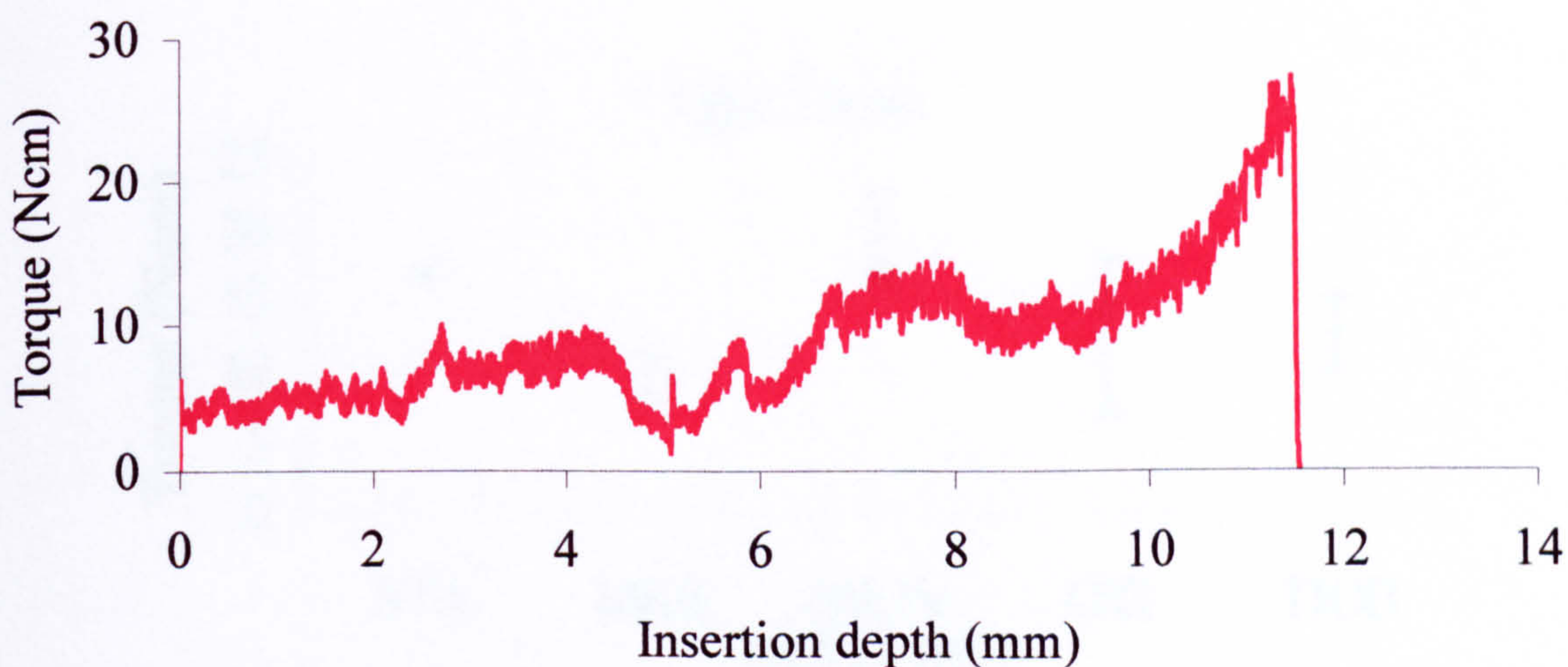


Figure 4.2: Insertion torque/displacement profile for a Mark IV implant

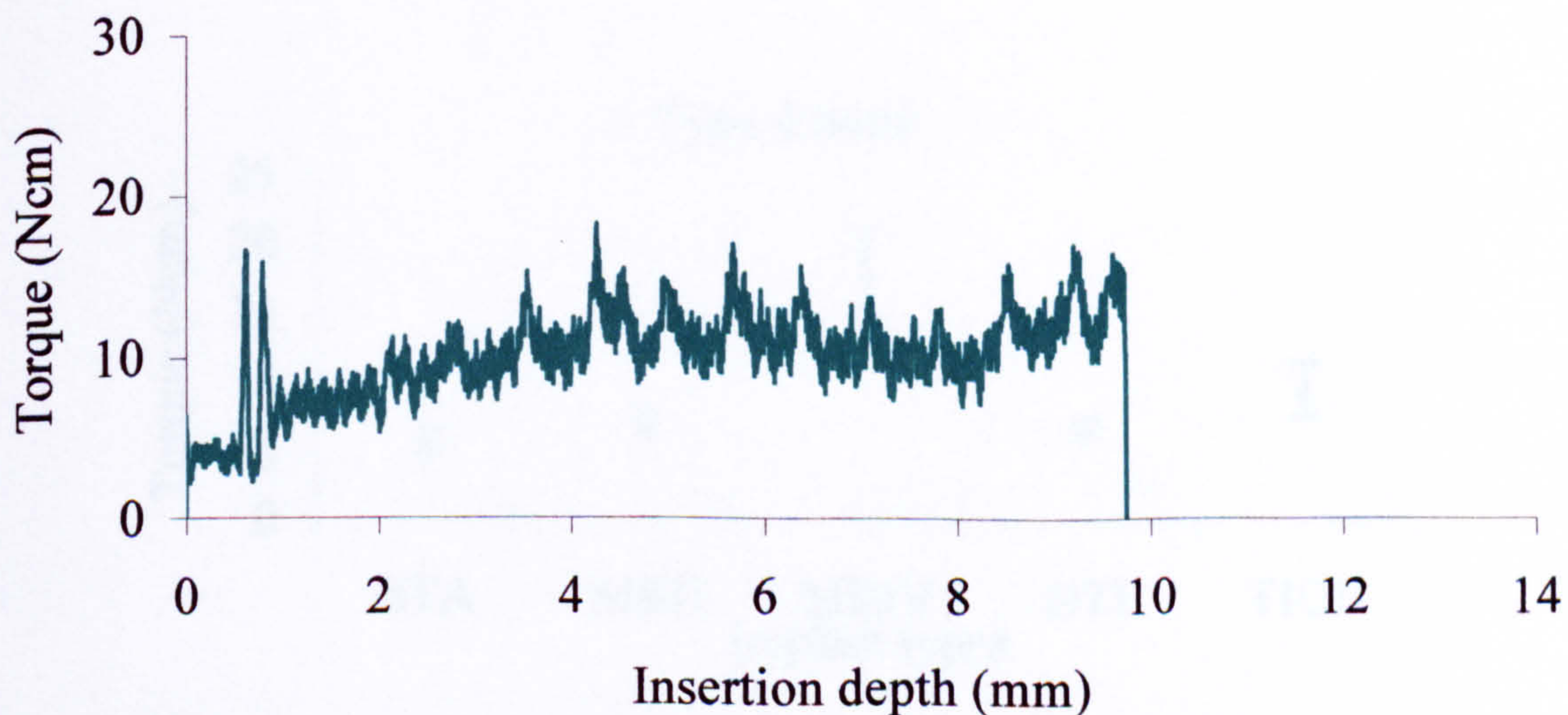


Figure 4.3: Insertion torque/displacement profile for an Osseotite implant

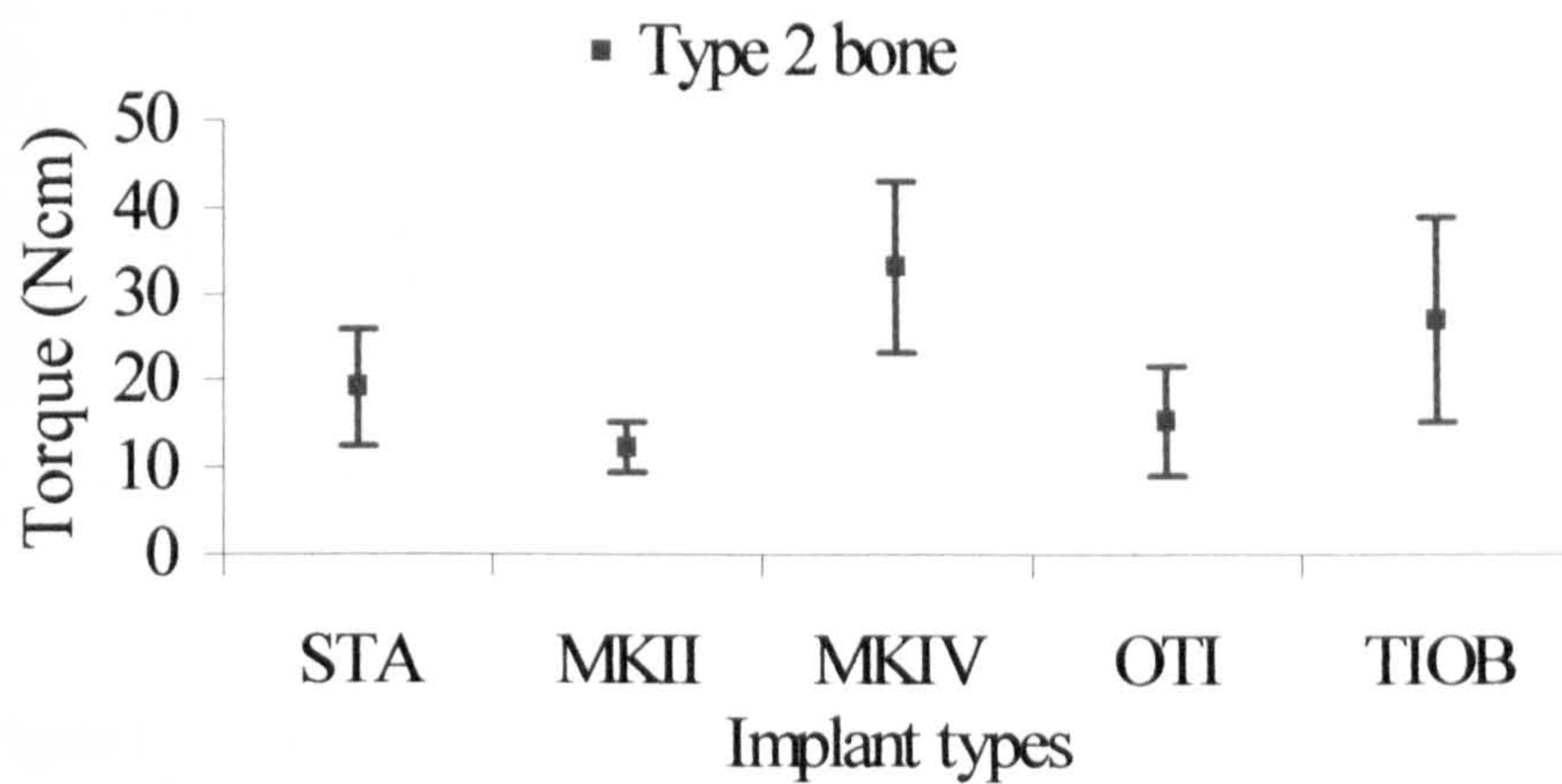


Figure 4.4: Peak insertion torque values for each implant type in Type 2 bone. Mean values and 95% confidence intervals are shown. (n=20).

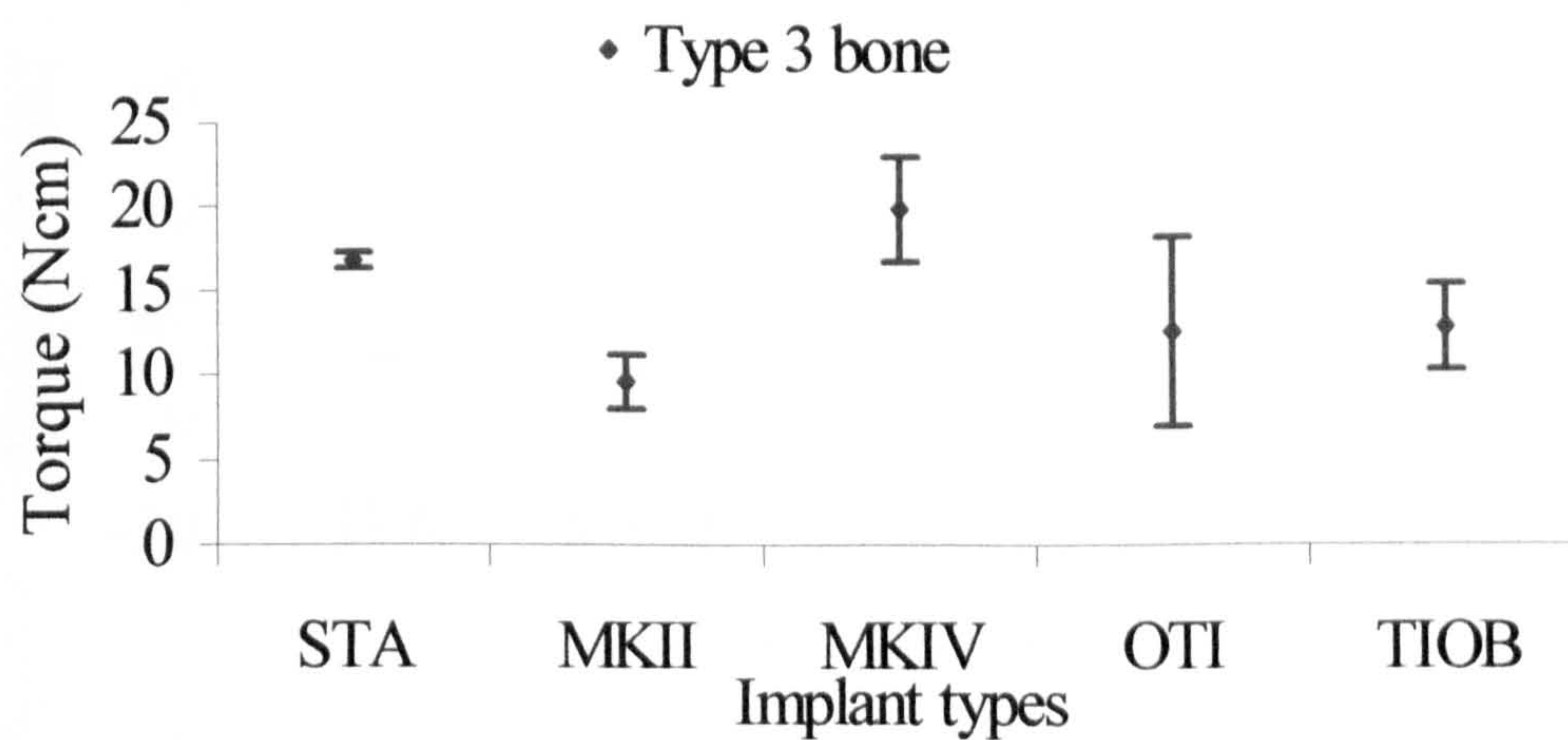


Figure 4.5: Peak insertion torque values for each implant type.in Type 3 bone Mean values and 95% confidence intervals are shown. (n=17).

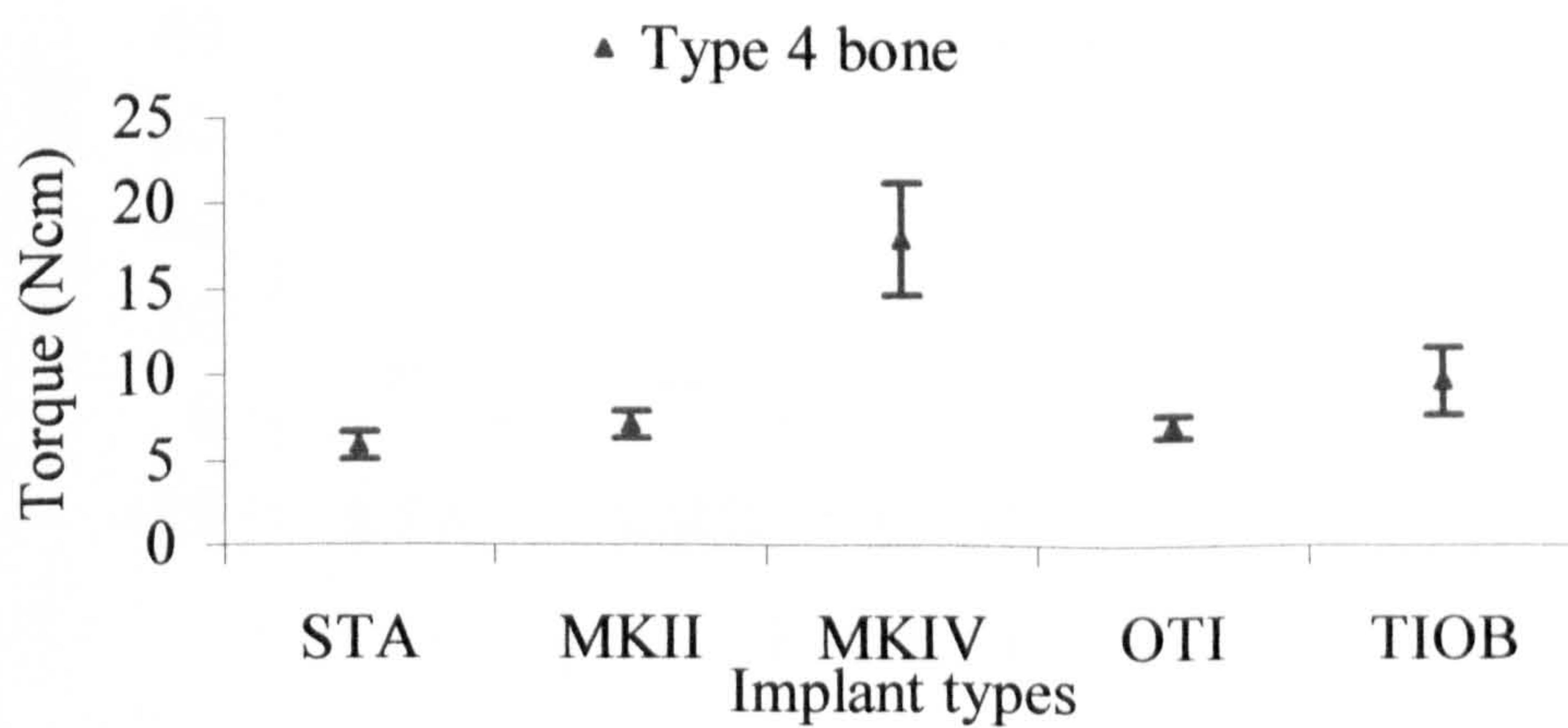


Figure 4.6: Peak insertion torque values for each implant type in Type 4 bone. Mean values and 95% confidence intervals are shown. (n=10).

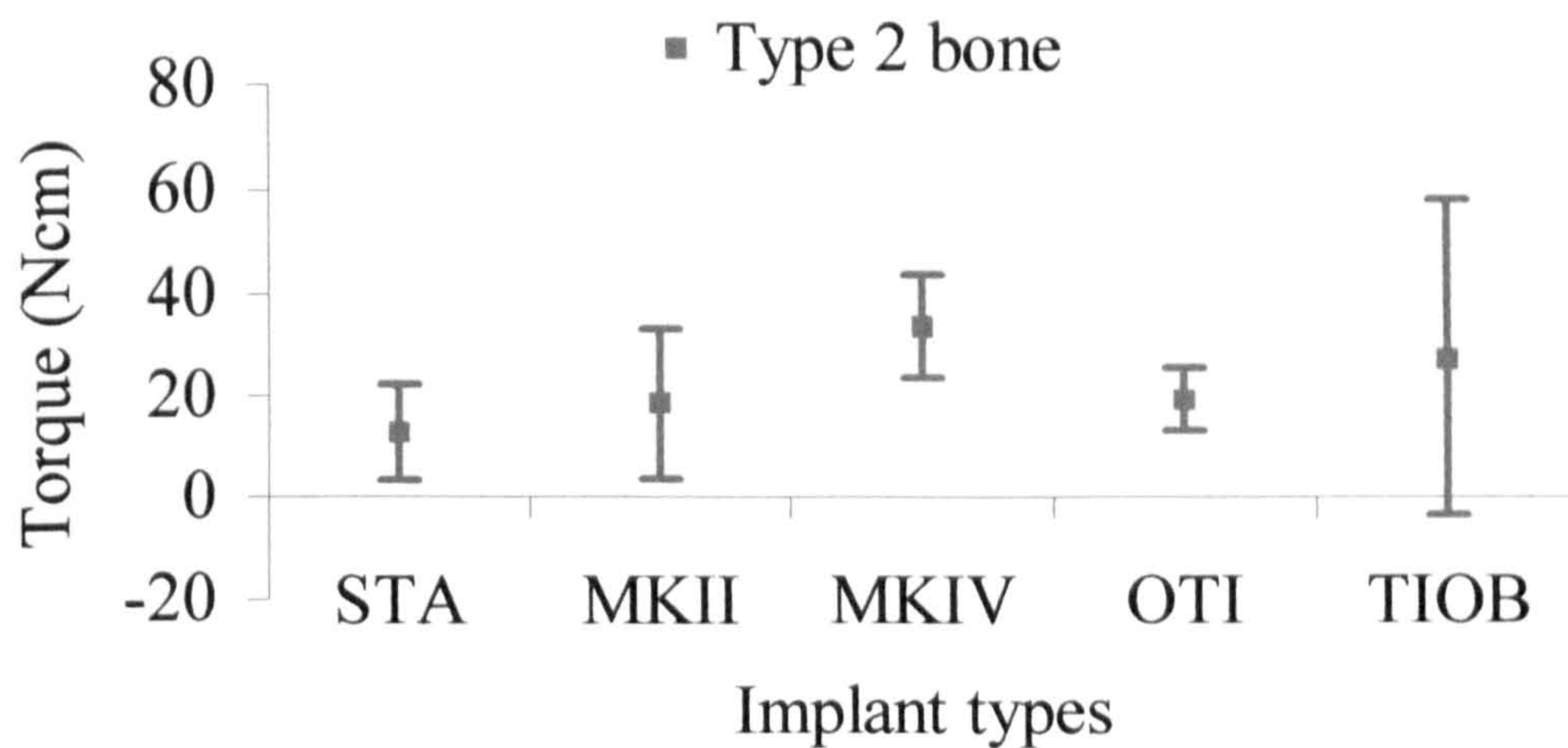


Figure 4.7: Peak immediate removal torque values for each implant type in Type 2 bone. Mean values and 95% confidence intervals are shown. (n=17).

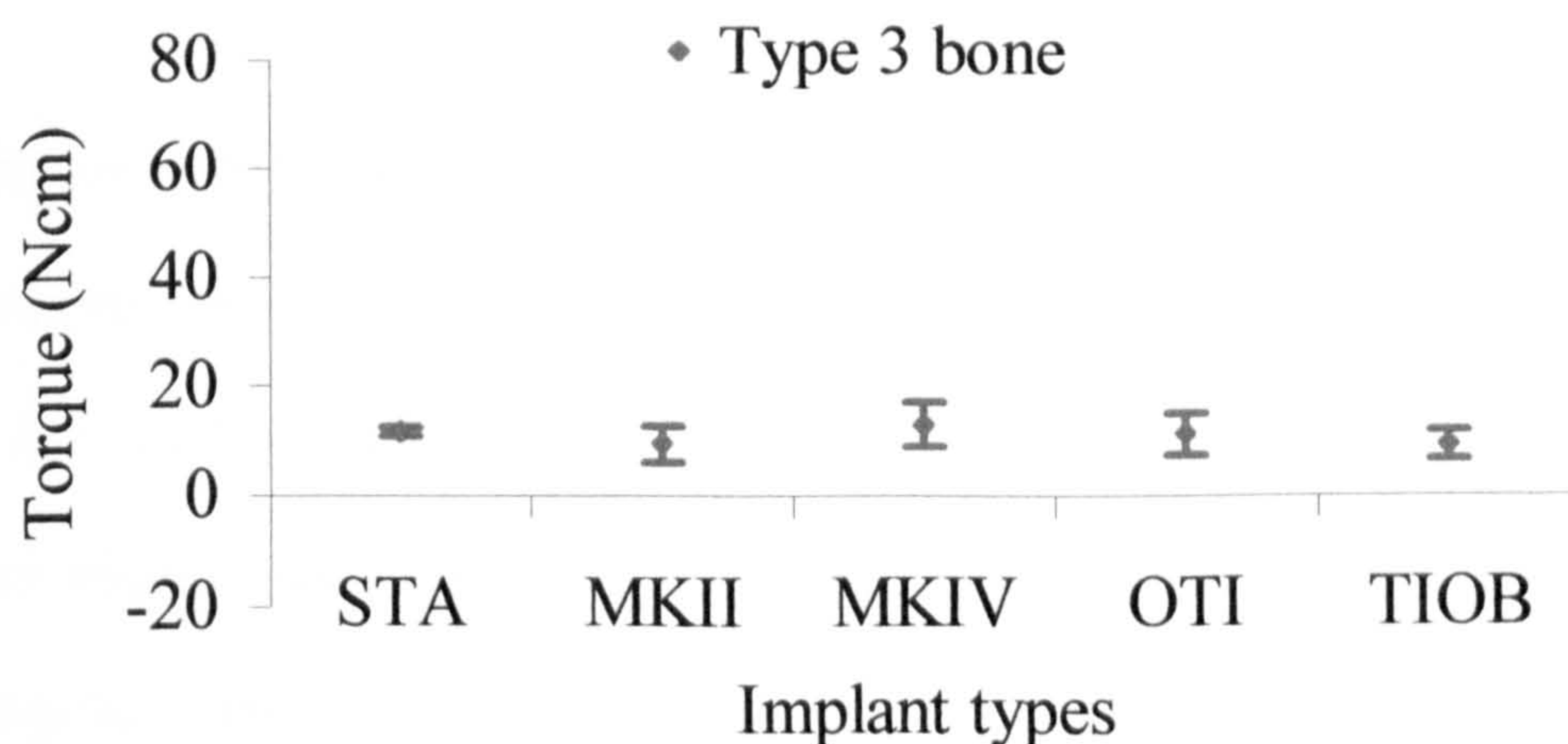


Figure 4.8: Peak immediate removal torque values for each implant type in Type 3 bone. Mean values and 95% confidence intervals are shown. (n=17).

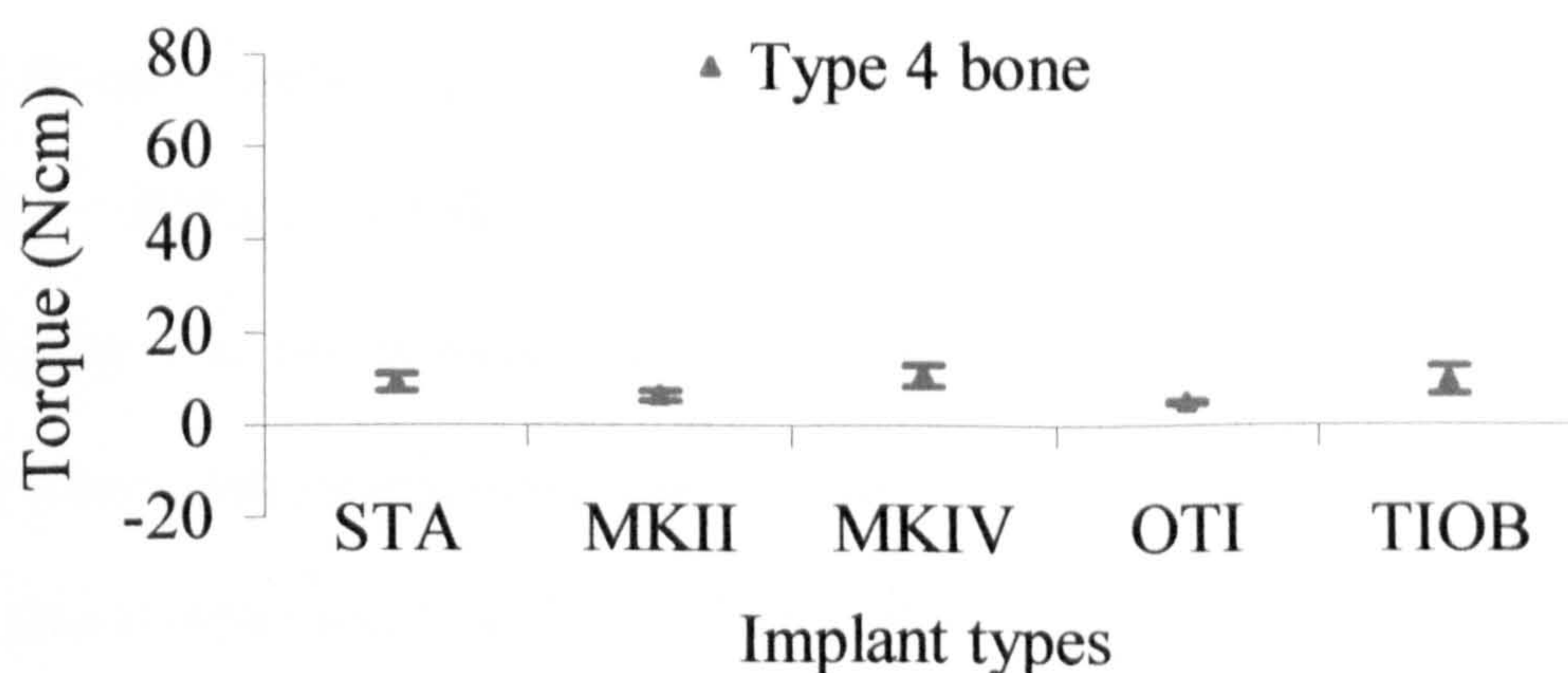


Figure 4.9: Peak immediate removal torque values for each implant type in Type 4 bone. Mean values and 95% confidence intervals are shown. (n=10).

torque one hour following implant insertion for bone types 2 to 4. Peak removal torque was calculated as the highest torque value obtained from the removal torque plot for each implant. Figure 4.10 illustrates a typical insertion torque plot against time for the MKIV, STA and MKII implants showing the reduced insertion time for the MKIV. When the peak insertion torque data from all bone qualities is pooled, using the Bonferroni multiple comparisons test a statistically significant difference ($p<0.05$) is evident between the MKIV and the STA, the MKIV and MKII, and between the MKIV and OTI. No significant difference was found between the immediate removal torque values for each implant type.

4.3.2 Resonance Frequency

The mean resonance frequency values with 95% confidence intervals for bone Types 2 to 4 are summarised in Figures 4.11 to 4.13. For STA, MKII, OTI and MKIV implants placed into Type 2 bone the RF values were greater than 7.10 kHz indicating high interfacial stiffness between the implant and the bone. The TIOB implants have a mean resonance frequency of 6.91 kHz, which although lower than the other implants tested would still be considered to indicate a good primary stability clinically. Very little change is seen in Type 3 bone, with the relative stability of each implant type remaining close to that seen in Type 2 bone. In Type 4 bone STA, MKII and OTI RF values were lower than those seen in bone Types 2 and 3, indicating that the primary stability of these implants in these bone types is reduced when compared to Type 2 and 3 bone. For TIOB implants the RF value also falls to give a value close to that of the OTI implant. The MKIV implants showed an increase in the mean resonance frequency to 7.99 kHz in Type 4 bone suggesting the highest primary stability of any of the implants tested. When the resonance frequency

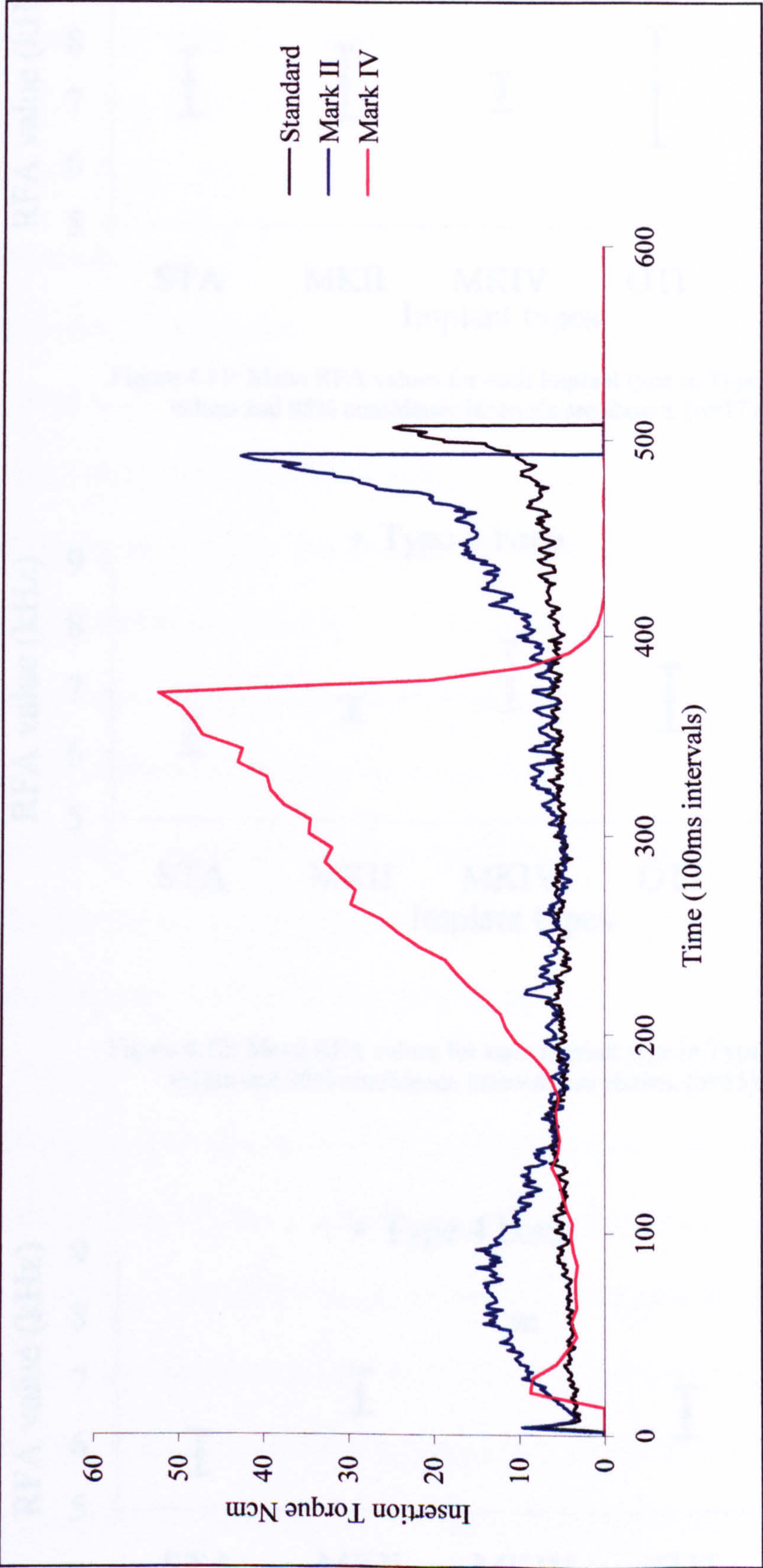


Figure 4.10: Insertion Torque profiles for standard Brånemark, Mark II, and Mark IV implants

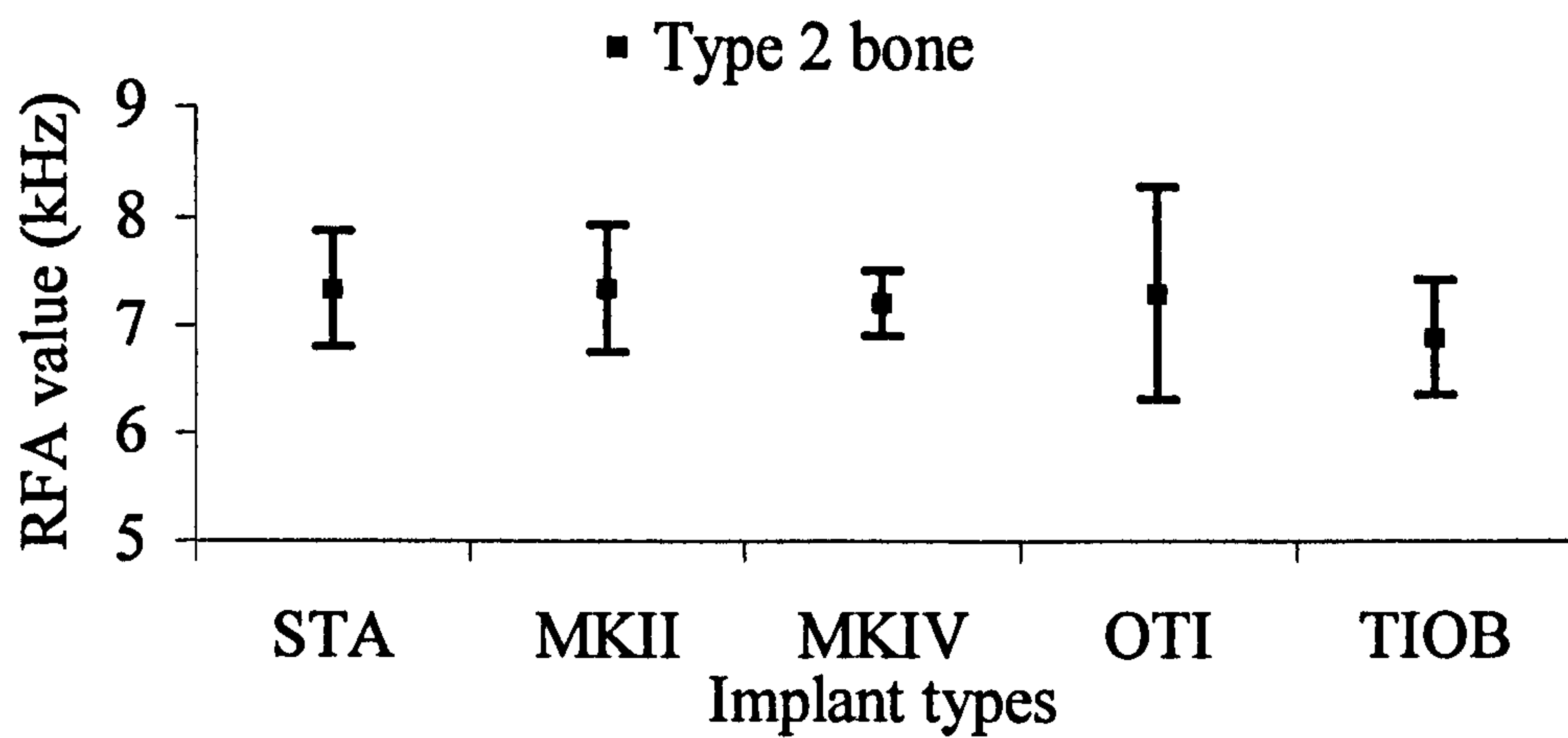


Figure 4.11: Mean RFA values for each implant type in Type 2 bone. Mean values and 95% confidence intervals are shown. (n=17).

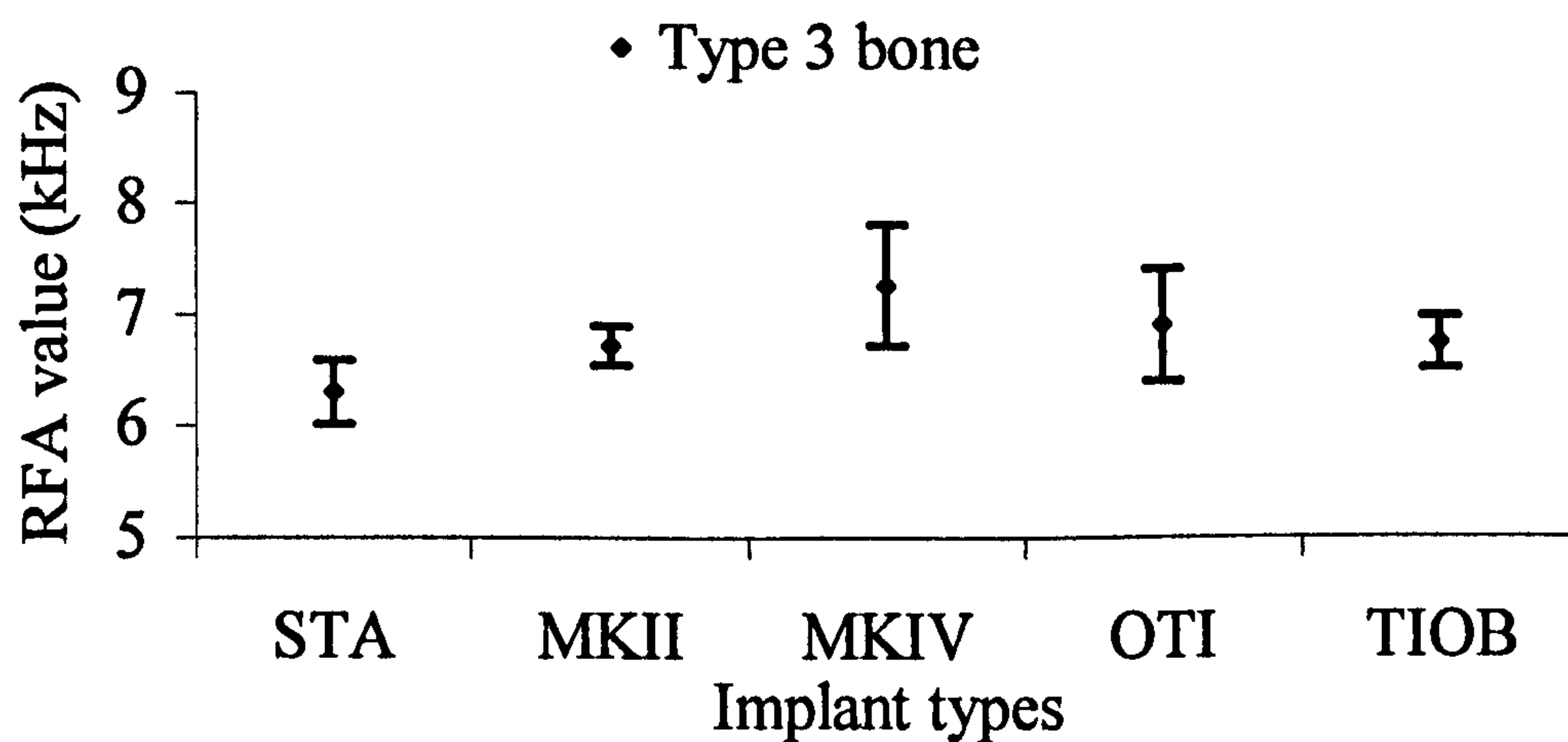


Figure 4.12: Mean RFA values for each implant type in Type 3 bone. Mean values and 95% confidence intervals are shown. (n=15).

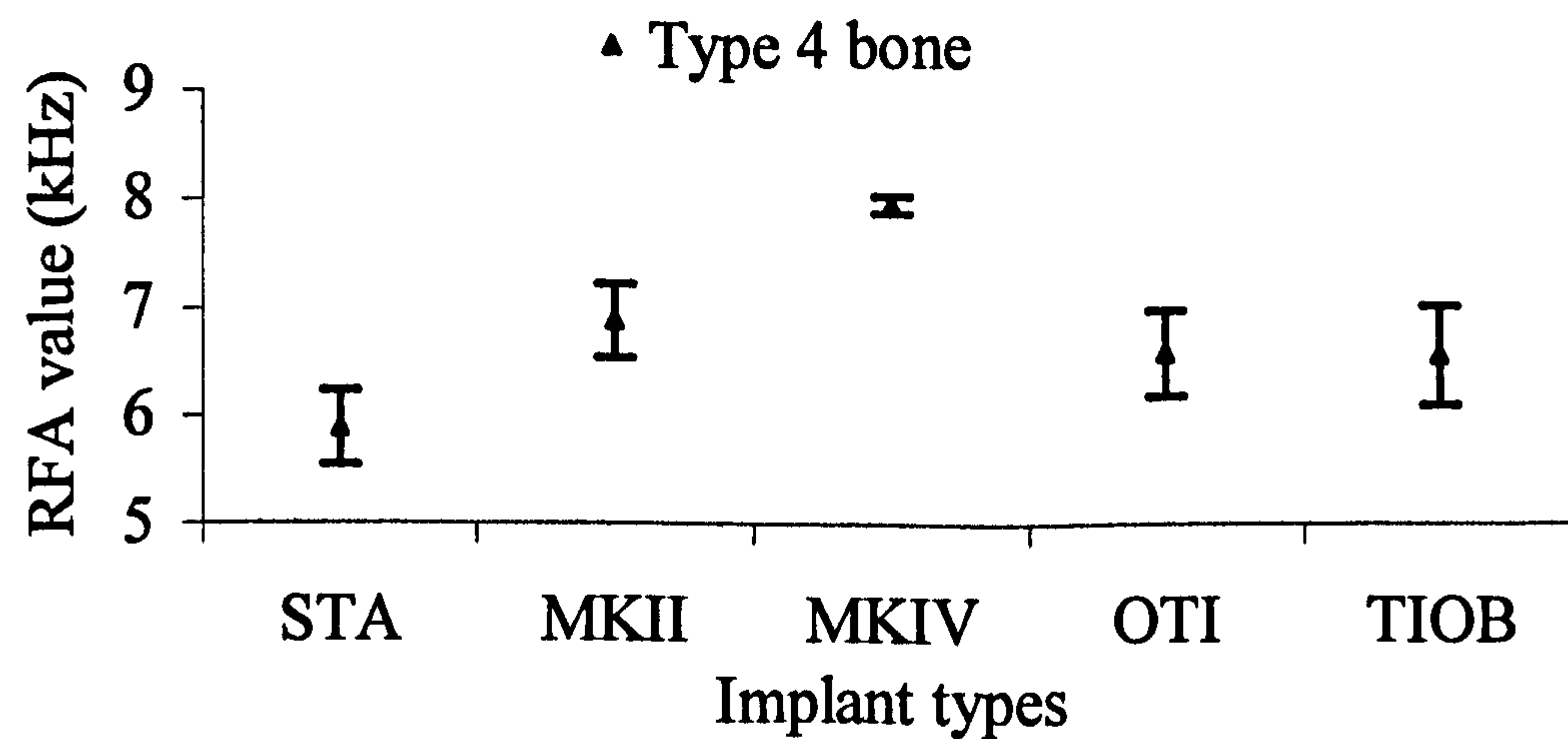


Figure 4.13: Mean RFA values for each implant type in Type 3 bone. Mean values and 95% Confidence intervals are shown. (n=11).

data from all bone qualities is pooled, using the Bonferroni multiple comparisons test a statistically significant difference ($p < 0.05$) is evident between the MKIV and the STA implants. No other significant differences were identified between implant types.

4.4 Discussion

4.4.1 Discussion of the method

The importance of good primary stability when implants are placed has been well documented. Poor initial stability is thought to play a significant part in the early loss of implants when this is coupled with an insufficient healing period. Primary stability of an implant at placement is a function of bone quality (the ratio of compact to trabecular bone), bone quantity; implant geometry and the placement technique (size of drills, whether self-tapping or not etc.). It is commonly stated by surgeons that bone quality and bone quantity influence the primary stability of dental implants, but this variation in the primary stability of a specific design of implant when placed into bone of varying qualities has not been quantified. The aim of this study was to compare the primary stability characteristics of five differing designs of implant and in particular to look at how the stability varies when these are placed into bone of varying qualities. Bone quality is often ranked clinically on a scale of 0-4 according to the bone density, perceived by the surgeon as resistance to drilling at implant placement. A quantitative technique was outlined by Johansson & Strid (1994) who calculated the resistance to cutting by measuring the electrical current used by a motorised handpiece. The reliability of this technique and its relationship to bone density was further investigated by Friberg et al (1995). The present study has utilised both the Lekholm and Zarb scoring method and measurement of insertion

torque to assess bone quality at each implant site. Although theoretically the lack of irrigation may affect lubrication and bone chip clearance, this did not appear to affect insertion torque values during preliminary tests prior to the study. Knowledge of the geometry of the implant and the insertion technique (e.g. the relative diameters of the implant and the pre-drilled hole) is essential, but with these in mind certain broad characteristics are apparent.

4.4.2 Discussion of the results

When considering the insertion torque profiles the curves for each of the implants are very similar for the first 3-4mm of insertion, corresponding to the blades of the tapping portion of each implant passing through the cortical bone. Following this, the curves correspond to the passage of the tapping portion of the implant passing through the trabecular bone and a frictional component as the threads of the remaining part of the implant pass through the tapped channel in the bone. With a tapered design of implant such as the MKIV used in this study there is an additional component to the curve as the upper threads of the implant are larger in diameter than the tapping portion. The increasing diameter of the inserting implant results in compression of the interfacial bone and leads to a steeper rise in the curve than that seen for a cylindrical implant (Figure 4.10). This effect was clearly seen in all of the insertion torque plots for the MKIV implants, which showed a steeper rise and higher peak insertion torque than the other implants tested. An additional design feature of the MKIV implant is the incorporation of a double thread in place of the single thread used in all of the other implant systems tested. The theoretical advantages of the double thread include an increased speed of insertion without increasing the energy generated at the implant/bone interface. The reduced insertion time can be

seen can be seen in Figure 4.10 when comparing the insertion torque graph for the MKIV implant with the STA and MKII implant plotted against time.

Primary stability of implants has traditionally been very difficult to assess and is often reduced to a simple assessment of mobility. This approach is subjective even when more sophisticated methods have been employed. One such method is the Periotest (Siemens Gmbh, Germany), which involves using a probe with a small metal slug containing an accelerometer. The probe is held in close proximity to the fixture/tooth and the metal slug is used to strike the surface under test, mobility being calculated from the contact time between the slug and the surface of the implant/tooth. There have been difficulties reported with this technique, the Periotest has been reported as being sensitive to changes in angulation, distance of the probe from the implant and variation of the area struck. These are problems, which are inherent with any hand-held mechanical test probe. A non-invasive technique for assessing the stability of an implant immediately after placement has been described by Meredith et al (1996a and b) and reported upon in a number of studies both in vitro and in vivo. The technique measures the resonance frequency of a small transducer which may be attached to an implant or to an abutment. The aim of the technique is to assess the interfacial stiffness between the implant and the bone and local bone stiffness in bending. This allows an initial assessment of stability to be made immediately after placement and to be able to monitor the increase in this stiffness with osseointegration.

For all of the implants, when placed into relatively good quality bone (Type 2), RF values were good (greater than 6.90 kHz). This was perhaps not surprising as in

good, dense bone it would be anticipated that the commercially available implants tested in this investigation would be able to achieve an acceptable primary stability. For the STA, and to a lesser extent the TIOB implants, RF values fell when they were inserted into poorer bone qualities indicating that the initial primary stability for these implants in this bone type is reduced when compared to Type 2 bone. For OTI and MKIV implants the RF values remained high even when placed into bone of quality Type 4, suggesting that the initial stability for these implants is less affected by the quality of the bone into which they are inserted.

Removal torque of an implant immediately after placement has been used to assess the initial stability of endosseous implants. Niimi et al (1997), used this technique to assess the bone quality and cortical bone thickness of fibula, iliac crest and scapula. They found a significant correlation between cortical bone thickness and removal torque, but not between bone quality and removal torque. They also compared the results from a cadaver model with data collected clinically and found no significant differences between them indicating that the cadaver is a suitable model for the assessment of initial stability. This was in agreement with Ueda et al (1991) who looked at the relationship between insertion torque and removal torque of endosseous fixtures when placed in cadaveric temporal bone. They noted that a high removal torque was always related to a higher initial insertion torque, but with the peak removal torque always of a lower magnitude than the peak insertion torque. This was a trend also seen in this investigation with the exception of two values. This would be expected as the frictional component of the removal torque curve would be the same as for the insertion torque but without the compressive component generated during insertion. There are obvious problems when drawing conclusions

from removal torque data gathered immediately after insertion. A high immediate removal torque might not indicate that a high removal torque would be gained once osseointegration has taken place. Immediate removal torque does however provide a measure of the resistance of an implant to rotational displacement in the vulnerable post insertion healing period. The measurement of removal torque following healing and osseointegration is a destructive test giving an indication of interfacial strength and may be used to determine the level of osseointegration of a cylindrical implant after a period of healing. The data obtained in this investigation confirmed the suitability of the cadaver model for the measurement of insertion and removal torque and also indicated that resonance frequency values are also comparable to those obtained clinically.

High insertion and therefore high removal torque are often seen as desirable, with a high insertion torque leading to an increase in the primary stability of the implant. The data in this investigation appeared to support this. The tapered experimental implant MKIV has been designed with this in mind but a concern must be that the taper may lead to high compression forces during placement. With high compression, disturbance of the local microcirculation may occur leading to necrosis of the osteocytes and bone resorption. It is reasonable to imagine that there is a balance point at which the degree of taper is such that there is an optimum level of primary stability without inducing resorption in the local bone. The degree of taper also prevents the full insertion of the implant into good quality Type 1 and Type 2 bone, to allow full insertion a larger initial drill size was needed and this appeared to reduce the initial stability of the implant. This is strong evidence that the MKIV implant should only be placed into bone of Type 4 or possibly Type 3 quality. From

the data it appears that the MKIV implant is more stable following placement than the other implants tested when placed into bone of Type 4 quality. When looking across all bone qualities the MKIV implant develops a significantly higher insertion torque than the STA, MKII and OTI implant types, and a significantly higher resonance frequency value than the STA implant indicating a higher interfacial stiffness at the implant/bone interface. Further studies are required to evaluate the clinical success of the fixture when compared to the other implant types.

CHAPTER 5

THE COMPARISON OF THE PRIMARY STABILITY OF IMPLANTS WITH DIFFERING GEOMETRY IN AN IN-VIVO RABBIT MODEL

THE COMPARISON OF THE PRIMARY STABILITY OF IMPLANTS WITH DIFFERING GEOMETRY IN AN IN-VIVO RABBIT MODEL

5.1 Aims and objectives

The results of previous studies appear to show an increase in the primary stability of a tapered implant placed into a cylindrical pre-drilled bone channel when compared to a cylindrical implant placed into a congruent cylindrical bone channel. It has been suggested that this may be due to the tapered implant generating compressive forces within the cortical bone at the implant site and this compression enhances the implant primary stability. This explanation appears reasonable from a purely mechanical perspective but bone is a vital tissue that responds to compression. It may be assumed that there is a threshold of compression above which, following implant insertion, the bone may undergo necrosis and the stability of the implant may be reduced. The aim of this study was to examine this problem, by studying the effect of implant taper upon implant primary and also secondary stability using a rabbit model.

5.2 Method

5.2.1 Animals and anaesthesia

Ethical approval was sought and confirmed in Sweden where the trial was conducted. Dr. Lars Sennerby of the Department of Biomaterials and Handicap Research, University of Gothenburg, Sweden was confirmed as the senior member of staff overseeing the study. Nine adult female New Zealand white rabbits were used in the study. They were kept in a purpose-designed facility and allowed free access to water and feed pellets. At surgery, general anaesthesia was induced by intramuscular

injection of Hypnorm (Janssen Pharmaceutica, Brussels, Belgium) 0.2ml/kg b wt and intraperitoneal injection of Stesolid (Dumex, Copenhagen, Denmark) 1.5mg/kg b wt. In addition, 0.8ml of local anaesthetic (2% lignocaine/ 1:80 000 adrenaline, Astra AB, Södertälje, Sweden) and analgesic (Temgesic, 0.05 mg/kg b wt, Reckitt and Coleman, Hull, U.K.) as single intramuscular injections. All surgery was performed under sterile conditions in an animal operating theatre. The tibial metaphyses and distal femoral condyles were used as experimental sites. The surgical areas were shaved. The feet were wrapped in gauze and the animals were draped with sterile drapes. The tibial metaphyses and distal femoral condyles were exposed via skin incisions and the tissues were blunt dissected down to the periosteum. The periosteum was incised and periosteal flaps raised. Implants were placed in accordance with the protocol outlined in Figure 5.1. The implant sites were prepared using standard surgical technique. Final drill diameters of 3.15mm were used. All drilling procedures were carried out under profuse sterile saline irrigation. After surgery the wounds were closed in layers with subcutaneous, resorbable sutures and superficially with silk sutures.

5.2.2 Implant materials

Thirty six implants were placed in total. Experimental implants were prepared with a 1° taper (EXP 0.2) at 6mm and 10mm in length. Experimental implants with a 2° taper (EXP 0.4) were prepared at 6mm in length and standard Brånemark implants (Nobel Biocare AB, Gothenburg, Sweden) the same length as the test implants were used as controls.

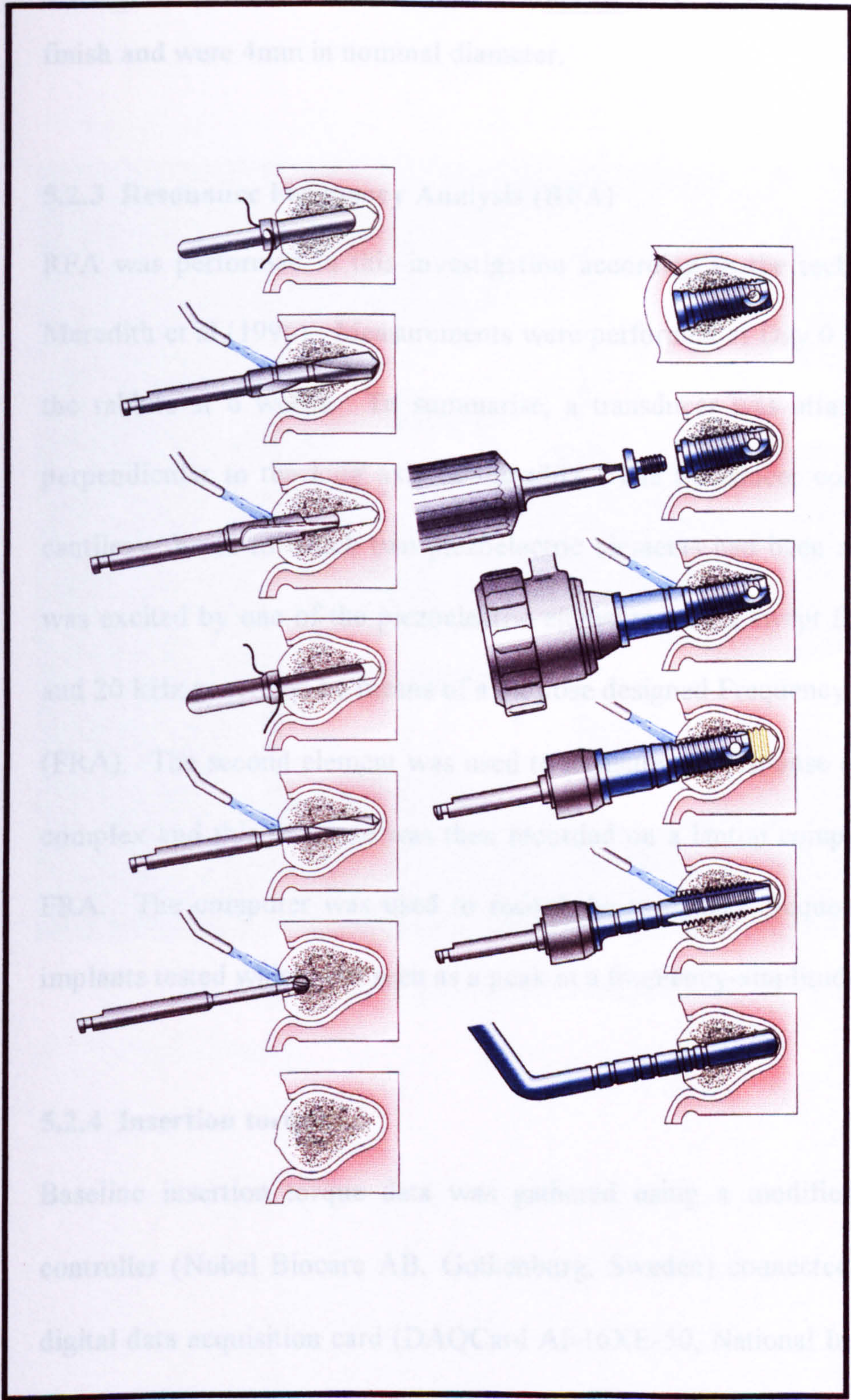


Figure 5.1: Surgical technique used in the placement of implants in the rabbit study.
(adapted from the Surgical Instruction manual – © Nobelbiocare AB, Gothenburg, Sweden).

Test and control implants were placed for each rabbit in accordance with the distribution in Figure 5.2. All experimental implants were custom made of c.p. titanium (Nobel Biocare AB, Gothenburg, Sweden) with the same machined surface finish and were 4mm in nominal diameter.

5.2.3 Resonance Frequency Analysis (RFA)

RFA was performed in this investigation according to the technique described by Meredith et al (1996). Measurements were performed at Day 0 and after sacrificing the rabbits at 6 weeks. To summarise, a transducer was attached to the implant perpendicular to the long axis of the tibia. The transducer comprised a modified cantilever beam to which two piezoelectric elements had been attached. The beam was excited by one of the piezoelectric elements with a swept frequency between 2 and 20 kHz generated by means of a purpose designed Frequency Response Analyser (FRA). The second element was used to measure the response of the beam/implant complex and this response was then recorded on a laptop computer attached to the FRA. The computer was used to record the resonance frequency for each of the implants tested which was seen as a peak in a frequency-amplitude plot.

5.2.4 Insertion torque

Baseline insertion torque data was gathered using a modified electronic torque controller (Nobel Biocare AB, Gothenburg, Sweden) connected to an analogue to digital data acquisition card (DAQCard AI-16XE-50, National Instruments, UK Ltd, UK) and laptop computer. Data were recorded at the rate of 10 samples per second. The system was calibrated using a Tonichi 15 BTG-N ® (Tohnici MFG, Japan) torque gauge which itself is factory calibrated with an error of 2%.

5.2.5 Results (continued)

At the end of the testing time, the rabbit legs were dissected and the implants were removed. The implants were then placed in a container and connected to the computer. The data was then analyzed and the results were as follows:

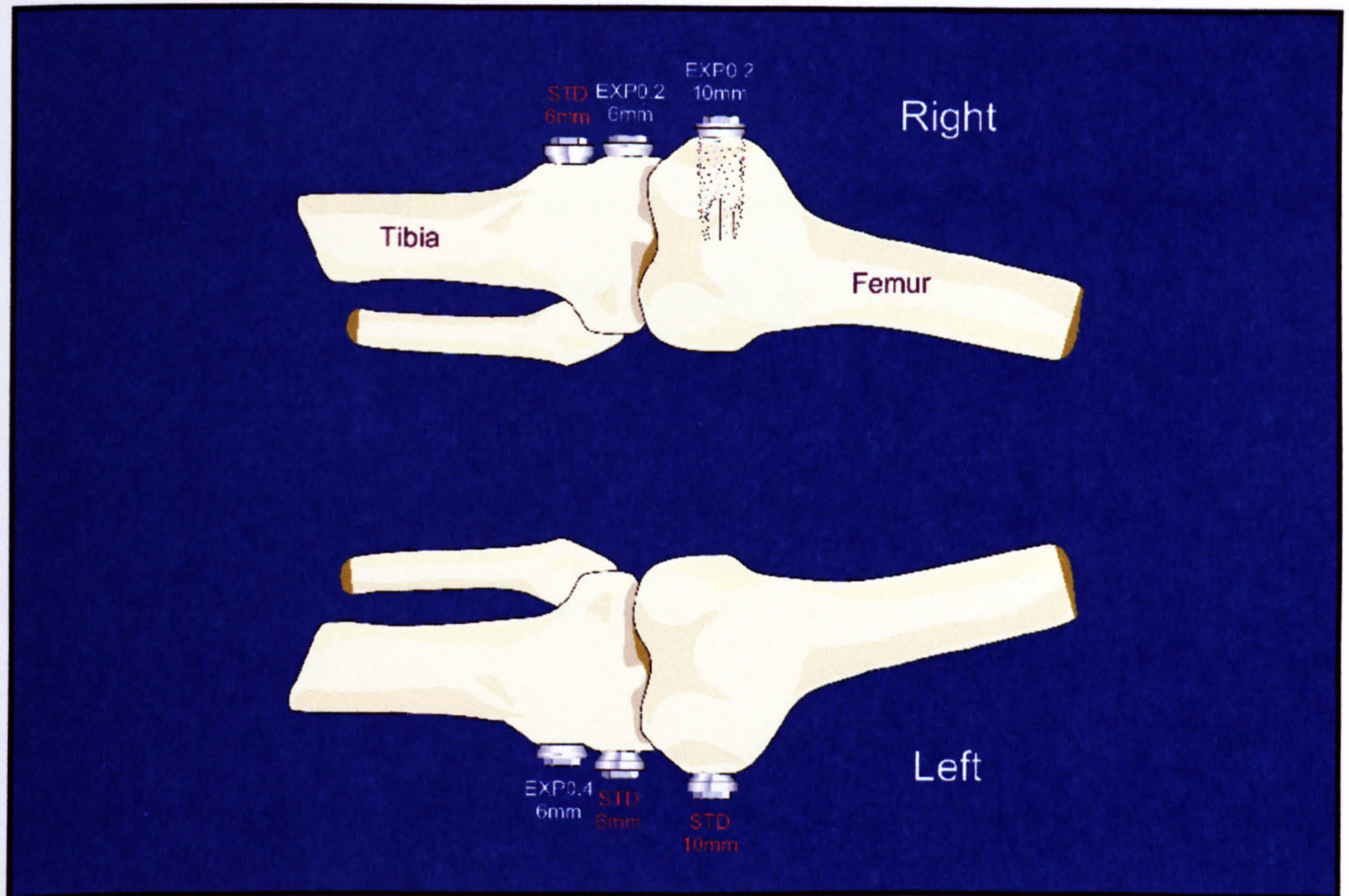


Figure 5.2: Implant distribution in the rabbit legs.

5.2.6 Results (continued)

Discussion

At 9 days post-implantation, the implants were removed and the data was analyzed. The results showed that the EXP0.4 implants had the highest success rate, followed by the STD implants. The EXP0.2 implants had the lowest success rate. The data also showed that the implants were well-tolerated by the rabbits and there were no significant differences in the bone density between the groups.

5.2.5 Removal torque

At the end of the healing period, the animals were sacrificed and the peak torque required to unscrew each implant was measured. The bone section containing the implant was fixed in a vice. An electric motor delivered the torque via a rigid shaft connected to the implant with a standard fixture mount (Nobel Biocare AB, Gothenburg, Sweden). A microprocessor converted the current used by the motor to a torque value. The current drain was also directly recorded using the data acquisition card and laptop used to record insertion torque to cross-check the calibration of the removal torque apparatus. (Figure 5.3).

5.2.6 Statistics

The unpaired t-test with Welch correction was used for statistical analysis. Significance was indicated at the $p \leq 0.05$ level.

5.3 Results

A summary of results is presented in Table 5.1.

RFA measurements

Placement

At 0 day no significant difference in RFA value was seen for the 10mm EXP 0.2 implants and controls placed into the femur or for the 6mm EXP 0.4 implants and the controls placed into the tibia. A statistically significant difference was seen between the 6mm EXP 0.2 implants and control implants placed into the tibia ($p=0.0275$) with the EXP 0.2 implants exhibiting a higher mean RFA value. If data for femur and

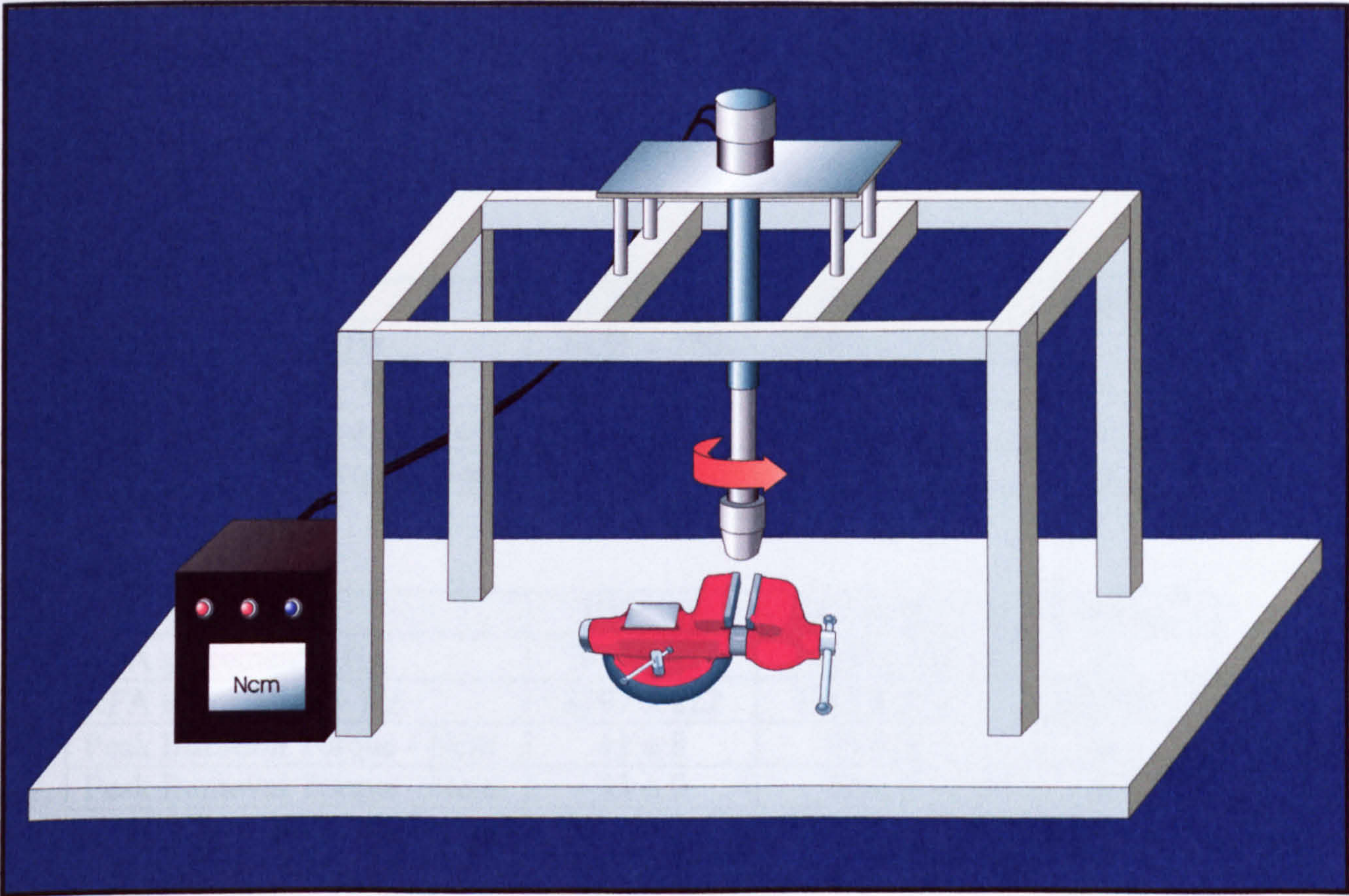


Figure 5.3: Removal Torque rig.

Femur

Test	EXP 0.2	Control	P value
RFA placement – Hz	8142 ± 377	7848 ± 107	ns
RFA termination – Hz	8328 ± 205	8458 ± 251	ns
Peak Insertion Torque - Ncm	46 ± 7	25 ± 3	0.0005
Peak Removal Torque - Ncm	66 ± 16	65 ± 8	ns

Tibia

Test	EXP 0.2	Control	P value
RFA placement – Hz	8131 ± 226	7782 ± 235	0.0275
RFA termination – Hz	8219 ± 315	8060 ± 194	ns
Peak Insertion Torque - Ncm	38 ± 9	28 ± 6	ns
Peak Removal Torque - Ncm	32 ± 4	31 ± 5	ns

Tibia

Test	EXP 0.4	Control	P value
RFA placement – Hz	7952 ± 114	7714 ± 352	ns
RFA termination – Hz	8197 ± 222	7913 ± 152	0.0329
Peak Insertion Torque - Ncm	41 ± 8	49 ± 9	ns
Peak Removal Torque - Ncm	33 ± 9	32 ± 8	ns

Mean ± SD values are shown.

Table5.1: Rabbit summary data.

tibia are combined a significant difference is seen overall for the EXP implants against the controls ($p=0.05$), again showing a higher mean RFA value for the EXP implants.

Termination

At 6 weeks no significant difference was seen between the EXP 0.2 implants and the controls in the femur or tibia. The EXP 0.4 implants showed a significantly lower mean RFA reading against the controls ($p=0.0329$).

Insertion torque

The difference in insertion torque between the EXP 0.4 implants and controls was not significant. The EXP 0.2 implants placed into the femur generated a significantly higher insertion torque than the controls ($p=0.0005$). Although the difference in insertion torque for the EXP 0.2 implants and controls in the tibia was not significant it should be noted that the p value ($p=0.0512$) was close to the level of significance used in this study.

Removal torque

No significant difference in removal torque was seen for any group.

5.4 Discussion

5.4.1 Discussion of the method

The experimental implants used in this study were manufactured with two different degrees of 1° and 2° taper. When a tapered implant is inserted into a cylindrical pre-drilled hole whose diameter is less than the maximum diameter of the implant a

degree of compression will take place at the surface of the bone. The insertion of threaded c.p. titanium implants have been reported to have a high success rate in favourable sites. The original technique outlined by Brånemark, and refined over several years of clinical experience, involved the use of drills of varying diameter used sequentially to produce a hole in the bone of suitable depth and diameter to accommodate an implant. A screw-tap was then used to prepare a threaded channel in the bone into which the implant was inserted under a slow rotational speed. All cutting and drilling of the bone was carried out under profuse saline irrigation and the aim of the technique was to minimise mechanical and thermal trauma to the bone at the implant site. This technique although having a good clinical success rate has been shown to be heavily affected by the quality and quantity of the bone at the implant site. Manufacturers now market a number of implant systems and although they differ in detail, systems generally still include the use of sequential twist drills to prepare a parallel-sided bone channel into which an implant with a basic cylindrical profile, with or without screw threads/fins, is inserted. Tapered and stepped cylindrical implant systems have been developed with a view to improving aesthetics and facilitating implant placement between adjacent natural teeth or in areas where the insertion of a cylindrical implant would lead to the apical area of the implant perforating the bone.

5.4.2 Discussion of the results

The theory behind the use of the tapered implants in this study is to induce a degree of compression of the cortical bone in a poor bone implant site. This degree of compression is related to three factors: the degree of taper of the implant; the relationship of the final drill diameter used to the maximum diameter of the implant;

and the mechanical properties of the bone itself. In this study the final drill diameters used were 3.15mm. At this diameter the EXP 0.2 implants seated fully without problems, however, it was not possible to fully seat the EXP 0.4 implants. In each rabbit the EXP 0.4 implants when placed had 3-4 threads left above the bone surface and this is reflected in the very high insertion torque's generated as the tapered upper portion of the implant engaged the cortical bone. When these more tapered implants are inserted initially a degree of compression will take place in the cortical bone layer but there will be a maximum limit to this compression and as this is reached the insertion torque increases until no further insertion of the implant is possible. This presents a number of potential problems in a clinical situation. An implant that fails to fully seat is of limited clinical value. Although the use of a larger drill size would allow the implant to seat, the degree of taper of the implant means that there is a danger that the lower threads of the implant do not engage the cancellous portion of the bone at all. In addition, the degree of compression generated by the implant is very high and may be expected to cause local cellular damage in the cortical bone. Very high compression of bone is known to cause cell death, necrosis and ultimately may lead to bone resorption in the cortical bone layer. Soltesz et al (1982) and Huiskes et al (1984) have shown a direct correlation between high stressed regions and bone resorption by comparing experimental observations with numerical calculations. If local bone resorption occurs then a reduction in RFA value over time would be expected. Bone resorption may occur around the neck of an implant or along the implant/bone interface. If resorption occurs around the neck of an implant it has the effect of increasing the effective length of the transducer/implant complex above bone, which in turn reduces the RFA value for that implant. Bone resorption along the length of the implant leads to a reduced

stiffness of the implant/bone interface and again is seen as a reduction in the RFA value over time. In both cases a reduction in RFA over the healing period would be expected, which was not observed in this study. An increase in implant stability, seen as a rise in RFA value during the healing period, was seen for all of the implants in this study. As successful integration of the implant occurs the RFA value may increase. This is seen in all of the implant types and there did not appear to be any group in which RF values would indicate that bone resorption is occurring over the time period of this study.

The generation of such high stresses within the bone with the use of EXP 0.4 implants may have a more immediate risk. The wedging effect may lead to crack propagation and fracture of the bone, particularly where more than one implant is placed in close proximity to another. At implant insertion EXP 0.4 implants did not have a significantly higher RFA value when compared to the control implants and this is almost certainly due to the failure of these implants to fully seat. RFA value is a measure of the stiffness of the implant/transducer/bone complex and is affected by the length of the transducer implant complex above the bone crest. In essence, the failure of the implant to seat increases the effective length above the bone crest and this reduces the RFA value. If this effect is corrected for then, as expected, the EXP 0.4 implant shows the highest primary stability of any of the implants tested. The EXP 0.2 implant is equivalent to the taper used in the commercially available MarkIV implant and this is specifically marketed for use only in bone of poor quality. There is however no convincing animal model for bone of poor quality. In this study the rabbit was used as there is a wealth of previously published work using the rabbit model in the field of oral implantology and its responses to standard

implant placement are well recorded. The rabbit bone cannot be considered to be representative of bone of poor quality/quantity, but can be seen as a useful guide to the behaviour of a tapered implant system in denser bone. If local bone compression was deleterious then its effects would be exaggerated in denser bone.

No difference in removal torque was observed in this study for any of the implant types. Removal torque is a measure of interfacial strength. The similar removal torque values for all the implants tested may be explained by their similar surface topography and since they all appeared to have successfully osseointegrated.

At placement significantly higher IT was needed to insert the EXP implants compared with the controls. Primary stability was statistically significantly higher for EXP 0.2 implants placed in the tibia but not in the femur. If pooled data from femur and tibia were considered there was a significant difference. The EXP 0.4 implants showed a lower RF value due to the exposed threads. This difference was not statistically significant, probably due to the higher insertion torque needed to seat these implants which may have increased the primary stability of some of these implants. At termination the EXP 0.4 showed lower RFA values as a result of the exposed threads. There was no difference observed when comparing the secondary stability for EXP 0.2 and the control implants, nor were there any differences in RT.

CHAPTER 6

MEASUREMENT OF THE SURFACE BONE STRAINS AND PRIMARY STABILITY OF IMPLANTS WITH DIFFERING GEOMETRY DURING IMPLANT PLACEMENT

MEASUREMENT OF THE SURFACE BONE STRAINS AND PRIMARY STABILITY OF IMPLANTS WITH DIFFERING GEOMETRY DURING IMPLANT PLACEMENT

6.1 Aims and objectives

The taper of an implant has been shown to affect the primary stability of that implant following surgical placement. Theoretically this has been suggested to be due to the taper generating compressive forces in the cortical bone as it is inserted. These forces and resultant strains have not been quantified for any implant system, let alone for a tapered implant system. The aim of this study was to quantify the surface bone strain generated during implant site preparation and when inserting three different implant types into bovine rib bone using electrical resistance strain gauges, and to look at the effect of the implant geometry upon that bone strain.

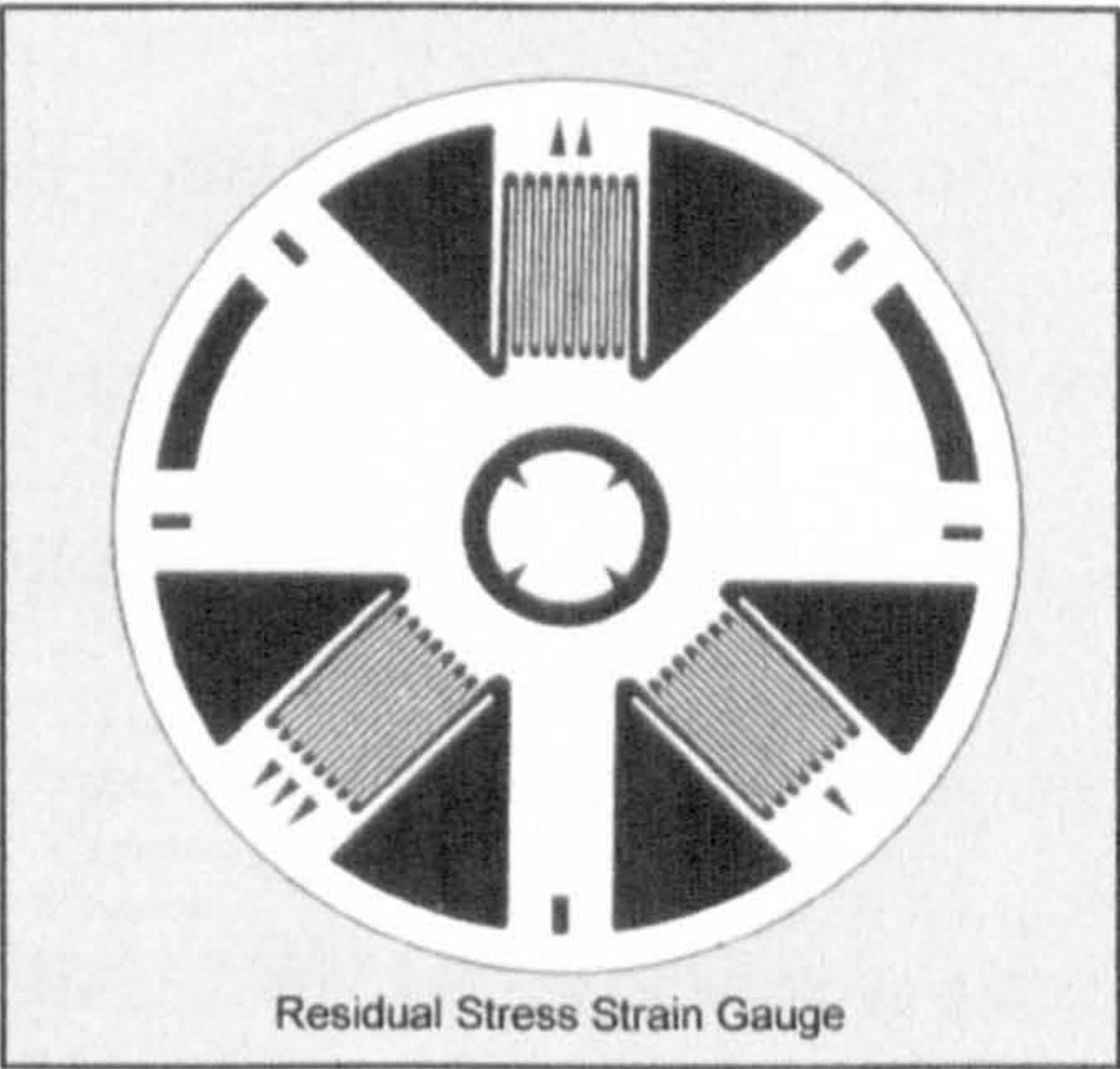
6.2 Method

6.2.1 Specimen Preparation

Specimens of bovine rib were obtained from an abattoir and returned to the laboratory within 1 hour of animal slaughter. The bone specimens were individually bagged and frozen at -22°C leaving the periosteum and adjacent musculature still in place to minimise dehydration of the bone. Prior to testing, each specimen was removed from the freezer, sectioned into 12cm lengths and thawed to room temperature submerged in isotonic saline. Once thawed the periosteum and musculature were dissected from the bone. All specimens were stored in isotonic saline prior to testing to prevent dehydration.

6.2.2 Strain gauge attachment

Three element electrical resistance residual stress strain gauges were used (FRS-3-11, TML, Tokyo Sokki Kenkyujo Co., Ltd, Tokyo 140, Japan). Details of the strain gauges used are summarized in Figure 6.1. Specimens were prepared by drying the surface with paper towel to remove excess moisture and then degreasing with propanone. The area for gauge attachment was abraded with fine diamond paper. A drop of methyl-2-cyanoacrylate (M-Bond 200, Vishay measurements group UK Ltd, Basingstoke, Hants., UK) was applied to the back of the strain gauge and spread into a thin film and the backing surface of the gauge applied to the bone and pressed firmly into place under a polyethylene sheet for 30 seconds. Terminals (CPF-75C, Vishay measurements group UK Ltd, Basingstoke, Hants., UK) were attached in a similar manner to the strain gauges as illustrated. The legs of the strain gauge were soldered to each terminal in turn and flat ribbon cable was soldered to connect the strain gauge to the strain gauge amplifier. Bond quality and electrical continuity was tested visually and by connecting the strain gauge to a strain gauge amplifier and gently tapping the gauge, if no response was elicited with tapping the bond quality was deemed satisfactory. As the testing was to be carried out under saline irrigation the gauges were waterproofed. The flux on the solder joints was removed by gently brushing with propanone and the assembly was allowed to air dry. A layer of air-drying acrylic resin (M-Coat D, Vishay measurements group UK Ltd., Basingstoke, Hants., UK) was applied and allowed to dry. A thin coating of microcrystalline wax



Residual Stress Strain gauge	
Manufacturer	TML Tokyo Sokki Kenkyujo Co., Ltd. Japan
Type	FRS-3-11
Gauge centre diameter	10.26mm
Gauge length (mm)	3
Gauge width (mm)	2.6
Backing diameter	17.5
Resistance in Ω	120
Operational Temperature ($^{\circ}\text{C}$)	-20 to +80
Coefficient of thermal expansion	$11.8 \times 10^{-6}/^{\circ}\text{C}$
Gauge factor	~ 2.1

Figure 6.1: Strain gauge details.

(W-1, TML, Tokyo Sokki Kenkyujo Co., Ltd, Tokyo 140, Japan) was applied as a final layer.

Each specimen was tested immediately after gauge attachment. The ends of the bone specimens, which were most vulnerable to dehydration, were wrapped in isotonic saline soaked tissue. Each specimen was mounted in a vice on the testing machine platform and connected to the strain gauge amplifier Figure 6.2. Each gauge arm was supplied with a D.C. 2-volt excitation the gain adjusted on each channel of the strain gauge amplifier prior to testing by switching a shunt resistor in parallel to the active element of each bridge simulating a mechanical strain of $1000\mu\epsilon$. Amplifier gain and excitation voltage were kept constant throughout the experiments but the amplifiers were set to zero where necessary to prevent over-ranging.

Strains were recorded for each gauge arm of the residual strain gauge during implant site preparation and implant insertion through the central hole of the gauge (Figure 6.3). An acrylic resin control specimen, to which an identical strain gauge had been mounted, was also placed adjacent to each test sample. Each arm of the gauge on the test specimen was connected as the active arm of a Wheatstone bridge circuit and gauges on the control specimen comprised the dummy arms of the bridge circuit. All tests were performed at ambient room temperature. As the testing machine was situated in the direct airflow from an air conditioning duct, all tests were performed at night when the air conditioning was not operating and the tests were less likely to be disturbed by electrical interference from work carried out in adjacent areas of the building. Temperature fluctuations were considered to be a potential source of error causing changes in gauge resistance and to reduce this effect the saline irrigant used



Figure 6.2: Experimental set-up for strain gauge work illustrating the instron testing machine with custom handpiece rig, electronic torque controller, strain gauge amplifier and thermocouple amplifier.

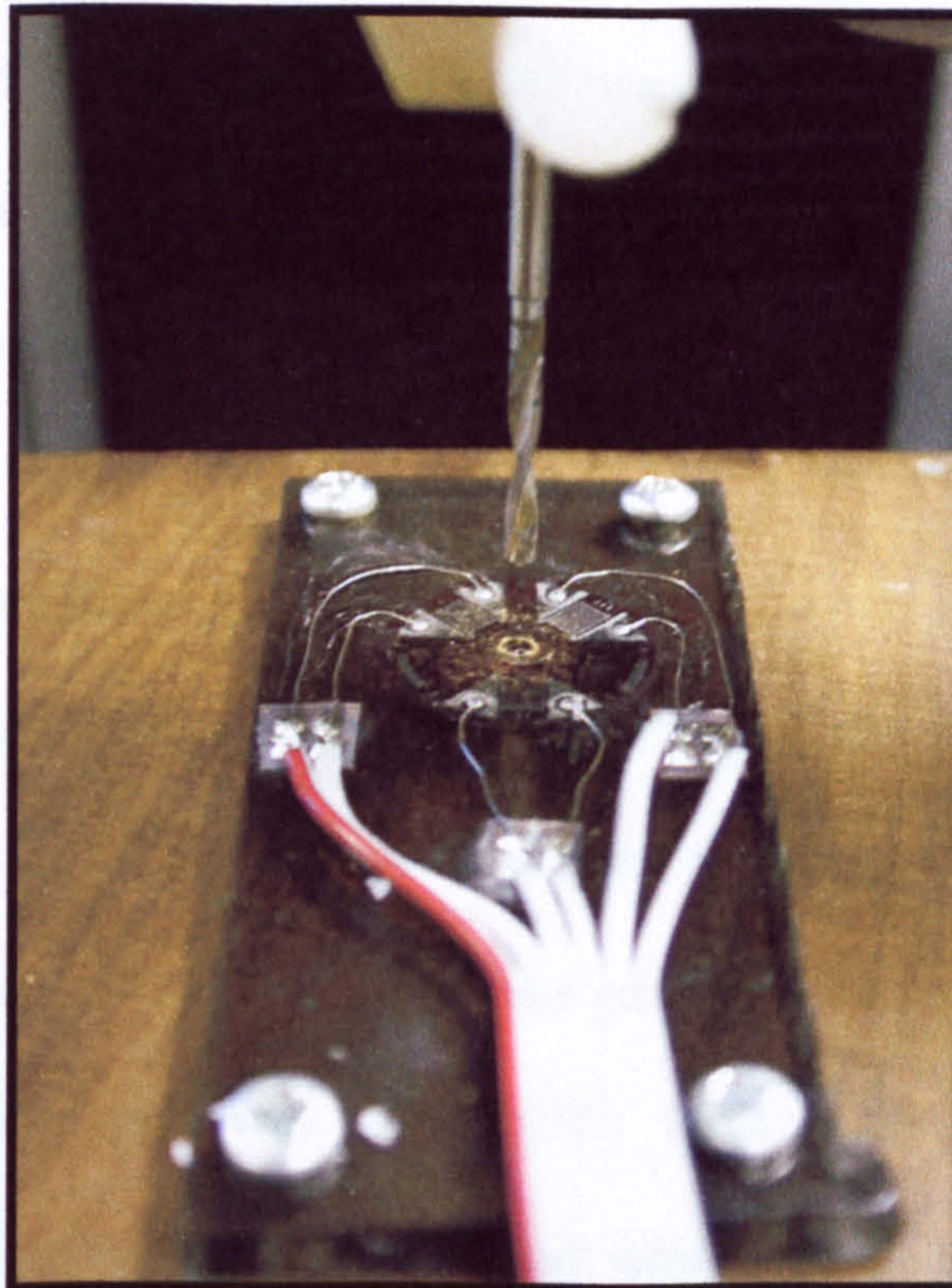


Figure 6.3(a): Implant site preparation through the strain gauge.

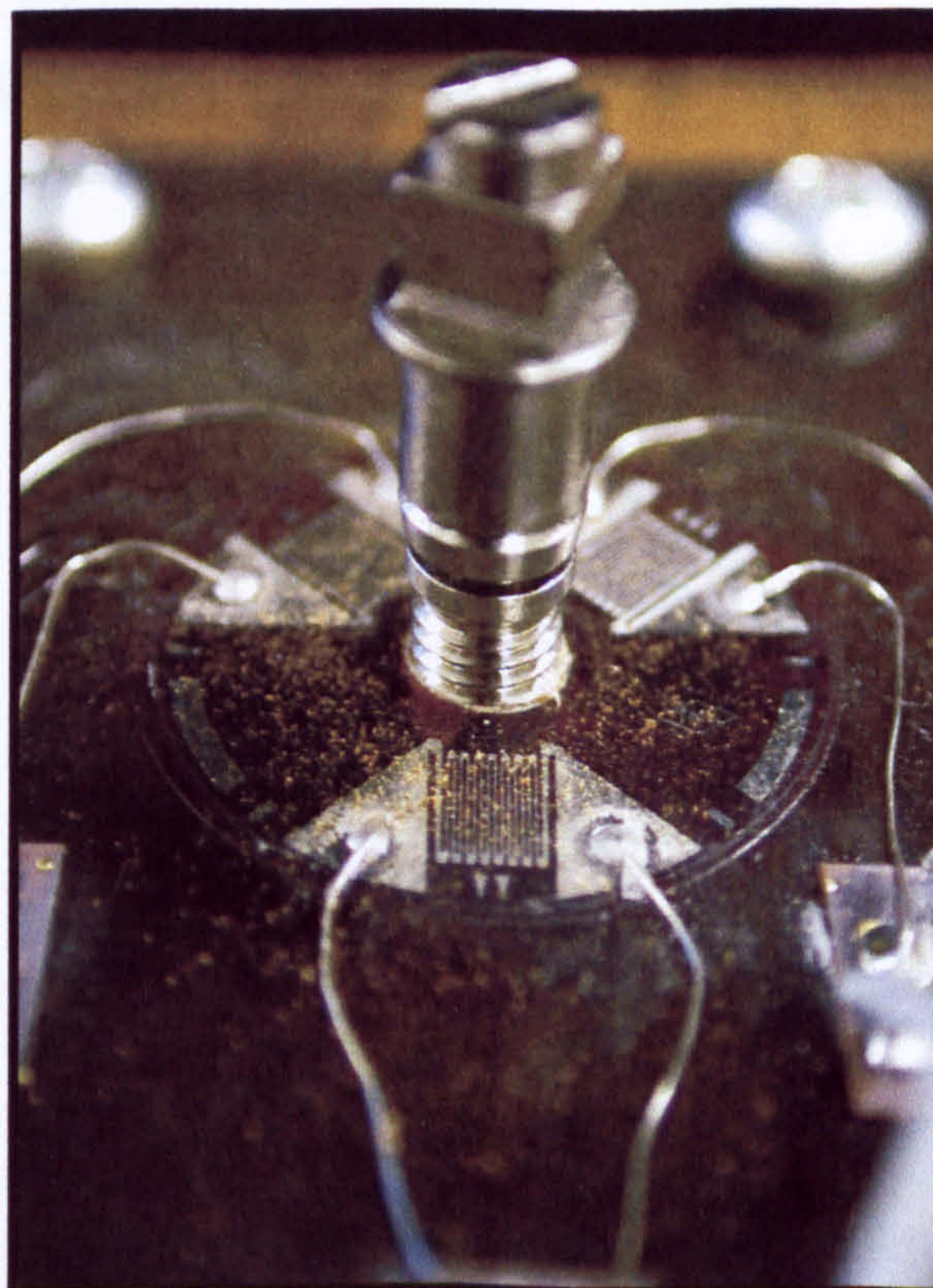


Figure 6.3(b): Implant inserted through the strain gauge.

during testing was kept at room temperature. A pilot test was performed with a thermocouple placed in the microcrystalline wax coating the active strain gauge. Temperature fluctuations measured in this way were less than 1°C which were not considered to be significant (Figure 6.4).

6.2.3 Strain gauge calibration

It was considered important that the drift in output of the strain gauge amplifiers should be assessed with respect to temperature and time. Figure 6.4 illustrates temperature measured at the 3-element rosette gauge over a period of 8 hours. It can be seen that temperature drift was within $\pm 1^\circ\text{C}$. Drift of the measured strain gauge was less than $\pm 10\mu\epsilon$ over a 30 minute period which was considered acceptable for this study. Calibrated values of strain were calculated for each element of the 3-element Rosette strain gauge using the digital data recorded from each element of the Rosette. The formula used for calculation of strains was:

$$\epsilon_x = \frac{1000}{(D_{1000} - D_0)X(D_x - D_0)}$$

where:

ϵ_x	=	Absolute strain in microstrain units ($\mu\epsilon$)
D_{1000}	=	Strain reading during 1000 $\mu\epsilon$ calibration test
D_0	=	Strain reading at zero strain
D_x	=	Strain reading at measured strain

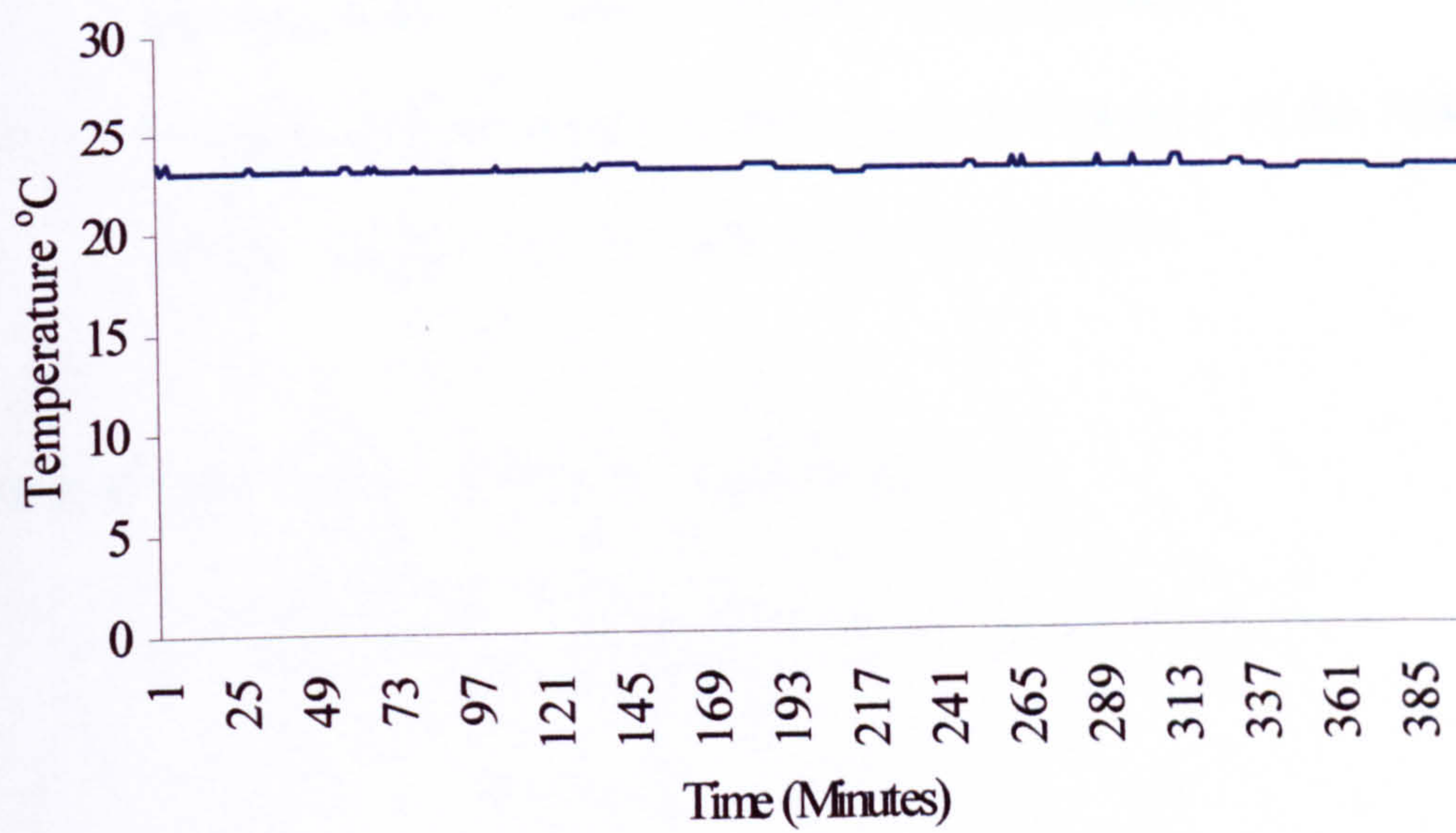


Figure 6.4: Temperature fluctuation of dummy strain gauge

The three individual strain readings were calculated for each 3-element rosette.

These strain readings were then used to calculate the following:

- a) the principal strain values for each specimen during preparation;
- b) the principal strain values for each specimen during implant insertion;
- c) the angle of principal strain with respect to element 1 on the 3-element rosette, for each specimen during preparation;
- d) the angle of principal strain with respect to element 1 of the 3-element rosette, for each specimen during implant insertion.

Principal strain values were calculated using the formula:

$$\varepsilon = \frac{\varepsilon_A + \varepsilon_B + \varepsilon_C}{3} \pm \frac{\sqrt{2}}{3} \sqrt{(\varepsilon_A - \varepsilon_B)^2 + (\varepsilon_B - \varepsilon_C)^2 + (\varepsilon_C - \varepsilon_A)^2}$$

where:

ε = Principal strain in microstrain units ($\mu\varepsilon$)

ε_x = Absolute strain value from strain gauge element x

The angle of principal strain was calculated by:

$$\tan 2\phi_1 = \frac{\sqrt{3}(\varepsilon_C - \varepsilon_B)}{2\varepsilon_A - (\varepsilon_B + \varepsilon_C)}$$

where $0 < \phi_1 < 90^\circ$ if $\varepsilon_C > \varepsilon_B$.

Principal strain values were also used to calculate the principal stresses during implant site preparation and implant insertion using the formula:

$$\sigma = \frac{E}{3} \left\{ \frac{\varepsilon_A + \varepsilon_B + \varepsilon_C}{1 - \nu} \pm \frac{\sqrt{2}}{1 + \nu} \sqrt{(\varepsilon_A - \varepsilon_B)^2 + (\varepsilon_B - \varepsilon_C)^2 + (\varepsilon_C - \varepsilon_A)^2} \right\}$$

where:

ρ	=	Principal stress
E	=	Young's modulus
ν	=	Poisson's ratio
ε_x	=	Absolute strain value from strain gauge element x

Using two values for Young's modulus taken from the literature (15 and 19 GNm⁻²) and two differing values for Poisson's ratio again taken from the literature (0.13 and 0.3) Wainwright et.al. (1982) the angle of the principal stress was calculated by:

$$\tan 2\phi_1 = \frac{\sqrt{3}(\varepsilon_C - \varepsilon_B)}{2\varepsilon_A - (\varepsilon_B + \varepsilon_C)}$$

where:

ε_x	=	Absolute strain value from strain gauge element x
-----------------	---	---

6.2.4 Testing procedures

Pilot tests had been performed to assess a suitable final drill diameter of 3.35mm diameter for use when preparing the implant sites. Due to the tapered profile of the Mark IV implants it is difficult to fully seat the implant in dense bone and it was determined that it was not possible to choose a drill diameter that would allow all implants to fully seat. A compromised drill diameter was selected that was the largest diameter advised for the insertion of standard and Mark II implants in dense bone which allowed their full insertion that allowed the partial insertion of the Mark IV implants. A standard implant insertion technique was used as recommended by

the implant manufacturers. None of the implant sites were countersunk as it is very difficult to standardize and control the amount of cortical bone removed with the countersink bit. Standard and Mark II implants were inserted until they were in a clinically acceptable position without the flange touching the bone surface, it was not possible to fully seat the Mark IV implants due to the taper of the implants and the bone density. The Mark IV implants were inserted into the bone until the automatic cut off of the torque controller occurred at approximately 50Ncm.

A standard implant insertion technique was used as recommended by the implant manufacturers (Figure 2.1). To standardize the implant insertion technique the dental handpiece used for drilling and implant insertion was mounted into a custom built jig which attached to the crosshead of a materials testing machine (Instron 5500, Instron Corporation, Canton, MA, USA.)(Figure 6.5). This allowed the axial speed of drilling and implant insertion to be controlled and allowed the load placed upon the specimen to be monitored. The use of the testing machine also allowed the drilled implant site and the path of implant insertion to be accurately and reproducibly aligned. During all of the drilling phases of implant site preparation a downward crosshead speed of 1mm/sec was used, whilst for tapping of the STA and MKII implant types a downward crosshead speed of 0.2mm/sec was used with this rate being doubled to 0.4mm/sec for the MKIV implant due to its double thread design. A summary of drill/tap/implant speeds and depths of penetration is presented in Tables 6.1 and 6.2. Drilling was performed at full speed, with implant insertion being performed at a lower speed which approximates to one revolution of the implant every 3 seconds; the cut out on the electronic torque controller (Nobel Biocare AB, Gothenburg, Sweden) was set to 45Ncm.

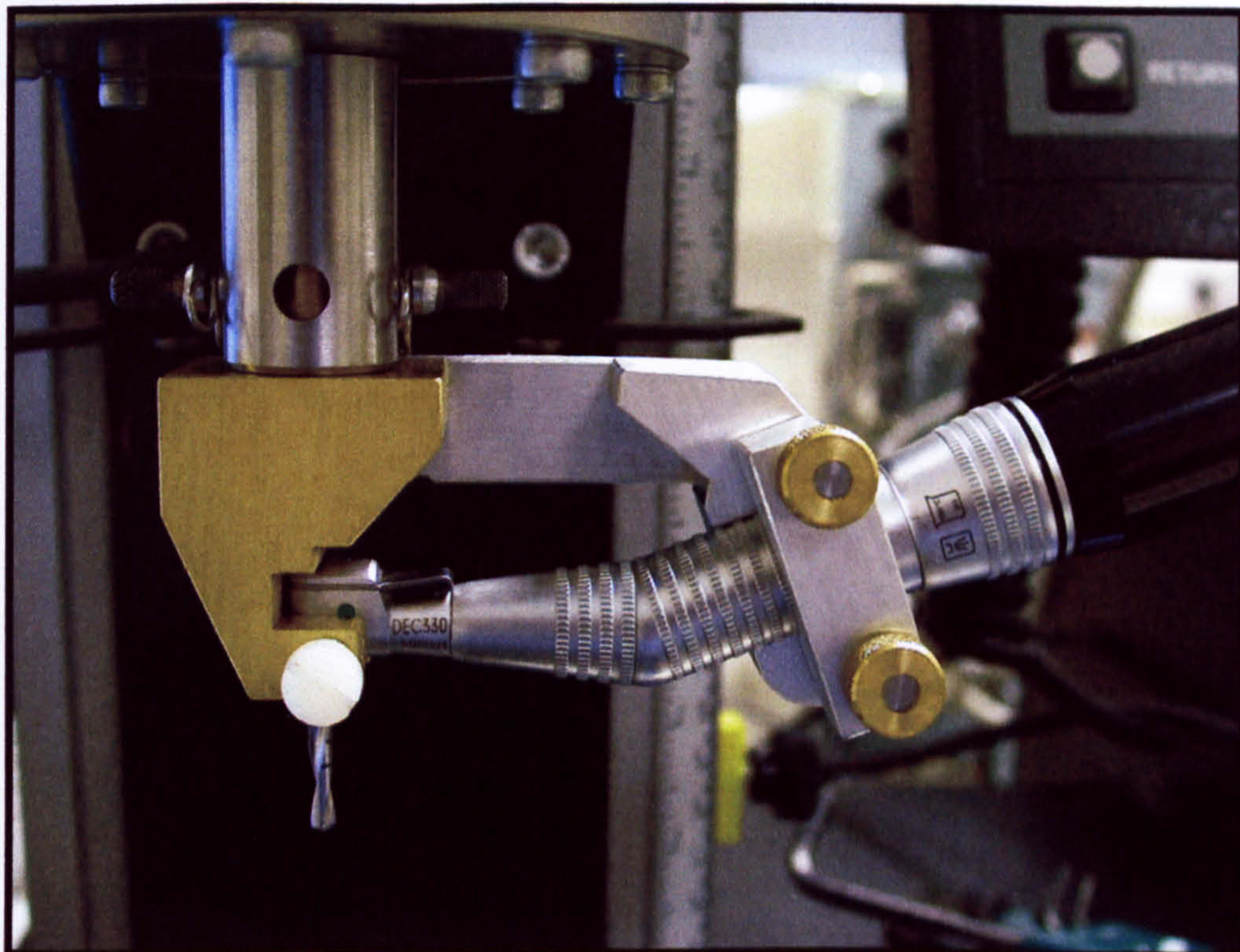
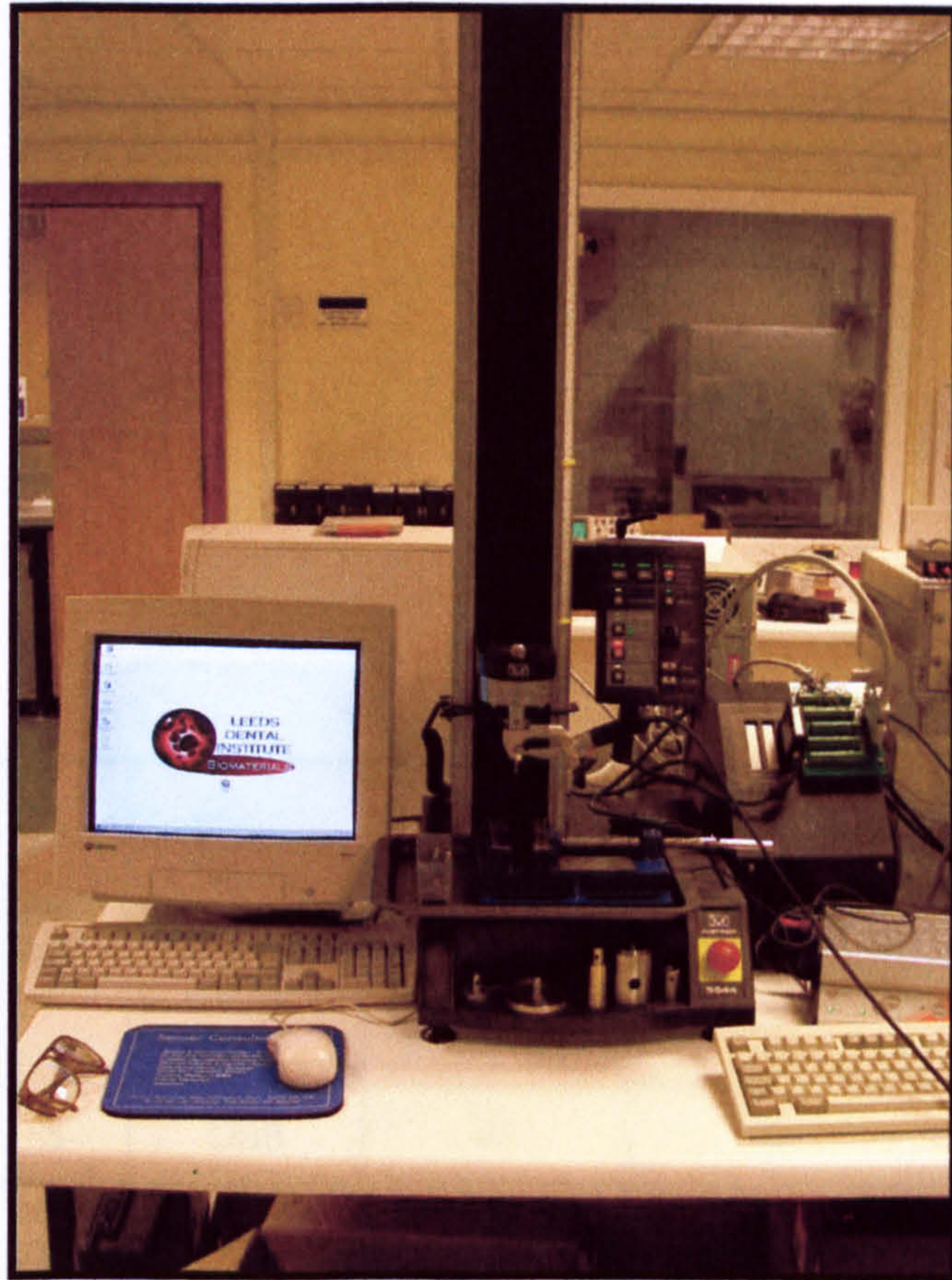


Figure 6.5: Instron mechanical testing machine and close view of handpiece rig.

	Feed Rate mm/sec	Depth mm	Torque Controller speed	Torque Controller Max. Torque Ncm	Data Logged				
					Load N	Extension mm	Strain gauge element		
							1	2	3
Guide Drill	1	5	Drill	45	✓	✓	✓	✓	✓
2mm Twist Drill	1	12	Drill	45	✓	✓	✓	✓	✓
Pilot Drill	1	7	Drill	45	✓	✓	✓	✓	✓
3.35mm Twist Drill	1	12	Drill	45	✓	✓	✓	✓	✓

Table 6.1: summary of implant site preparation stages.

	Feed Rate mm/sec	Depth Mm	Torque Controller speed	Torque Controller Max. Torque Ncm	Data Logged				
					Load N	Extension mm	Strain gauge element		
							1	2	3
Standard	0.2	12	High	45	✓	✓	✓	✓	✓
Mark II	0.2	12	High	45	✓	✓	✓	✓	✓
Mark IV	0.4	12	High	45	✓	✓	✓	✓	✓

Table 6.2: summary of implant insertion details.

6.2.5 Data acquisition

During implant site preparation and implant insertion, axial load and crosshead displacement were monitored and logged from the testing machine. Strain gauge data was collected as a voltage output from the strain gauge amplifier and insertion torque was recorded from a modified electronic torque controller (Nobel Biocare AB, Gothenburg, Sweden) by measuring the voltage drop across a resistor to infer the current drain from the handpiece motor. Temperature was monitored by using a thermocouple. All data was logged simultaneously into separate analogue inputs of a data acquisition card (National Instruments). The channel allocation used is outlined below:

- 1) Strain gauge element 1
- 2) Strain gauge element 2
- 3) Strain gauge element 3
- 4) Insertion torque, torque controller
- 5) Load cell output, testing machine
- 6) Crosshead displacement, testing machine
- 7) Temperature, thermocouple amplifier

Pilot studies were carried out in order to identify the appropriate sampling rate and a sampling rate of 10Hz was found to be appropriate. The data acquisition was controlled via a graphical user interface software package (Labview 5.1, National Instruments, Newbury, Berkshire, UK). This allows the operator to control the data as inputs to a specifically programmed virtual instrument. Data from all channels were converted within the software package and saved to disc as ASCII files with 7

columns, one for each channel of data (Figure 6.6). The ASCII file data was logged as the following:

1)	Strain gauge element 1	$\mu\epsilon$
2)	Strain gauge element 2	$\mu\epsilon$
3)	Strain gauge element 3	$\mu\epsilon$
4)	Insertion torque, torque controller	Ncm
5)	Load cell output, testing machine	N
6)	Crosshead displacement, testing machine	mm
7)	Temperature, Thermocouple amplifier	$^{\circ}\text{C}$

6.2.6 Statistics

Statistical comparison was performed using analysis of variance (ANOVA). Where a significant difference was indicated the Bonferroni multiple comparison test was carried out with the significance set at $p=0.05$.

6.3 Results

The results of this study are summarized in Figures 6.7 to 6.24.

Figure 6.7 illustrates the response of a 3-element rosette gauge to implant site preparation. Figure 6.8 shows the same data plotted against insertion depth rather than time. Figures 6.9 to 6.11 show typical responses for different implant types during insertion into the bovine rib specimens. Figures 6.12 to 6.14 show the implant insertion responses plotted against insertion depth.



Figure 6.6(a): Labview display used in Chapter 6.

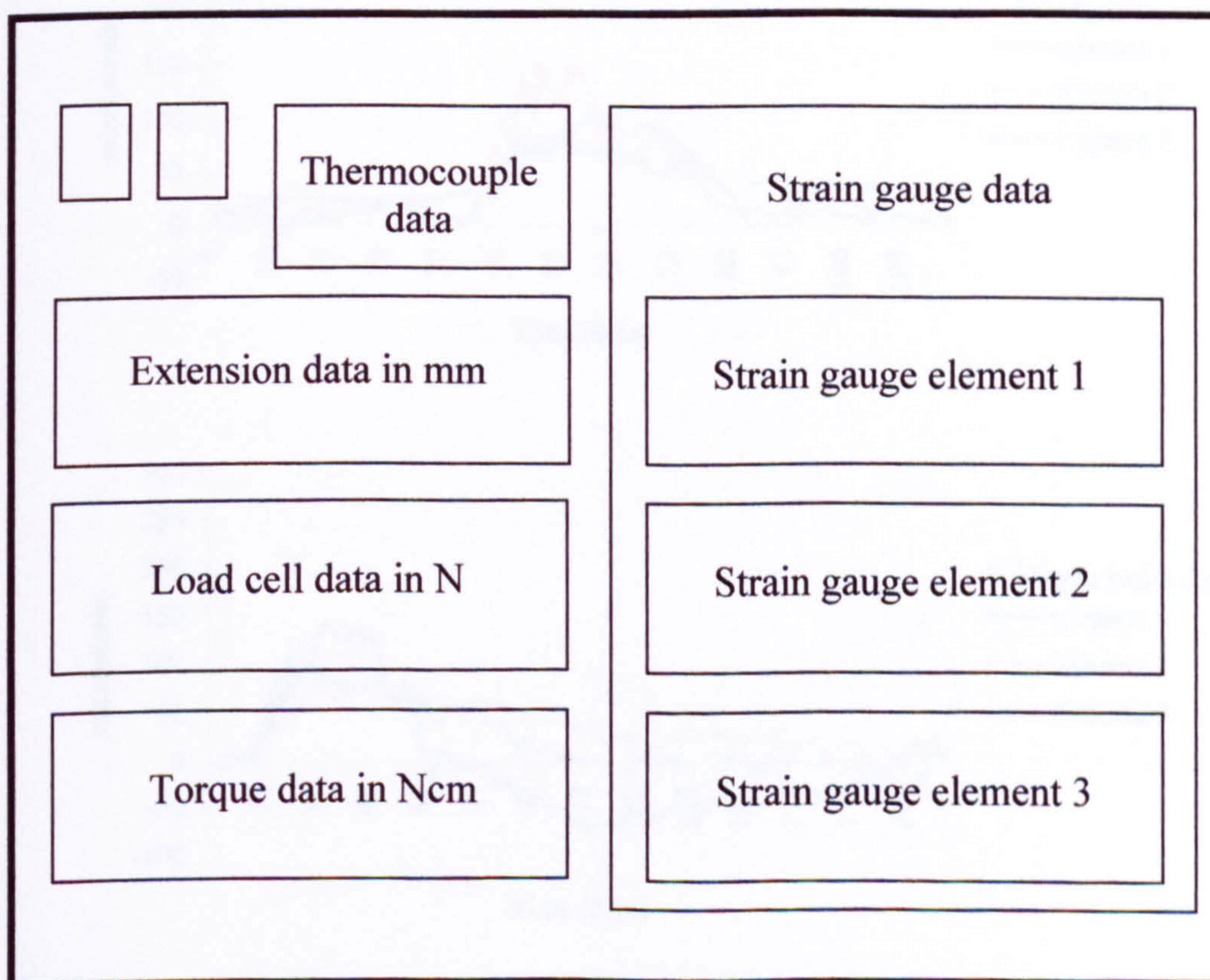


Figure 6.6(b): Labview display schematic.

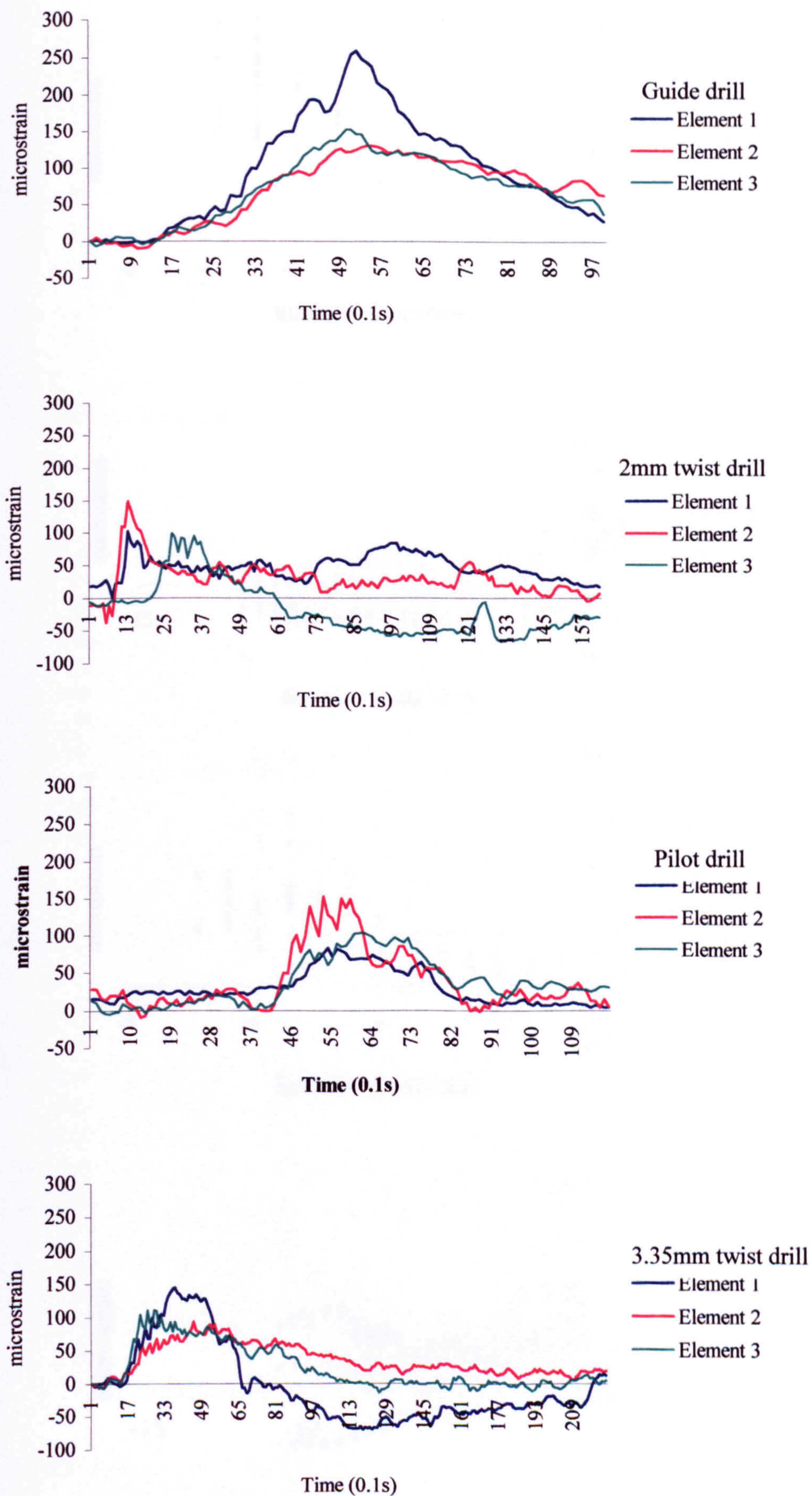


Figure 6.7: Strain gauge response to implant site preparation.

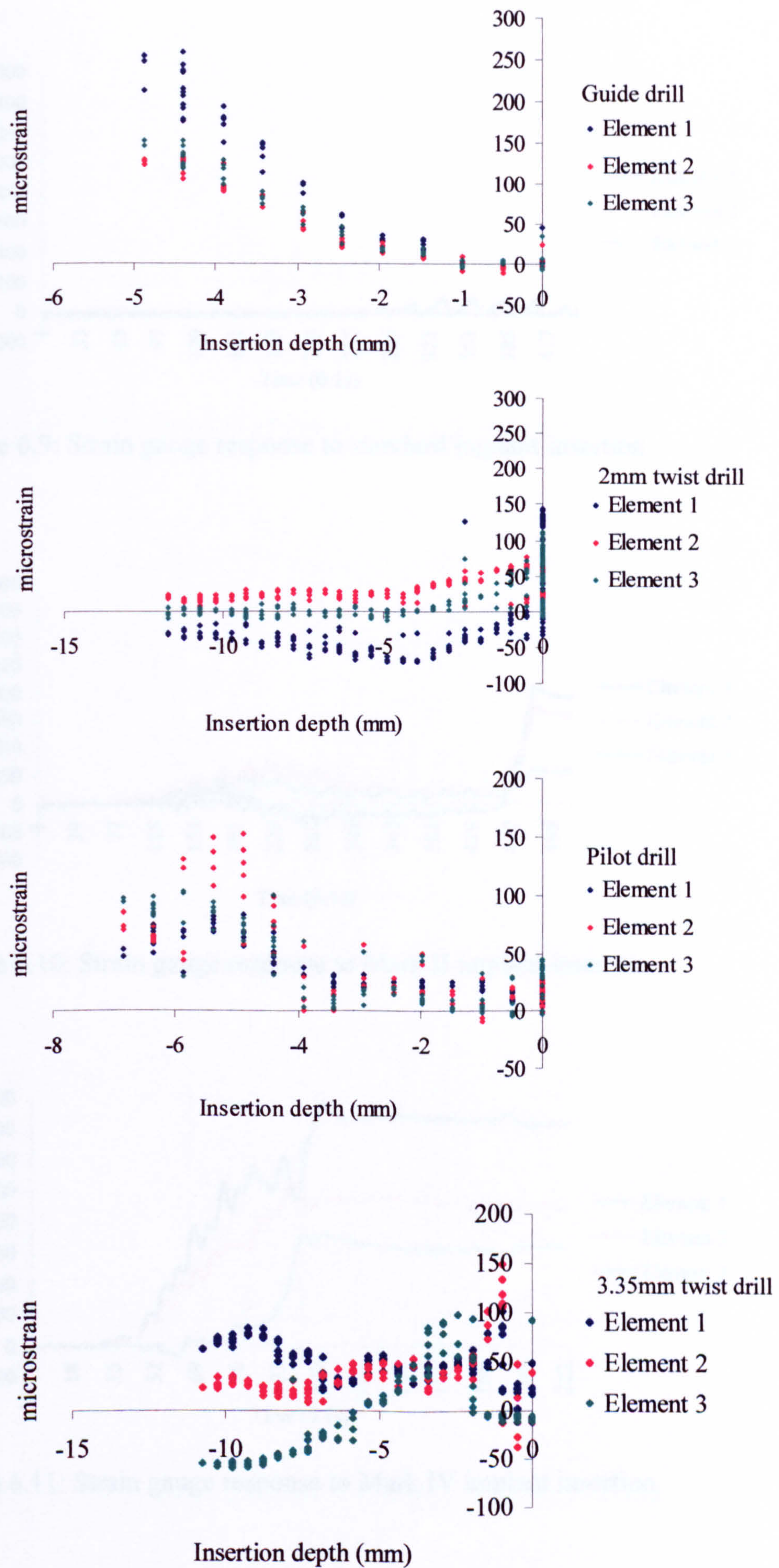


Figure 6.8: Strain gauge response to implant site preparation.

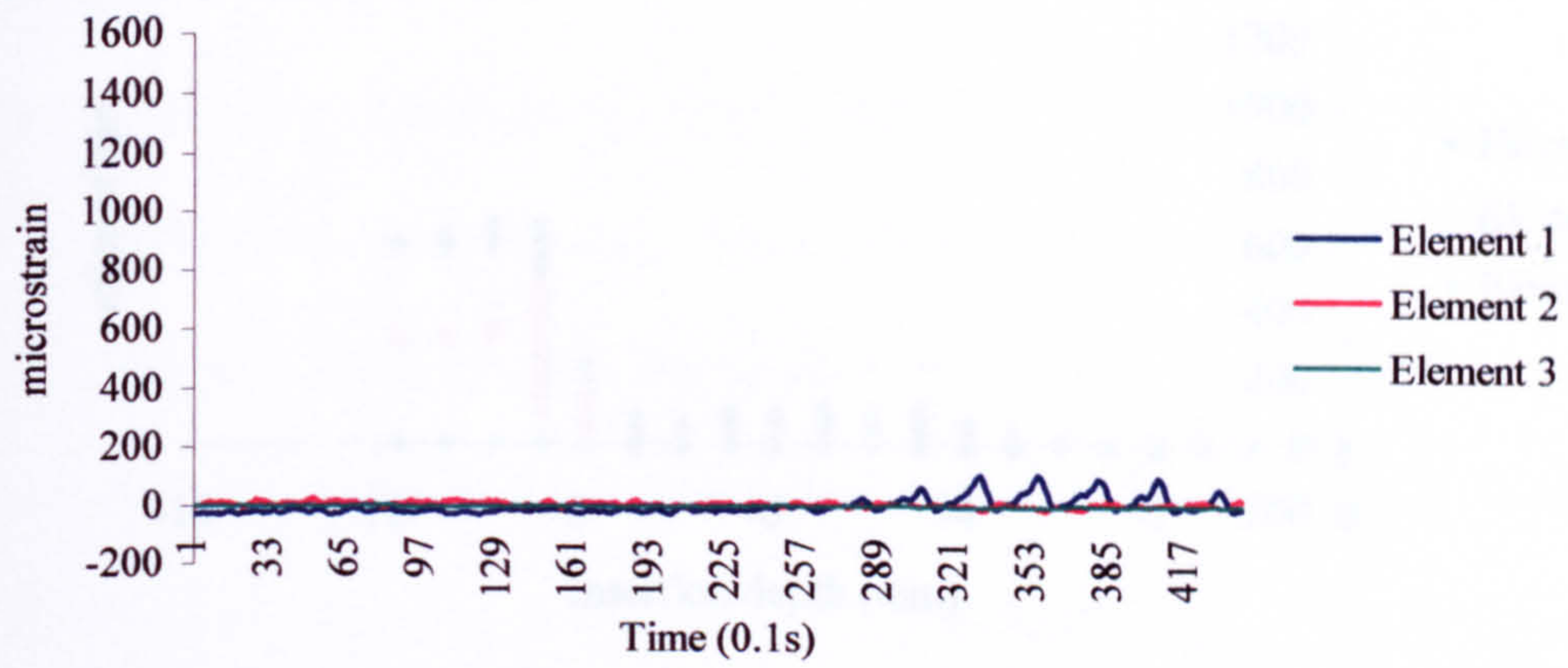


Figure 6.9: Strain gauge response to standard implant insertion.

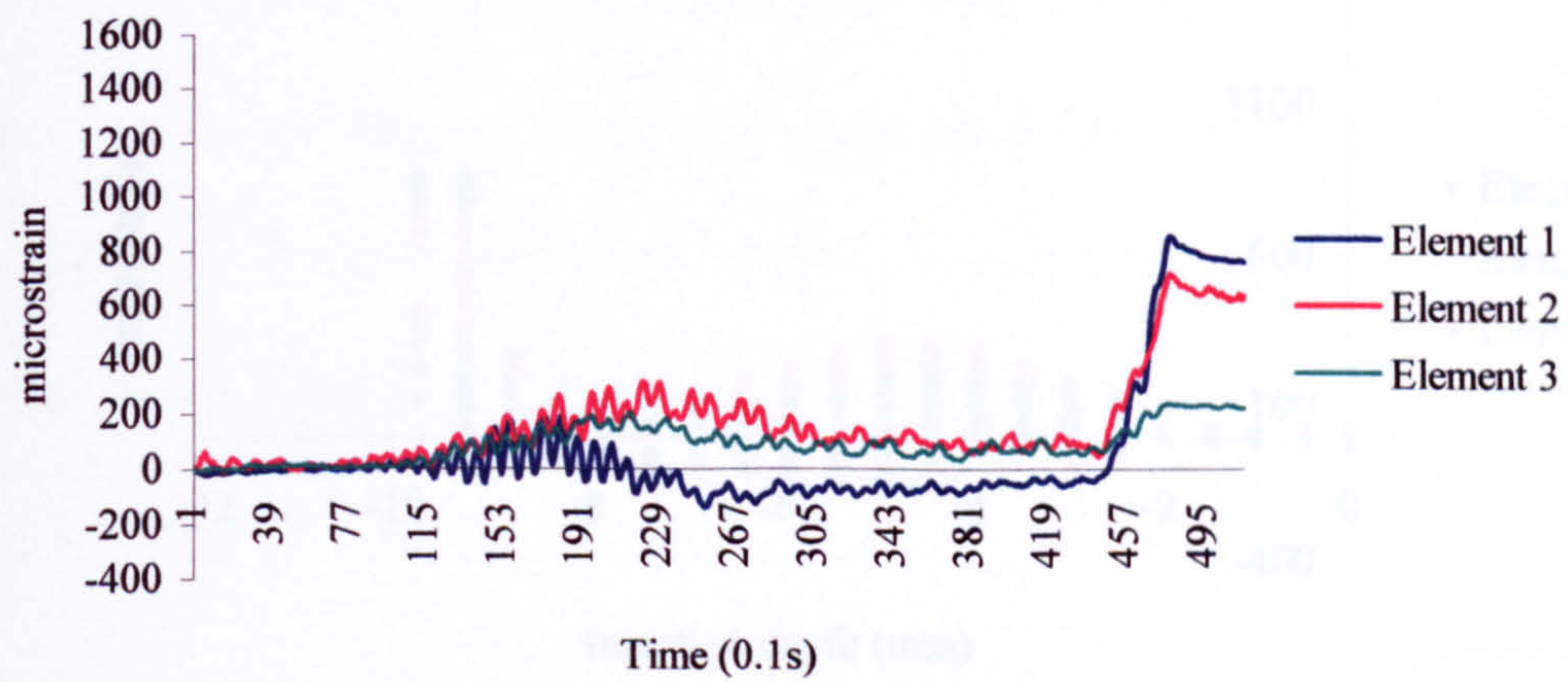


Figure 6.10: Strain gauge response to Mark II implant insertion.

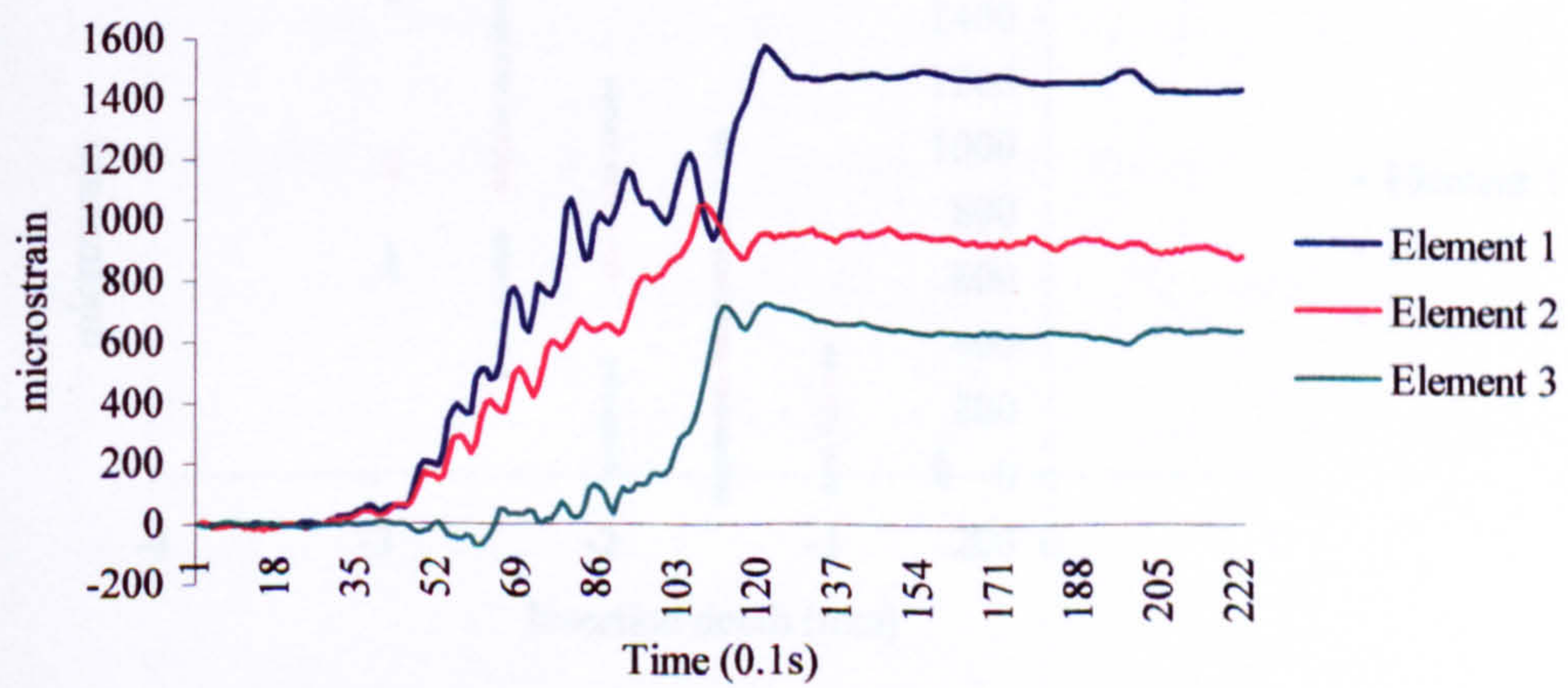


Figure 6.11: Strain gauge response to Mark IV implant insertion.

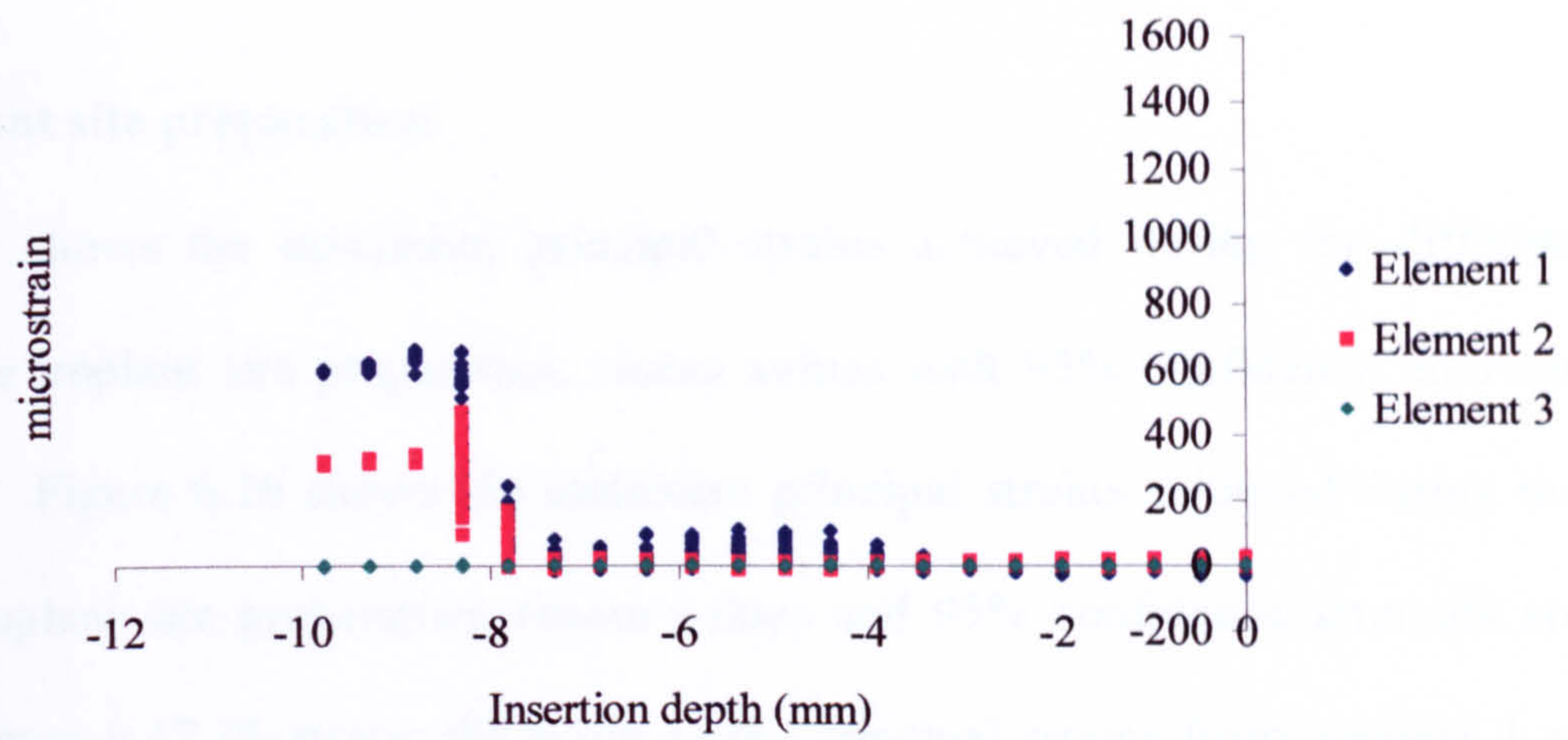


Figure 6.12: Strain gauge response to standard implant insertion.

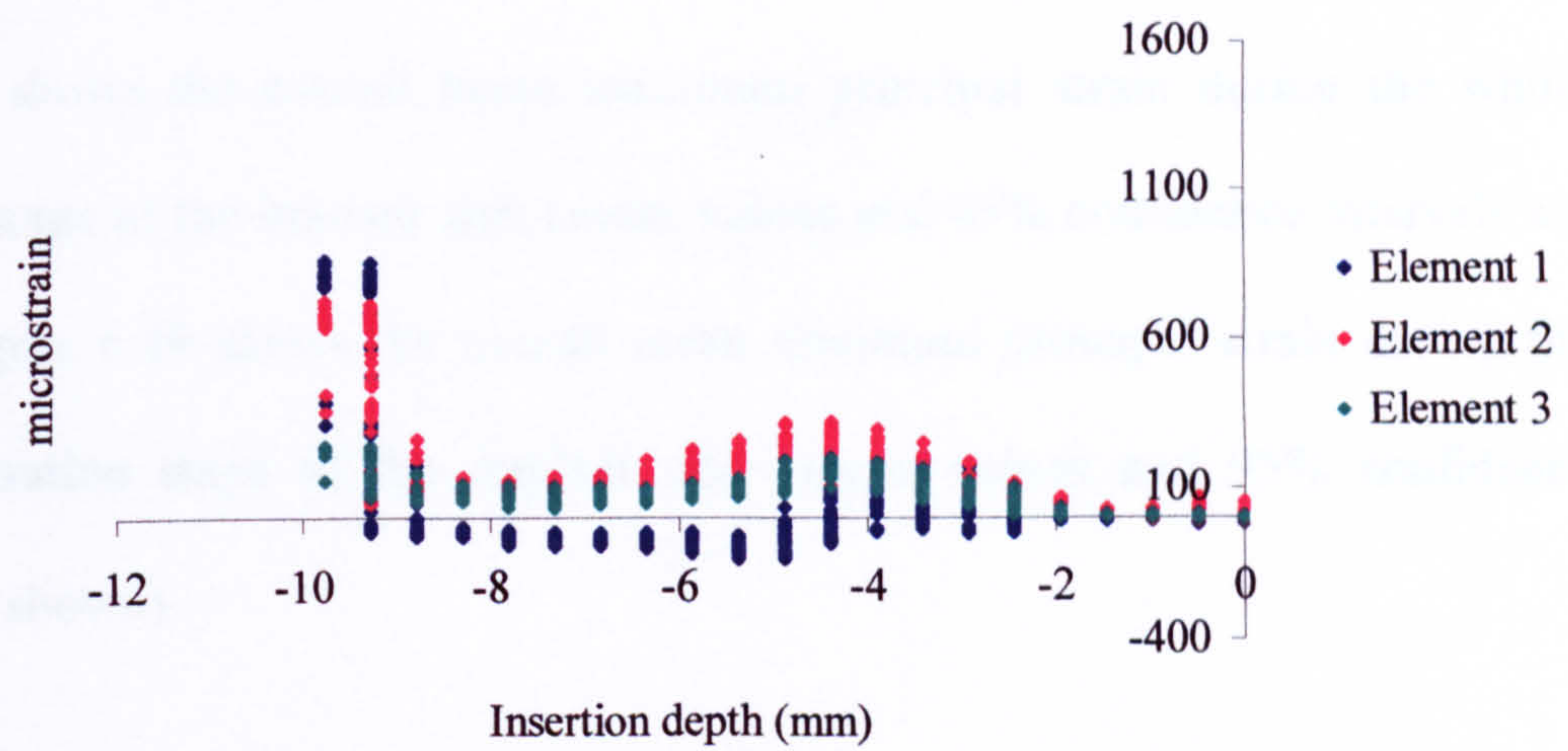


Figure 6.13: Strain gauge response to Mark II implant insertion.

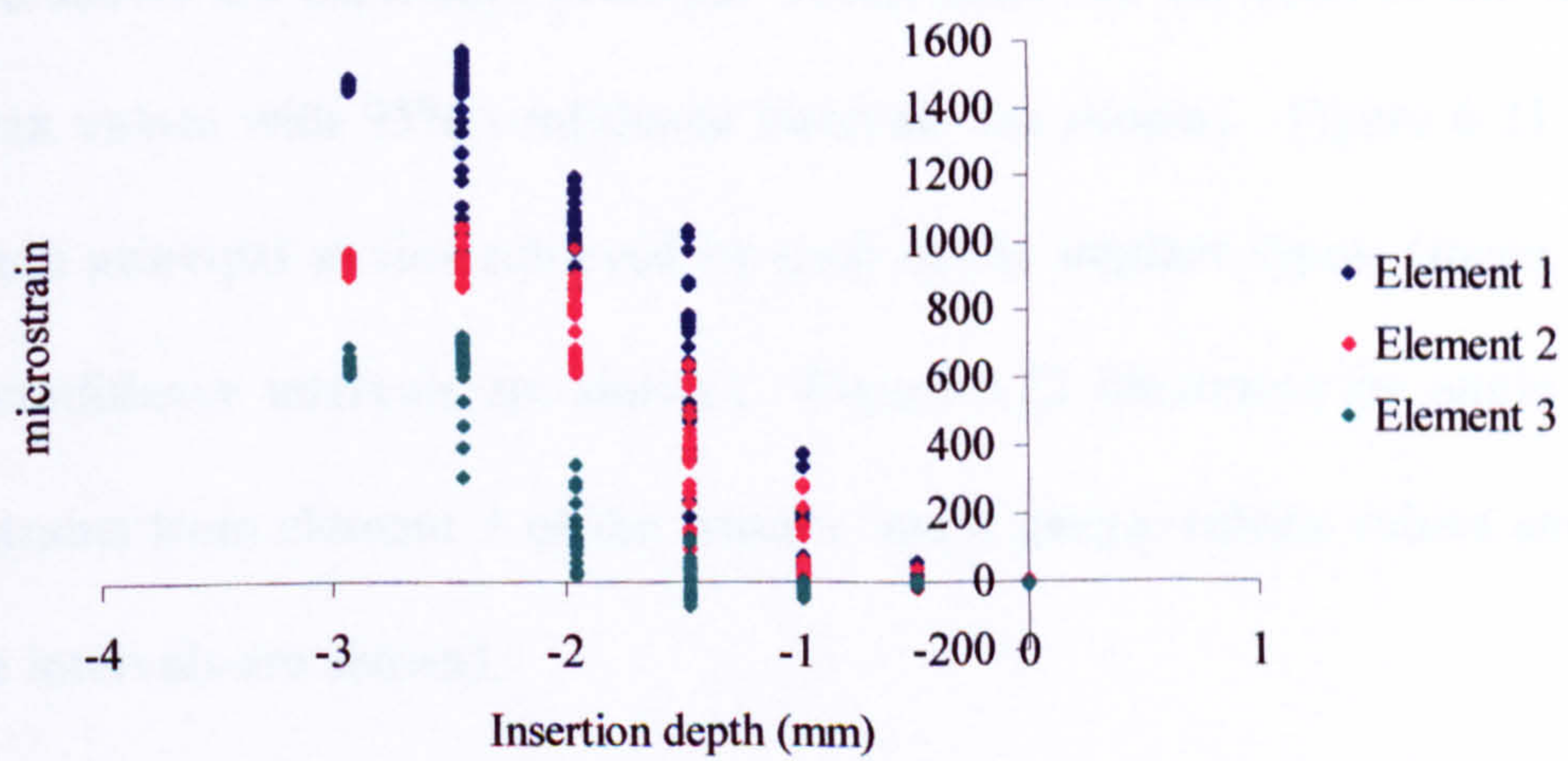


Figure 6.14: Strain gauge response to Mark IV implant insertion.

6.3.1 Implant site preparation

Figure 6.15 shows the maximum principal strains achieved during the different stages of the implant site preparation; (mean values with 95% confidence intervals are shown). Figure 6.16 shows the minimum principal strains achieved during the stages of implant site preparation; (mean values and 95% confidence intervals are shown). Figure 6.17 illustrates the angle of the principal strains from element 1 of the Rosette strain gauge; (mean values and 95% confidence intervals are shown).

Figure 6.18 shows the overall mean maximum principal strain during the whole preparation stage of the implant site; (mean values and 95% confidence intervals are shown). Figure 6.19 shows the overall mean minimum principal strain during the whole preparation stage of the implant site; (mean values and 95% confidence intervals are shown).

6.3.2 Implant insertion

Figure 6.20 shows the maximum principal strains achieved for each of the implant types; (mean values with 95% confidence intervals are shown). Figure 6.21 shows the minimum principal strains achieved by each of the implant types; (mean values and 95% confidence intervals are shown). Figure 6.22 illustrates the angle of the principal strains from element 1 of the Rosette strain gauge; (mean values and 95% confidence intervals are shown).

Figure 6.23 shows the overall mean maximum principal strain during the whole duration of placing the implant; (mean values and 95% confidence intervals are shown). Figure 6.24 shows the overall mean minimum principal strain during the

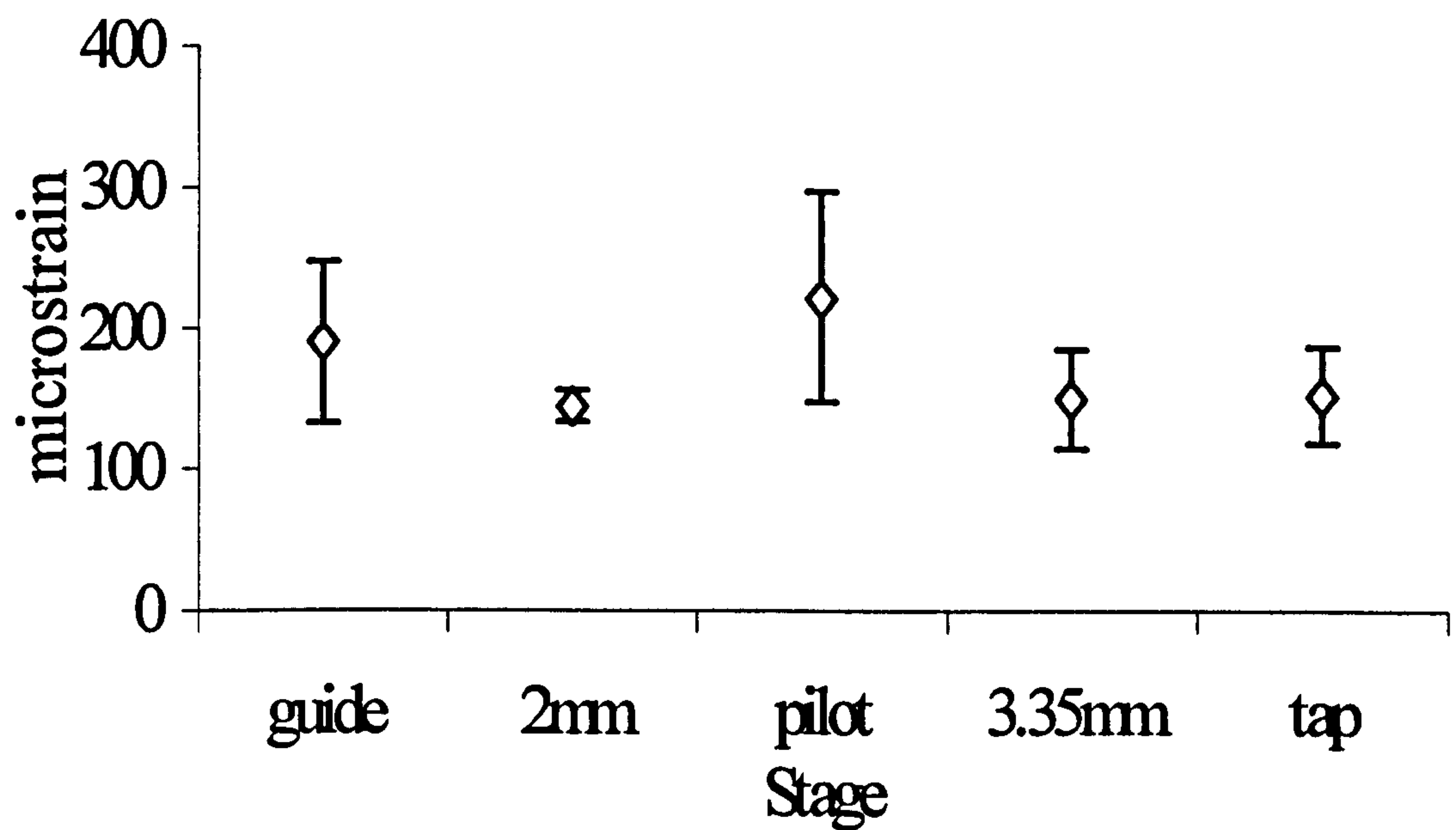


Figure 6.15: Maximum principal strains during the stages of implant site preparation. Mean values and 95% confidence intervals are shown. (n=36).

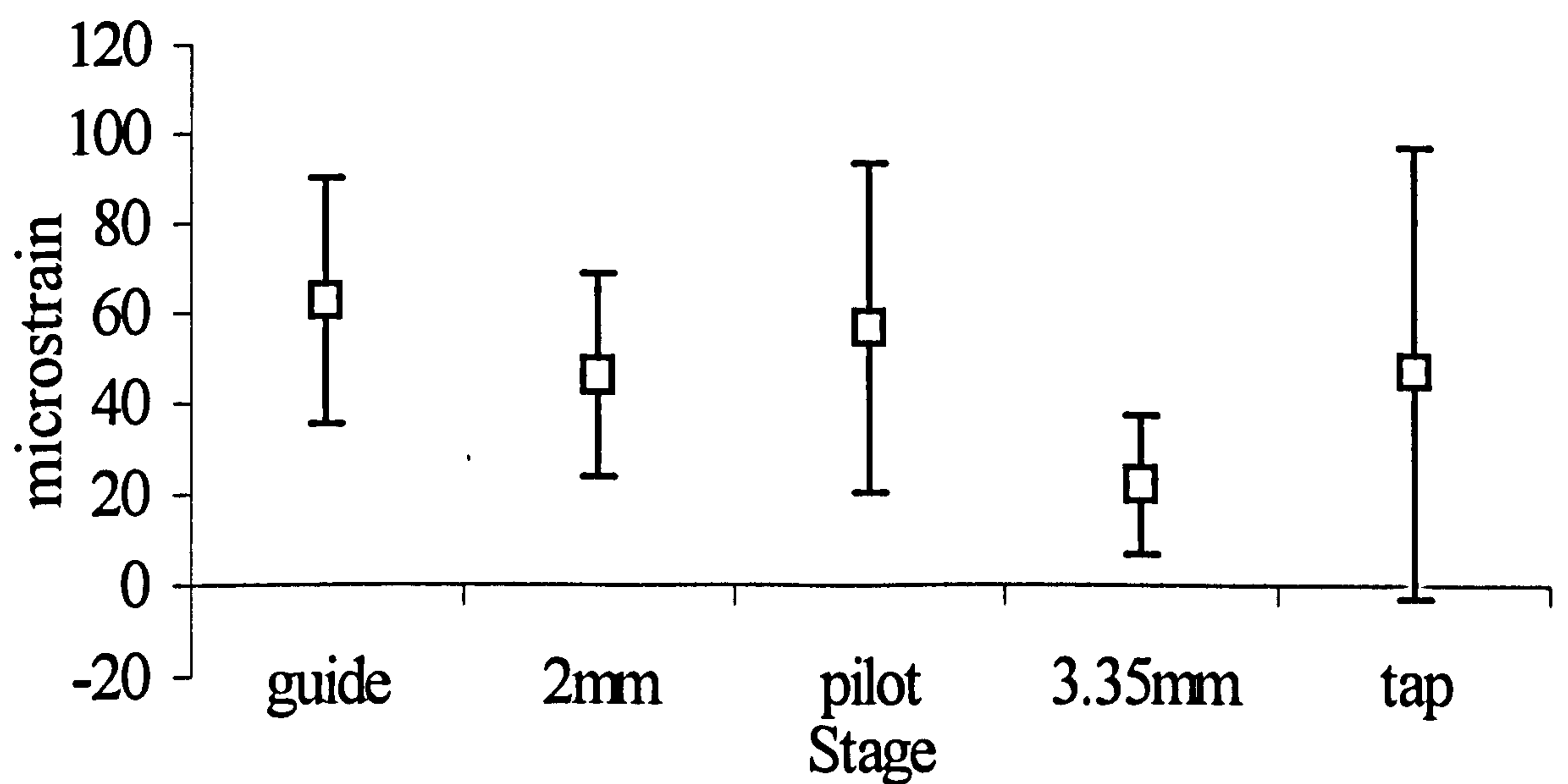


Figure 6.16: Minimum principal strains during the stages of implant site preparation. Mean values and 95% confidence intervals are shown. (n=36).

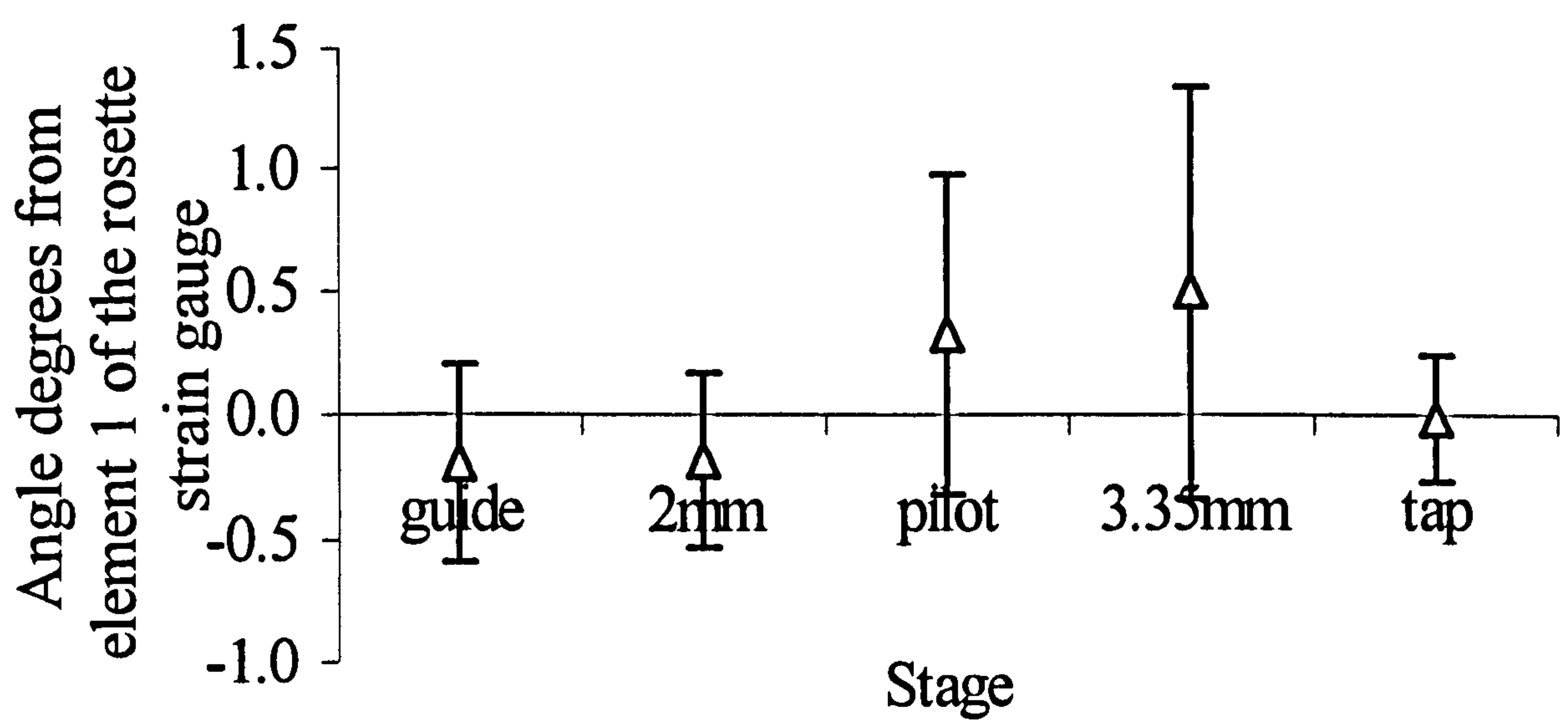


Figure 6.17: Angle of the principal strains during the stages of implant site preparation. Mean values and 95% confidence intervals are shown. (n=36).

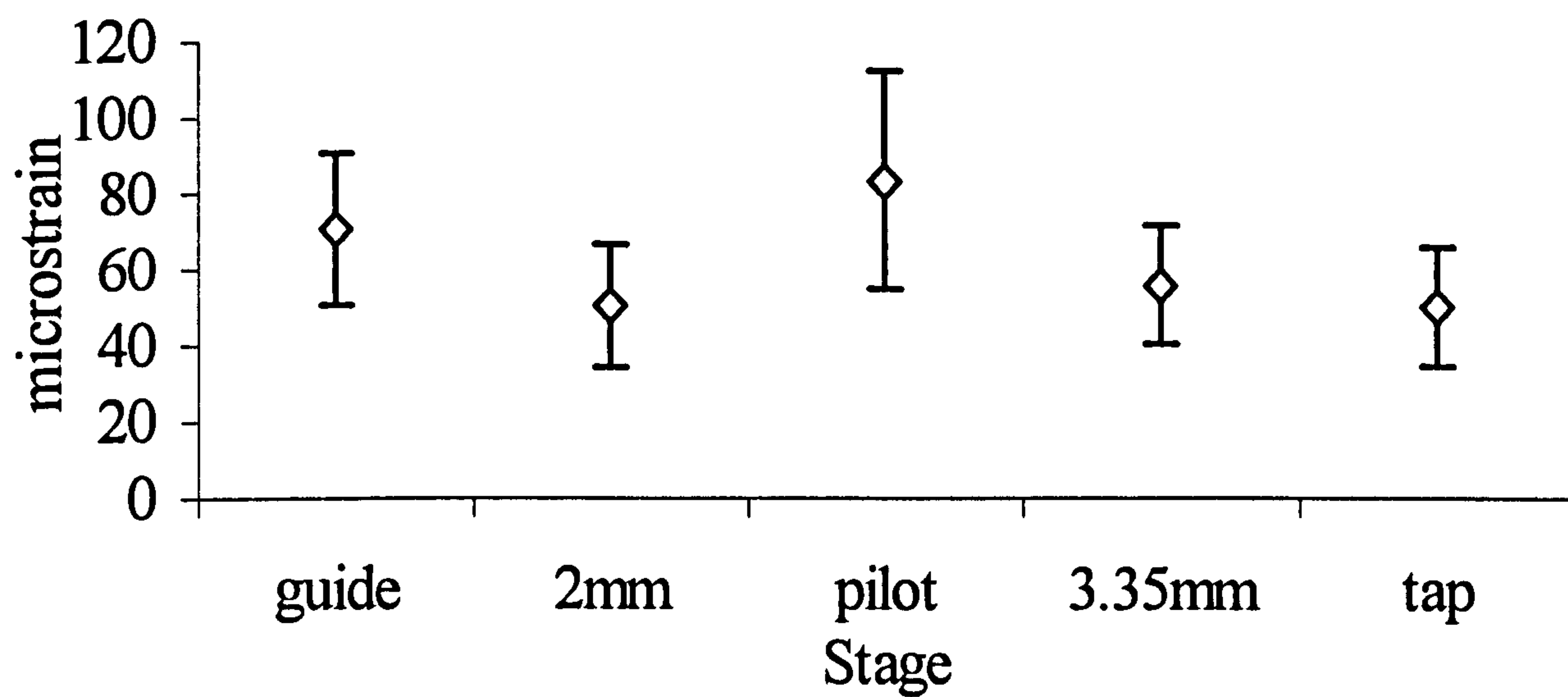


Figure 6.18: Mean maximum principal strain during implant site preparation. Mean values and 95% confidence intervals are shown. (n=36).

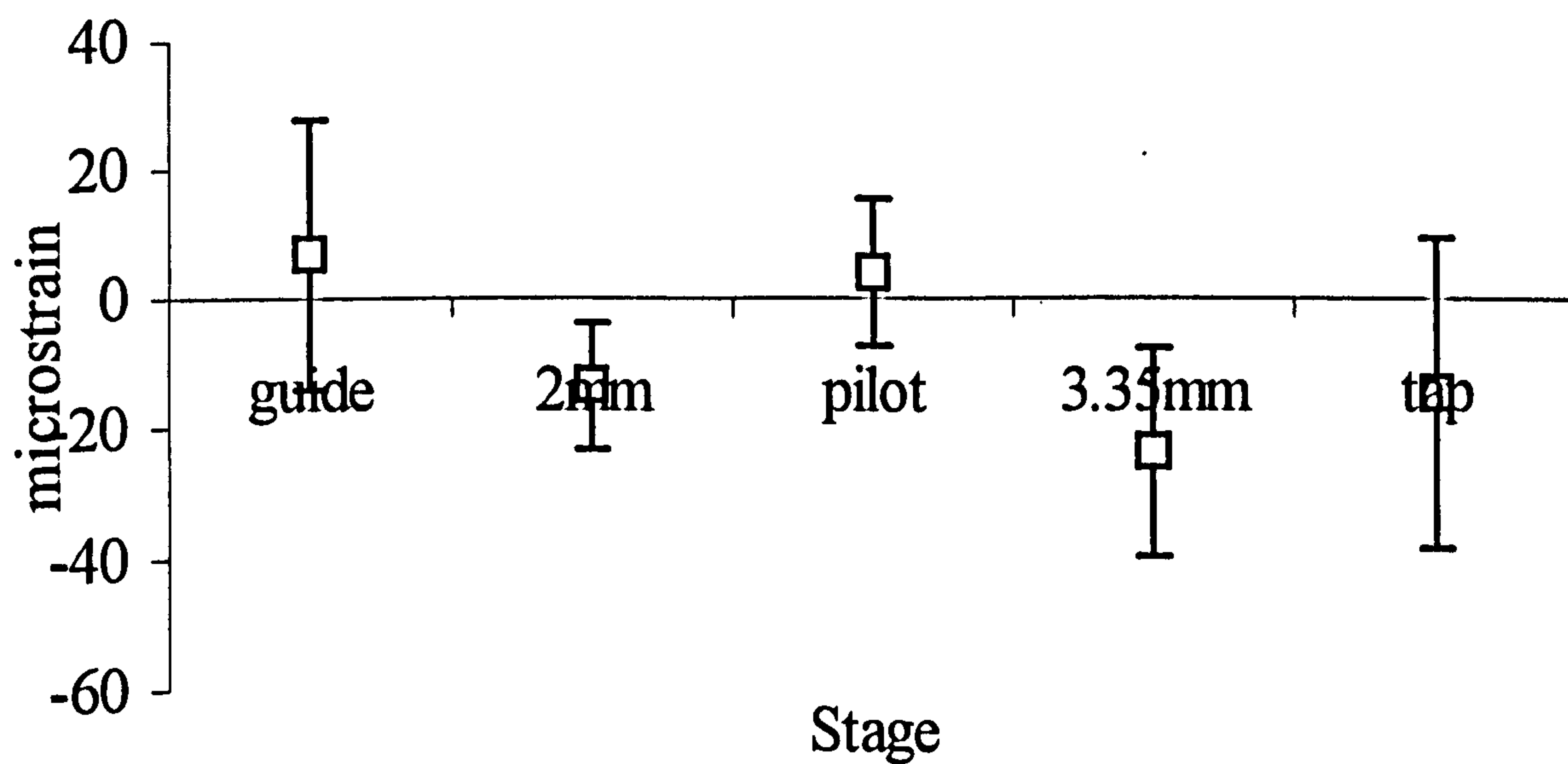


Figure 6.19: Mean minimum principal strain during implant site preparation. Mean values and 95% confidence intervals are shown. (n=36).

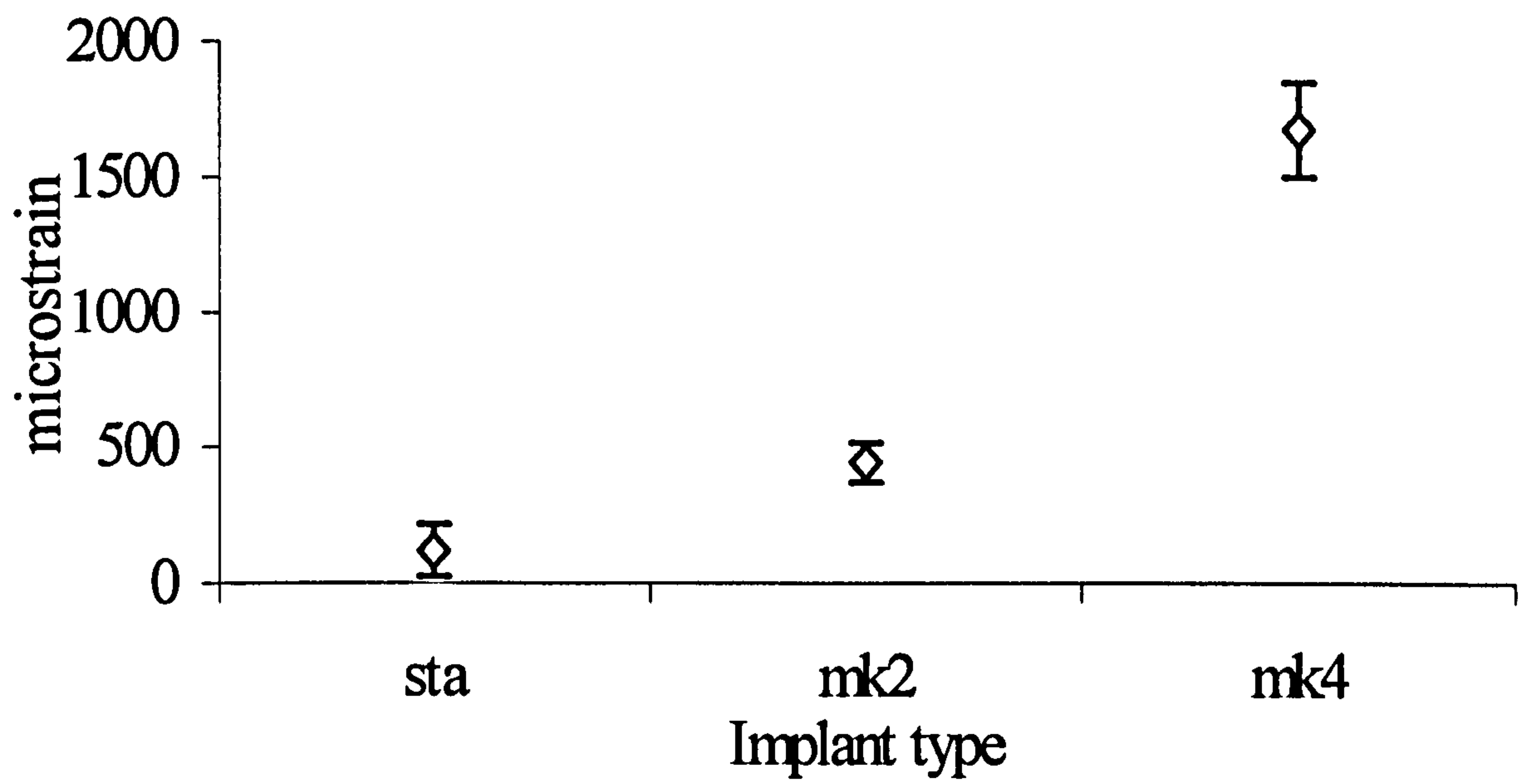


Figure 6.20: Maximum principal strain during implant insertion. Mean values and 95% confidence intervals are shown. (n=9).

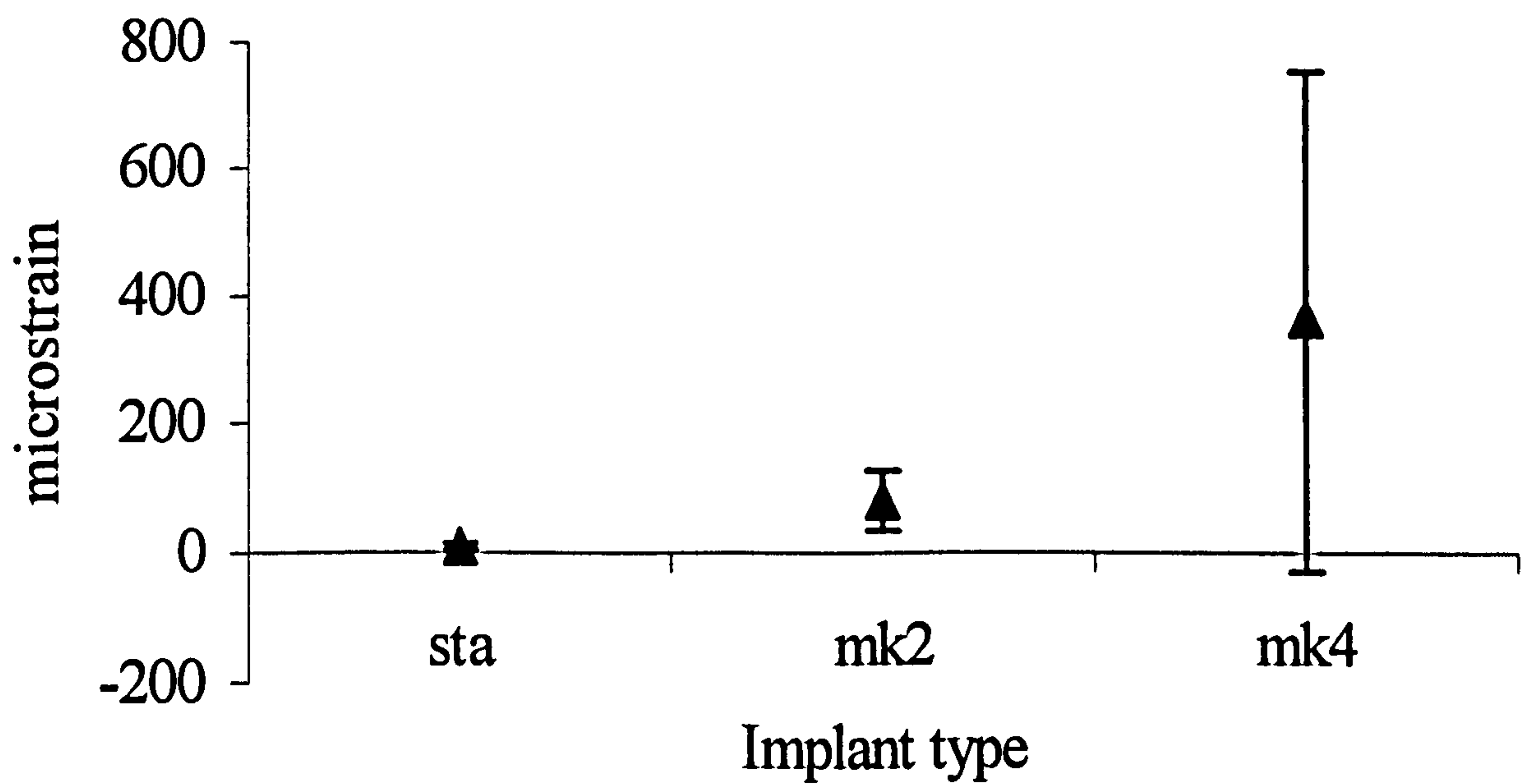


Figure 6.21: Minimum principal strain during implant insertion. Mean values and 95% confidence intervals are shown. (n=9).

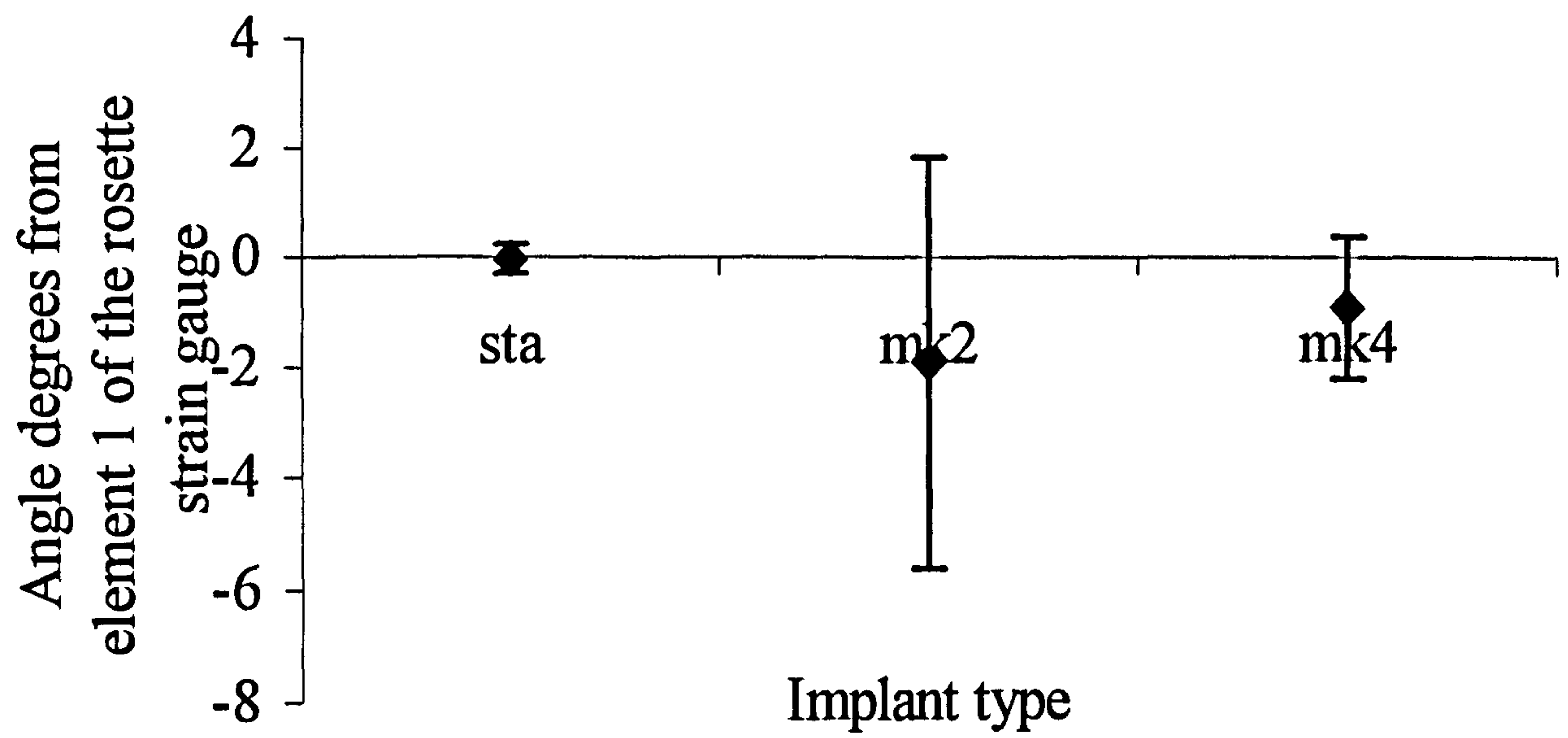


Figure 6.22: The angle of principal strain during implant insertion. Mean values and 95% confidence intervals are shown. (n=9).

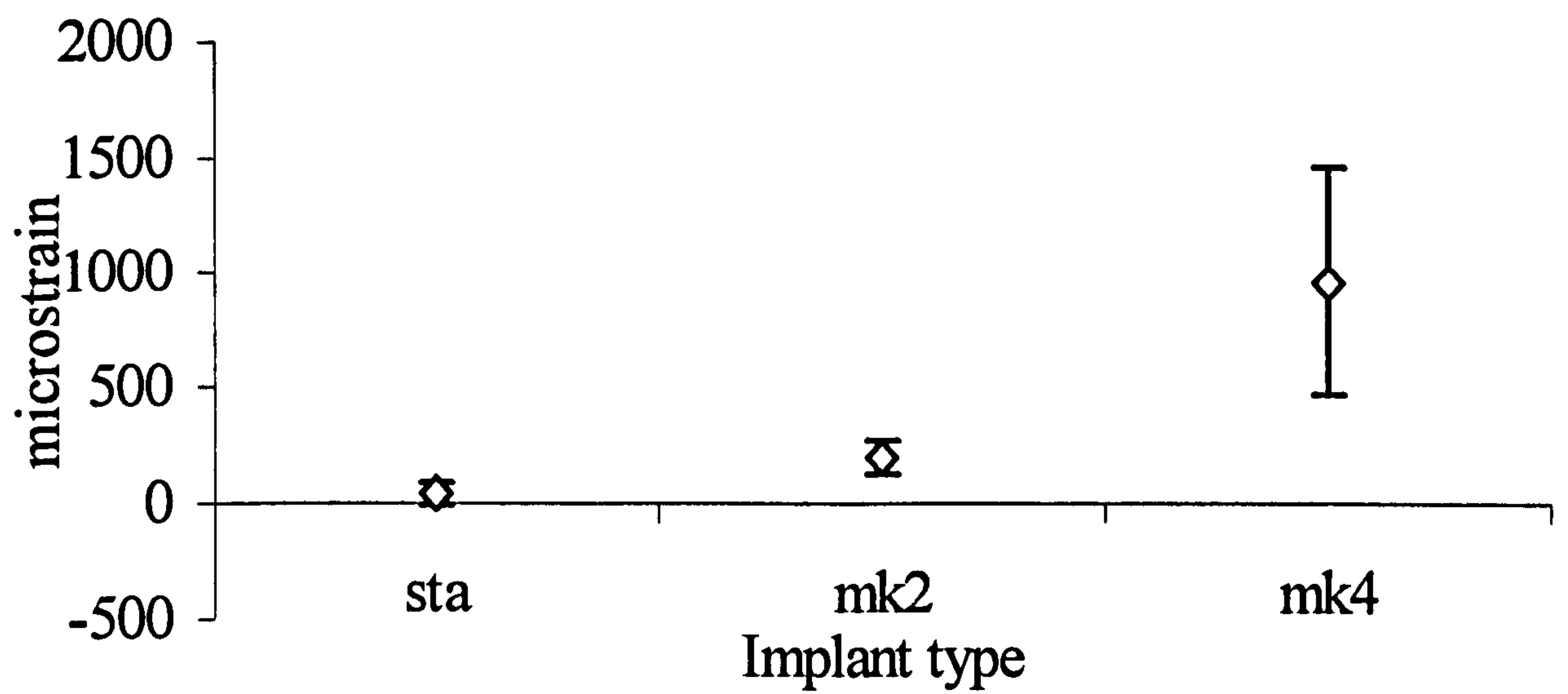


Figure 6.23: Mean maximum principal strain during implant insertion. Mean values and 95% confidence intervals are shown. (n=9).

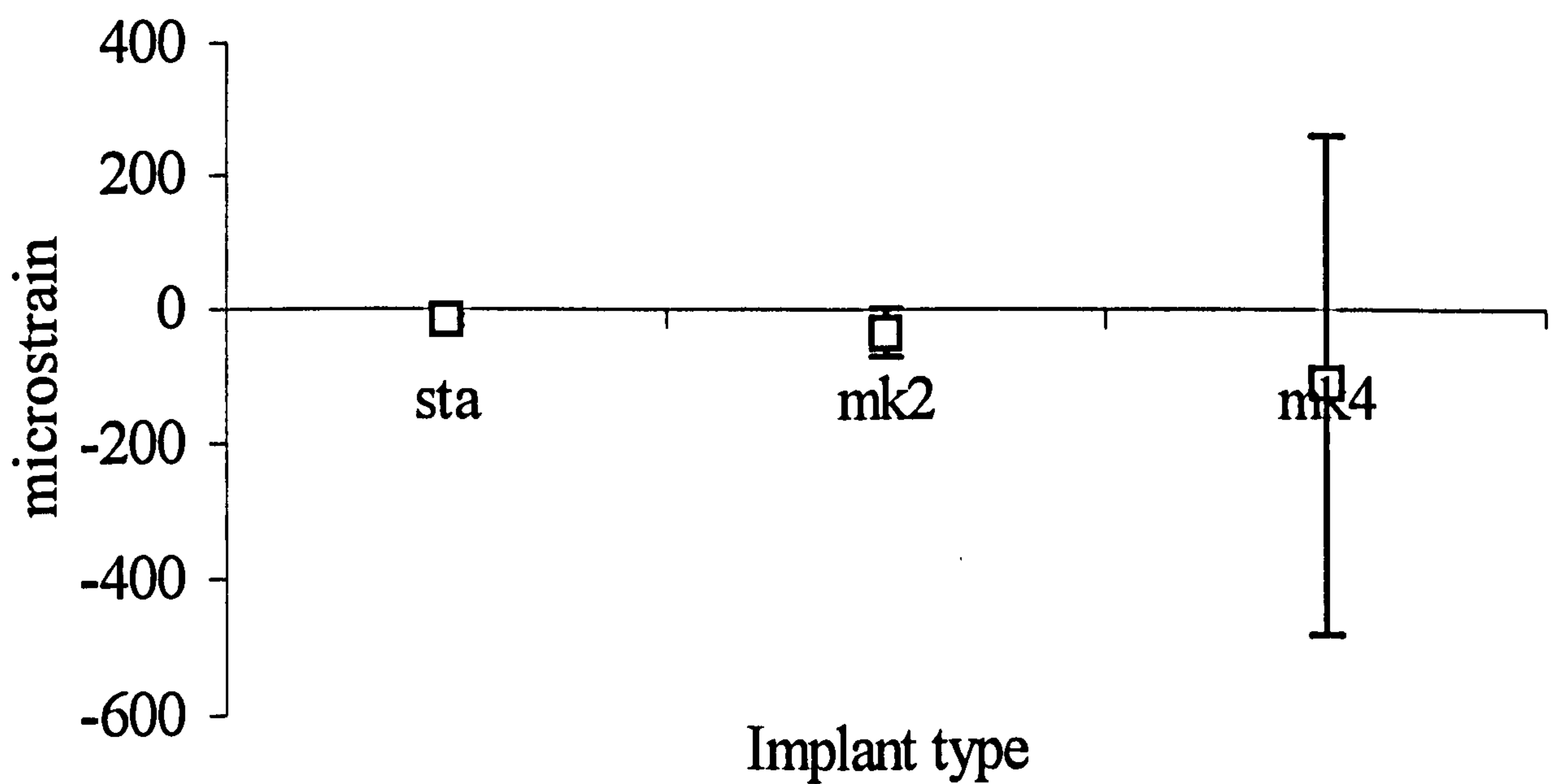


Figure 6.24: Mean minimum principal strain during implant insertion. Mean values and 95% confidence intervals are shown. (n=9).

whole duration of placing the implant; (mean values and 95% confidence intervals are shown). Figures 6.25 to 6.28 show principal stress values calculated from the data using a range of values for Poisson's ratio and Young's modulus. A summary of the results is shown in Table 6.3 and Table 6.4

6.4 Discussion

6.4.1 Discussion of the method

The aim of the study should be to reproduce in-vitro the in-vivo moisture state, temperature, applied stress, strain rate, material properties of the implant and the host site. The in-vitro study cannot truly replicate the in-vivo situation, a problem found with all biological systems when studied with strain gauge techniques. The moisture state in this study was close to the ideal since the bone was kept saturated throughout the preparation and test period with normal saline. Dehydration was avoided as this would have two main effects upon testing. Firstly, the direct effect upon the strain gauge/adhesive properties and secondly Dempster and Liddicoat (1952) reported that dehydration of bone alters its mechanical properties finding that dry bone was significantly more brittle than wet bone. Bone specimen preparation was carried out according to the guidelines suggested by Dabestani in 1992 based upon his review of the literature.

Temperature was difficult to match to the in-vivo situation. Pilot tests were conducted at both 4°C and 37°C but it was found that tests conducted at room temperature were the most temperature stable. Sedlin and Hirsch (1966) found no difference in the mechanical properties of femoral bone tested at 21°C and 37°C, with no detectable differences in maximal stress and energy absorption. In this

	Guide drill	2mm twist drill	Pilot drill	3.35mm twist drill	Tap
Max Principal strain ($\mu\epsilon$)	190 ± 92	144 ± 16	222 ± 126	150 ± 54	154 ± 30
Min Principal strain ($\mu\epsilon$)	63 ± 43	46 ± 32	57 ± 61	22 ± 23	47 ± 44
Angle of Principal strain (degree)	-0.19 ± 0.6	-0.18 ± 0.5	0.33 ± 1.1	0.50 ± 1.2	-0.02 ± 0.2
Average Max Principal strain during insertion ($\mu\epsilon$)	71 ± 32	50 ± 23	84 ± 46	56 ± 24	51 ± 14
Average Min Principal strain during insertion ($\mu\epsilon$)	7 ± 33	-13 ± 14	4 ± 19	-24 ± 24	-15 ± 21

Mean values \pm s.d are shown

Table 6.3: Implant site preparation – summary of data.

	Standard Implant	Mark II Implant	Mark IV Implant
Max Principal strain ($\mu\epsilon$)	118 ± 97	443 ± 64	1680 ± 156
Min Principal strain ($\mu\epsilon$)	9 ± 5	79 ± 41	363 ± 346
Angle of Principal strain (degrees)	-0.04 ± 0.3	-1.91 ± 3.3	-0.93 ± 1.1
Average Max Principal strain during insertion ($\mu\epsilon$)	43 ± 48	198 ± 65	969 ± 439
Average Min Principal strain during insertion ($\mu\epsilon$)	-17 ± 9	-34 ± 32	-110 ± 329

Mean values \pm s.d are shown

Table 6.4: Implant types – summary of data.

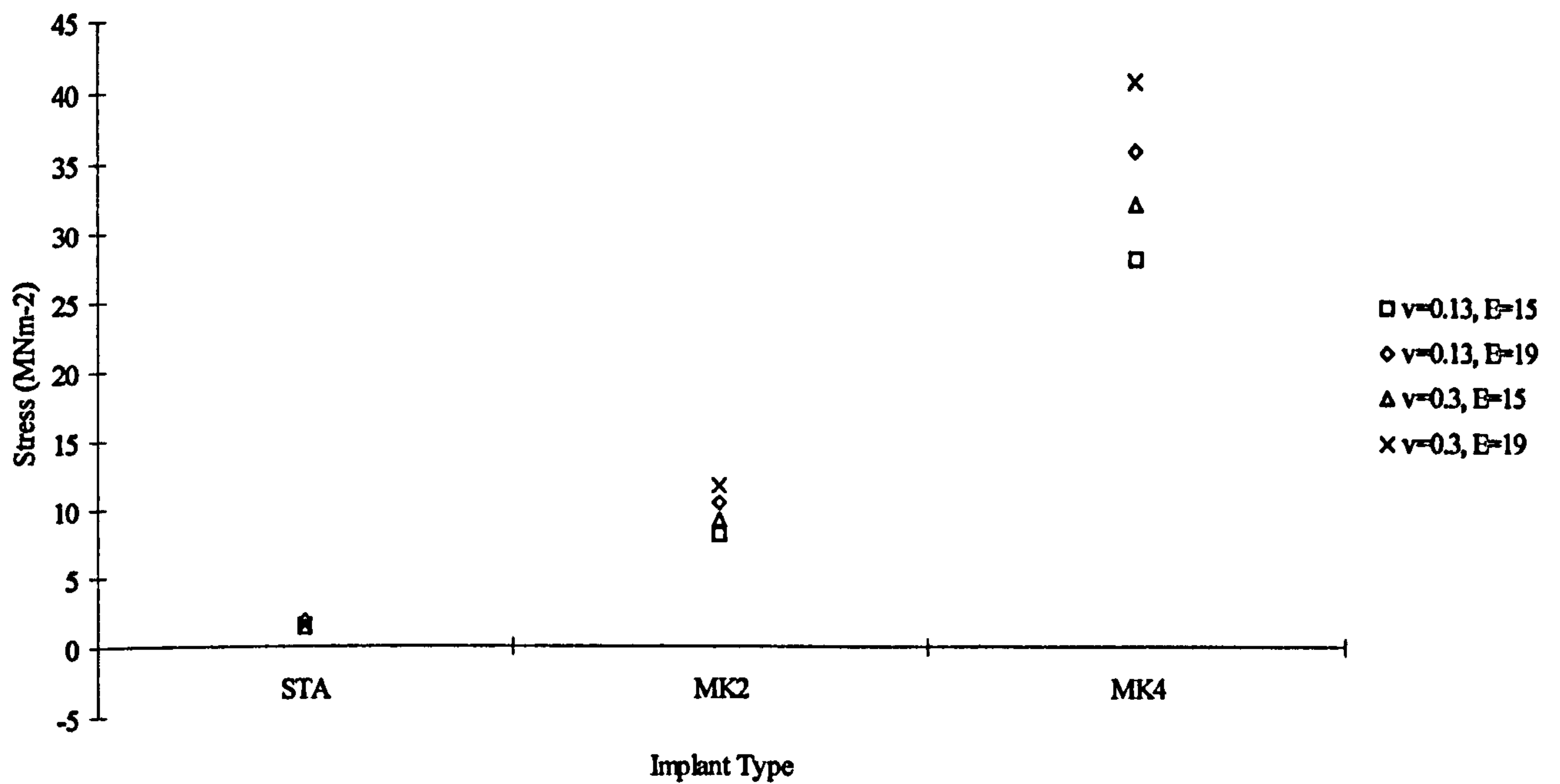


Figure 6.27: Mean maximum principal stresses during implant insertion calculated with a range of values for Poisson's ratio (ν) and Young's modulus (E).

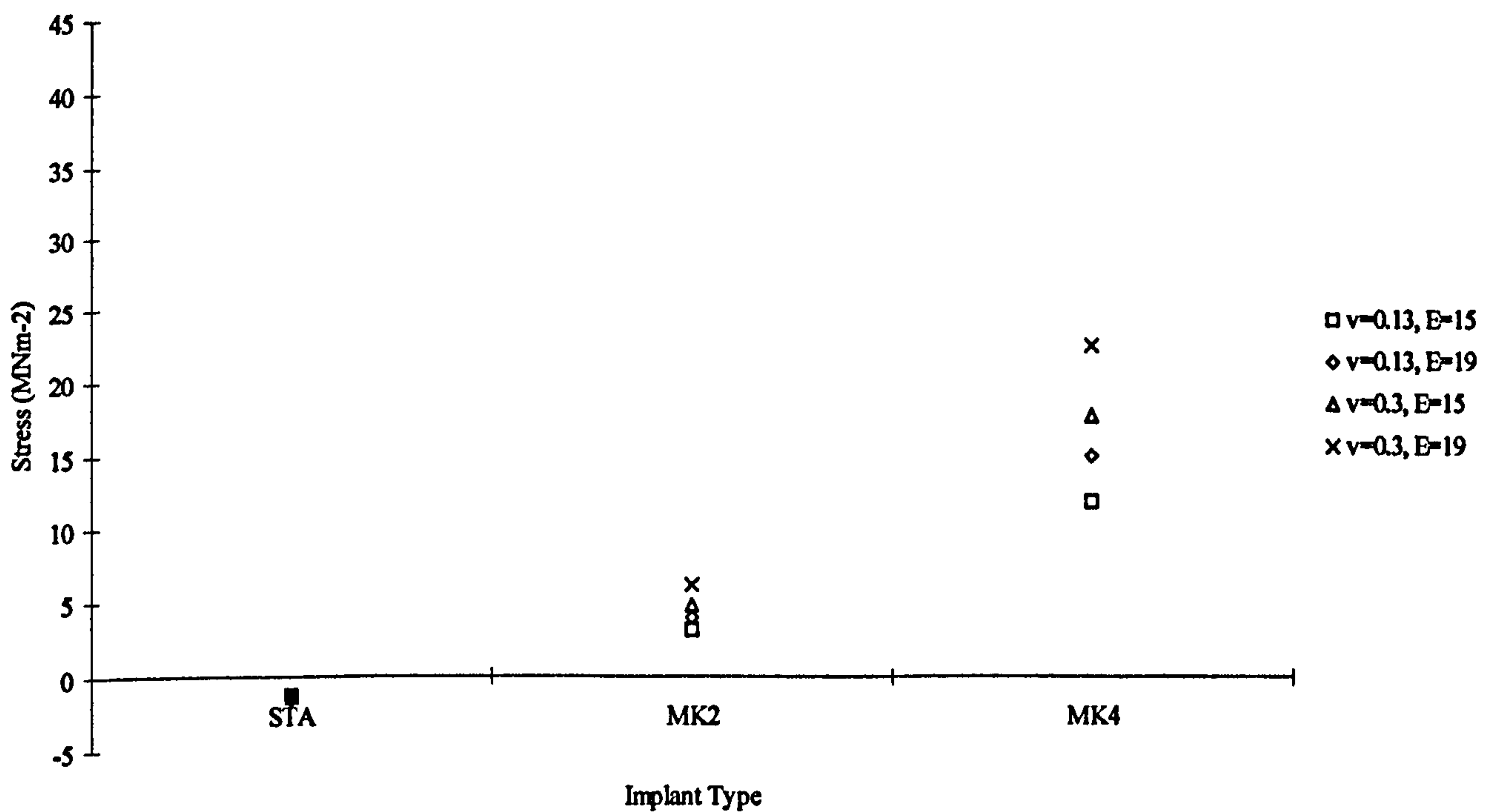


Figure 6.28: Mean minimum principal stresses during implant insertion calculated with a range of values for Poisson's ratio (ν) and Young's modulus (E).

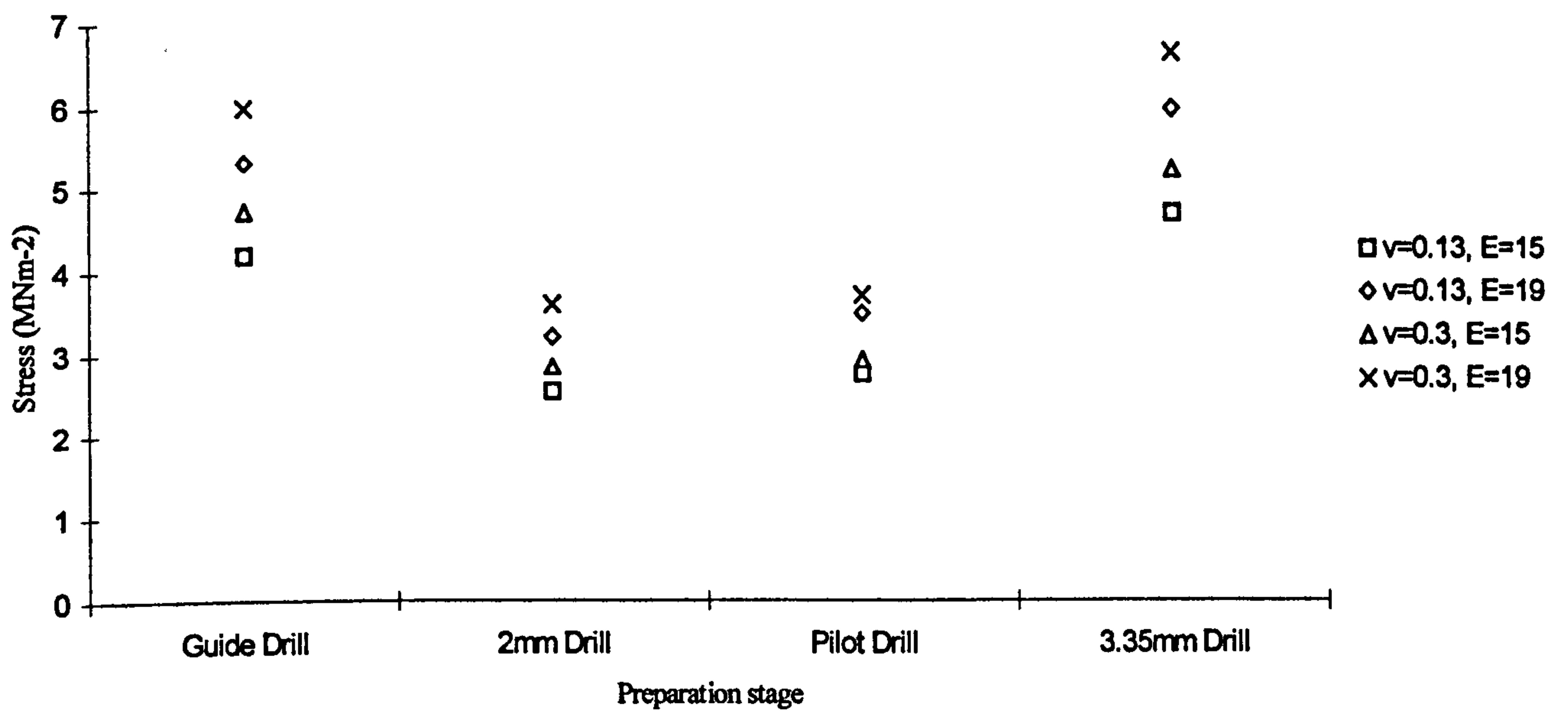


Figure 6.25: Mean maximum principal stresses during implant site preparation calculated with a range of values for Poisson's ratio (v) and Young's modulus (E).

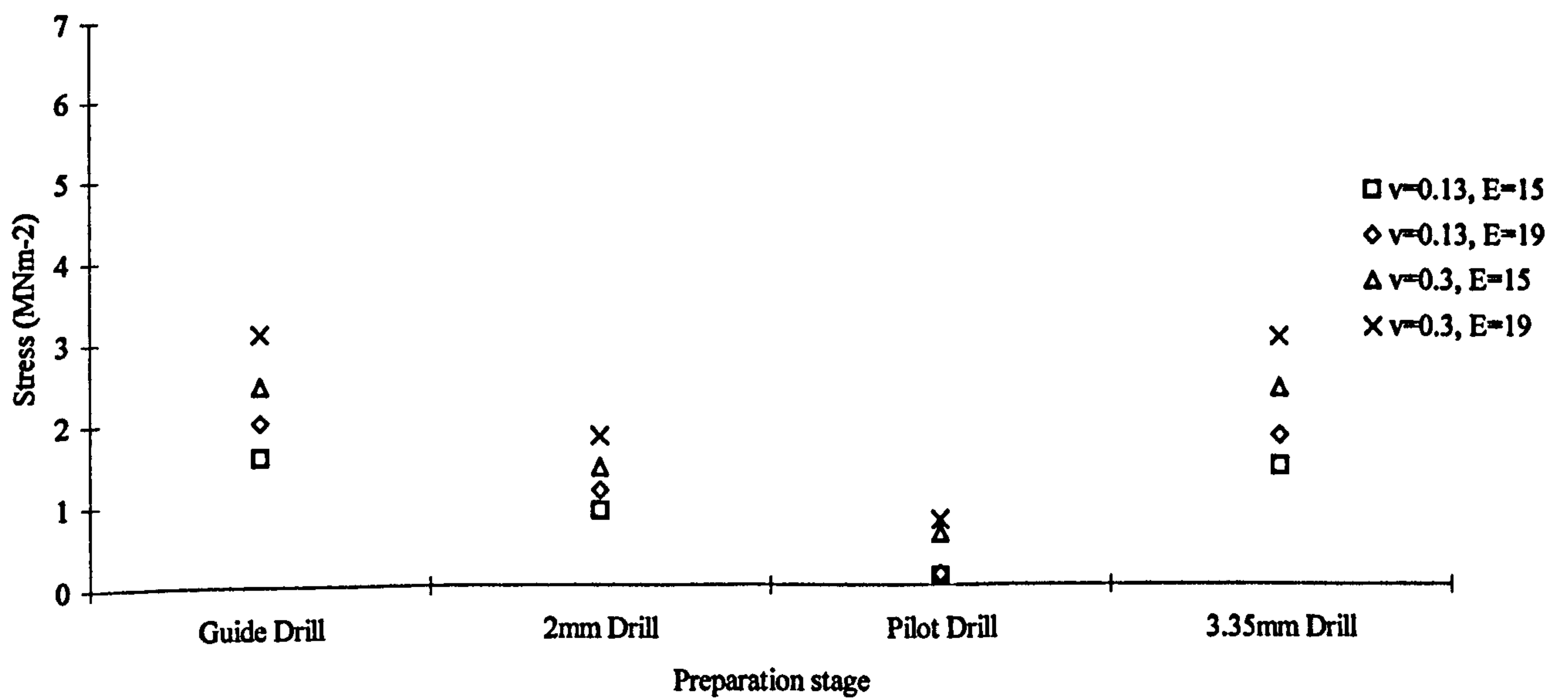


Figure 6.26: Mean minimum principal stresses during implant site preparation calculated with a range of values for Poisson's ratio (v) and Young's modulus (E).

investigation a decision was taken that stability of temperature during the test would be of most importance, rather than attempting to maintain human body temperature in-vitro. In clinical practice during implant insertion it is unlikely that the temperature of cortical bone remains constant as the conflicting elements of increased temperature from heat generation during drilling and the cooling effect of irrigants used alter the underlying tissue temperature. If a strain gauge is bonded to a test material with a coefficient of thermal expansion significantly different to that of the strain gauge backing fluctuations in temperature can result in 'apparent strain' being recorded in the strain gauge.

The quality of the adhesive bond between the strain gauge and the test material is of paramount importance. It is assumed in all calculations that the strain appearing in the gauge is the same as that occurring on the surface of the cortical bone. The adhesive used in this study was a cyanoacrylate, (M-Bond 200, Vishay measurements group UK Ltd, Basingstoke, Hants., UK). The ideal adhesive material should have minimum curing time, should not require mixing, be applicable in a thin layer, require low clamping pressure, have a wide operating temperature range be insoluble in isotonic saline and show linearity with minimal creep and hysteresis (Dabestani, 1992). Cyanocrylate fulfills many of the ideal criteria. Dabestani, (1989) showed that the adhesive bond to bone is unaffected within the temperature range -5°C to 55°C . Morden (1982) has demonstrated that cyanoacrylate has a creep free performance and an elongation capability of approximately 15% (150 000 microstrain). The test conditions of this study lie well within these ranges.

6.4.2 Discussion of the results

6.4.2.1 Implant site preparation

Figure 6.15 shows the maximum principal strains achieved during the different stages of the implant site preparation; mean values with 95% confidence intervals are shown. The maximum principal strains during all stages of the implant site preparation were relatively consistent with mean values ranging from 144 to 222 microstrain. The stages related to the use of a twist drill (2mm and 3.35mm diameter) or the surgical tap showed the smallest variation in value with mean values from between 144 and 154 microstrain. This consistency in value is probably due to the higher cutting efficiency of these instruments, which produce more consistent bone cutting. This is in contrast to the design and performance of the guide drill and pilot drills that have a lower cutting efficiency and have mean values of 190 and 222 microstrain. As illustrated in Figure 6.7, the strain induced in the bone at each stage of implant preparation is related only to the period that the bone is instrumented and strain values return to zero once the stage is completed. This conforms to the theoretical ideal of an atraumatic surgical technique. When considering the highest value of the minimum principal strains (Figure 6.16) during the stages of implant site preparation a similar overall pattern is seen with mean values ranging from 22 to 63 microstrain. The angle of the principal strain varies from -0.19 to 0.5 degrees from element 1 of the Rosette strain gauge (Figure 6.17). The range of the angle of the principal strains was small, indicating that the strain distribution during implant site preparation was relatively even between stages around the circumference of the implant site. The approximation of the maximum principal strain to zero (i.e. orientation of element 1 on the strain gauge rosette) means that it may be more

appropriate to consider the orientations of the maximum principal strain in relation to the orientation of the bone samples themselves (Figure 6.29).

Figure 6.18 shows the overall mean maximum principal strain during the whole preparation stage of the implant. The mean maximum principal strain for the 2mm twist drill, the 3.35mm twist drill and the surgical tap is, again very consistent with a spread of values between 50 and 56 microstrain. Again the guide drill and pilot drill stages develop higher strains than those of the twist drills and taps. The variation in mean values is more consistent with 95% confidence intervals of between 16 and 29 microstrain. Figure 6.19 shows the overall mean minimum strain during the whole preparation stage of the implant site, with mean values from between -24 and 7 microstrain.

6.4.2.2 Implant insertion

Figure 6.20 shows the maximum principal strains achieved for each of the implant types. Clear differences are seen between the three implant types. The standard implants generate the lowest mean principal strains (118 microstrain), with the Mark II implants inducing the next highest strain (443 microstrain) and the Mark IV implants generating an extremely high strain (1680 microstrain). These findings can be explained since the standard implants when placed into a pre-tapped channel induce the least strain in the bone since no cutting takes place as the implant is inserted and there is a minimal degree of compression in the interfacial bone. Once the implant is inserted the pre-insertion strain level is restored. The Mark II implant has cutting facets placed into the apical portion of the implant and the strain induced in the bone is higher than for the standard implant. As predicted by the previous

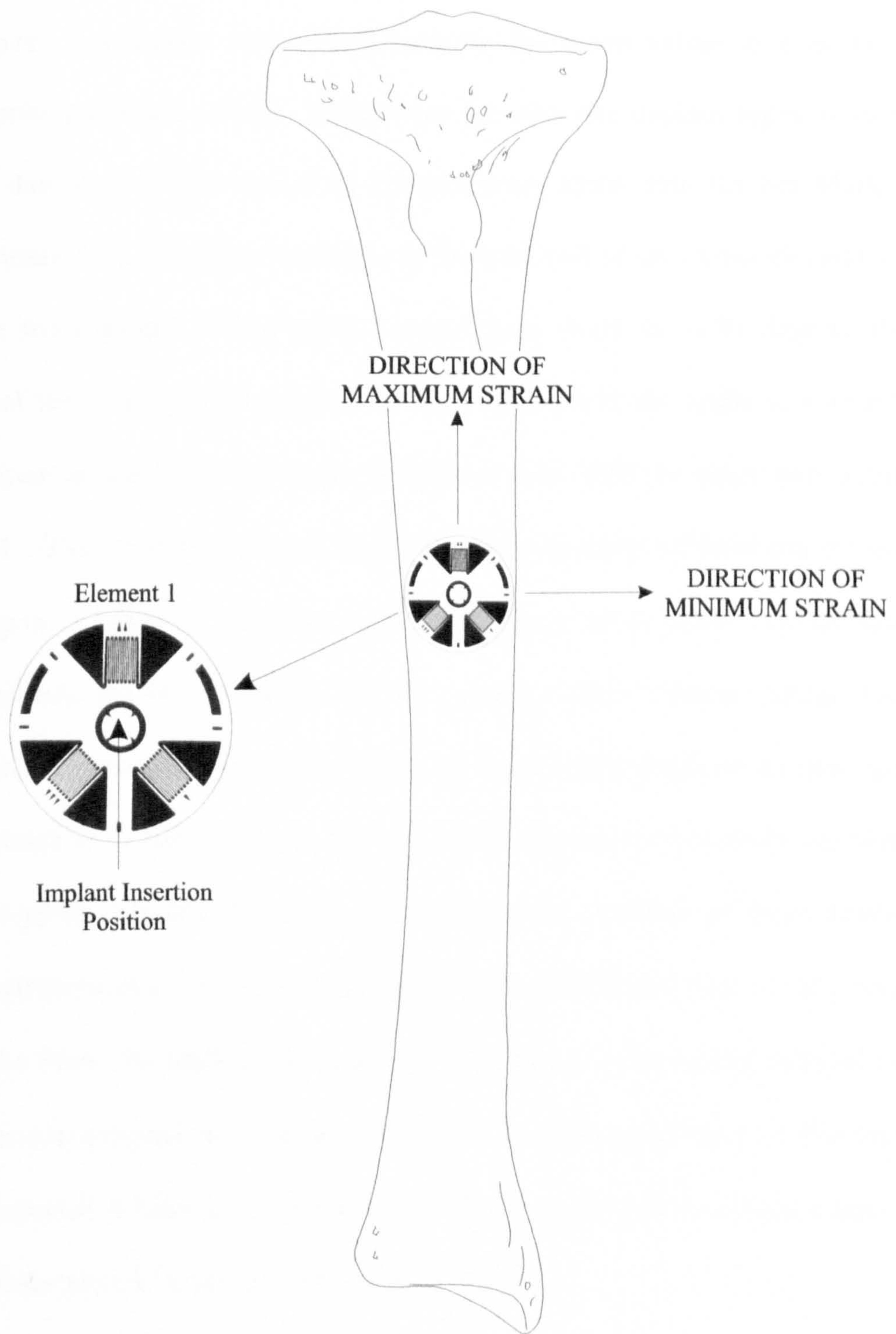


Figure 6.29: Illustration of maximum and minimum principal strain directions in relation to anatomical form.

studies in this work, the greatest magnitude of maximum principal strain was generated by the Mark IV implant. The tapered design of the implant induces a high degree of compression of the interfacial bone and deformation of the cortical bone in the region. Figure 6.21 shows the minimum principal strains achieved by each of the implant types. A similar relationship between the mean values is seen in the minimum principal strain values. Differences between the implant types were not significant due to the wide spread of the minimum strain data for the Mark IV implant. Figure 6.22 illustrates the angle of the principal strains from element 1 of the Rosette strain gauge. Mean values ranged from -0.04 to -1.91 degrees from element 1 of the rosette strain gauge. Greater variation in the angle of maximum principal strain is seen with the Mark II implant than with the other two implant types tested. This may be expected from the differing mode of insertion for these implant types. Mark II implants are self-tapping with three cutting facets incorporated into the apical portion of the implant design. These cutting facets would clearly be expected to produce points of strain within the bone as they rotate and cut through the bone structure. The standard implants in this study are placed into a pre-tapped hole and it would be expected that the insertion of these implants would be symmetrical with equal compression of the interfacial bone as they rotate. Although the Mark IV implants have four cutting facets in the apical third of their design these are minimal and, due to the size of the pre-drilled hole in this study, would be expected to have a negligible effect as the pre-drilled hole is larger than the diameter of the implant at the level of the cutting facets.

Figure 6.23 shows the overall mean maximum principal strain during the whole duration of placing the implant. These show the mean values for the implant types to

follow the same distribution as the plots of maximum and minimum principal strains with the Mark IV implant developing a statistically significantly ($p=0.05$) higher mean maximum principal strain value than the other two implant types. Figure 6.24 shows the overall mean minimum principal strain during the whole duration of placing the implant. There was no statistically significant difference between the implant types when looking at the mean minimum principal strains due to the wide variation in the values for the Mark IV implant.

Principal stresses were calculated from the strain gauge data using a range of values for Poisson's ratio and Young's modulus taken from the literature (Wainwright et al, 1982). Caution should be exercised when examining these results, as there is considerable difficulty in establishing true values for these variables (Odgaard et al, 1991). Values are derived from experimental data for human and animal bone specimens, these values are affected by the manner of testing (Linde et al, 1991) and specimen size and shape (Linde et al, 1992) as well as the site of the bone samples and orientation in relation to anatomy in the living organism (Goldstein, 1987). It does appear from the data that the Mark IV implant is able to induce stress levels that are of a magnitude sufficient to induce bone resorption (Rieger 1990). This emphasises that the Mark IV implant should not be placed into good quality bone. Clinically the Mark IV would only be placed into bone of much poorer quality where the magnitude of the induced stresses will be lower. It is currently not possible to calculate the stresses generated in poor quality bone as reliable values for Poisson's ratio and Young's modulus in poor bone have not been reported in the literature. In addition a suitable poor quality bone model does not exist which would be reliable enough for strain gauge testing.

CHAPTER 7

THE MEASUREMENT OF PRIMARY STABILITY AND STRESS RELAXATION OF IMPLANTS WITH DIFFERING GEOMETRY IMMEDIATELY FOLLOWING IMPLANT PLACEMENT

THE MEASUREMENT OF PRIMARY STABILITY AND STRESS RELAXATION OF IMPLANTS WITH DIFFERING GEOMETRY IMMEDIATELY FOLLOWING IMPLANT PLACEMENT

7.1 Aims and objectives

Implant primary stability has been discussed in the literature as a measure of stability of an implant immediately after insertion into bone, with secondary stability relating to a measure of stability of the implant at a variable time after implant insertion. Secondary stability is affected by the primary implant stability, and the quality and quantity of bone apposition and deposition adjacent to the implant during the variable healing period. This implies that during the healing phase the stability of an implant is in a state of change. It is not known for how long after the implant is placed that the term implant primary stability retains its validity. Pilot studies and unpublished clinical immediate loading studies using Resonance Frequency Analysis (personal communications Meredith 2000 + 2001, O'Sullivan et al 2000) appear to demonstrate a change in RFA value immediately following implant placement. The aim of this study was to investigate whether the immediate post insertion change in RFA value (within 12 hours of insertion) relates to a mechanical stress relaxation in the bone following implant insertion and whether, if such relaxation occurs, there is a relationship between the degree of strain placed upon the bone due to the implant design and insertion technique and the degree of stress relaxation.

7.2 Method

7.2.1 Specimen Preparation

Specimens of bovine rib were obtained from an abattoir and returned to the laboratory within 1 hour of animal slaughter. The bone specimens were individually bagged and frozen at -22°C leaving the periosteum and adjacent musculature in place to minimise dehydration of the bone. Prior to testing each specimen was removed from the freezer, sectioned into 12cm lengths and thawed to room temperature submerged in normal saline. Once thawed, the periosteum and musculature were dissected from the bone.

7.2.2 Strain gauge attachment

Three element electrical resistance residual strain gauges were used in this study (FRS-3-11, TML, Tokyo Sokki Kenkyujo Co., Ltd, Tokyo 140, Japan). Details of the strain gauges used are summarized in Figure 6.1. Strain gauges were attached to the bone specimens using the method described in 6.2.2.

Each specimen was tested immediately after gauge attachment. The ends of the bone specimens, which were most vulnerable to dehydration, were wrapped in isotonic saline soaked tissue. Each specimen was mounted in a vice on the testing machine platform and connected to the strain gauge amplifier. Each gauge arm was supplied with a D.C. 2-volt excitation and the gain was adjusted on each channel of the strain gauge amplifier prior to testing by switching a shunt resistor in parallel to the active element of each bridge simulating a mechanical strain of $1000\mu\epsilon$. Amplifier gain and excitation voltage were kept constant throughout the experiments but the amplifiers were set to zero where necessary to prevent over-ranging.

Strains were recorded for each gauge arm of the residual strain gauge following implant insertion through the central hole of the gauge (Figure 6.3). An acrylic resin control specimen, to which an identical strain gauge had been mounted, was also placed adjacent to each test sample. Each arm of the gauge on the test specimen was connected as the active arm of a Wheatstone bridge circuit and gauges on the control specimen comprised the dummy arms of the bridge circuit.

Calibrated values of strain were calculated for each element of the 3-element Rosette strain gauge using the digital data recorded from each element of the Rosette. The formula used for calculation of strains was:

$$\epsilon_x = \frac{1000}{(D_{1000} - D_0)X(D_x - D_0)}$$

where:

ϵ_x	=	Absolute strain in microstrain units ($\mu\epsilon$)
D_{1000}	=	Strain reading during 1000 $\mu\epsilon$ calibration test
D_0	=	Strain reading at zero strain
D_x	=	Strain reading at measured strain

The three individual strain readings were calculated for each 3-element rosette. These strain readings were then used to calculate the principal maximum and minimum strain values for each specimen during the test period following implant insertion.

Principal strain values were calculated using the formula:

$$\varepsilon = \frac{\varepsilon_1 + \varepsilon_2 + \varepsilon_3}{3} \pm \frac{\sqrt{2}}{3} \sqrt{(\varepsilon_1 - \varepsilon_2)^2 + (\varepsilon_2 - \varepsilon_3)^2 + (\varepsilon_3 - \varepsilon_1)^2}$$

where:

ε = Principal strain in microstrain units ($\mu\varepsilon$)

ε_x = Absolute strain value from strain gauge element x

The angle of principal strain was calculated by:

$$\tan 2\phi_1 = \frac{\sqrt{3}(\varepsilon_c - \varepsilon_B)}{2\varepsilon_A - (\varepsilon_B + \varepsilon_c)}$$

where $0 < \phi_1 < 90^\circ$ if $\varepsilon_c > \varepsilon_B$

7.2.3 Data acquisition

All data was logged simultaneously into separate analogue inputs of a data acquisition card (National Instruments, Newbury, Berkshire, UK), the channel allocation used is outlined below:

- 1) Strain gauge element 1
- 2) Strain gauge element 2
- 3) Strain gauge element 3
- 4) Temperature, Thermocouple amplifier

Pilot studies were carried out in order to identify the appropriate sampling rate, a sampling rate of 1 sample per minute was considered to be appropriate. The sampling rate and data acquisition were controlled via a software programmed virtual instrument (Labview 5.1, National Instruments, Newbury, Berkshire, UK), data from all channels were converted within the software package and saved to disc as ASCII files with 4 columns, one for each channel of data. Resonance Frequency data

was recorded using automatic test software (Brian Pavlovic, Imperial College, Kensington, London, UK) that performed a resonance frequency sweep every minute and logged the data as an ASCII file. All test parameters were recorded simultaneously and the ASCII data were later pulled into a spreadsheet programme (Excel 97, Microsoft Corporation, Redmond, WA, USA) for data analysis. The setup used for testing and data acquisition is summarised in Figure 7.1.

7.2.4 Testing procedures

Initial pilot studies were carried out over 8 hours post implant insertion and from these a suitable test period of 4 hours was decided upon as test traces for Resonance Frequency and strain levelled off after 2.5 to 3 hours. It was also felt desirable that the test period should not exceed this area of stable Strain/Resonance Frequency value as degradation of the bone specimens would begin to play an important role with potential changes in the test parameters. All tests were performed at night when the air conditioning was not operating and the tests were less likely to be disturbed by electrical interference from work carried out in adjacent areas of the building. Temperature fluctuations were considered to be a potential source of error causing changes in gauge resistance. A pilot test was performed with a thermocouple placed in the microcrystalline wax coating the active strain gauge. Temperature fluctuation measured in this way was less than 1°C which was not considered to be of significance.

Pilot tests had been performed to assess a suitable final drill diameter of 3.35mm diameter for use when preparing the implant sites. Due to the tapered profile of the Mark IV implants it was difficult to fully seat the implant in dense bone and it was

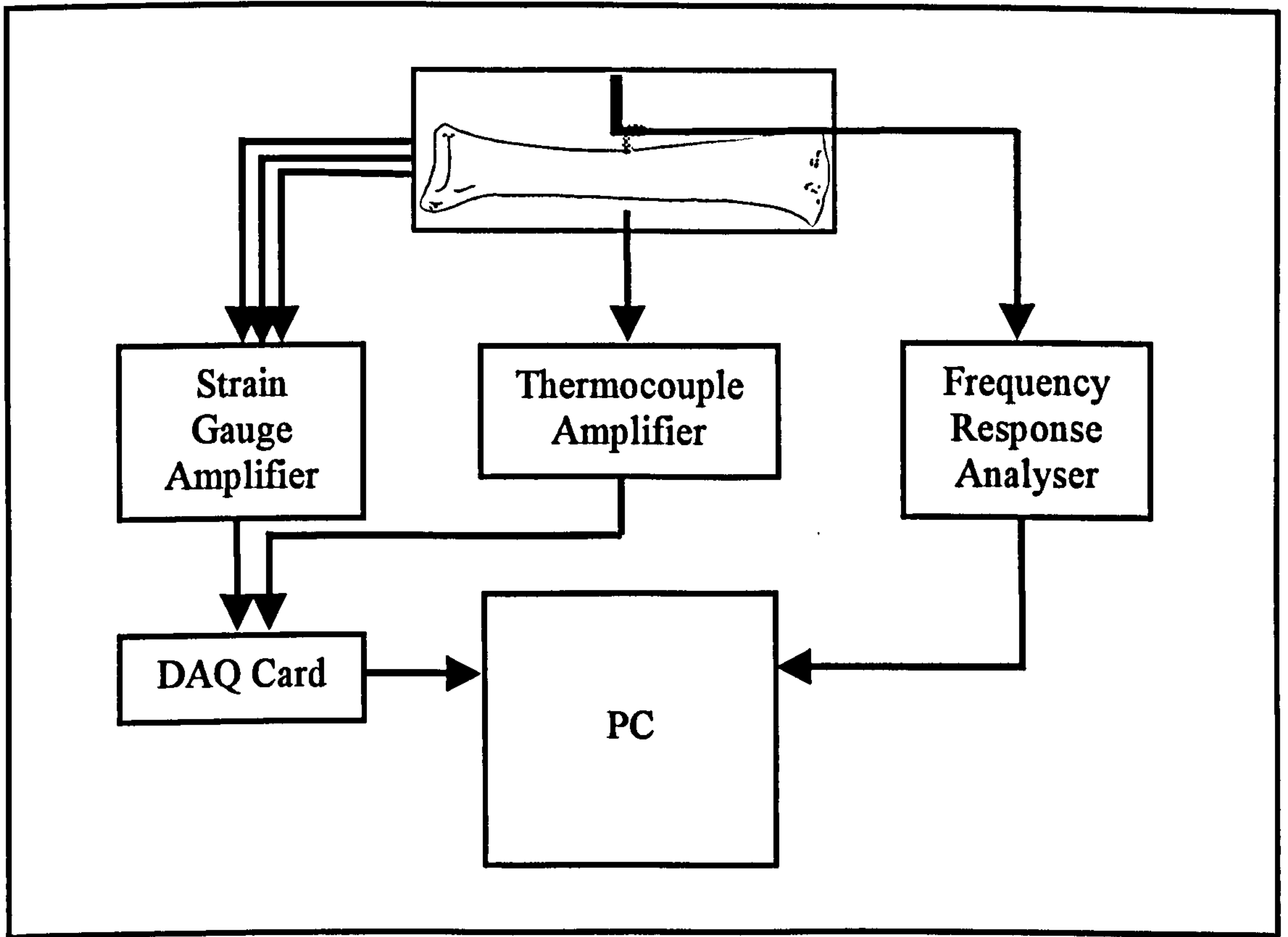


Figure 7.1: Stress relaxation set-up.

determined that it was not possible to choose a drill diameter that would allow all implants to fully seat. A compromised drill diameter (3.35mm) was selected that was the largest diameter advised for the insertion of standard and Mark II implants in dense bone which allowed their full insertion, and that allowed the partial insertion of the Mark IV implants.

A standard implant insertion technique was used as recommended by the implant manufacturers. None of the implant sites were countersunk as it is very difficult to standardise and control the amount of cortical bone removed with the countersink bit. Standard and Mark II implants were inserted until they were in a clinically acceptable position just prior to the flange touching the bone surface (Figure 7.2). It was not possible to fully seat the Mark IV implants due to the taper of the implants and the bone density. The Mark IV implants were inserted into the bone until the automatic cut off of the torque controller occurred at approximately 50Ncm. During the drilling and implant insertion the bone specimens were held in a vice to stabilize them. Care was taken to hold the specimens lightly so that minimal force was placed onto the bone and no change in the strain state of the specimens was registered from the strain gauges. Following implant insertion a Resonance Frequency transducer was attached to the implant head and data recording was commenced. The specimens were then immediately removed from the implant insertion area and placed into the test tray. The specimens were lightly supported in polyurethane foam blocks in an aluminium tray. The exposed ends of the bone were wrapped in saline soaked gauze and 1cm depth of normal saline was used to bathe the bone specimens, the tray was then covered with plastic film to prevent the specimens from drying out

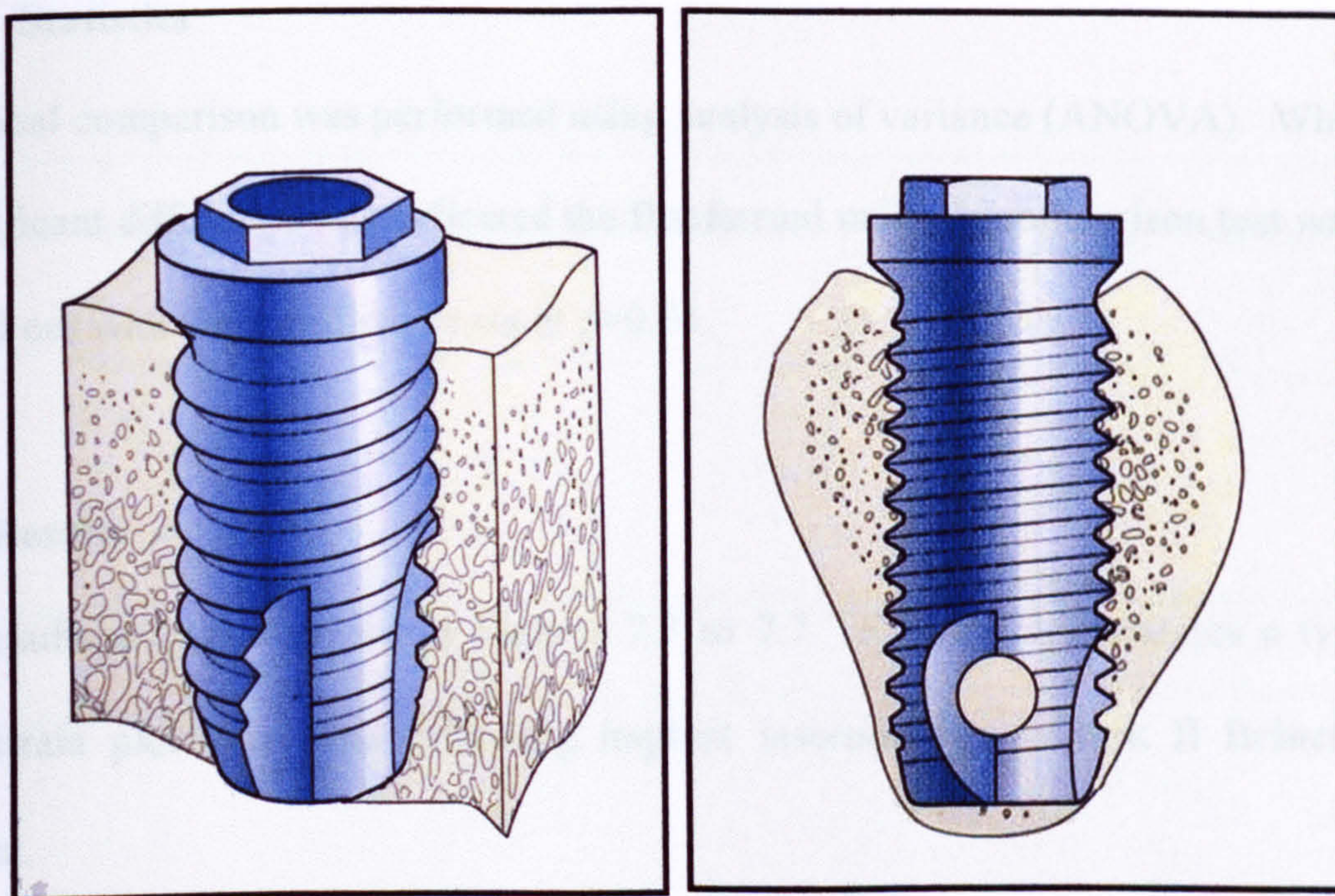


Figure 7.2: Implant insertion stopping position. Demonstrating space between implant flange and cortical bone surface

and to ensure that the air surrounding the specimen was as close to 100% humidity as possible.

7.2.5 Statistics

Statistical comparison was performed using analysis of variance (ANOVA). Where a significant difference was indicated the Bonferroni multiple comparison test was carried out with the significance set at $p=0.05$.

7.3 Results

The results are summarized in Figures 7.3 to 7.7. Figure 7.3 illustrates a typical RFA/strain plot over time following implant insertion for a Mark II Brånemark implant.

A summary of the results is displayed in Table 7.1. Figure 7.4 shows the mean RFA values immediately after implant insertion for each implant type shown with 95% confidence intervals. Figure 7.5 shows the mean changes in RFA value over the test period for each implant type; mean values and 95% confidence intervals are shown. The standard Brånemark implant shows a mean increase in RFA value of 70Hz over the test period, whilst the Mark II and Mark IV implants show a reduction in mean RFA value over the same period of 36Hz and 123Hz respectively. The differences in RFA value over the test period were not significant ($p=0.08$).

Figure 7.6 shows the mean changes in maximum principal strain for each of the implant types studied; mean values and 95% confidence intervals are shown. The Mark IV implant shows the largest initial rise in strain and maintains a level higher

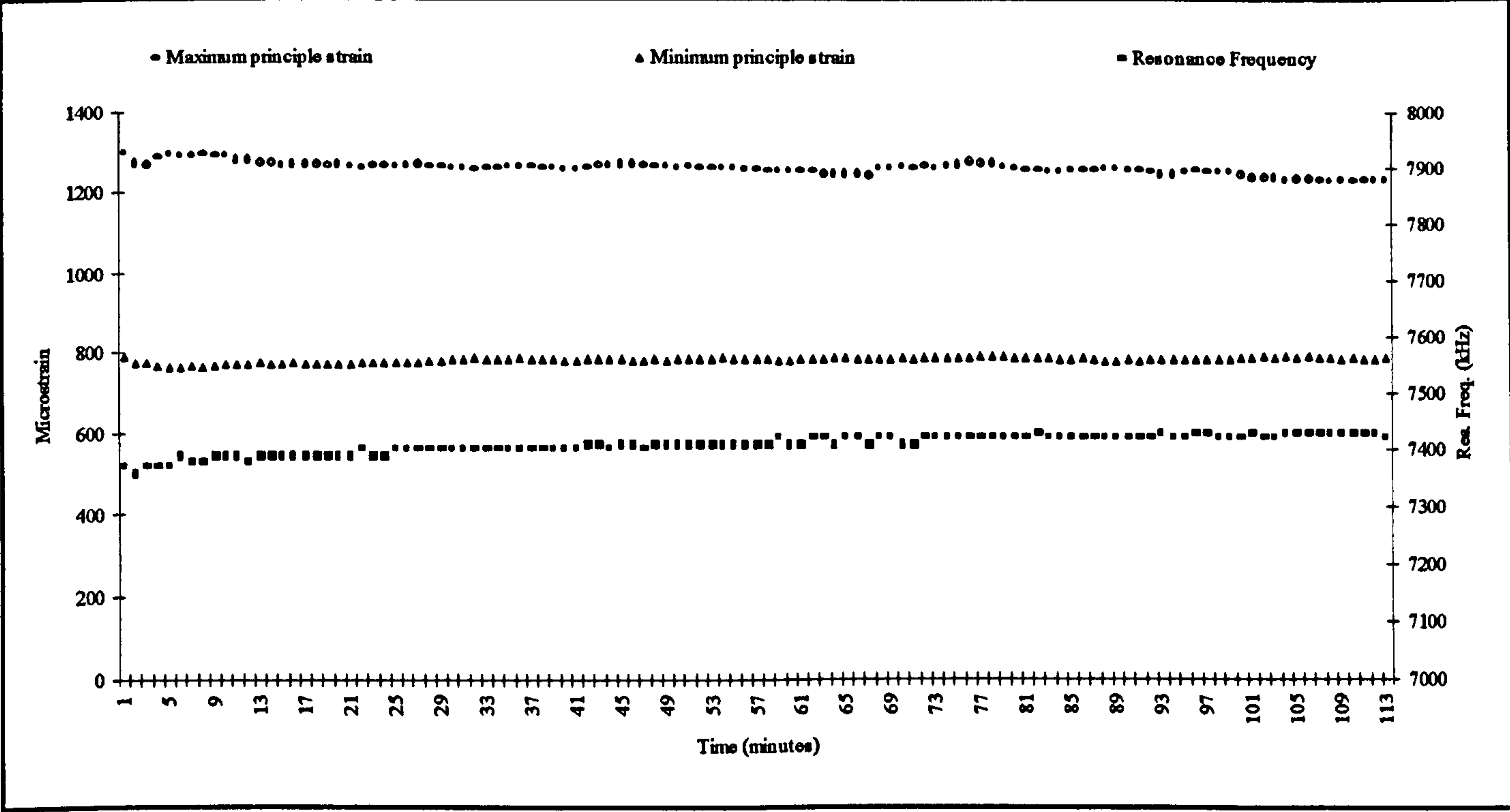


Figure 7.3: Strain/RFA changes for a Mark II implant in bovine rib following insertion.

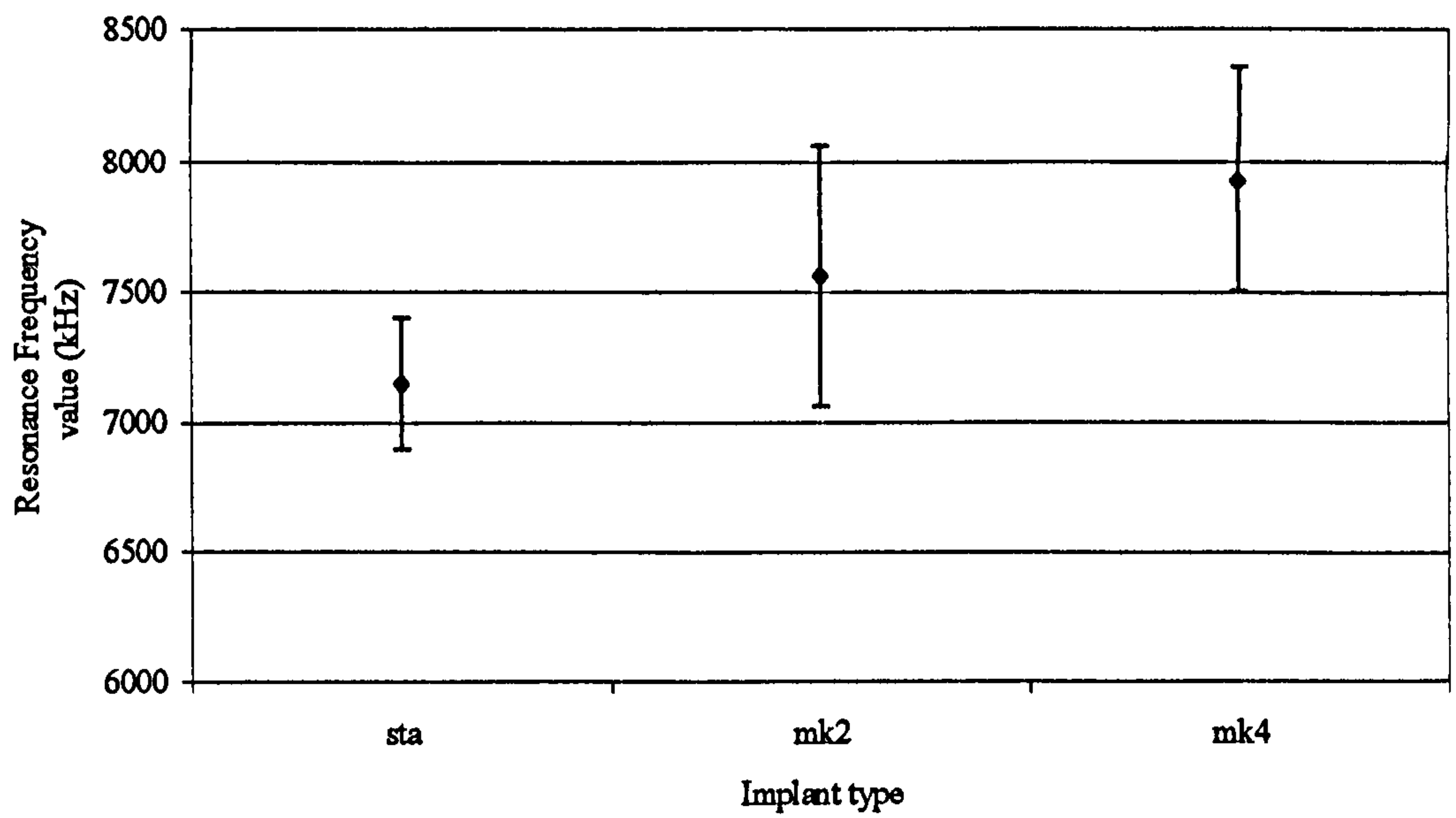


Figure 7.4: Mean Starting RFA values. Mean values with 95% confidence intervals are shown. (n=12).

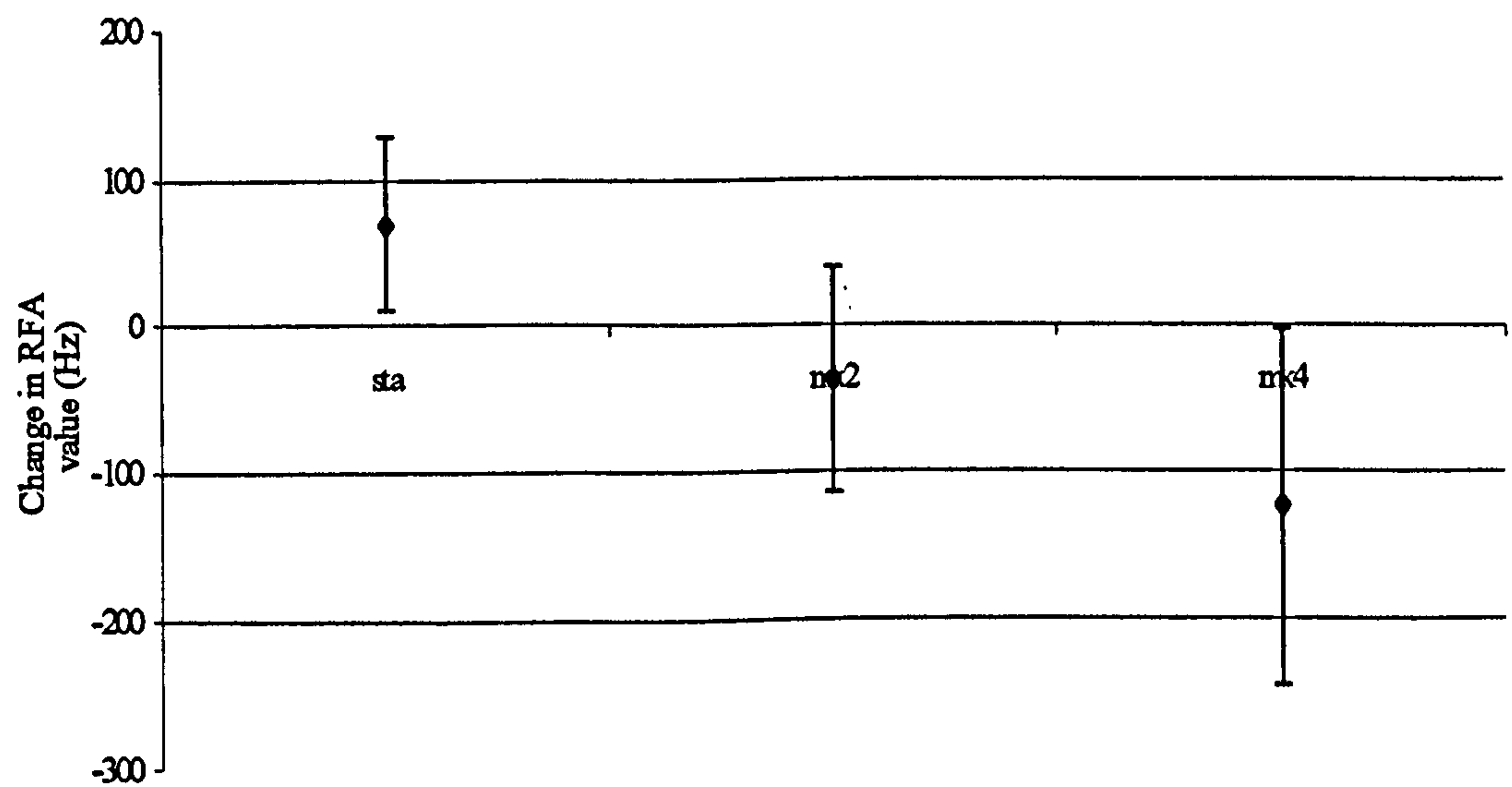


Figure 7.5: Change in RFA value over the test period. Mean values with 95% confidence intervals are shown. (n=12).

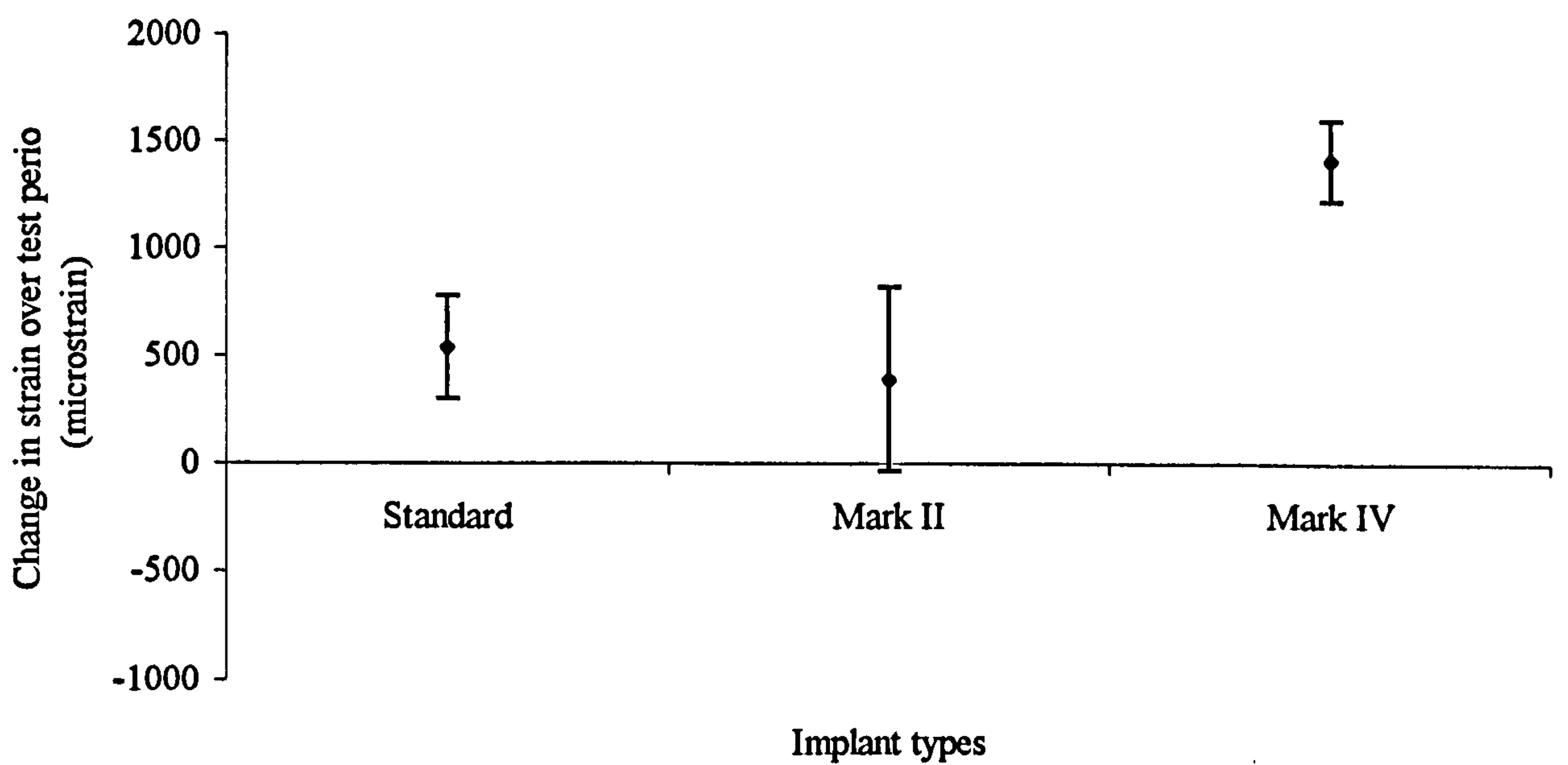


Figure 7.6: Mean changes in maximum principal strain over the test period. Mean values and 95% confidence intervals are shown. (n=12).

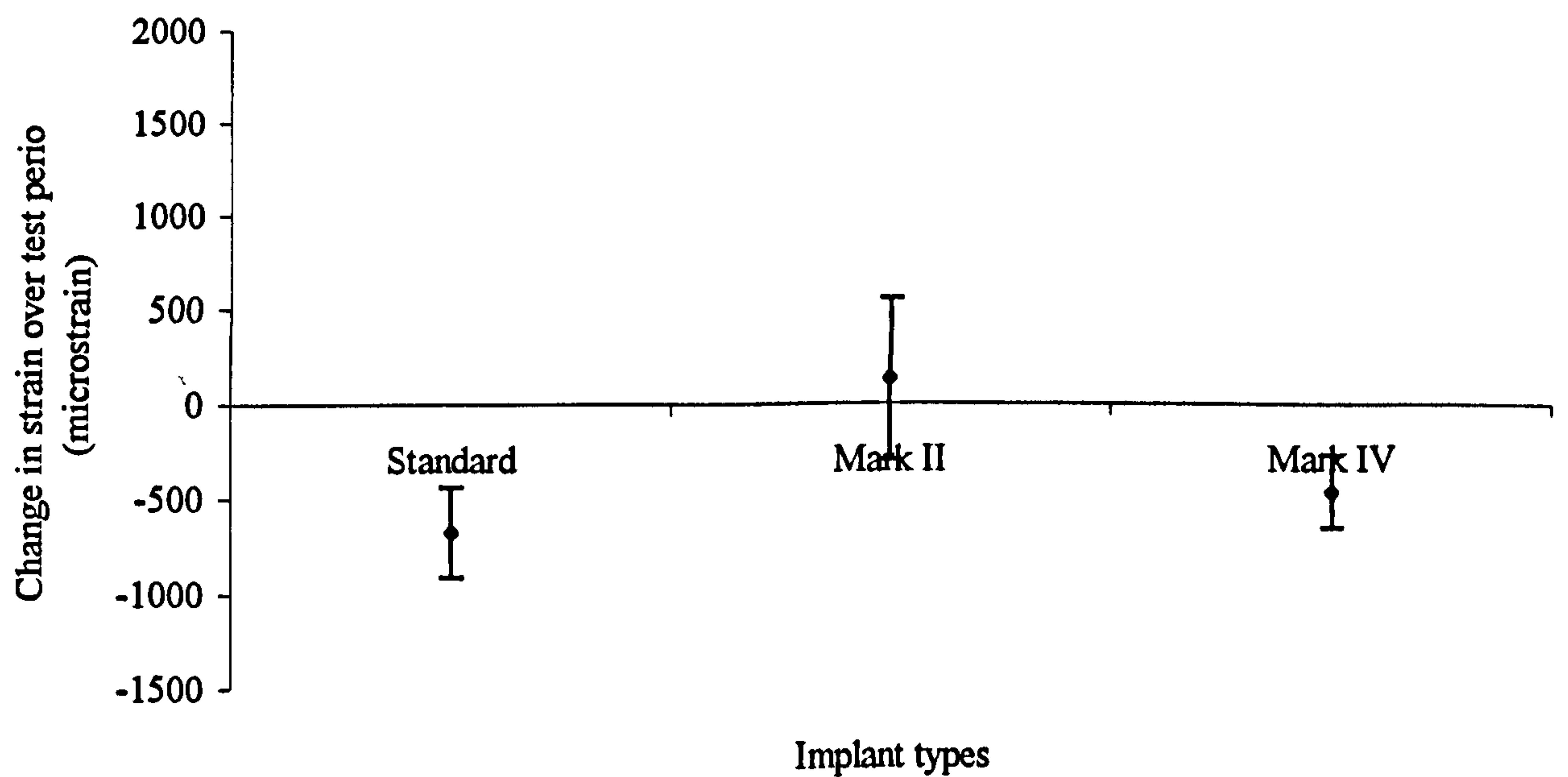


Figure 7.7: Mean changes in minimum principle strain over the test period. Mean values and 95% confidence intervals are shown. (n=12).

	Standard Implant	Mark II Implant	Mark IV Implant
Starting RFA values	7150 ± 220	7563 ± 441	7933 ± 378
Change in RFA value during test period	70 ± 52	-37 ± 68	-123 ± 106

Mean RFA values in Hz are shown ± s.d. (n=12)

Table 7.1: Summary of RFA data.

than the values for the other implant types during the test period. The Mark II implant and standard Brånemark implant showed similar changes in maximum principle strain during the test period with an increase in value. The difference in value between the Mark IV and the standard Brånemark implant was statistically significant at the $p=0.05$ level. The mean changes in minimum principal strain are shown in Figure 7.7, mean values and 95% confidence intervals are displayed. The Mark IV and standard implants show a decrease in mean value following implant insertion. The Mark II implant shows the highest mean value for the three implant types tested, showing a continued rise over the test period. The standard Brånemark implant shows a similar strain pattern to the Mark IV implant but displaying the lowest absolute values of the three implant types.

7.4 Discussion

7.4.1 Discussion of the method

Bone is a viscoelastic composite material. A great deal of information is available in the literature regarding the response of bone to strain, and the effect of varying the rate of change in strain upon the bone response. The plastic energy absorbing qualities of bone have a clear physiological advantage. In normal function bone is subject to dynamic loading within an identifiable range, depending upon the bones position and function. The limb bones and jaw bones are subject to these physiological loads but may also be subject to rapid increases in loading. Such rapid increases in load are seen when a person jumps from a great height onto hard ground or when a blow is directed to the jaw bones or a hard object is bitten into unexpectedly in soft food. These are not infrequent events in the average human lifespan and there is a clear adaptive advantage in the bones' ability to respond to

rapid load application *in extremis*. In a rapid tension test (taking about 0.5 seconds to failure) cow femoral cortical bone gives the load deformation curve seen in Figure 7.8. There is a straight, elastic part of the curve up to a definite yield point and the curve then bends over into a region of plastic flow. The break, when it occurs, is sudden and appears brittle. The ultimate strain is about 4% and the elastic strain is about 1%.

When an implant is placed into bone it has traditionally been the case that the surgery should be as atraumatic as possible and the implant is placed into a prepared bone channel, which closely matches the implant geometry. With most implant insertions the implant slightly compresses the interfacial bone but no greater deformation is expected. With the advent of the Mark IV implant design, which is specifically shaped to induce higher levels of compression, there is uncertainty about exactly how bone responds to these higher levels of interfacial bone compression. Previous chapters have investigated the immediate response of the local bone to implant insertion but as many authors have shown bone can exhibit slow deformation over time. There are no reports in the literature of work carried out to look at the response of bone in the immediate postoperative period although clinically this time relates to the closure of the surgical wound and the discharge of the patient. During this period the implant site is vulnerable to micromotion. Resonance Frequency analysis has allowed the provision of an objective test of the mechanical stability of an implant immediately after insertion. It is known from a number of papers using Resonance Frequency analysis that the RFA value changes during the healing period. The changes in RFA value over the healing period have been attributed to bone remodelling around the neck of the implant and the bone resorption and deposition in

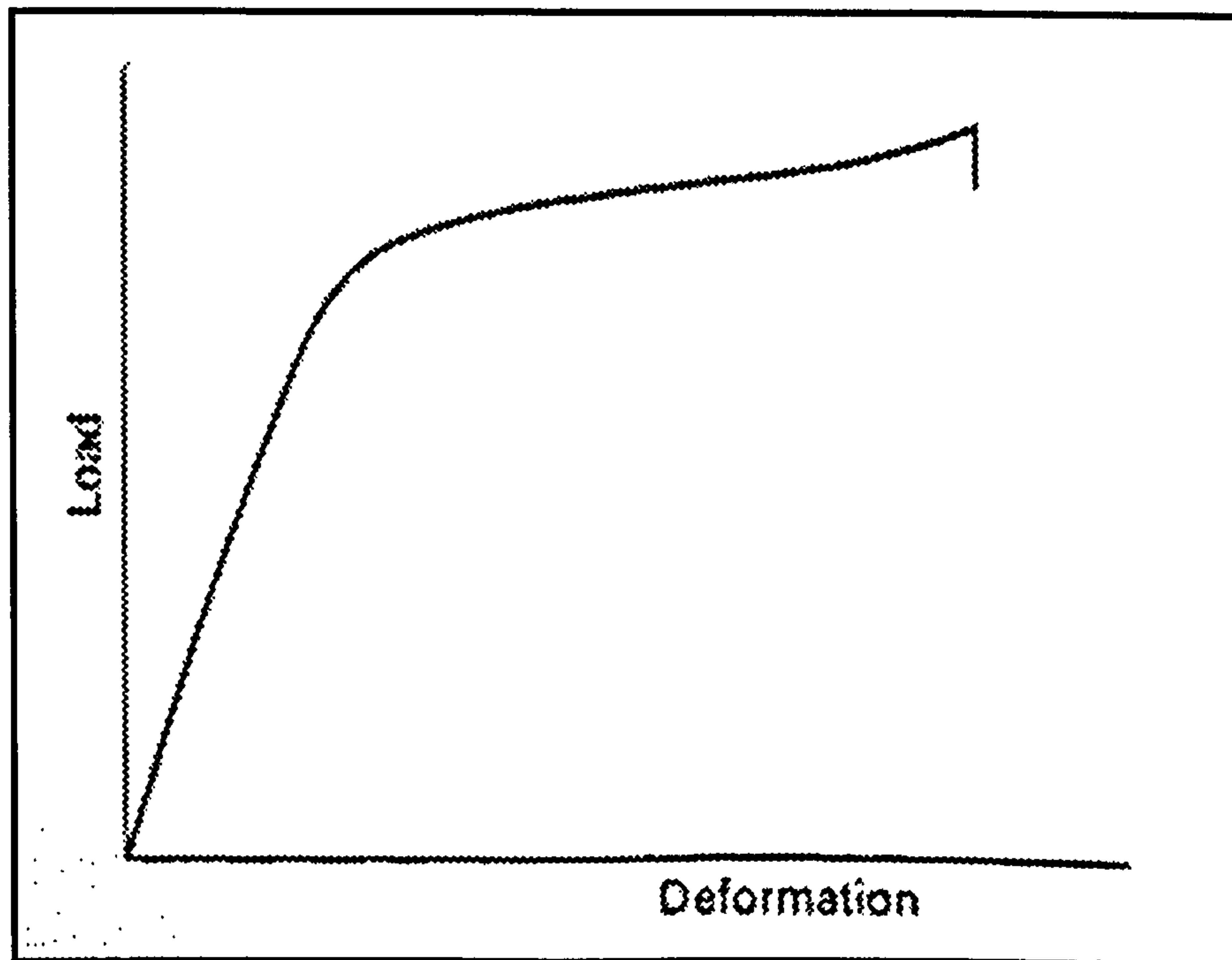


Figure 7.8: Load-deformation curve for bovine bone specimen

(from Mechanical design in organisms – Princeton University Press, Princeton, New Jersey, USA. (eds.) Wainwright S.A., Biggs W.D., Currey J.D., Gosline J.M.).

the interfacial region. Although these factors are certainly significant there are no reported studies evaluating the extent of any mechanical changes in the implant-adjacent bone in the immediate postoperative period.

Work by several authors (Smith et al, 1959; Linde, 1994) has shown that testing temperature has a significant effect on the mechanical properties of bone. It would obviously be preferable to keep the test conditions as close to the physiological situation as possible, this includes matching body temperature. Bonfield and Li (1967) found a reduction in the measured Young's modulus with increasing temperature in the range of -58°C to 25°C. Linde (1994) found a drop in Young's modulus, a reduction in strength and a decrease in ultimate strain with increasing temperature from 20°C to 37°C. In the present study, initial pilot tests were performed with the bone specimens in a water bath at 37°C, however at this temperature bone decomposition was accelerated to an unacceptable degree. Apparent changes in RFA value would have been seen due to bone decomposition. To avoid perceived changes in strain and stiffness due to thermal changes during the test it was decided to maintain as constant a temperature as possible. Provisional tests at 4°C proved problematic and since it was not possible to place the implants under refrigeration and commence the test without wide variations in the temperature of the bone specimens it was decided to run the tests at room temperature. This allowed the temperature of the specimens to be maintained with greater constancy. It is inevitable that decomposition will take place during the tests but it is assumed that these effects will be consistent during all tests and would not interfere unduly with any differences seen between implant types.

7.4.2 Discussion of the results

The mean RFA value for each implant type at the start of the test period is shown in Figure 7.4. The relative mean values for each implant type displayed the pattern seen in previous sections of this work. The standard Brånemark implant had the lowest mean RFA value at the start of the test period. It has previously been theorized that this is due to the use of the surgical tap to prepare the implant site. This additional stage leads to the increased possibility that the implant bed may not be congruent with the implant site leading to a reduced implant primary stability. The Mark II implant has a slightly higher mean starting RFA value; this again matches the relationship between these two implant types referred to elsewhere. It is suggested that this may be due to the self-tapping design of this implant, which, due to the reduced number of surgical steps, may lead to an increased primary implant stability. The Mark IV implants demonstrated the highest starting RFA value of the three implant types tested. This has been investigated in previous studies and appears related to the tapered design of the implant inducing high compressive forces in the interfacial bone region. The circumferential stresses generated at the implant insertion stage lead to a higher primary implant stability. The differences in initial RFA values were statistically significant ($p=0.05$) between the standard Brånemark implant and the Mark IV implant.

When comparing RFA values for each implant type changes in RFA value were seen for all of the implants studied. All of the standard Brånemark implants tested showed an increase in RFA value over the test period. The Mark II implants showed a decrease in mean RFA value during the test, although the spread of values for the Mark II implant makes it difficult to draw firm conclusions for this implant type. All

of the Mark IV implants tested showed a decrease in their RFA value, with a mean decrease of 123Hz over the test period. The change in RFA value between the implant types was not statistically significant ($p=0.08$).

When considering changes in maximum principal strains for each of the implant types the standard Brånemark implant showed the least change in strain value during the test period. The Mark II implant showed the greatest variation in value, mirroring the variation seen in the RFA value for this implant type. The mean change in the principal strain value during the test period was of a similar magnitude as that seen for the standard Brånemark implant. The Mark IV implant showed the largest rise in strain value following implant insertion and maintained a higher level than the other two implant types throughout the testing period

The mean change in the minimum principal strain for the standard Brånemark implant gave the lowest magnitude of the three implant types, after implant insertion the minimum principal strain decreases and then rises towards the immediate post-insertion value. The Mark II implants showed the highest mean change in the minimum principal strains of those tested showing a gradual rise in value throughout the test period. The Mark IV implants showed a similar pattern to the standard Brånemark implants, with a drop in minimum principal strain value and a rise towards the immediate post-insertion value at the end of the test period. The magnitude of the Mark IV values lie between the standard Brånemark implant and the Mark II implants.

The results appear to suggest that a degree of deformational change continues to take place following implant placement. The standard Brånemark implant placed into a pre-tapped hole has the lowest initial RFA value indicating the lowest primary stability of the implant types tested. During the test there is a small change in strain and RFA value indicating little change in the stiffness of the implant/bone interface taking place following implant insertion. The Mark II implant when placed into bone has an initial RFA value higher than that for the standard implant and demonstrates a mean decrease in RFA value during the test period and although there is little change in minimum principal strain there is a small increase in mean minimum principal strain value. These changes are not statistically significantly different from the values obtained from the standard Brånemark implant. The use of a self-tapping implant may reduce the chances of variation between the implant and the implant site by removing a surgical stage. This in turn would be expected to result in an RFA value higher for the Mark II than the standard Brånemark implant. The change in strain following implant insertion could be largely related to the difference between the implant diameter and the prepared implant site, and therefore the degree of compression induced in the interfacial bone region. In this regard there is little difference between the standard implant and the Mark II and this may explain the small overall changes in RFA and strain following implant insertion. The Mark IV implant appears to behave differently with the initial RFA values and strain values being much higher when compared to the other two implant types, with a statistically significant difference between the Mark IV and the Standard Brånemark implant. There is a much larger fall in the RFA value over time and a much larger rise in the maximum principal strain value.

Several authors have investigated the effect of strain rate on the mechanical properties of bone. Currey (1975) investigated the effect of relatively low strain rates (0.00013 to 0.16 s⁻¹). Wright and Hayes (1976) tested at higher strain rates, up to 237 s⁻¹. They found that at low strain rates bone exhibits viscoelastic properties while at higher strain rates (>0.174 s⁻¹) the apparent bone stiffness increases with a linear stress/strain curve until the point of fracture is reached. Bonfield and O'Connor (1978) reported that residual strains during the mechanical testing of bone under greater and greater stresses. These strains eventually recovered after a given amount of time up to 37 hours post testing. The viscoelastic effects seen in bone have been associated with the movement of fluids within and between compartments in the bone structure. The restricted movements of these fluids between compartments give rise to increasing internal pressures within the compartment under greatest deformation. Deformation can also occur within the collagen matrix.

Although further work is necessary to confirm the nature of the peri-implant changes in the bone site, the results of this study appear to confirm that changes do occur. Little change is seen for the standard Brånemark implant and the Mark II implant. The surgical and design philosophy behind these implant types revolved around the idea of a minimally traumatic surgical approach, with only a small difference between the final drill diameter and implant diameters. Little interfacial bone compression occurs and, although changes in strain are seen during implant insertion as described in Chapter 6 the strain values appear to return close to pre-insertion levels when implant insertion ceases. In the immediate post operative period little change appears to occur in interfacial stiffness or peri-implant bone strain.

The Mark IV implant behaves differently. During insertion much higher strains are induced in the peri-implant bone and they do not return to the pre-insertion values following implant insertion. Over the immediate post-operative period changes in RFA value indicate that changes in interfacial stiffness occur with changes in strain also observed. The relationship of these changes is complex but it may be theorized that during implant insertion the application of a high rate of compression due to the implant taper leads to an initial high RFA value. The bone will deform initially but will then reach a level at which immediate elastic deformation cannot accommodate the rapid change. Plastic, energy-absorbing behaviour will then occur. In a composite like bone, plastic flow can occur in a number of ways:

- a) plastic deformation of the mineral crystals, with elastic or plastic deformation of the collagen matrix;
- b) fracture of the crystals, with plastic deformation of the fibrous matrix;
- c) delamination of the matrix from the crystals.

When a bone is loaded to fracture a small amount of plastic flow has been shown to occur prior to a relatively brittle fracture (Currey and Brear, 1974). If the load is removed prior to fracture the bone will remain deformed permanently. The energy of the load is absorbed in the plastic phase with little energy being absorbed during the fracture itself (Wainwright et al, 1982). When the Mark IV implant is inserted it may be theorized that plastic flow begins to occur but does not cease when the implant is inserted. Plastic flow will continue after the rotation of the implant stops and results in reduced stiffness of the bone immediately adjacent to the implant (leading to a lower RFA value) and the changes in strain seen in this study.

Changes occurring immediately following implant insertion are complex but it is clear from this study that the changes seen between primary implant stability and secondary implant stability are not entirely due to bone apposition and remodelling. The mechanical response of bone also has a role to play.

CHAPTER 8

CLINICAL IMPLICATIONS, PROPOSED FURTHER WORK AND CONCLUSIONS

CLINICAL IMPLICATIONS, PROPOSED FURTHER WORK AND CONCLUSIONS

8.1 Clinical implications

The standard Brånemark implant is without doubt the most closely researched design of oral implant. It has been shown to have an acceptable clinical survival rate. The surgical protocol was developed in order to minimise surgical trauma to hard and soft tissues.

The use of a surgical tap to prepare the implant bed appears to reduce the induced cortical bone strain, which is in line with this atraumatic principle. It must be noted that this involves an additional stage in the implant site preparation and as such, it increases surgical time. From the in-vitro results presented it also appears that the use of a surgical tap may increase the variability in implant primary stability although this was less obvious in the work utilising cadavers. The most likely reason for this is variation between the threaded bone channel and the implant itself due to variations in angulation during bone tapping. In bone of good quality this variation in implant primary stability, if it occurs, does not appear to be important as judged by the clinical success rate. In good quality bone, even if variation in implant primary stability occurs, the absolute primary stability value is still high. In bone of poor quality it is known that implant success is greatly reduced. It may be hypothesised that in this case variation during site preparation may begin to be more important as the absolute mean value is reduced any variation from the mean may lead to a very low absolute primary stability value.

In order to remove this surgical variable the manufacturers introduced a self-tapping implant, the Mark II. By using the implant to tap the bone channel surgical time is reduced and the likelihood of mismatch between the path of the implant and the implants own dimensions is reduced. Results from this study show that although a surgical stage is undoubtedly removed this does not result in a significant increase in the implants primary stability. The Resonance Frequency results are not significantly better than for the standard Brånemark implant. The reason is unclear but may be attributed to the cutting facets incorporated into the apical third of the Mark II implant. Large bone clearance chambers are necessary adjacent to the cutting facets and these chambers reduce the surface area of the titanium in contact with the walls of the bone channel. It may be that the reduced stability due to these chambers offsets any advantage from the reduced number of surgical stages. The Osseotite implant is very similar in design to the Mark II implant and is placed in a similar manner. From the cadaver study it behaves very similarly to the Mark II. It appears from the mean values obtained that the differing surface of the Osseotite does not enhance the implants primary stability. From the results in Chapter 6 and 7 it also appears that, due to the reduced cutting efficiency of the Mark II implant when compared with the tap greater resultant strains are induced in the cortical bone during the implants insertion, the impact of this is unclear. Another method employed by surgical operators to increase the stability of standard Brånemark implants in poor bone is to omit the use of the surgical tap and place the implant into the predrilled hole. The implant then becomes a thread forming implant with compression occurring in the interfacial bone. It appears when comparing the results from Chapter 1 and Chapter 4 that this does appear to enhance the implant's primary stability but this is at the cost of increased friction between the implant and the bone

surface. The Mark IV implant was designed to increase the primary implant stability by preferentially inducing circumferential stresses in the cortical bone layer but without increasing the energy imparted to the bone site. The clinical results in this study appear to confirm that this is the case. The Mark IV implant demonstrates an increased implant primary stability when compared to the other implants tested. The double thread design reduces the insertion time to approximately 60% of the standard Brånemark implant and a lower energy level is imparted to the bone at the implant site. As a result of this a lower temperature rise in the interfacial bone would be expected. The increased magnitude of the strains in the cortical bone layer have also been confirmed and are of the order of 10 times those seen for the standard implant. It may be assumed that high levels of cortical bone compression are detrimental to bone healing but we were unable to identify a level at which this occurred when looking at the rabbit model. Caution should be exercised, however, when extrapolating the results to the clinical setting as the rabbit has a rapid bone turnover and very rapid healing capacity, human bone response to those levels of compression may not be the same. It is very difficult to simulate poor bone quality in an animal model. High strain rates in the cortical bone may give rise to bone loss around the neck of an implant, and long term follow-up of the patients in Chapter 1 must be made. The Mark IV implant used in this study appears to be a suitable implant for enhancing primary implant stability when used in bone of poor quality. Experimental evidence suggests that it should not be placed into bone of type 1 or 2 on the Lekholm and Zarb bone scoring system as excessively high levels of cortical bone compression may be induced which may give rise to bone necrosis and even bone fracture upon implant insertion.

8.2 Proposed further work

Continued clinical studies into the use of the Mark IV implant are required and in particular its effect upon cortical bone remodeling at the neck of the implants. It is important to investigate if the bone compression identified in this work is of clinical significance. Long term radiographic follow up is continuing for patients treated with Mark IV implants as part of a multi-centered worldwide trial. If cortical bone loss occurs in the longer term it would be important to establish the relationship between implant taper/bone compression and bone resorption at the implant site. Further work is needed to accurately quantify the peri-implant changes that occur in bone following implant insertion. The work in Chapter 7 could be extended to look at the effect of alteration in the surgical technique upon cortical bone strain. The bone quality at the implant site is of particular importance and currently there is no reliable technique for identifying the mechanical properties of bone at the implant site prior to implant insertion. It may be possible to identify the quality of the bone by the use of a small diameter tap inserted into the implant site prior to implant insertion. Further study of the significance of peak insertion torque and the slope of the peak insertion torque graph may provide a better means of bone quality identification. At present it appears unlikely that a universal implant is possible that will behave comparably in all bone types. The future may lie in tailoring implant design to bone quality and quantity. Improved bone quantity and quality is possible with grafting but this is expensive and still not reliable for all patients. The work presented here has confirmed that surgical technique and implant design can be altered to enhance implant primary stability and efforts should continue to enhance the success rate of implants in bone of poor quality.

8.3 Conclusions

The results from this study indicate that:

- The Mark IV implant makes a significant contribution to improve the primary stability of implants in poor bone quality. Its design features appear to indicate that this enhanced stability is produced with the generation of less thermal energy than that produced during standard implant insertion.
- The Mark IV generates 10 times and the Mark II generates 4 times the level of cortical bone strain seen when inserting a standard Brånemark implant.
- The omission of the surgical tap during the preparation of the standard Brånemark implant site increases the implant primary stability but also increases the thermal energy imparted to the bone at the implant site.
- The Mark II implant reduces surgical time but does not appear to enhance implant primary stability significantly.
- Surface treatment of the implant with etching or blasting does not significantly enhance the primary stability of those implants.
- Caution seems sensible in view of the potentially high stresses produced when placing the implants into better bone qualities and although no negative effects were seen in the rabbit model this should be viewed with caution as the rabbit has a rapid bone turnover and results may not be applicable to the human maxilla

or mandible. The Mark IV implant should only be inserted into bone types 3 or 4 of the Lekholm and Zarb scoring system.

- Following implant insertion changes occur within the peri-implant bone which are affected by implant geometry. The changes affect implant stability and bone strains and may relate to the viscoelastic deformation and relaxation of bone following surgery.

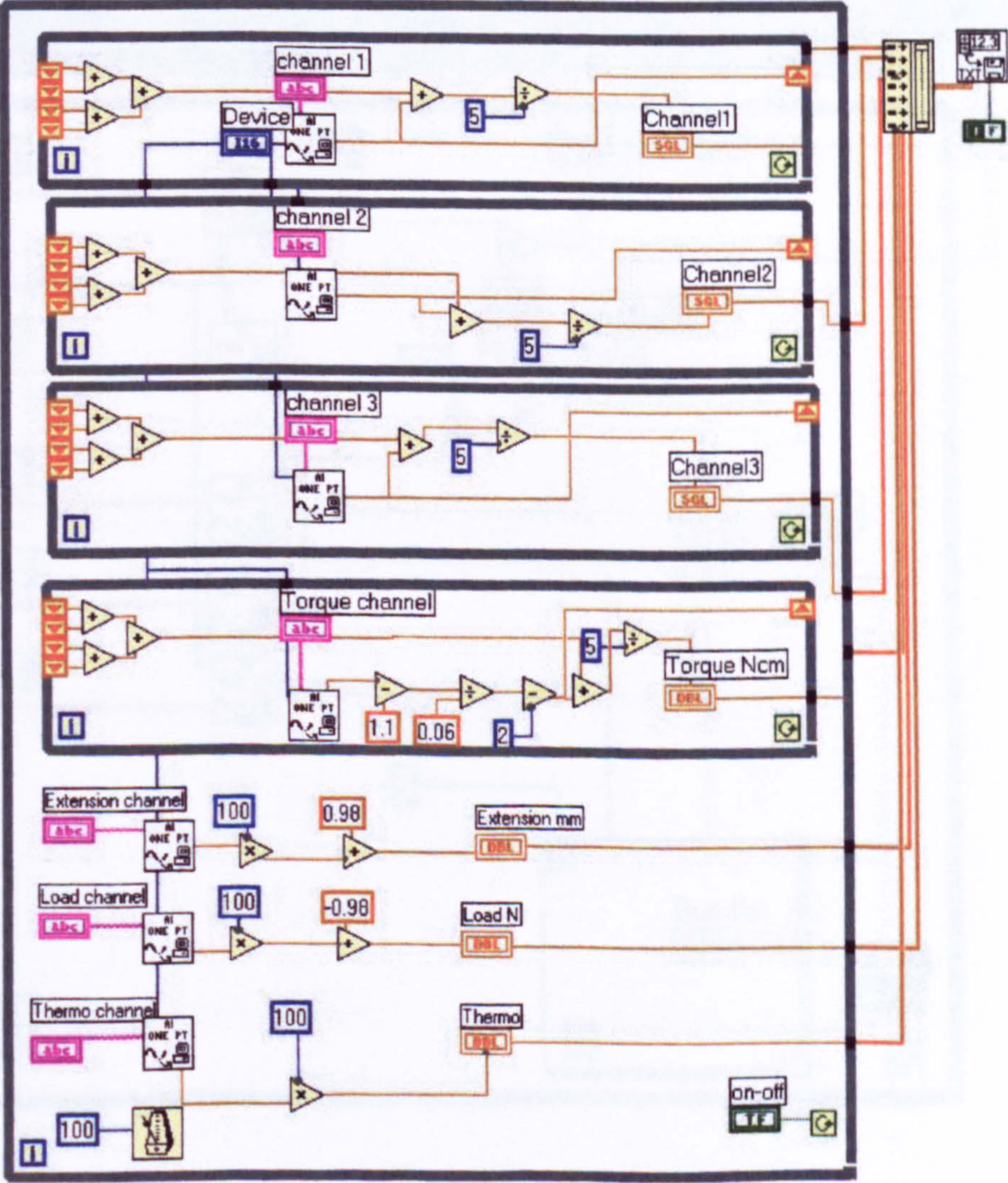
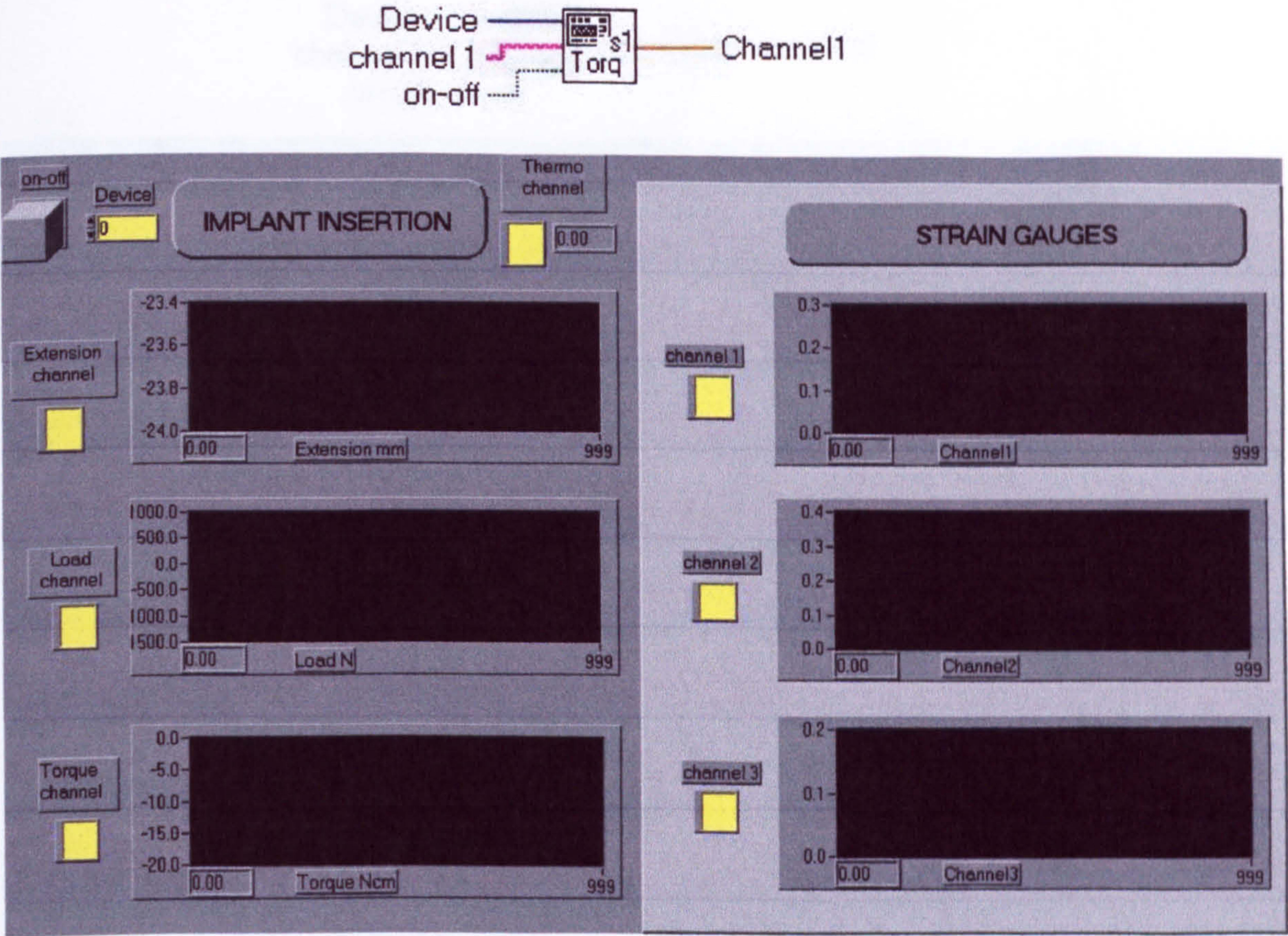
Appendix I – Labview 5.1 virtual instruments used in this work

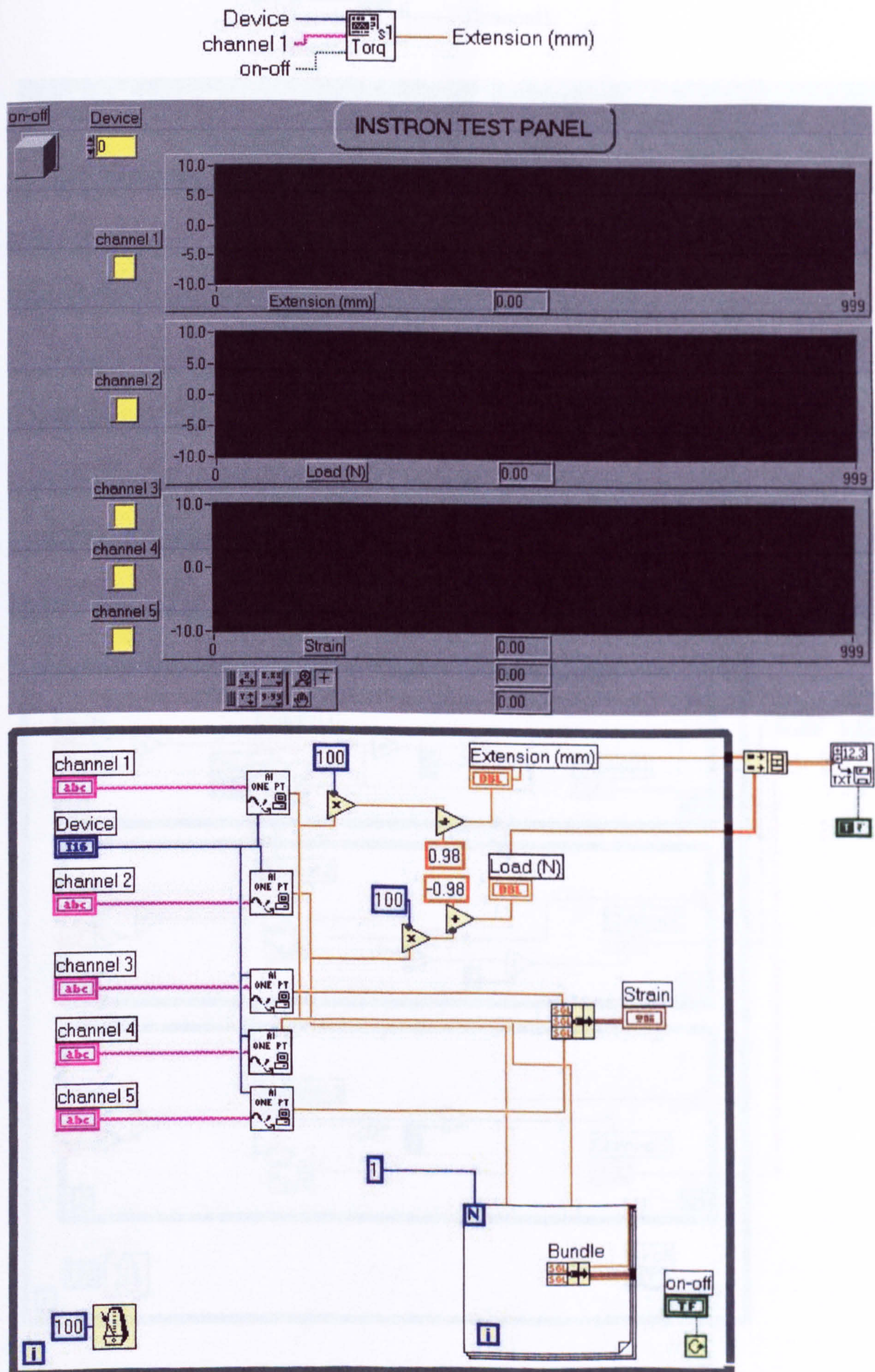
Several virtual instruments were designed and programmed in this work, using a windows based graphical user interface software package Labview 5.1 (National Instruments Ltd, Newbury, Berkshire, UK). Details of the virtual instruments are given.

- **Implant Insertion – Used in Chapter 6**
- **Instron Test – Used in Chapter 6**
- **Strain gauge calibration – Chapters 6 & 7**
- **Stress Relaxation – Chapter 7**
- **Torque and Encoder – Chapter 2**
- **Torque Measurement – Chapters 3,4 & 5**

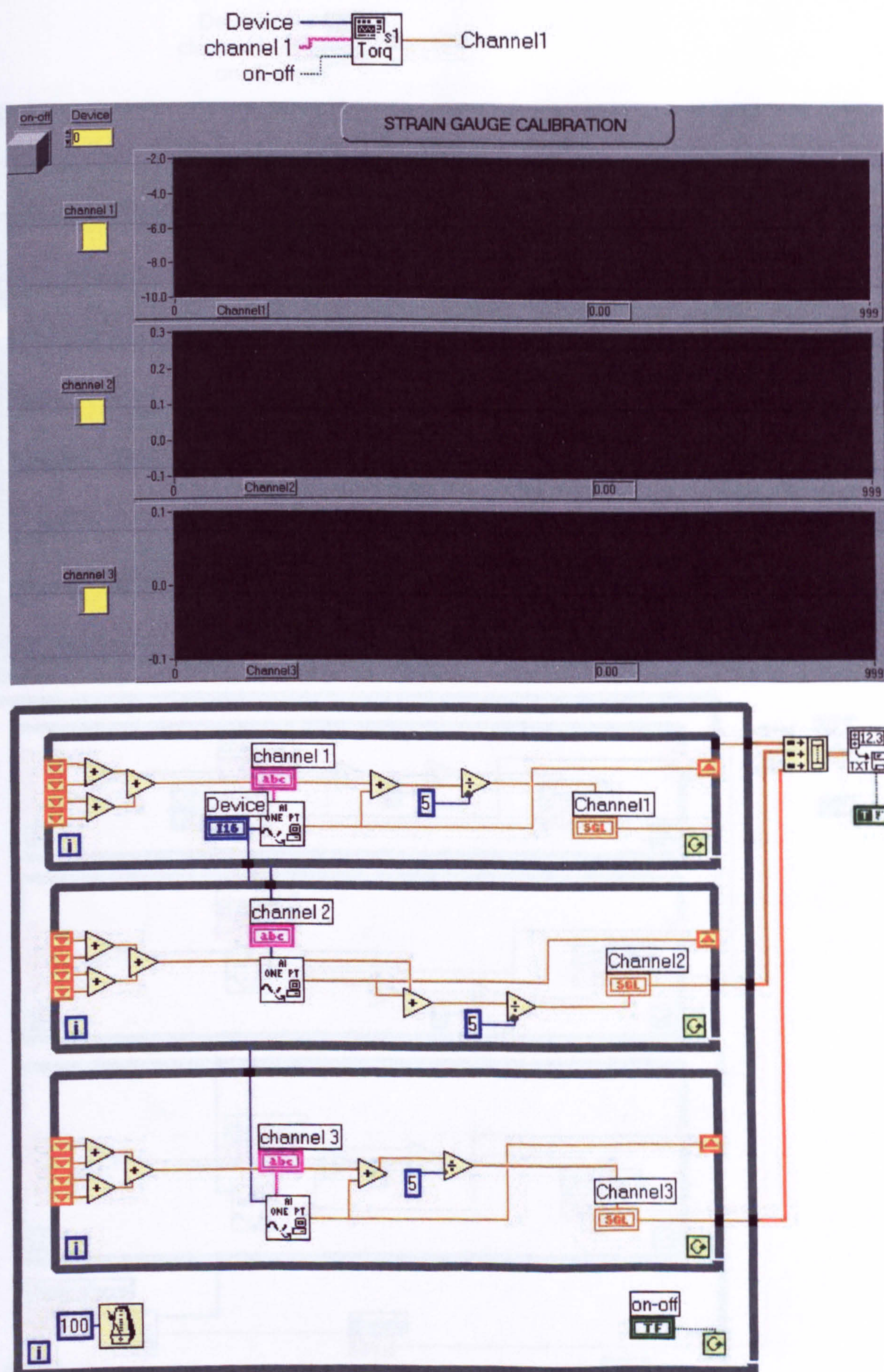
Appendix 1 Figure 1.

Virtual Instrument Labview 5.1 - IMPLANT INSERTION

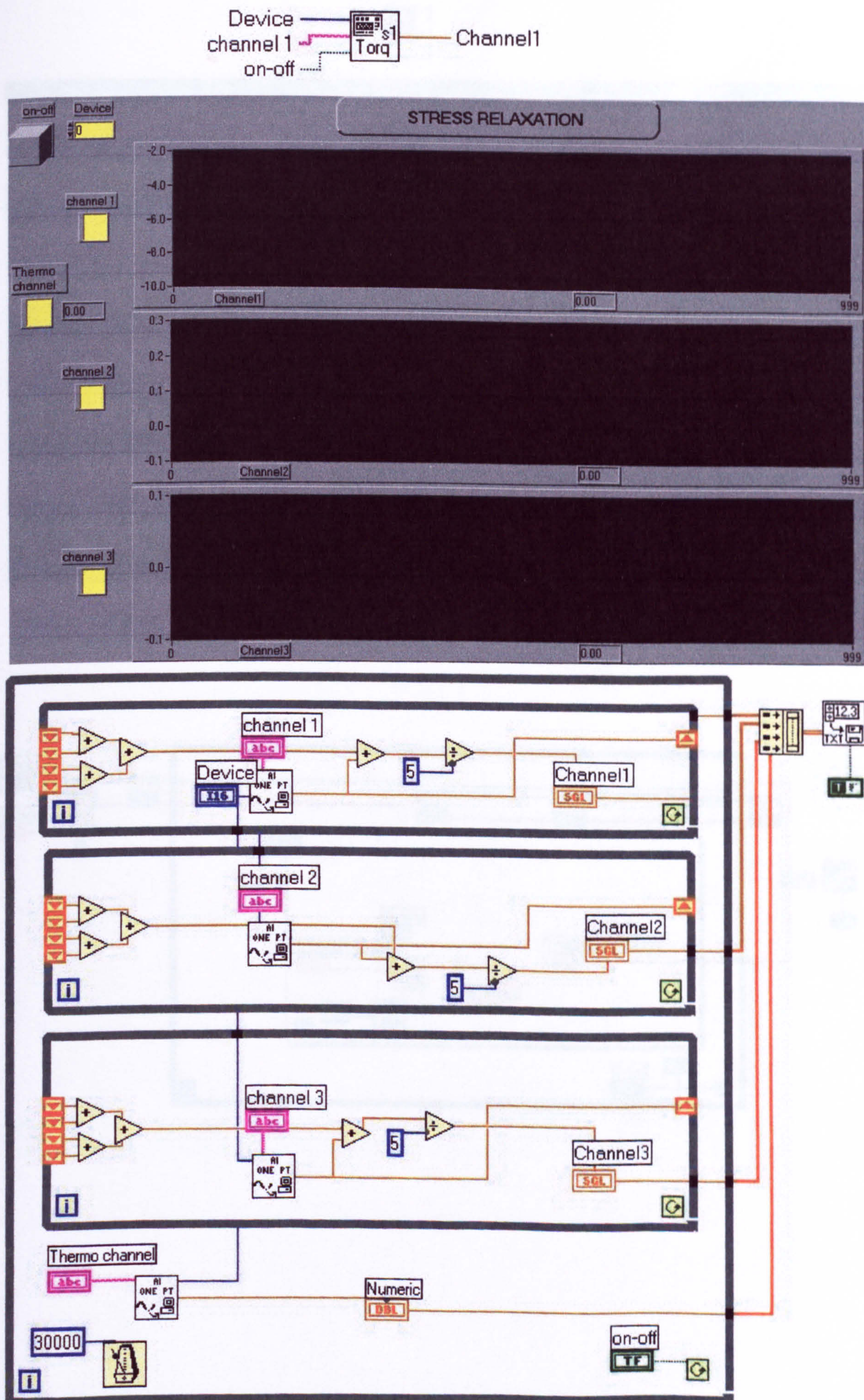




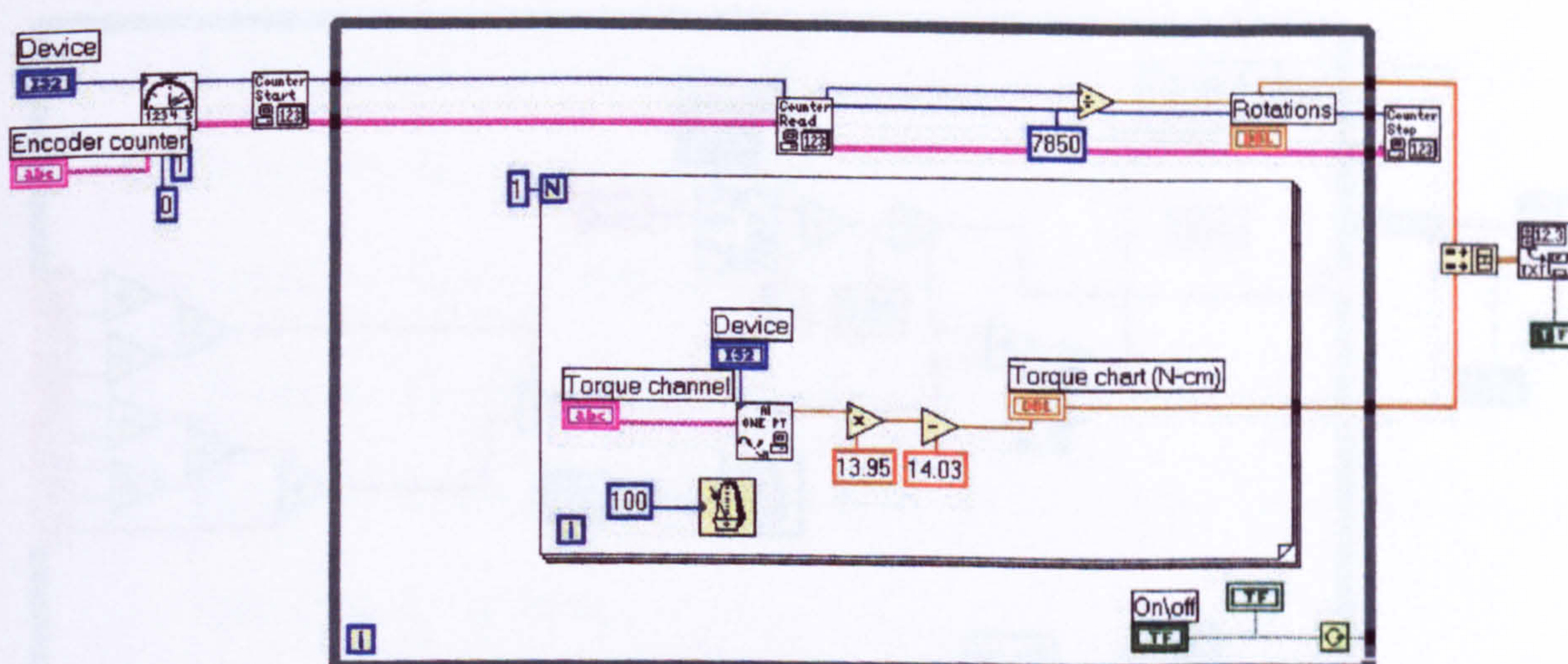
Virtual Instrument Labview 5.1 – STRAIN GAUGE CALIBRATION



Virtual Instrument Labview 5.1 – STRESS RELAXATION

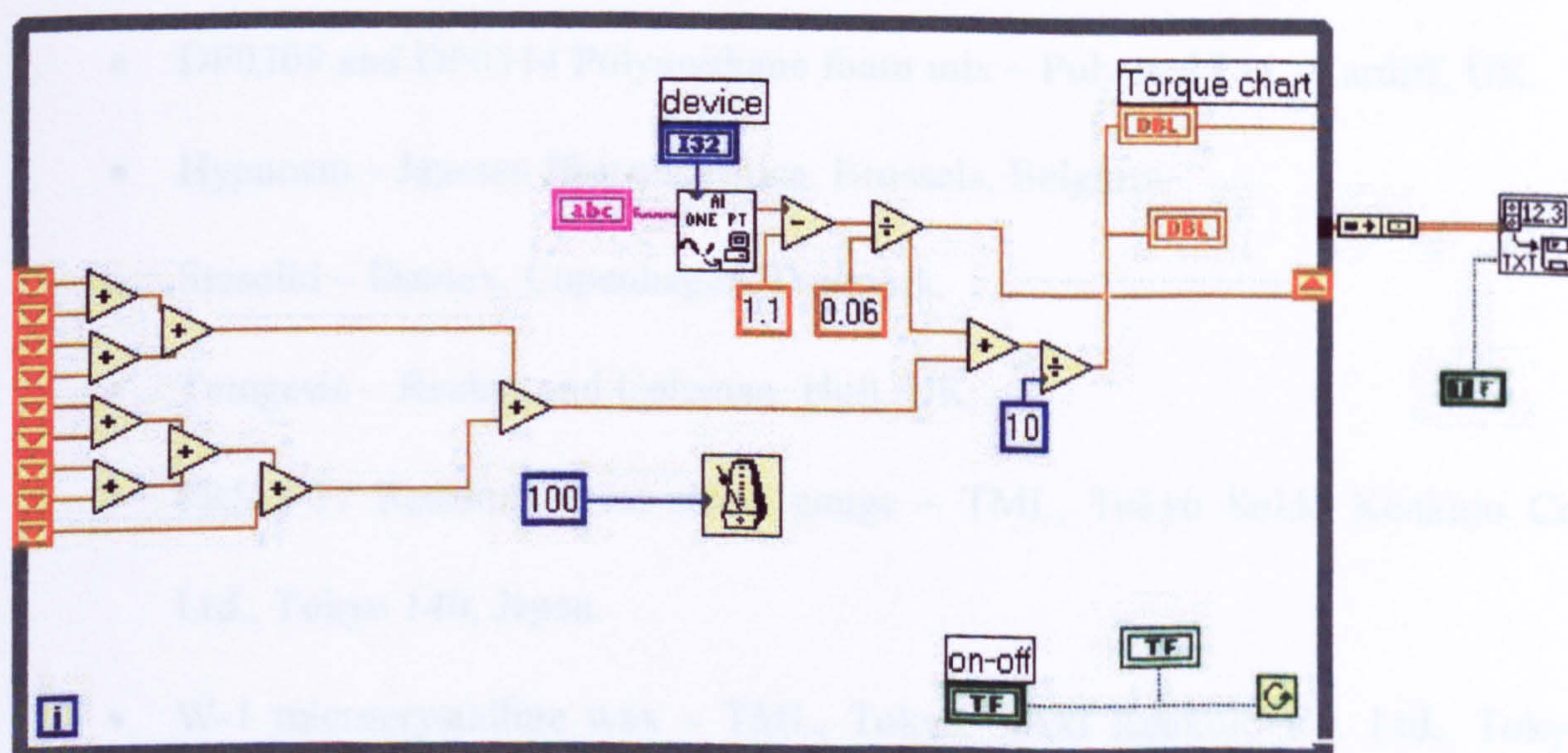
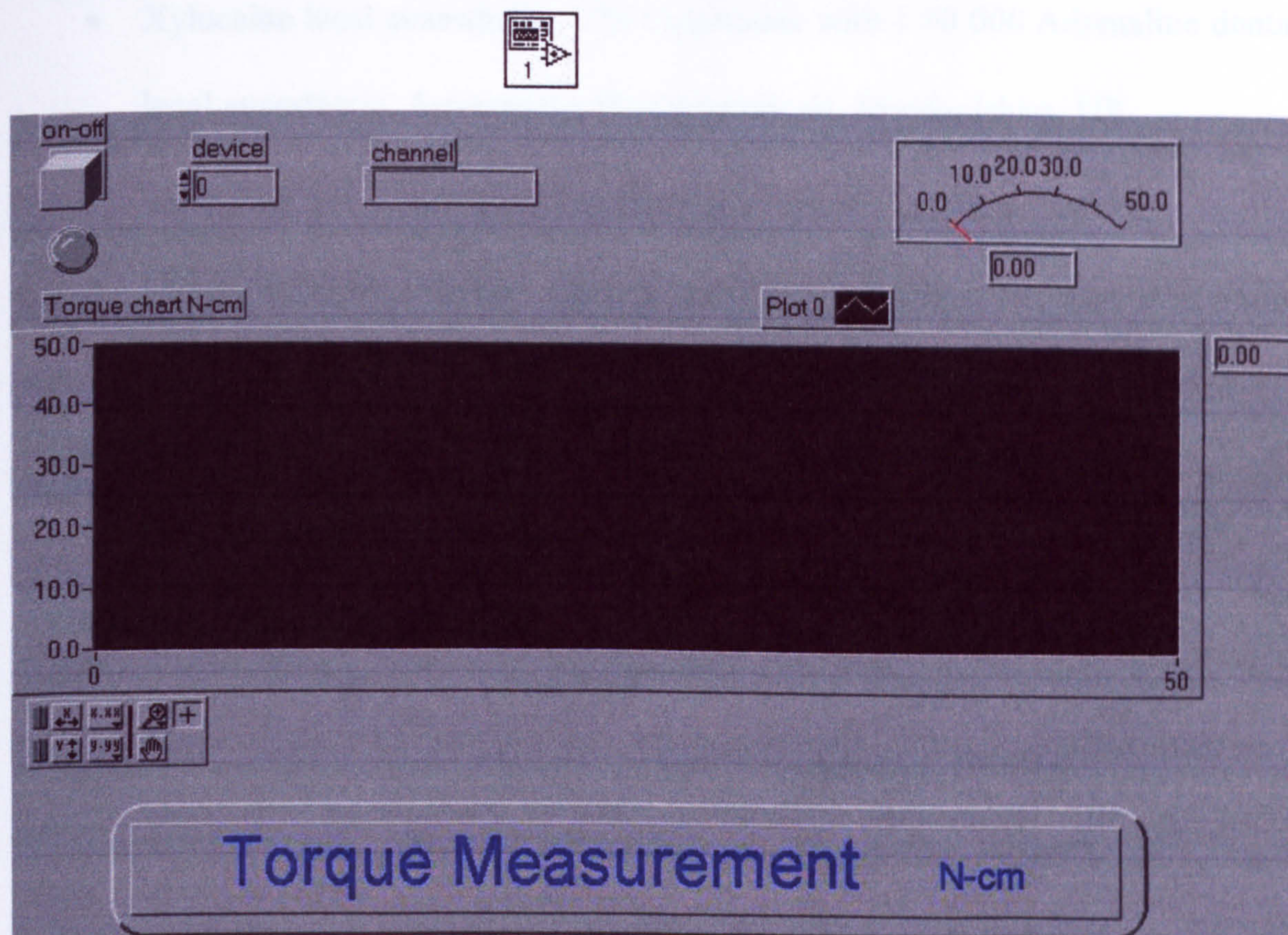


Virtual Instrument Labview 5.1 – TORQUE AND ENCODER



Appendix 1 Figure 6.

Virtual Instrument Labview 5.1 – TORQUE MEASUREMENT



Appendix II – Materials

- **Xylocaine local anaesthetic - 2% Lignocaine with 1:80 000 Adrenaline dental local anaesthetic, Astrazeneca Pharmaceuticals, Hertfordshire, UK.**
- **Osseocare drill controller – Nobelbiocare AB, Gothenburg, Sweden.**
- **PE122 Smart card reader – Philips electronics UK Ltd, Croydon, Surrey, UK.**
- **15-BTGN – Tohnichi Torque gauge, Tohnichi MFG, Japan.**
- **HEDS-550S optical rotary encoder – Hewlett-Packard Ltd, Bracknell, Berkshire, UK.**
- **MIO A10-16XE-50 Data acquisition card – National Instruments Ltd, Newbury, Berkshire, UK.**
- **Labview 5.1 Software package - National Instruments Ltd, Newbury, Berkshire, UK.**
- **RM520W Polyurethane foam mix – Baxenden Chemicals Ltd., Lancashire, UK.**
- **DF0309 and DF0314 Polyurethane foam mix – Polymed Ltd., Cardiff, UK.**
- **Hypnorm – Janssen Pharmaceutica, Brussels, Belgium.**
- **Stesolid – Dumex, Copenhagen, Denmark.**
- **Temgesic – Reckitt and Coleman, Hull, UK.**
- **FRS-3-11 Residual stress strain gauge – TML, Tokyo Sokki Kenkujo Co. Ltd., Tokyo 140, Japan.**
- **W-1 microcrystalline wax – TML, Tokyo Sokki Kenkujo Co. Ltd., Tokyo 140, Japan.**
- **M Bond 200 – cyanoacrylate adhesive and M Coat D – air drying acrylic resin – Vishay measurements group, UK Ltd., Basingstoke, Hants, UK.**

Appendix III -Work from this thesis previously published

Paper

O'Sullivan D.J., Sennerby L., Meredith N. 2000 'Measurements comparing the initial stability of five designs of dental implants: a human cadaver study'. *Clinical Implant dentistry and Related Research*; 2:2:85-91.

Measurements Comparing the Initial Stability of Five Designs of Dental Implants: A Human Cadaver Study

Dominic O'Sullivan, BDS, FDS, RCS;* Lars Sennerby, DDS, PhD;† Neil Meredith, BDS, FDS RCS, PhD‡

ABSTRACT

Background: A number of different dental implant designs are currently in clinical use. A successful outcome of implant placement is thought, at least in part, to be due to the primary stability of an implant after placement. Few data are available for comparing the primary stability characteristics of different implant designs.

Purpose: This investigation compared the primary stability of five types of endosseous dental implant of varying geometry and surface topography.

Materials and Methods: Comparison was made between a standard threaded commercially pure titanium implant (Nobel Biocare AB, Göteborg, Sweden), the Mark II self-tapping implant (Nobel Biocare AB, Göteborg, Sweden), the Mark IV tapered self-tapping implant (Nobel Biocare AB, Göteborg, Sweden), the Astra Tioblast (AstraTech AB, Mölndahl, Sweden), and the 3i Osseotite (3i [Implant Innovations Incorporated], Palm Beach, Florida, USA). Fifty-two fixtures were placed in the maxillary bone of nine unembalmed human cadavers. Implant stability as a function of peak insertion torque and resonance frequency values was recorded for each fixture site after placement. Removal torque was also measured 1-hour postinsertion. Assessment of bone quality at each site was made.

Results: All of the implants tested demonstrated good primary stability in type 2 and 3 bone. The Standard, Mark II, Osseotite, and Tioblast were less stable when placed into bone type 4. The Mark IV implants appeared to maintain a high primary stability even in Type 4 bone.

Conclusion: When looking across all bone qualities, the Mark IV implant develops a significantly higher insertion torque than the Standard, Mark II, and Osseotite implant types, and a significantly higher resonance frequency value than the Standard implant, indicating a higher interfacial stiffness at the implant–bone interface.

KEY WORDS: endosseous implants, jawbone, resonance frequency analysis, stability, torque

The use of endosseous dental implants to restore the missing or incomplete dentition has, over the last 30 years, become increasingly widespread. Excellent results can be claimed for implants placed into bone of good quality and quantity. The long-term success for implant therapy unfortunately becomes less certain when fixtures are placed into bone of poor quality and/or quantity. The

early loss of dental implants is thought to be due to excessive mechanical loads applied too early to the implant coupled with poor primary stability at placement.^{1–3} Commercially, a number of implant designs have been shown to have comparable results when used in bone of sufficient quantity and density to provide good mechanical stability to the implant immediately following placement.⁴ As confidence in the outcome of implant treatment in good bone has increased, manufacturers have now turned their attention to increasing the success rate of implants placed in bone of poorer quality. What both implant manufacturers and clinicians seek is a design of implant that ensures good primary stability even when placed into bone of reduced quality and quantity. Attempts have been made to achieve this with altered surface characteristics and/or changes to the geometric design of the implant. Surfaces can be abrasive blasted,

*Clinical Research Fellow, Leeds Dental Institute, University of Leeds, Leeds, United Kingdom; †Professor, Department of Biomaterials and Handicap Research, Institute for Surgical Sciences, University of Göteborg and the Brånemark Clinic, Göteborg, Sweden; ‡Professor of Clinical Biomaterials in Relation to Restorative Dentistry, Leeds Dental Institute, University of Leeds, Leeds, United Kingdom

Reprint requests: Dominic O'Sullivan, BDS, FDS, RCS, Leeds Dental Institute, University of Leeds, Clarendon Way, Leeds LS2 9LU, United Kingdom

chemically etched, or have a surface coating applied in an attempt to provide an optimal surface for bone apposition and osseointegration. The effect on osseointegration of changes to the surface of implant fixtures has been investigated using histology, histomorphometry, and removal torque analysis.⁵⁻⁷ Such changes may enhance the osseointegration of implants during the healing period but have little effect on the initial primary stability of the fixtures immediately after placement. In order to enhance the primary stability of dental implants, attention has recently shifted toward changes in the overall geometry of the implants. The rationale behind implant design changes has often not been clear, and little has been done to attempt to quantify any increase in the primary stability of such implants. The original implant technique as described by Brånemark and co-workers⁸ relied on the use of a tap to cut a threaded channel in the bone prior to implant placement. The use of a surgical tap is, however, an additional step in the implant placement process, and several implant manufacturers have now adopted the use of a self-tapping design of implant. Self-tapping implants used in this investigation incorporate cutting facets into the lower portion of the implant, which allow the insertion of the implant without the prior use of the tap. However, there are no published data available regarding the effect of this change in implant geometry on the primary stability of the implants. A new self-tapping implant has been specifically designed for use in poorer bone quality (type 3 and type 4), with the design emphasis placed on enhancing the primary stability of the implant. To do this, the implant has been designed with a 1-degree taper. The tapered implant is placed into a cylindrical hole. As the implant is inserted, it is thought that the denser cortical bone is compressed, with this compression increasing the primary stability of the implant.

The aim of this study was to assess the primary stability characteristics of five differing designs of dental implants when placed into bone of varying qualities. To do this, we have used a human cadaver model in an attempt to closely approximate the clinical situation.

MATERIALS AND METHODS

Subjects

Nine human cadavers were used in the investigation, of which five were female and four male. Their ages ranged from 65 to 79, with a mean of 71 years. All

cadavers were less than 48 hours postmortem with most being tested within 30 hours; specimens were stored at 4°C. All of the included subjects were free from bone pathology and fully edentulous. All implants were placed in maxillary bone, as it was frequently impossible to gain access to the mandible due to the rigor of the facial tissues.

Implant Characteristics

Five dental implant types were used (Figure 1). The Standard Brånemark implant (STA) (Nobel Biocare AB, Göteborg, Sweden), Mark II self-tapping implant (MKII) (Nobel Biocare AB, Göteborg, Sweden), the Mark IV self-tapping tapered implant (MKIV) (Nobel Biocare AB, Göteborg, Sweden), the Astra Tioblast (TIOB) (AstraTech, Mölndahl, Sweden), and the 3i Osseotite (OTI) (3i [Implant Innovations Incorporated]), Palm Beach, Florida, USA). All of the implants used were 13 mm in length.

Surgical Technique and Implant Placement

A standard surgical technique was used to prepare the sites for implant placement in the maxillary bone of each cadaver. Manufacturers' guidelines were followed for each of the implant systems tested. A 2-mm pilot drill was used for all implant sites. Final drill diameters of 3 mm were used in bone of type 3 and 4 quality when placing MKIV; however, difficulty was experienced in fully seating the MKIV implants in type 2 bone, and a final diameter of 3.35 mm was used in these sites. The same final drill diameters were used when placing STA and MKII to allow comparison with the MKIV implants. To place the OTI, 3.35-mm diameter drills were used, and a 3.75-mm final drill was used for the TIOB in accordance with the manufacturer's

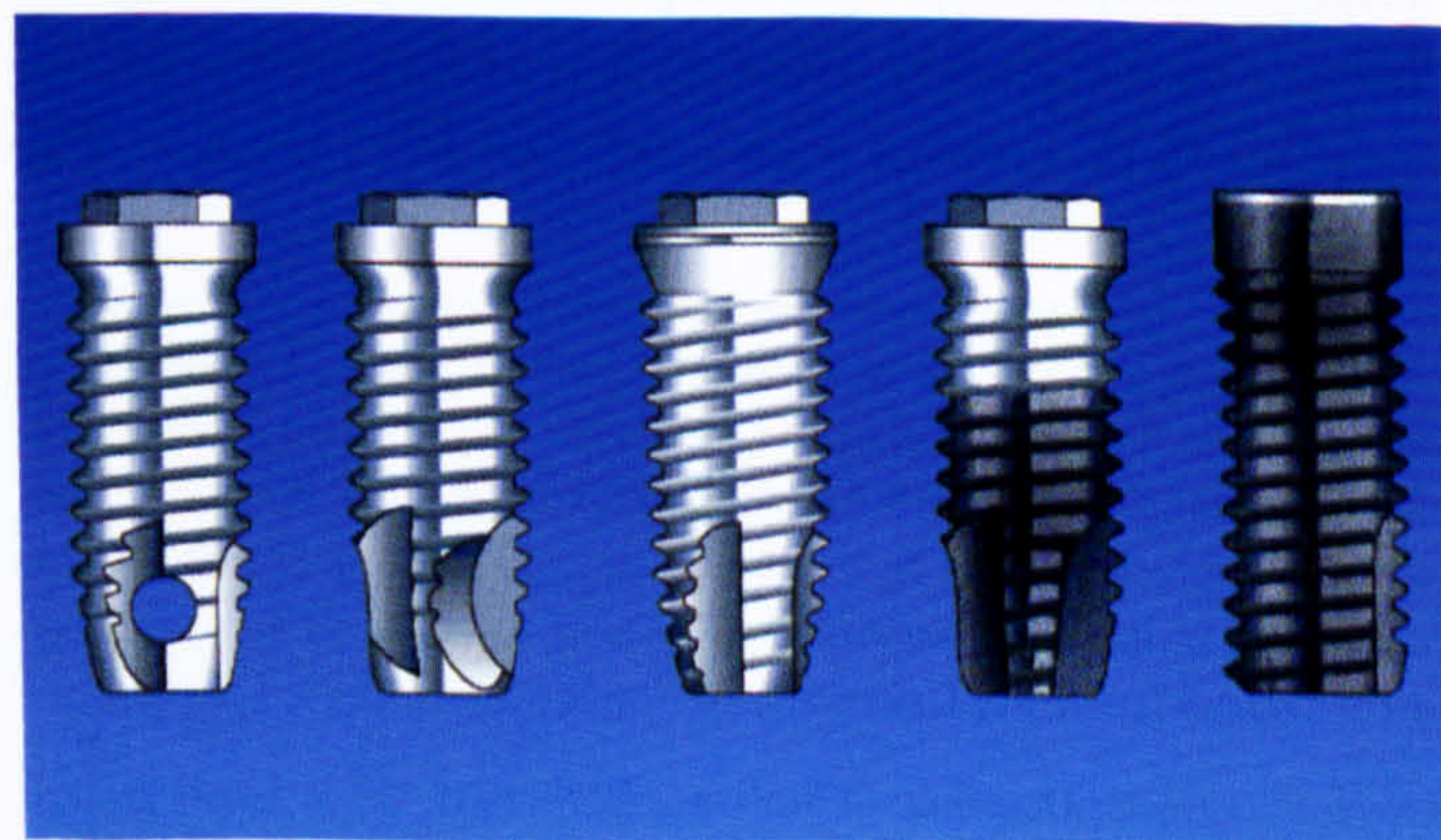


Figure 1. Illustration of five implant types: STA-Standard Brånemark, MKII-Mark II implant, MKIV-Mark IV implant, OTI-Osseotite implant, TIOB-Tioblast implant.

guidelines for implant insertion into maxillary bone. None of the implant sites were countersunk. Because the mean temperature of the cadavers was only 4°C, irrigation was not used, and all of the implants were inserted at the same low rotational speed. To enable direct comparison of different implants in bone of comparable quality and quantity, implants were placed symmetrically in opposing sides of the maxilla, with comparison implants (STA, NBC, TIOB, and OTI) in the left side of the maxilla and the MKIV in the right side. Fifty-two implants were placed in total. Table 1 illustrates the distribution of implant placement.

Assessment of Bone Quality

The bone quality at each placement was assessed by the operator according to the system described by Lekholm and Zarb in 1985.⁹ The assessment of bone quality was achieved by the combined tactile impression of bone quality at placement and the appearance of the bone at the implant site following implant removal. Due to the subjective nature of this test, care was taken to obscure computer measurement of insertion torque from the operator making the bone quality assessment.

Data Collection

Following site preparation, torque during implant insertion was recorded using a modified electronic torque controller (Nobel Biocare AB, Göteborg, Sweden) connected to an analogue to digital data acquisition card (DAQCard AI-16XE-50, National Instruments, UK Ltd., UK) and a laptop computer. Data were recorded at the rate of 10 samples per second. Angular displacement of each implant was measured using a hall effect rotary encoder mounted on the handpiece motor. Following implant placement, resonance frequency measurements were made according to the method originally described by Meredith et al in 1996.¹⁰⁻¹³ The resonance frequency

analysis equipment consists of a transducer, which attaches to the implant; this, in turn, connects to a custom-designed frequency response analyzer and a portable laptop computer. The transducer is an L-shaped cantilever beam, which connects to the implant via a screw attachment. A piezoelectric crystal on the vertical of the L-shaped beam is used to stimulate the implant/transducer complex across a swept frequency range of approximately 2 to 20 kHz; this range is generated by the frequency response analyzer. A second piezoelectric crystal on the opposite side of the beam is used as the receiving element to detect the resonance frequency peak. The data were analyzed, collected, and stored on the computer.

Statistical Analysis

The small number of samples for each implant/bone quality subset precluded statistical analysis between these subsets. Overall comparison between implant types across all bone qualities was possible using analysis of variance. Where a significant difference was indicated, the Bonferroni multiple-comparison test was performed with the significance set at *p* = .05.

RESULTS

Insertion Torque

The insertion depth (ID) was calculated as a function of the angular displacement (θ) and the thread pitch (TP) of each implant:

$$\frac{\theta}{TP} = ID$$

Figure 2, A to C, illustrates three plots showing typical insertion torque/displacement plots for the MKII, MKIV, and OTI implant types when placed into type 2 bone. Mean values for peak insertion torque with 95% confidence intervals for bone types 2 to 4 are illustrated in Figure 3, A to C. Peak insertion torque was calculated as the highest torque value obtained from the insertion torque plot for each implant. Figure 4, A to C, shows mean values with 95% confidence intervals for peak removal torque 1 hour following implant insertion for bone types 2 to 4. Peak removal torque was calculated as the highest torque value obtained from the removal torque plot for each implant. Figure 5 illustrates a typical insertion torque plot against time for the MKIV, STA, and MKII implants showing the reduced insertion time for the MKIV. When the peak insertion torque data

TABLE 1. Implant Distribution

Implant Type	Bone Type 2	Bone Type 3	Bone Type 4	Total
STA	4	3	3	10
MKII	3	3	3	9
MKIV	8	4	3	15
OTI	3	3	3	9
TIOB	3	3	3	9
Total	21	16	15	52

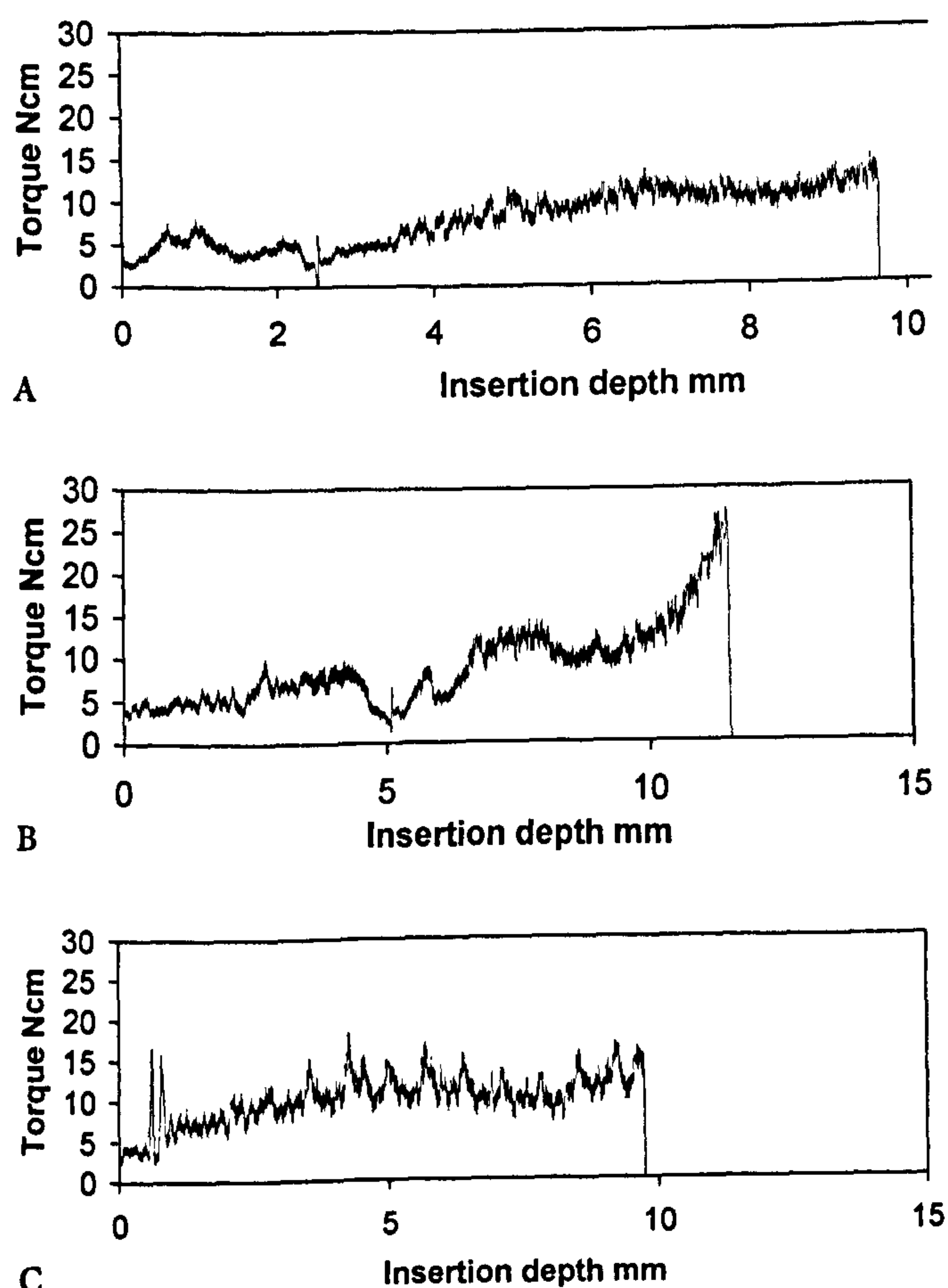


Figure 2. A, Mark II implant insertion torque profile plot. Insertion torque plotted against insertion depth in mm. B, Mark IV implant insertion torque profile plot. Insertion torque plotted against insertion depth in mm. C, Osseotite implant insertion torque profile plot. Insertion torque plotted against insertion depth in mm.

from all bone qualities are pooled, using the Bonferroni multiple-comparison test, a statistically significant difference ($p < .05$) is evident between the MKIV and the STA, the MKIV and MKII, and the MKIV and OTI implants; these data are summarized in Table 2. No significant difference was found between the immediate removal torque values for each implant type.

Resonance Frequency

The mean resonance frequency values with 95% confidence intervals for bone types 2 to 4 are summarized in Figure 6, A to C. For STA, MKII, OTI, and MKIV implants placed into type 2 bone, the resonance frequency values were greater than 7.10 kHz, indicating high interfacial stiffness between the implant and the bone. The TIOB implants have a mean resonance frequency of 6.91 kHz, which, although lower than the other implants tested, would still be considered to indicate a good primary stability clinically. Very little

change is seen in type 3 bone, with the relative stability of each implant type remaining close to that seen in type 2 bone. In type 4 bone, STA, MKII, and OTI resonance frequency values were lower than those seen in bone types 2 and 3, indicating that the primary stability of these implants in these bone types is reduced when compared to type 2 and 3 bone. For TIOB implants, the resonance frequency value also falls to give a value close to that of the OTI implant. The MKIV implants showed an increase in the mean resonance frequency to 7.99 kHz in type 4 bone, suggesting the highest primary stability of any of the implants tested. When the resonance frequency data from all bone qualities are pooled, using the Bonferroni multiple-comparison test, a statistically significant difference ($p < .05$) is evident between the MKIV and the STA implants. No other significant differences were identified between implant types. These data are summarized in Table 2.

DISCUSSION

The importance of good primary stability when implants are placed has been well established. Poor initial stability is thought to play a significant part in the early loss of implants when this is coupled with an insufficient healing.^{2,3} Primary stability of an implant at placement is a function of bone quality (the ratio of compact to trabecular bone), bone quantity, implant geometry, and the placement technique (size of drills, whether self-tapping or not, etc.). It is commonly cited by surgeons that bone quality and quantity influence the primary stability of dental implants, but this variation in the primary stability of a specific design of implant when placed into bone of varying qualities has not been quantified. The aim of this study was to compare the primary stability characteristics of five differing designs of implant and in particular to look at how the stability varies when these are placed into bone of varying qualities. Bone quality is often ranked clinically on a scale of 0 to 4⁹ according to bone density, perceived by the surgeon as resistance to drilling at implant placement. A quantitative technique was outlined by Johansson and Strid in 1994, who calculated the resistance to cutting by measuring the electrical current used by a motorized handpiece.¹⁴ The reliability of this technique and its relationship to bone density was further investigated by Friberg et al in 1995.¹⁵ The present study has used both the Lekholm and Zarb scoring method and measurement of insertion torque to assess bone quality at each implant site. It is important to exer-

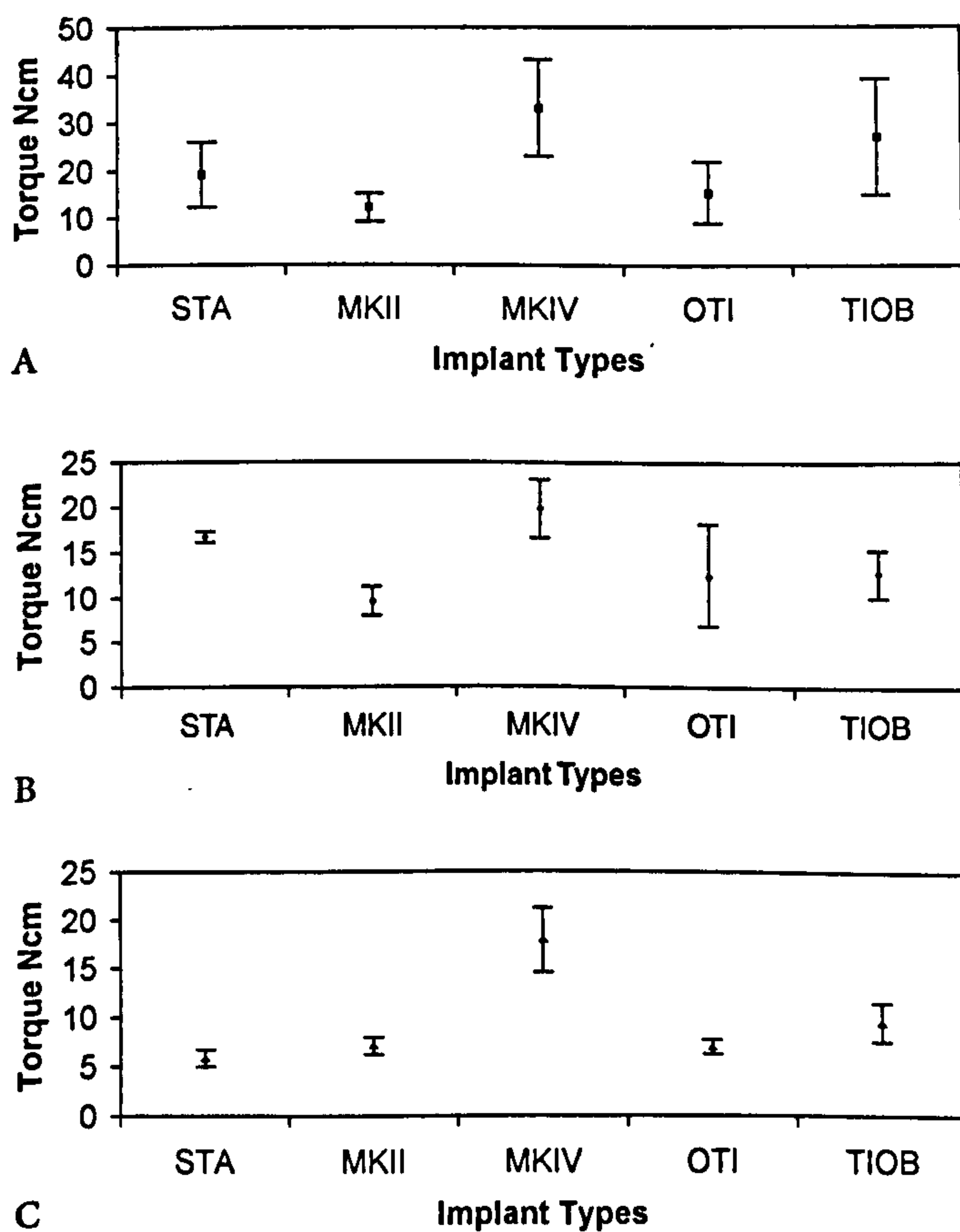


Figure 3. A, Mean peak insertion torque values for each implant type in type 2 bone; 95% confidence intervals shown. B, Mean peak insertion torque values for each implant type in type 3 bone; 95% confidence intervals shown. C, Mean peak insertion torque values for each implant type in type 4 bone; 95% confidence intervals shown.

cise caution when interpreting the insertion torque plots for each of the implants. Although, theoretically, the lack of irrigation may affect lubrication and bone chip clearance, this did not appear to affect insertion torque values during preliminary tests prior to the study. Knowledge of the geometry of the implant and the insertion technique (e.g., the relative diameters of the implant and the predrilled hole) is essential, but with these in mind, certain broad characteristics are apparent. The curves for each of the implants are very similar for the first 3 to 4 mm of insertion, corresponding to the blades of the tapping portion of each implant passing through the cortical bone. Following this, the curves correspond to the passage of the tapping portion of the implant passing through the trabecular bone and a frictional component as the threads of the remaining part of the implant pass through the tapped channel in the bone. With a tapered design of implant such as MKIV used in this study, there is an additional component to the curve as the upper threads of the implant are larger in diameter than the tapping portion. The increasing

diameter of the inserting implant results in compression of the interfacial bone and leads to a steeper rise in the curve than that seen for a cylindrical implant (see Figure 5). This effect was clearly seen in all of the insertion torque plots for the MKIV implants, which showed a steeper rise and higher peak insertion torque than the other implants tested. An additional design feature of the MKIV implant is the incorporation of a double thread in place of the single thread used in all of the other implant systems tested. The theoretical advantages of the double thread include an increased speed of insertion without increasing the energy generated at the implant-bone interface. The reduced insertion time can be seen in Figure 5 when comparing the insertion torque graph for the MKIV implant with the STA and MKII implant plotted against time.

Primary stability of implants has traditionally been very difficult to assess and is often reduced to a simple

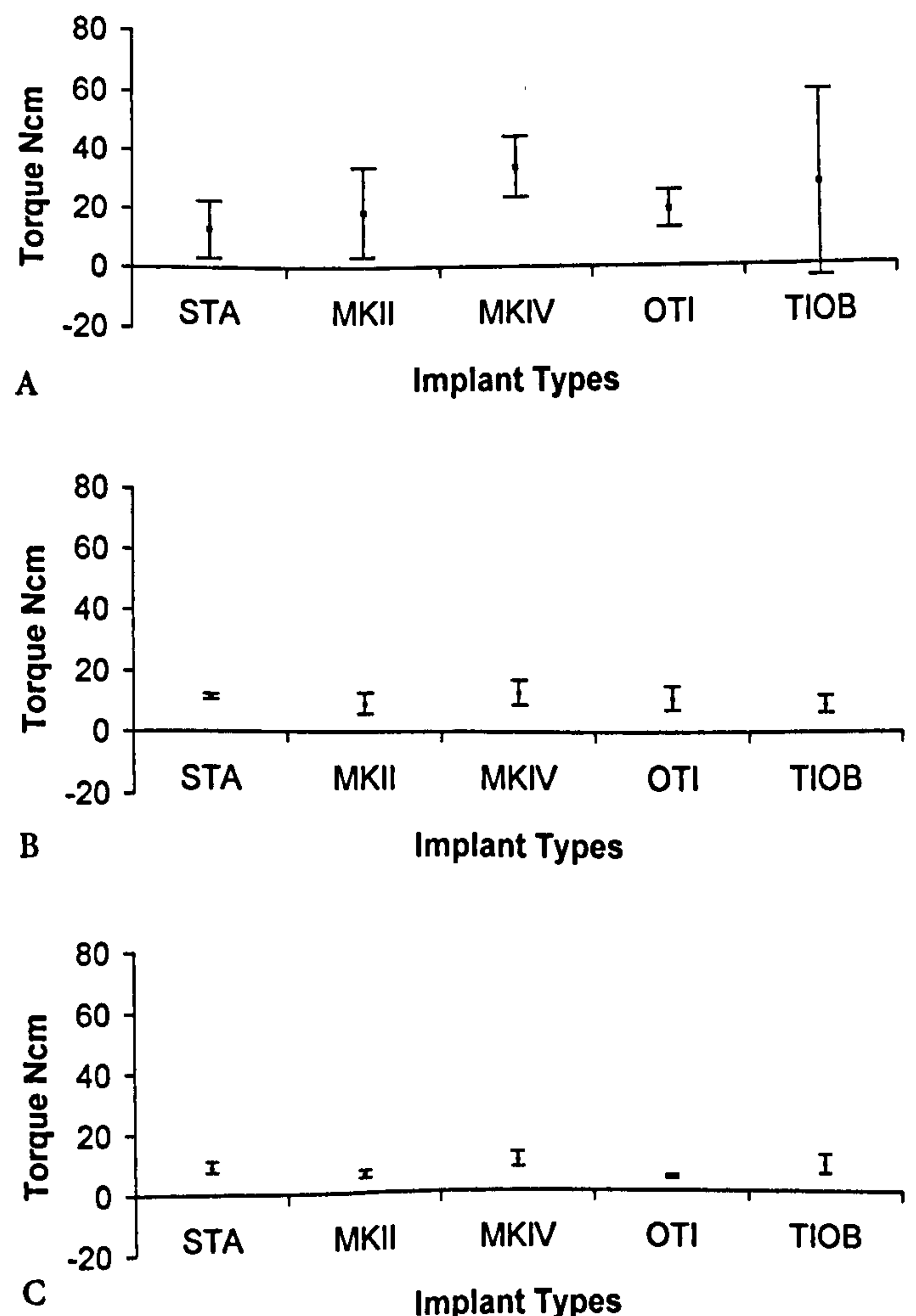


Figure 4. A, Mean peak removal torque 1 hour after placement for each implant type in type 2 bone; 95% confidence intervals shown. B, Mean peak removal torque 1 hour after placement for each implant type in type 3 bone; 95% confidence intervals shown. C, Mean peak removal torque 1 hour after placement for each implant type in type 4 bone; 95% confidence intervals shown.

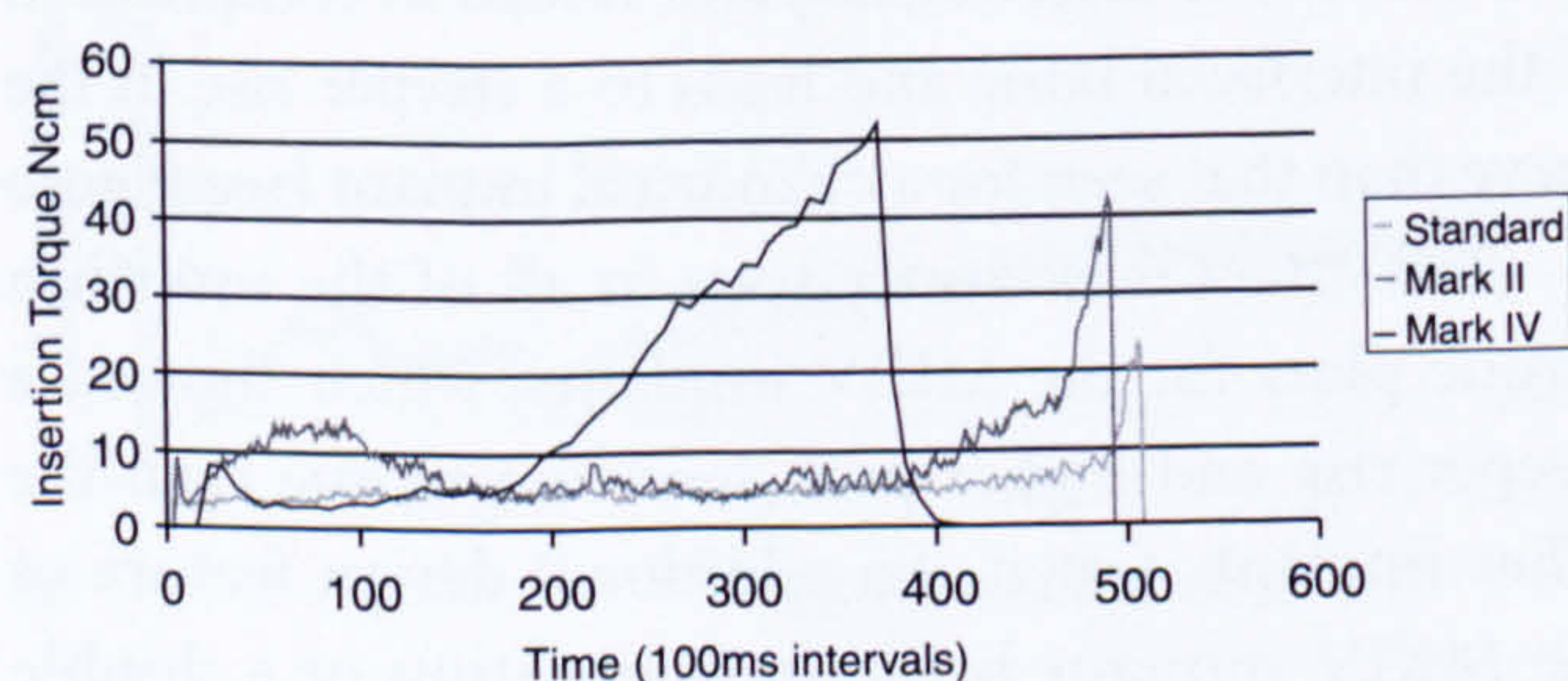


Figure 5. Insertion torque profiles for a Standard implant, a Mark II implant, and a Mark IV implant; insertion torque plotted against time.

assessment of mobility. This is very subjective even when more sophisticated methods have been employed. One such method is the Periotest (Siemens GmbH, Germany), which involves using a probe with a small metal slug containing an accelerometer. The probe is held in close proximity to the fixture/tooth and the metal slug is used to strike the surface under test, mobility being calculated from the contact time between the slug and the surface of the implant/tooth.¹⁶⁻¹⁹ There have been reported difficulties with this technique. The Periotest has been reported as being sensitive to changes in angulation, distance of the probe from the implant, and variation of the area, which is struck.^{19,20} These are problems that are inherent with any handheld mechanical test probe. A noninvasive technique for assessing the stability of an implant immediately after placement has been described by Meredith et al and reported on in a number of studies both in vitro and in vivo.¹⁰⁻¹³ The technique measures the resonance frequency of a small transducer, which may be attached to an implant or to an abutment. The aim of the technique is to assess the interfacial stiffness between the implant and the bone and local bone stiffness in bending. This allows an initial assessment of stability to be made immediately after placement and to be able to monitor the increase in this stiffness with osseointegration.

For all of the implants, when placed into relatively good quality bone (type 2), resonance frequency values were good (greater than 6.90 kHz). This was perhaps not surprising as in good, dense bone, it would be anticipated that the commercially available implants tested in this investigation would be able to achieve an acceptable primary stability. For the STA and to a lesser extent the TIOB implants, resonance frequency values fell when they were inserted into poorer bone qualities, indicating that the initial primary stability for these implants in this bone type is reduced when compared to type 2 bone. For OTI and MKIV implants, the resonance frequency values remained high even when placed into bone of quality type 4, suggesting that the initial stability for these implants is less affected by the quality of the bone into which they are inserted.

Removal torque of an implant immediately after placement has been used to assess the initial stability of endosseous implants. Niimi et al in 1997²¹ used this technique to assess the bone quality and cortical bone thickness of fibula, iliac crest, and scapula. They found a significant correlation between cortical bone thickness and removal torque but not between bone quality and removal torque. They also compared the results from a cadaver model with data collected clinically and found no significant differences between them, indicating that the cadaver is a suitable model for the assessment of initial stability. This was in agreement with Ueda et al,²² who looked at the relationship between insertion torque and removal torque of endosseous fixtures when placed in cadaveric temporal bone. They noted that a high removal torque was always related to a higher initial insertion torque, but with the peak removal torque always of a lower magnitude than the peak insertion torque. This was a trend also seen in this investigation with the exception of two values. This would be expected as the frictional component of the removal torque curve would be the same as for the

TABLE 2. Data for Implant Types—Bone Qualities 2, 3, and 4 Combined

	STA	MKII	MKIV	OTI	TIOB
Peak insertion torque (Ncm)	14.46 ± 7.22	9.62 ± 2.66	26.08 ± 12.35*	11.63 ± 5.28	16.44 ± 5.28
Immediate removal torque (Ncm)	11.36 ± 5.89	11.43 ± 8.71	23.80 ± 15.29	11.71 ± 6.60	14.41 ± 14.21
Resonance frequency (kHz)	6.59 ± 0.76	6.98 ± 0.42	7.39 ± 0.49†	6.93 ± 0.61	6.70 ± 0.35

Mean ± SD. Combined data from all bone qualities.

*Statistically significantly different ($pH < .05$) compared to STA, MKII, and OTI.

†Statistically significantly different ($pH < .05$) compared to STA.

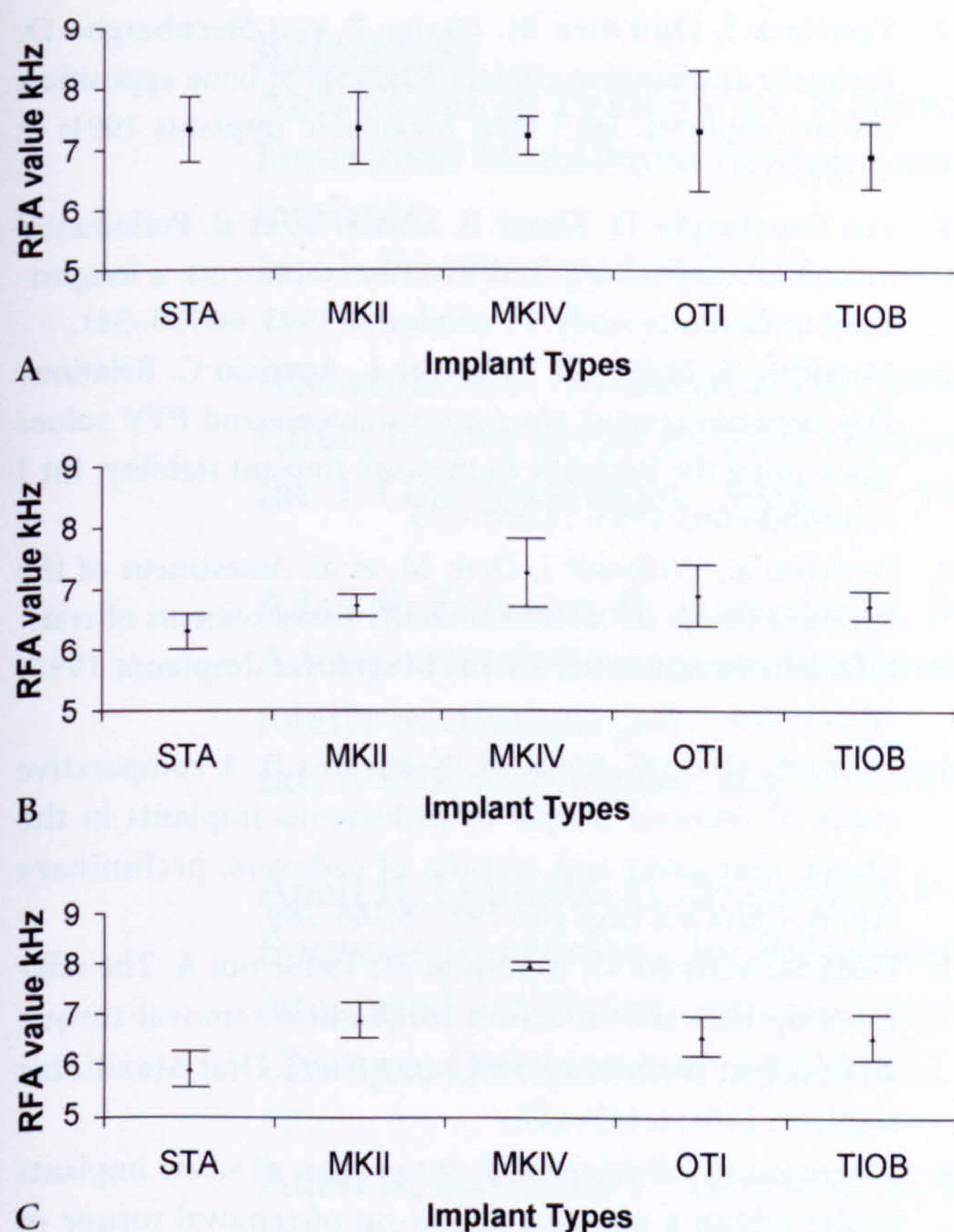


Figure 6. A, Mean RFA measurements for each implant type in type 2 bone. B, Mean RFA measurements for each implant type in type 3 bone. C, Mean RFA measurements for each implant type in type 4 bone.

insertion torque but without the compressive component generated during insertion. There are obvious problems when drawing conclusions from removal torque data gathered immediately after insertion. A high immediate removal torque may not indicate that a high removal torque would be gained once osseointegration has taken place. Immediate removal torque does, however, provide a measure of the resistance of an implant to rotational displacement in the vulnerable postinsertion healing period. The measurement of removal torque following healing and osseointegration is a destructive test giving an indication of interfacial strength and may be used to determine the level of osseointegration of a cylindrical implant^{23,24} after a period of healing. The data obtained in this investigation confirmed the suitability of the cadaver model for insertion and removal torque and also indicated that resonance frequency values are also comparable to those obtained clinically.

High insertion and therefore high removal torque are often seen as desirable, with a high insertion torque leading to an increase in the primary stability of the

implant. The data in this investigation appear to support this. The tapered experimental implant MKIV has been designed with this in mind, but a concern must be that the taper may lead to high compression forces during placement. With high compression, disturbance of the local microcirculation may occur, leading to necrosis of the osteocytes and bone resorption.²¹ It is reasonable to imagine that there is a balance point at which the degree of taper is such that there is an optimum level of primary stability without inducing resorption in the local bone. The degree of taper also prevents the full insertion of the implant into good quality type 1 and type 2 bone. To allow full insertion, a larger initial drill size was needed, and this appeared to reduce the initial stability of the implant. It may be strongly suggested from this that the MKIV implant should be placed only into bone of type 4 or possibly type 3 quality. From our data, it appears that the MKIV implant is more stable following placement than the other implants tested when placed into bone of type 4 quality. When looking across all bone qualities, the MKIV implant develops a significantly higher insertion torque than the STA, MKII, and OTI implant types and a significantly higher resonance frequency value than the STA implant, indicating a higher interfacial stiffness at the implant–bone interface. Further studies are needed to evaluate the clinical success of the fixture when compared to the other implant types.

REFERENCES

1. Albrektsson T. On long-term maintenance of the osseointegrated response. *Aust Prosthet J* 1993; 7(Suppl):15–24.
2. Friberg B, Jemt T, Lekholm U. Early failures in 4641 consecutively placed Brånemark dental implants. A study from stage I surgery to the connection of completed prostheses. *Int J Oral Maxillofac Implants* 1991; 6:142–146.
3. Jaffin RA, Berman CL. The excessive loss of Brånemark fixtures in type IV bone: a 5-year analysis. *J Periodontol* 1991; 62:2–4.
4. Roos J, Sennerby L, Albrektsson T. An update on the clinical documentation on currently used bone anchored endosseous oral implants. *Dent Update* 1997; 24:194–200.
5. Wennerberg A, Albrektsson T, Andersson B. Design and surface characteristics of 13 commercially available oral implant systems. *Int J Oral Maxillofac Implants* 1993; 8:622–633.
6. Wennerberg A, Albrektsson T, Anderson B, Krol J. A histomorphometric and removal torque study of screw-shaped titanium implants with three different surface topographies. *Clin Oral Impl Res* 1995; 6:24–30.
7. Wennerberg A. On surface roughness and implant incorporation. Thesis, University of Göteborg, Göteborg, Sweden, 1996.

8. Brånemark P-I, Breine U, Lindström J, et al. Intra-osseous anchorage of dental prostheses. I. Experimental studies. *Scand J Plast Reconstr Surg* 1969; 3:81.
9. Lekholm U, Zarb GA. Patient selection and preparation. In: Brånemark P-I, Zarb G, Albrektsson T, eds. *Osseointegration in clinical dentistry*. Chicago: Quintessence, 1985:199–209.
10. Meredith N, Cawley P, Alleyne D. Quantitative determination of the stability of the implant-tissue interface using resonance frequency analysis. *Clin Oral Impl Res* 1996; 7:261–267.
11. Meredith N, Book K, Friberg B, et al. Resonance frequency measurements of implant stability in vivo. A cross sectional and longitudinal study of R.F.M. on implants in the edentulous and partially dentate maxilla. *Clin Oral Impl Res* 1997; 8:226–233.
12. Meredith N, Shagaldi F, Alleyne D, et al. The application of resonance frequency measurements to study the stability of titanium implants during healing in the rabbit tibia. *Clin Oral Impl Res* 1997; 8:234–243.
13. Meredith N, Book K, Friberg B, et al. Resonance frequency measurements of implant stability in vivo. *Clin Oral Impl Res* 1997; 8:226–233.
14. Johansson P, Strid KG. Assessment of bone quality from cutting resistance during implant surgery. *Int J Oral Maxillofac Implants* 1994; 9:279–288.
15. Friberg B, Sennerby L, Roos J, et al. Evaluation of bone density using cutting resistance measurements and microradiography: an in vitro study in pig ribs. *Clin Oral Impl Res* 1995; 5:164–171.
16. Olive J, Aparicio C. The Periotest method as a measure of osseointegrated oral implant stability. *Int J Oral Maxillofac Implants* 1990; 5:390–400.
17. Teerlinck J, Quirynen M, Darius P, van Steenberghe D. Periotest: an objective clinical diagnosis of bone apposition toward implants. *Int J Oral Maxillofac Implants* 1991; 6: 55–61.
18. van Steenberghe D, Klinge B, Linden U, et al. Periodontal indices around natural and titanium abutments: a longitudinal multicentre study. *J Periodontol* 1993; 64:538–541.
19. Meredith N, Friberg B, Sennerby L, Aparicio C. Relationship between contact time measurements and PTV values when using the Periotest to measure implant stability. *Int J Prosthodontics* 1998; 11:269–275.
20. Derhami K, Wolfaadt J, Dent M, et al. Assessment of the Periotest device in baseline mobility measurements of craniofacial implants. *Int J Oral Maxillofac Implants* 1995; 10:221–229.
21. Niimi A, Ozeki K, Ueda M, Nakayama B. A comparative study of removal torque of endosseous implants in the fibula, iliac crest and scapula of cadavers: preliminary report. *Clin Oral Impl Res* 1997; 8:286–289.
22. Ueda M, Matsuki M, Jacobsson M, Tjellstrom A. The relationship between insertion torque and removal torque analysed in fresh temporal bone. *Int J Oral Maxillofac Implants* 1991; 6:442–447.
23. Johansson C, Albrektsson T. Integration of screw implants in the rabbit: a one-year follow-up of removal torque of titanium implants. *Int J Oral Maxillofac Implants* 1987; 2: 69–75.
24. Johansson C, Albrektsson T. A removal torque and histomorphometric study of commercially pure niobium and titanium implants in rabbit bone. *Clin Oral Impl Res* 1991; 2:24–49.

References

- Abdel-Latif H, Hobkirk JA, Kelleway JP (2000).
Functional Mandibular deformation in edentulous subjects treated with dental implants.
Int. J. Prosthodont.; 13:513-519.
- Abouzgia MB, Symington JM (1996).
Effect of drill speed on bone temperature.
Int. J. Oral Maxillofac. Surg.; 25:394-399.
- Adell R, Eriksson B, Lekholm U, Brånemark P-I, Jemt T (1990) [a].
A long-term follow-up study of osseointegrated implants in the treatment of the totally edentulous jaw.
Int. J. Oral Maxillofac. Impl.; 5:347-359.
- Adell R, Lekholm U, Brånemark P-I (1985)
Surgical procedures. In: Brånemark P-I, Zarb GA, Albrektsson T, (eds): Tissue-integrated prostheses: osseointegration in clinical dentistry.
Chicago, Quintessence; pp211-232.
- Adell R, Lekholm U, Gröndahl K, Brånemark P-I, Lindström J, Jacobsson M (1990) [b].
Reconstruction of severely resorbed edentulous maxillae using osseointegrated fixtures in immediate autogenous bone grafts.
Int. J. Oral Maxillofac. Impl.; 5:233-246.
- Adell R, Lekholm U, Rockler B., Brånemark P-I (1981).
A 15-year study of osseointegrated implants in the treatment of the edentulous jaw.
Int. J. Oral Surg.; 10:387-416.
- Albrektsson T (1988).
A multicentre report on osseointegrated oral implants.
J. Prosthet. Dent.; 60:75-84.
- Albrektsson T (1993).
On long-term maintenance of the osseointegrated response.
Aust. Prosthodont. J.; 7(suppl):15-24.
- Albrektsson T, Zarb G, Worthington P, Eriksson AR (1986).
The long-term efficacy of currently used dental implants: A review and proposed criteria of success.
Int. J Oral Maxillofac. Impl.; 1:11-25.
- Albrektsson T, Sennerby L (1991).
State of the art in oral implants.
J. Clin. Periodontol.; 18:474-81.
- Ansell R, Scales J (1968).
A study of some factors which affect the strength of screws and their holding power in bone.
J. Biomechanics; 1:279-302.

Atmaran GH, Mohammed H (1981).

Photoelastic stress analysis of dental implants with different root configurations.
N.Y. State Dent. J.; 47:30-33.

Atmaran GH, Mohammed H, Schoen (1979).

Stress analysis of single-tooth implants. I. Effect of elastic parameters and geometry of implant.

Biomat. Med. Dev. Art Org.; 7:99-104.

Bahat O (1993).

Treatment planning and placement of implants in the posterior maxillae: Report of 732 consecutive Nobelpharma implants.

Int. J. Oral Maxillofac. Impl.; 8:151-161.

Bassett CA, Becker RO (1962).

Generation of electric potentials by bone in response to mechanical stress.

Science; 137:1063-1064.

Blum AE (1977).

The use and understanding of photoelastic coatings.

Strain; 13: 96-101.

Bobbio A (1972).

The first endosseous alloplastic implant in the history of man.

Bull Hist. Dent.; 20:1-6.

Bonfield W, Li CH (1967).

Anisotropy of non-elastic flow in bone.

J. App. Phys.; 38:2450.

Bonfield W, O'Connor P (1978).

Anealastic deformation and friction stress of bone.

J. Mater. Sci.; 13:202.

Bonwill W (1895).

Implantation of metal tubes or pins of gold or iridium into the solid alveolar process to retain teeth.

Dental Cosmo.; 37:611-612.

Brånemark P-I, Breine U, Lindström J, Adell R, Hansson B-O, and Ohlsson P (1969). Intra-osseous anchorage of dental prostheses. I. Experimental studies.

Scand. J. Plast. Reconstr. Surg.; 3:81

Brånemark P-I, Hansson BO, Adell R, Breine U, Lindström J, Hallén O, Öhman A

(1977). Osseointegrated implants in the treatment of the edentulous jaw. Experience from a 10-year period.

Scand. Reconst. Surg.; II: suppl 16.

Brånemark P-I, Zarb G, Albrektsson T, (eds) (1985):
Tissue-integrated prostheses: osseointegration in clinical dentistry. Quintessence Publishing Co, Chicago.

Brosh I, Pilo R., Sudai D (1998).
The influence of abutment angulation on strains and stresses along the implant/bone interface: comparison between two experimental techniques.
J. Prosthet. Dent.; 79:328-34.

Brunski JB (1988).
Biomaterials and biomechanics in dental implant design.
Int. J. Oral Maxillofac. Implants; 3:85-97.

Brunski JB (1992).
Review paper. Biomechanical factors affecting the bone-dental implant interface.
Clin. Mater.; 10:153-201.

Bryant SR (1998).
The effects of age, jaw site, and bone condition on oral implant outcomes.
Int. J. Prosthodont.; 11:470-490.

Carlsson L, Röstlund T, Albrektsson B, Albrektsson T (1986).
Removal torques for polished and rough implants.
Acta. Orthop. Scand.; 57:285-289.

Carlsson L, Röstlund T, Albrektsson B and Albrektsson T (1988).
Removal torques for polished and rough titanium implants.
Int. J. Oral Maxillofac. Implants; 3:21-24.

Cameron HU, Pilliar RM, Macnab I (1973).
The effect of movement on the bonding of porous metal to bone.
J. Biomed. Mater. Res.; 7:301-311.

Carter DR (1982).
The relationship between in vivo strains and cortical remodeling.
In: Bourne JR, (ed.). CRC critical reviews in bioengineering.
Boca Raton: CRC Press Inc. p1-28.

Carter DR, Smith DJ, Spengler DM, Daly CH, Frankel VH (1980).
Measurement and analysis of in vivo bone strains on the canine radius and ulna.
J. Biomech.; 13:27-38.

Casino A, Harrison P, Tarnow D, Morris H, Ochi S (1997).
The influence of type of incision on the success rate of implant integration at stage II uncovering surgery.
J. Oral Maxillofac. Surg.; 55:31-37.

Caton J, Zander HA (1976).
Osseous repair of an infrabony pocket without new attachment of connective tissue.
J Clin Periodontol.; 3:54-58.

Chavez H, Ortman LF, DeFranco RL, Medige J (1993).
Assessment of oral implant mobility.
J. Prosthet. Dent.; 70:421-426.

Clift SE, Fisher J, Watson CJ (1992).
Finite element stress and strain analysis of the bone surrounding a dental implant:
effect of variations in bone modulus.
Proc. Inst. Mech. Engrs.; 206:233-241.

Cox JF, Zarb GA (1987).
The longitudinal clinical efficacy of osseointegrated dental implants: A 3-year report.
Int. J. Oral Maxillofac. Impl.; 2:91-100.

Cranin AN, Sher J, Schilb TP (1986).
The transosteal implant: a 17-year review and report.
J. Prosthet. Dent.; 55:709-718.

Currey JD, Brear K (1974).
Tensile yield in bone.
Calc. Tiss. Res.; 15:173-9.

Currey JD (1975).
The effects of strain rate, reconstruction and mineral content on some mechanical
properties of bovine bone.
J. Biomechanics. 8:81-86.

Dabestani M (1989).
The deformation behaviour of human compact bone, PhD thesis, University of
London.

Dabestani M (1992).
In vitro measurement in bone. In: Miles AW, Tanner KE (eds.) Strain
measurements in biomechanics. Chapman and Hall. pp58-69.

DeCoster T, Heetderks D, Downey D, Ferries J, Jones W (1990).
Optimizing bone screw pullout force.
J. Orthop. Trauma; 4:169-174.

Dempster WT, Liddicoat RT (1952).
Compact bone as a non-isotropic material.
Am. J. Anat.; 91:331-362.

Derhami K, Wolfaardt J, Dent M, Faulkner G, and Grace M (1995).
Assessment of the Periotest device in baseline mobility measurements of craniofacial
implants.
Int. J. Oral Maxillofacial. Implants; 10:221 – 229.

Dougherty G (1996).

Quantitative CT in the measurements of bone quantity and bone quality for assessing osteoporosis.

Med. Eng. Phys.; 18:557-568.

Duckmanton NA, Austin BW, Lechner SK, Klineberg IJ (1994).

Imaging for predictable maxillary implants.

Int. J. Prosthodont.; 7:77-80.

Duncan JL, MacKenzie AK (1989).

A comparative study of stress distribution in human bone under simple and complex loading conditions and as modified by the insertion of a metallic prosthesis. SPIE Stress and Vibration: Recent developments in Industrial Measurement and Analysis.; 184:111-114.

Duncan JL, Nicol AC (1985).

Experimental stress analysis of fresh bone using a thermoelastic technique.

Proc. Inst. Phys/Biol. Eng. Soc.; Uxbridge, UK.

Edmunds J (1889).

Metallic capsule implantation.

Dental. Cosmos.; 31:371-372, 550, 944.

Engquist B, Bergendahl T, Kallus T, Linden U (1988).

A retrospective multicenter evaluation of osseo-integrated implants supporting overdentures.

Int. J. Oral Maxillofac. Impl.; 2:129-134.

Eriksson AR (1984).

Heat-induced bone tissue injury. An in-vivo investigation of heat tolerance of bone tissue and temperature rise in the drilling of cortical bone. Thesis, University of Göteborg, Göteborg, Sweden.

Esposito M, Hirsch J-M, Lekholm U, Thomsen P (1998) [a].

Biological factors contributing to failures of osseointegrated oral implants. (1). Success criteria and epidemiology.

Eur. J. Oral Sci.; 106:527-551.

Esposito M, Hirsch J-M, Lekholm U, Thomsen P (1998) [b].

Biological factors contributing to failures of osseointegrated oral implants. (2). Etiopathogenesis.

Eur. J. Oral Sci.; 106:721-764.

Farah JW, Craig RG, Yapp RA (1979).

Stress distribution caused by blade type dental implants.

Implantologist; 1:82-85.

Friberg B (1994).

Bone Quality Evaluation during implant placement. MDS dissertation, University of Gothenburg, Sweden.

- Friberg B (1996).
Sterile operating conditions for the placement of intraoral implants.
J. Oral Maxillofac. Surg.; 54:1334-1336.
- Friberg B, Jemt T, and Lekholm U (1991).
Early failures in 4641 consecutively placed Brånemark dental implants. A study from stage I surgery to the connection of completed prostheses.
Int. J. Oral Maxillofacial. Implants; 6:142 – 146.
- Friberg B, Nilson H, Olsson M, Palmquist C (1997).
Mk II: the self-tapping Brånemark implant. 5-year result of a prospective 3-center study.
Clin. Oral Impl. Res.; 8:279-285.
- Friberg B, Sennerby L, Meredith N, Lekholm U (1999).
A comparison between cutting torque and resonance frequency measurements of maxillary implants.
Int. J. Oral Maxillofac. Surg.; 28(4):297-303.
- Friberg B, Sennerby L, Roos J, Johansson P, Strid CG, and Lekholm U (1995).
Evaluation of bone density using cutting resistance measurements and microradiography: an in vitro study in pig ribs.
Clin. Oral. Impl. Res.; 5:164-171.
- Frost HM (1987).
Bone “mass” and the “mechanostat”: a proposal.
Anat. Rec.; 219:1-9.
- Frost HM (1989) [a].
The biology of fracture healing. An overview for clinicians. Part I.
Clin. Orthop. Rel. Res.; 248:283-293.
- Frost HM (1989) [b].
The biology of fracture healing. An overview for clinicians. Part II.
Clin. Orthop. Rel. Res.; 248:294-309.
- Goldberg N, Gershkoff A (1949).
Implant lower denture.
Dental Digest.; 55:490-494.
- Goldstein SA (1987).
The mechanical properties of trabecular bone: dependence on anatomic location and function.
J. Biomechanics.; 1055-1061.
- Goodman S, Wang JS, Doshi A, Aspenberg P (1993).
Difference in bone ingrowth after one versus two daily episodes of micromotion: experiments with titanium chambers in rabbits.
J. Biomed. Mater. Res.; 27:1419-1424.

- Greenfield E (1913).
Implantation of artificial crown and bridge abutments.
Dental Cosmos.; 55:364-369.
- Grenoble DE (1974).
Design criteria for dental implants.
Oral Implantol.; 5:44-64.
- Gröndahl K, Ekestubbe A, Gröndahl HG, (eds.) (1996).
Radiography in Oral Endosseous Prosthetics.
NobleBiocare AB, Goteborg, Sweden.
- Gröndahl K, Lekholm U (1997).
The predictive value of radiographic diagnosis of implant instability.
Int. J. Oral Maxillofac. Impl.; 12:59-64.
- Haider R, Watzek G, Plenk H (1993).
Effects of drill cooling and bone structure on IMZ implant fixation.
Int. J. Oral Maxillofac. Implants.; 8:83-91.
- Hans D, Fuerst T, Lang T, Majumdar S, Lu Y, Genant HK, Glüer C (1997).
How can we measure bone quality?
Bailliere's Clin. Rheum.; 11:495-515.
- Haraldson T (1980).
A photoelastic study of some biomechanical factors affecting the anchorage of
osseointegrated implants in the lower jaw.
Scand. J. Plast. Reconstr. Surg.; 14:209-214.
- Hassler C, Rybicki E, Cummings K, Clark L (1977).
Quantitation of compressive stress and its effects upon bone remodeling.
Bull Hosp. Joint Diseases.; 38:90-93.
- Henry P, Laney W, Jemt T, Harris D, Krogh P, Polizzi G, Zarb G, Herrman I (1996).
Osseointegrated implants for single-tooth replacement: a prospective 5-year
multicentre study.
Int. J. Oral Maxillofac. Implants; 11:450-455.
- Heywood RB (1969).
Photoelasticity for Designers. Pergamon Press, Oxford.
- Hirschmann PH (1998).
Magnetic resonance imaging: a possible alternative to CT prior to dental implants.
Br. Dent. J.; 184:603-607.
- Hobkirk JA (1983).
Progress in implant research.
Int. Dent. J.; 33:341-349.

Hobkirk JA, Havthoulas TK (1998).

The influence of mandibular deformation, implant numbrs, and loading position on detected forces in abutments supporting fixed implant superstructures.
J. Prosthet. Dent.; 80:169-74.

Hobkirk JA, Rusiniak K (1977).

Investigation of variable factors in drilling bone.
J. Oral Surgery; 35:968-973

Holmgren EP, Seckinger RJ, Kilgren LM, Mante F (1998).

Evaluating parameters of osseointegrated dental implants using finite element analysis – a two-dimensional comparative study examining the effects of implant diameter, implant shape, and load direction.
J. Oral Implantol.; 24:80-8.

Hongo M, Abe E, Shimada Y, Murai H, Ishikawa N, Sato K (1999).

Surface strain distribution on thoracic and lumbar vertebrae under axial compression. The role in burst fractures.
Spine; 24:1197-202.

Horner K, Devlin H (1998) [a].

The relationships between two indices of mandibular bone quality and bone mineral density measured by dual energy X-ray absorptiometry.
Dentomaxillofac. Radiol.; 27: 17-21.

Horner K, Devlin H (1998) [b].

The relationship between mandibular bone mineral density and panoramic radiographic measurements.
J. Dent.; 26:337-343.

Hoshaw SJ, Brunski JB, Cochran GVB (1994).

Mechanical loading of Branemark implants affects interfacial bone modeling and remodeling.
Int. J. Oral Maxillofac. Impl.; 9:345-360.

Hossdorf H (1974).

Model Analysis of Structures, Van Nostrand Reinhold, Wokingham.

Huiskes R, Nunamaker D (1984).

Local stresses and bone adaptation around orthopedic implants.
Calcif. Tissue Int.; 36:110-117.

Ivanoff C-J (1999).

On surgical and implant related factors influencing integration and function of titanium implants – experimental and clinical aspects. Thesis. University of Göteborg, Sweden.

Ivanoff C-J, Sennerby L, Lekholm U (1996).

Influence of mono- and bicortical anchorage on the integration of titanium implants. A study in the rabbit tibia.

Int. J. Oral Maxillofac. Surg.; 25:229-235.

Iyer S, Weiss C, Mehta A (1997).

Effects of drill speed on heat production and the rate and quality of bone formation in dental implant osteotomies. Part I: relationship between drill speed and heat production.

Int. J. Prosthodont.; 10:411-414.

Jaffin RA, Berman CL (1991).

The excessive loss of Brånemark fixtures in type IV bone. A 5-year analysis.

J. Periodontol.; 62:2-4.

Jemt T (1991).

Failures and complications in 391 consecutively inserted fixed prostheses supported by Brånemark implants in the edentulous jaws: A study of treatment from the time of prosthesis placement to the first annual checkup.

Int. J. Oral Maxillofac. Impl.; 6:270-276.

Jemt T, Lekholm U (1993).

Oral implant treatment in posterior partially edentulous jaws : a 5-year follow-up report.

Int. J. Oral Maxillofac. Implants; 5:347-359

Jemt T, Lekholm U (1995).

Implant treatment in edentulous maxillae: a 5-year follow-up report on patients with different degrees of jaw resorption.

Int. J. Oral Maxillofac. Impl.; 10:303-311.

Jemt T, Pettersson P (1993).

A 3-year follow-up study on single implant treatment.

J. Dent.; 21:203-208.

Jensen OT (1989).

Site classification for the osseointegrated implant.

J. Prosthet. Dent.; 61:228-234.

Johannsson CB, Albrektsson T (1987).

Integration of screw implants in the rabbit: a one-year follow-up of removal torque of titanium implants.

Int. J. Oral Maxillofac. Impl.; 2:69-75.

Johannsson CB, Albrektsson T (1991).

A removal torque and histomorphometric study of commercially pure niobium and titanium implants in rabbit bone.

Clin. Oral Impl. Res.; 2:24-29.

Johansson P, Strid KG (1994).

Assessment of bone quality from cutting resistance during implant surgery.

Int. J. Oral and Maxillofac. Impl.; 9:279-288.

- Klemetti E, Kolmakov S, Heiskanen P, Vainio P, Lassila V (1993) [a].
Panoramic mandibular index and bone mineral densities in postmenopausal women.
Oral Surg. Oral Med. Oral Pathol.; 75:774-779.
- Klemetti E, Vainio P, Lassila V, Alhava E (1993) [b].
Trabecular bone mineral density of mandible and alveolar height in postmenopausal women.
Scand. J. Dent. Res.; 101:166-170.
- Klinge B, Johansson CB, Albrektsson T, Hallstrom H, Engdahl T (1995).
A new method to obtain bone biopsies at implant sites peri-operatively: technique and bone structure.
Clin. Oral Impl. Res.; 6:91-95.
- Kody MH, Kabo JM, Markolf KL, Dorey FJ, Amstutz HC (1990).
Strength of initial mechanical fixation of screw ring acetabular components.
Clin. Orthop.; 257:146-153.
- Kraut RA (1996).
Clean operating conditions for the placement of intraoral implants.
J. Oral Maxillofac. Surg.; 54:1337-1338.
- Kuske A, Robertson G (1977).
Photoelastic Stress Analysis. John Wiley, Chichester, UK.
- Lambert P, Morris H, Ochi S (1997).
Positive effect of surgical experience with implants on second-stage implant survival.
J. Oral Maxillofac. Surg.; 55:12-18.
- Langer B, Langer L, Herrmann I, Jorneus L (1993).
The wide fixture. A solution for special bone situations and a rescue for the compromised implant.
Int. J. Oral Maxillofac. Impl.; 8:400-8.
- Lanyon LE (1976).
The measurement of bone strain in vivo.
Acta. Orthop. Belg.; 42:98-108.
- Lekholm U, van Steenberghe D, Herrmann I, et. al. (1994).
Osseointegrated implants in the treatment of partially edentulous jaws: a prospective 5-year multicenter study.
Int. J. Oral Maxillofac. Impl.; 9:627-635.
- Lekholm U, and Zarb GA (1985).
Patient selection and preparation. In: Brånemark PI, Zarb G, Albrektsson T, eds. Osseointegration in clinical dentistry, Quintessence Publishers, Chicago; pp199-209.
- Linde F (1994).
Elastic and viscoelastic properties of trabecular bone by a compression testing approach.

Danish Medical Bulletin; 41:119-138.

Linde F, Nørgaard P, Hvid I, Odgaard A, Søballe K (1991).
Mechanical properties of trabecular bone. Dependency on strain rate.
J.Biomechanics; 24:803-809.

Linde F, Hvid I, Madsen F (1992).
The effect of specimen geometry on the mechanical behaviour of trabecular bone specimens.
J. Biomechanics; 25:359-368.

Lindh C, Nilsson M, Klinge B, Petersson A (1996) [a].
Quantitative computed tomography of trabecular bone in the mandible.
Dentomaxillofac. Radiol.; 25:146-150.

Lindh C, Petersson A, Rohlin M (1996) [b].
Assessment of the trabecular pattern before endosseous implant treatment: diagnostic outcome of periapical radiography in the mandible.
Oral Surg. Oral Med. Oral Pathol. Oral Radiol. Endod.; 82:335-343.

Little EG, Finlay JB (1992).
Perspectives of strain measurement techniques. In: Miles AW, Tanner KE (eds.)
Strain measurements in biomechanics. Chapman and Hall. pp1-13.

Lundskog J (1972).
Heat and bone tissue. An experimental investigation of the thermal properties of bone tissue and threshold levels for thermal injury.
Scand. J. Plast. Reconstr. Surg.; (Suppl 9): 1-80.

Marshall PD, Evans PD, Richards J (1993).
Laboratory comparison of the cannulated Herbert bone screw with ASIF cancellous lag screws.
J.Bone Joint Surg. Br.; 75:89-92.

Martin RB (1991).
Determinants of the mechanical properties of bone.
J. Biomechanics; 24:79-88.

Masuda T, Salvi S, Offenbacher S, Felton D, Cooper L (1997).
Cell and matrix reactions at titanium implants in surgically prepared rat tibiae.
Int. J. Oral Maxillofac. Implants; 12:472-485.

Meredith N (1997).
On the clinical measurement of implant stability and osseointegration. PhD thesis, University of Gothenburg, Sweden.

Meredith N (1998) [a].
Assessment of implant stability as a prognostic determinant.
Int. J. Prosthodont.; 11:491-501.

Meredith N (1998) [b].

A review of non-destructive test methods and their application to measuring the stability of osseointegration of bone anchored endosseous implants.

Crit. Rev. Biomed. Eng.; 26:275-91.

Meredith N, Book K, Friberg B, Jemt T, & Sennerby L (1997) [a].

Resonance Frequency measurements of implant stability in vivo. A cross sectional and longitudinal study of R.F.M. on implants in the edentulous and partially dentate maxilla.

Clinical Oral Implants Research; 8:226-233.

Meredith N, Cawley P, & Alleyne D (1996) [a].

Quantitative determination of the stability of the implant-tissue interface using Resonance Frequency Analysis.

Clinical Oral Implants Research; 7:261-267.

Meredith N, Friberg B, Sennerby L, Aparicio C (1998).

Relationship between contact time measurements and PTV values when using the Periotest to measure implant stability.

The Int. J. Prosthodontics; 11:269-275.

Meredith N, Rasmusson L, Sennerby L, Alleyne D (1996) [b].

Mapping implant stability by resonance frequency analysis.

Med. Sci. Res.; 24:191-193.

Meredith N, Shagaldi F, Alleyne D, Sennerby L, & Cawley P (1997) [b].

The application of resonance frequency measurements to study the stability of titanium implants during healing in the rabbit tibia.

Clinical Oral Implants Research; 8:234-243.

Misch CE (1990).

Density of bone: Effect on treatment plans, surgical approach, healing and progressive bone loading.

Int. J. Oral Impl.; 6:23-31.

Morden GC (1982).

Adhesives and installation techniques, in Strain gauge Technology. Window AL and Holister GS (eds.). Applied Sciences Publishers, Barking, UK. pp43-54.

Morris HF, Ochi S (1992).

The influence of implant design, application, and site on clinical performance and crestal bone: a multicentre, multidisciplinary clinical study. Dental Implant Clinical Research Group (Planning Committee).

Implant Dent.; 1:49-55.

Murphy W, Williams KR, Gregory MC (1995).

Stress in bone adjacent to dental implants.

J. Oral Rehabil.; 22:897-903.

Natiella J, Armitage J, Greene G, Meenaghan M (1972).
Current evaluation of dental implants.
J. Am. Dent. Assoc.; 84:1358-1372.

Nevins M, Langer B (1993).
The successful application of osseointegrated implants to the posterior jaw: A long-term retrospective study.
Int. J. Oral Maxillofac. Impl.; 8:428-432.

Niimi A, Ozeki K, Ueda M, Nakayama B (1997).
A comparative study of removal torque of endosseous implants in the fibula, iliac crest and scapula of cadavers: preliminary report.
Clin. Oral Implants Res.; 8:286 – 289.

Odgaard A, Linde F (1991).
The underestimation of Young's modulus in compressive testing of cancellous bone specimens.
J. Biomechanics; 24:691-698.

Oka H, Yamamoto T, Sarantani K, Kawazoe T (1990).
Automatic diagnosis system of tooth mobility for clinical use.
Medical Progress through Technology; 16:117-124.

Olivé J, and Aparicio C (1990).
The Periotest method as a measure of osseointegrated oral implant stability.
Int. J. Oral. Maxillofac. Implants; 5:390-400.

Pilliar RM, Lee JM, Maniopoulos C (1986).
Observations on the effect of movement on bone ingrowth into porous-surfaced implants.
Clin. Orthop. Rel. Res.; 208:108-113.

Pople J (1979).
BSSM Strain Measurement Reference Book, British Society for Strain Measurement, Newcastle Upon Tyne, UK.

Privitzer E, Widera O, Tesk JA (1975).
Some factors affecting dental implant design.
J. Biomed Mater. Res.; 9:251-255.

Quirynen M, Naert I, van Steenberghe D (1992).
Fixture design and overload influence marginal bone loss and fixture success in the Branemark system.
Lin. Oral Impl. Res.; 3:104-111.

Rasmusson L, Meredith N, Kahnberg KE, Sennerby L (1998).
Stability assessments and histology of titanium implants placed simultaneously with autogenous onlay bone in the rabbit tibia.
Int. J. Oral Maxillofac. Surg.; 27:229-35.

- Rasmusson L, Meredith N, Sennerby L (1997).
Measurements of stability changes of titanium implants with exposed threads subjected to barrier membrane induced bone augmentation. An experimental study in the rabbit tibia.
Clin. Oral Implants Res.; 8:316-22.
- Rieger MR, Adams WK, Kinzel GL (1990).
A finite element survey of eleven endosseous implants.
J. Prosthet. Dent.; 63:457-465.
- Roberts E, Smith R, Zilberman Y, Mozsary P, Smith R (1984).
Osseous adaptation to continuous loading of rigid endosseous implants.
Am. J. Orthod.; 86:95-111.
- Roberts E, Garetto L, Brezniak N (1993).
Bone physiology and metabolism. In: Misch C, (ed): Contemporary implant dentistry. St. Louis, Mosby Year Book. pp327-353.
- Roos J, Sennerby L and Albrektsson T (1997).
An update on the clinical documentation on currently used bone anchored endosseous oral implants.
Dent. Update; 24:194-200.
- Rubin CT, Lanyon LE (1987).
Osteoregulatory nature of mechanical stimuli: function as a determinant for adaptive remodeling in bone.
J. Orthop. Res.; 5:300-310.
- Salonen M., Oikarinen K., Virtanen K., Pernu H (1993).
Failures in the osseointegration of endosseous implants.
Int. J. Oral Maxillofac. Implants; 8:92-97.
- Sandy JR, Farndale RW, Meikle MC (1993).
Recent advances in understanding mechanically induced bone remodelling and their relevance to orthodontic theory and practice.
Am. J. Orthod. Dentofac. Orthop.; 103:212-222.
- Scharf DR, Tarnow DP (1993).
The effect of crestal versus mucobuccal incisions on the success rate of implant osseointegration.
Int. J. Oral Maxillofac. Implants; 8:187-190.
- Schatzker JG, Horne JG, Sumner Smith G (1975).
The effects of movement on the holding power of screws in compact bone.
Clin. Orthop. 111:257
- Schenk RK (1994).
Bone regeneration: biological basis. In: Buser D., Dahlin C., Schenk R.K., (eds.): Guided bone regeneration in implant dentistry. Quintessence Publ Co, Inc, Chicago. pp49-100.

Schenk RK, Willenegger HR (1977).

Histology of primary bone healing: modifications and limits of recovery of gaps in relation to extent of the defect.

Unfallheilkunde; 80:155-160.

Schulte W, Lucas D, Mulbradt L, et. al. (1983).

Periotest – ein neues Verfahren zur Messung der Funktion des Parodontiums. Zahnartzl Mitt.; 73:1229.

Sedlin ED, Hirsch C (1966).

Factors affecting the determination of the physical properties of femoral cortical bone.

Acta. Orthop. Scand.; 37:29.

Sennerby L (1991).

On the bone tissue response to titanium implants. Thesis, University of Göteborg, Göteborg, Sweden.

Sennerby L, Roos J (1998).

Surgical determinants of clinical success of osseointegrated oral implants: A review of the literature.

Int. J. Prosthodont.; 11:408-420.

Sennerby L, Thomsen P, Ericsson L (1992).

A morphometric and biomechanic comparison of titanium implants inserted in rabbit cortical and cancellous bone.

Int. J. Oral Maxillofac. Implants; 7:62-71.

Sennerby L, Thomsen P, Ericsson L (1993).

Early tissue response to titanium implants inserted in rabbit cortical bone. Part I. Light microscopic observations.

J. Mater. Sci. Mater. Med.; 4:240-250.

Seong W, Koriath TW, Hodges JS (2000).

Experimentally induced abutment strains in three types of single-molar implant restorations.

J. Prosthet. Dent.; 84:318-26.

Small IA. (1975).

Chalmers J Lyons memorial lecture: Metal implants and the mandibular staple bone plate.[Review].

J. Oral Surg.; 33:571-585.

Smith JW, Walmsley R (1959).

Factors affecting the elasticity of bone.

Acta. Anat.; 93:503.

- Soltész U, Siegele D, Riedmüller J, Schultz P (1982).
Stress concentration and bone resorption in the jaw for dental implants with shoulders. In Lee AJC, Albrektsson T, Branemark P-I (eds): Clinical applications of Biomaterials. Chichester, England, Wiley and Sons Ltd. pp115-122.
- Strid K-G (1985).
Radiographic results. In osseointegration in clinical dentistry. Branemark P-I, Zarb G, Albrektsson T, (eds.), Quintessence Publishers, Chicago.pp 187-197.
- Stulberg BN, Bauer TW, Watson JT, Richmond B (1989).
Bone quality. Roentgenographic versus histologic assessment of hip bone structure. Clin. Orthop. Rel. Res.; 240:200-205.
- Sullivan DY, Sherwood RL, Collins TA and Krogh PHJ (1996).
The reverse-torque test: a clinical report.
Int. J. Oral Maxillofac. Implants.; 11:179-185.
- Sundén S, Gröndahl K and Gröndahl H-G (1995).
Accuracy and precision in the radiographic diagnosis of clinical instability in Brånemark dental implants.
Clin. Oral Impl. Res.; 6:220-226.
- Taguchi A, Tanimoto K, Ogawa M, Sunayashiki T, Wada T (1991).
Effect of size of region of interest on precision of bone mineral measurements of the mandible by quantitative computed tomography.
Dentamaxillofac. Radiol.; 20:25-29.
- Tashkandi EA, Lang BR, Edge MJ (1996).
Analysis of strain at selected bone sites of a cantilevered implant-supported prosthesis.
J. Prosthet. Dent.; 76:158-64.
- Teixeira ER, Sato Y, Akagawa Y, Shindoi N (1998).
A comparative evaluation of mandibular finite element models with different lengths and elements for implant biomechanics.
J. Oral Rehabil.; 25:299-303.
- Tricio J, Laohapand P, van Steenberghe D, Quirynen M, Naert I (1995).
Mechanical state assessment of the implant-bone continuum: A better understanding of the Periotest method.
Int. J. Oral Maxillofac. Implants; 10:43-49.
- Turner CH (1991).
Homeostatic control of bone structure: an application of feedback theory.
Bone; 12: 203-217.
- Turner CH (1998).
Three rules for bone adaptation to mechanical stimuli.
Bone; 23:399-407.

- Ueda M, Matsuki M, Jacobsson M, and Tjellstrom A (1991).
The relationship between insertion torque and removal torque analysed in fresh temporal bone.
Int. J. Oral Maxillofac. Implants; 6:442 – 447.
- Van Steenberghe D (1991).
Oral implants.
Curr. Opin. Dent.; 1:138-145.
- Van Steenberghe D, Quirynen M, Calberson L, Demanet M (1987).
A prospective evaluation of the fate of 697 consecutive intra-oral fixtures ad modum Brånemark in the rehabilitation of edentulism.
J. Head and Neck Pathol.; 6:53-58.
- Volmer D, Meyer U, Joos U, Vegh A, Piffko J (2000).
Experimental and finite element study of a human mandible.
J. Craniomaxillofac. Surg.; 28:91-6.
- Von Wowern N, Lyager N, Storm T, Olgaard K (1988).
Bone mineral content by photon absorptiometry of the mandible compared with that of the forearm and the lumbar spine.
Calcif. Tissue Int.; 42:157-161.
- Von Wowern N, Harder F, Hjorting-Hansen E, Gotfredsen K (1990).
ITI implants with overdentures: a prevention of bone loss in edentulous mandibles?
Int. J. Oral Maxillofac. Impl.; 5:135-139.
- Wainwright SA, Biggs WD, Currey JD, Gosline JM (1982). In “Mechanical design in Organisms”; pp174; Princetown University Press, Princetown, New Jersey, USA.
- Walker JD (1978).
Applied Mechanics. Hodder and Stoughton Ltd., London, UK.
- Wang S, Hobkirk A (1996).
Load distribution on implants with a cantilevered substructure: an in vitro pilot study.
Implant Dent.; 5:36-42.
- Wennerberg A, Albrektsson T, Andersson B and Krol J (1995).
A histomorphometric and removal torque study of screw-shaped titanium implants with three different surface topographies.
Clin. Oral Impl. Res.; 6:24-30.
- Worthington P, Bolender CL, Taylor TD (1987). The Swedish system of osseointegrated implants: problems and complications encountered during a 4-year trial period. Int. J. Oral Maxillofac. Impl.; 2:77-84.
- Wright TM, Hayes WC (1976).
Tensile testing of bone over a wide range of strain rates: effects of strain rate, microstructure and density.
Med. Biol. Eng.; 14:671-679.

Wyatt C, Zarb GA (1998). Treatment outcomes of patients with implant-supported fixed prostheses. *Int. J. Oral Maxillofac. Impl.*; 13:204-211.

Zarb GA, Schmitt A (1990). The longitudinal clinical effectiveness of osseointegrated dental implants: The Toronto study. Part III: Problems and complications encountered. *J. Prosthet. Dent.*; 64:185-194.

Znamensky N (1891).
The implantation of artificial teeth.
Brit. J. Dent. Science; 34:314-316.

